Modulation of the endogenous *MBNL1* expression via RNA activation (RNAa) as a novel therapeutic approach towards myotonic dystrophy type 1 (DM1)

Nikola Musiała-Kierklo

PhD Thesis

Doctoral Supervisor: **Prof. UPP dr hab. inż. Ewa Stępniak-Konieczna**

Laboratory of RNA Biology

Department of Biochemistry and Biotechnology

Faculty of Agriculture, Horticulture and Biotechnology

Poznań University of Life Sciences

ADAM MICKIEWICZ UNIVERSITY POZNAŃ

DOCTORAL SCHOOL OF NATURAL SCIENCES

Poznań 2025

Modulacja endogennej ekspresji *MBNL1* poprzez aktywację RNA (RNAa) jako nowe podejście terapeutyczne w dystrofii miotonicznej typu 1 (DM1)

Nikola Musiała-Kierklo

Rozprawa doktorska

Promotor: **Prof. UPP dr hab. inż. Ewa Stępniak-Konieczna**

Zespół Biologii RNA

Katedra Biochemii i Biotechnologii

Wydział Rolnictwa, Ogrodnictwa i Biotechnologii

Uniwersytet Przyrodniczy w Poznaniu

UNIWERSYTET IM. ADAMA MICKIEWICZA W POZNANIU

SZKOŁA DOKTORSKA NAUK PRZYRODNICZYCH

Poznań 2025

I would like to thank my Doctoral Supervisor,

Prof. UPP dr hab. inż. Ewa Stępniak-Konieczna, for giving me an opportunity to develop myself as a scientist, sharing knowledge, counselling and mentoring.

I would also like to thank,

Scientific Community from Adam Mickiewicz University, Institute of Molecular Biology and Biotechnology led by prof. Krzysztof Sobczak, and Poznań University of Life Sciences, Department of Biochemistry and Biotechnology led by prof. prof. UPP dr hab. inż. Joanna Zeyland, for their support, collaboration and inspiration.

My husband, Jakub, for his patience, empathy and invaluable support, especially when I doubted myself.

My family and friends, for believing in me and supporting me through good and bad times.

Dedicated to my husband, Jakub

and our daughter, Amelia

TABLE OF CONTENTS

FUNDING

This PhD project was carried out within the framework of the National Science Centre grant OPUS nr UMO-2020/37/B/NZ5/01263 (to Ewa Stępniak-Konieczna)

Additional sources of funding included:

1. National Science Centre grant SONATA BIS nr UMO-2022/46/E/NZ5/00088 (to Ewa Stępniak-Konieczna)
2. ID-UB (Inicjatywa doskonałości – Uczelnia Badawcza; Excellence Initiative - Research University) Doctoral mini-grant for the Academic Year 2022/2023 nr 054/13/SNP/0013 (to Nikola Musiała-Kierklo)

The PhD scholarship was funded by the National Science Centre grant OPUS nr UMO-2020/37/B/NZ5/01263 (to Ewa Stępniak-Konieczna)

ABSTRACT

Myotonic Dystrophy (DM) is an autosomal dominant neuromuscular disorder and is the most common form of muscular dystrophy in adults. Myotonic dystrophy type 1 (DM1) is caused by expansion of a CTG triplet repeat in the 3′ untranslated region (3′UTR) of dystrophia myotonica protein kinase (*DMPK*) gene and involves variable spectrum of symptoms including most characteristic myotonia, cardiomyopathy, insulin-resistance as well as muscular weakness and atrophy. Mutated *DMPK* transcripts containing expanded CUG repeat tracts (CUG^{exp}) form hairpin-like structures which are retained in the nuclei where they sequester distinct RNA-binding proteins, including Muscleblind-like (MBNL) family members, eventually accumulating as discrete ribonuclear foci. MBNL proteins control cellular RNA metabolism through the regulation of alternative splicing, alternative polyadenylation as well as stability and localization of mRNAs. Amongst the three *MNBL* paralogs, *MBNL1* is predominantly expressed in majority of tissues and plays major roles in alternative splicing regulation (except for the brain where *MBNL2* predominates). Importantly, there are three promoters (P1, 2 and 3) and three transcription start sites (TSS1, 2 and 3) involved in *MBNL1* expression, among which P2 is the major driver in most tissues. Moreover, only P2/TSS2-derived transcripts undergo MBNL-dependent regulation of the alternative splicing of first coding exon (e1), while P1/TSS1- and P3/TSS3-derived mRNAs exhibit always skipped or included e1, respectively. E1-depleted *MBNL1* mRNAs give rise to unstable MBNL1 protein isoforms with decreased functionality, due to loss of first two of four zinc fingers (ZnFs) that are essential for RNA target recognition and splicing, thus unable to further repress e1 inclusion and resulting in translation of a fully functional protein from e1-containing mRNAs. This e1-based autoregulatory feedback loop ensures appropriate MBNL1 protein level according to cellular demands. Notably, the impact of upregulation of the endogenous P2-mediated *MBNL1* expression has not been tested previously in the context of experimental therapy against DM. Modulating P2 activity could give a rise to a balanced MBNL1 splice isoforms diversity regulating its own protein level via e1 alternative splicing, hence protecting the cells from uncontrolled and possibly toxic MBNL1 overexpression.

Currently, there is no effective therapy for DM patients. The most explored types of molecular strategies for treating DM target either the expanded CUG^{exp} RNA for degradation via distinct antisense-based mechanisms, or inhibit and / or disrupt the toxic RNA:MBNL complex via distinct small molecule compounds and ligands. Alternatively, MBNLs

overexpression has shown promising therapeutic potential in DM *in vivo*, such as delivery of recombinant adeno-associated (rAAV) vectors carrying MBNL1 or endogenous modulation of *MBNL1* expression via small molecules and antisense oligomers.

The therapeutic upregulation of endogenous *MBNL1,* investigated in this PhD Thesis, is based on a conserved cellular mechanism of gene activation - RNAa (RNA activation). RNAa can be induced by artificially designed promoter-targeted duplex (double-stranded) RNAs termed small activating RNAs (saRNAs). The therapeutic utility of RNAa was demonstrated with several genes in distinct cancer models. This novel approach, when applied to *MBNL1*, allowed to develop a new type of possible treatment strategy for DM1. Two identified saRNAs, directed at specific *MBNL1* promoter 2 (P2) sequences, led to upregulation of *MBNL1* pre-mRNA, mRNA and protein level up to ~2-fold and reversed alternative splicing alterations linked to DM1 in distinct cellular models. Mechanistically, saRNAs stimulated *MBNL1* transcription specifically through the involvement of AGO2-mediated loading of the antisense strand of saRNA duplex onto *MBNL1* promoter, and recruitment of crucial RNAa pathway components (RHA and CTR9) and RNAPII. Additionally, contribution of two transcription factors (MEIS1 and MEIS2) in saRNA-mediated *MBNL1* upregulation was detected. Furthermore, presented data ruled out potential involvement of lncRNA *MBNL1-AS1* in *MBNL1* RNAa. Moreover, data included in the published original article that are part of this dissertation, but not part of my PhD Thesis, excluded the mechanistic involvement of short promoter-associated RNAs and indicated that the potential off-target effect of lncRNA *MBNL1-AS1* downregulation by saRNA depends on the activity of the sense (passenger) strand of the duplex and can be eliminated by chemical modification. In summary, saRNA-mediated upregulation of the endogenous *MBNL1* offers a new opportunity to achieve therapeutic effects in DM1 with lower level of *MBNL1* upregulation compared to exogenous overexpression, and hence may limit side effects associated with high protein levels.

STRESZCZENIE

Dystrofia miotoniczna (DM) to autosomalnie dominujące zaburzenie nerwowo-mięśniowe i najczęstsza postać dystrofii mięśniowej u dorosłych. Dystrofia miotoniczna typu 1 (DM1) jest spowodowana ekspansją trójnukleotydowego powtórzenia CTG w nieulegającym translacji regionie 3' (3'UTR) genu kinazy białkowej dystrofii miotonicznej (*DMPK*) i obejmuje zróżnicowane spektrum objawów, w tym najbardziej charakterystyczną miotonię, kardiomiopatię, insulinooporność, a także osłabienie i zanik mięśni. Zmutowane transkrypty *DMPK* zawierające nadmiernie wydłużone ciągi powtórzenia CUG (CUG^{exp}) tworzą w jądrach komórkowych struktury przypominające spinki do włosów, gdzie sekwestrują różne białka wiążące RNA, w tym tez rodziny białek typu muscleblind-like (MBNL), gromadząc się jako ziarnistości jądrowe (foci). Białka MBNL kontrolują metabolizm RNA w komórce poprzez regulację alternatywnego splicingu, alternatywnej poliadenylacji, a także biogenezy, stabilności i lokalizacji mRNA. Spośród trzech paralogów *MNBL*, *MBNL1* jest głównie eksprymowanym w większości tkanek i odgrywa kluczową rolę w regulacji alternatywnego splicingu (z wyjątkiem mózgu, gdzie dominuje *MBNL2*). Co ważne, transkrypcja *MBNL1* kontrolowana jest przez trzy promotory (P1, 2 i 3) oraz trzy miejsca startu transkrypcji (TSS1, 2 i 3), spośród których P2 jest najbardziej aktywnym promotorem w większości tkanek. Co więcej, tylko transkrypty pochodzące z P2/TSS2 podlegają zależnej od białek MBNL regulacji alternatywnego splicingu pierwszego eksonu kodującego (e1), podczas gdy mRNA pochodzące z P1/TSS1 i P3/TSS3 zawsze wykazują odpowiednio pominięty lub włączony e1. Obecność mRNA *MBNL1* bez e1 prowadzi do powstania niestabilnych izoform białka MBNL1 o obniżonej funkcjonalności, z powodu utraty pierwszych dwóch z czterech palców cynkowych (ZnF), które są niezbędne do rozpoznawania i splicingu RNA. W rezultacie uniemożliwiają one dalszą represję inkluzji e1 i prowadzą do translacji w pełni funkcjonalnego białka z mRNA zawierających e1. Ta oparta na e1 autoregulacyjna pętla sprzężenia zwrotnego zapewnia odpowiedni poziom białka MBNL1, zgodnie z zapotrzebowaniem komórki. Co istotne, wpływ zwiększenia endogennej ilości transkryptu *MBNL1*, zależnej od P2, nie był dotychczas badany w kontekście terapii eksperymentalnej w DM. Modulacja aktywności P2 może prowadzić do powstania zrównoważonej i różnorodnej ilości wariantów splicingowych MBNL1, regulującej poziom własnego białka poprzez alternatywny splicing e1, chroniąc w ten sposób komórki przed niekontrolowaną i potencjalnie toksyczną nadekspresją MBNL1.

Obecnie nie ma skutecznej terapii dla pacjentów z DM. Najlepiej zbadane strategie molekularne w leczeniu DM polegają albo na degradacji wydłużonego RNA CUG^{exp} za pomocą mechanizmów opartych na sekwencjach antysensowych, albo na inhibicji i/lub rozbijaniu toksycznego kompleksu RNA:MBNL za pomocą związków drobnocząsteczkowych i ligandów. Alternatywnie, w badaniach *in vivo* nad DM nadekspresja MBNL wykazała obiecujący potencjał terapeutyczny, na przykład poprzez dostarczanie MBNL1 przy użyciu rekombinowanych wektorów wirusowych związanych z adenowirusami (rAAV) lub endogenną modulację ekspresji *MBNL1* za pomocą małych cząsteczek i oligomerów antysensowych.

Terapeutyczna regulacja ekspresji endogennego *MBNL1*, badana w niniejszej rozprawie doktorskiej, opiera się na konserwatywnym komórkowym mechanizmie aktywacji genów – RNAa (aktywacja RNA). RNAa może być indukowana przez sztucznie zaprojektowane, ukierunkowane na promotor dwuniciowe RNA, zwane małymi aktywującymi RNA (saRNA). Terapeutyczna użyteczność RNAa została wykazana w przypadku kilku genów w różnych modelach nowotworowych. Te nowatorskie podejście, zastosowane do *MBNL1*, pozwoliło na opracowanie nowej strategii terapeutycznej dla DM1. Dwa zidentyfikowane saRNA, skierowane na specyficzne sekwencje docelowe promotora 2 (P2) genu *MBNL1*, doprowadziły do ~2-krotnego wzrostu poziomu pre-mRNA, mRNA i białka MBNL1 oraz do skorygowania nieprawidłowego alternatywnego splicingu związanego z DM1 w różnych modelach komórkowych.

Mechanistycznie, saRNA specyficznie stymulowały transkrypcję *MBNL1* poprzez zależne od AGO2 ładowanie nici antysensowej (wiodącej) z dwuniciowego saRNA na promotor *MBNL1* oraz rekrutację kluczowych czynników szlaku RNAa (RHA i CTR9) i RNAPII. Ponadto wykryto udział dwóch czynników transkrypcyjnych (MEIS1 i MEIS2) w regulacji ekspresji *MBNL1* związanej z jednym ze zidentyfikowanych dupleksów saRNA., Przedstawione dane wykluczyły mechanistyczny udział długiego niekodującego RNA (lncRNA) *MBNL1-AS1,* powstającego z niekodującej nici DNA genu *MBNL1* i nakładającego się częściowo na jego promotor P2 .Co więcej, dane wchodzące w skład pracy opublikowanej w ramach tej rozprawy, natomiast nie będące częścią tej rozprawy, wykluczyły mechanistyczny udział krótkich RNA związanych z promotorem i wskazały, że potencjalny efekt off-target w postaci obniżenia lncRNA *MBNL1-AS1* pod wpływem saRNA zależny jest od aktywności nici sensowej (pasażerskiej) dupleksu i może być wyeliminowany chemiczną modyfikacją. Podsumowując, regulacja ekspresji endogennego

MBNL1 przy udziale saRNA oferuje nową strategię terapeutyczną w DM1, przy niższym poziomie *MBNL1* w porównaniu z egzogenną nadekspresją, co tym samym może ograniczyć skutki uboczne związane z wysokim poziomem białka.

ABBREVIATIONS

2’- F - 2’-fluoro

2’- OMe - 2’-O-methyl

AGO - argonaute

AltS - alternative splicing

APP - amyloid beta precursor protein

AS - antisense

ASD - autism spectrum disorder

ASO - antisense oligonucleotides

BCG - Bacillus Calmette-Guérin

BIN1 - bridging integrator-1

C/EBPα - CCAAT/enhancer-binding protein alpha

C9ORF72-FTD/ALS - C9ORF72 frontotemporal dementia and/or amyotrophic lateral sclerosis

Cas9 - CRISPR-associated protein 9

Ccnb1 - cyclin b1

CDH1 - Cadherin-1/E-cadherin

CDKN1A/p21 - cyclin dependent kinase inhibitor 1A

CELF1 - CUGBP, Elav-like family member 1

CLCN1 - chloride voltage-gated channel 1

CNBP - cellular nucleic acid-binding protein

CRISPR - clustered regularly interspaced short palindromic repeats

Ct - cycle threshold

Ctrl - control

CUG^{exp} - CUG expansion

CUT&RUN - cleavage under target and release using nuclease

DM - myotonic dystrophy

DM1 - myotonic dystrophy type 1

DM2 - myotonic dystrophy type 2

DMPK - dystrophia myotonica protein kinase

dsRNA - double-stranded RNA

dTdT - deoxythymidine dinucleotide

EPD - Eukaryotic Promoter Database

FXS/FXTAS - fragile X syndrome and fragile X tremor ataxia syndrome

GSK3β - glycogen synthase kinase-3β

GSP - gene-specific primer

HCC - hepatocellular carcinoma

HD - Huntington's disease

HDAC - histone-deacetylase inhibitors

HSA^{LR} - human α-skeletal muscle actin long-repeat

hU7-snRNAs - engineered human U7 small nuclear RNAs

INSR - insulin receptor

KLF4 - Kruppel-Like Factor 4

KO - knockout

KRAB-ZFP - KRAB-containing zinc finger protein

LNA - locked nucleic acid

lncRNA - long non-coding RNA

MAPT - microtubule-associated protein tau

MBNL - Muscleblind-like

miRNA, miR - microRNA

MTMR1 - myotubularin-related 1

NMDAR1 - NMDA receptor 1

NMIBC - non-muscle invasive bladder cancer

PAWR - pro-apoptotic WT1 regulator

PKC - protein kinase C

rAAV - recombinant adeno-associated virus

RACE - rapid amplification of cDNA ends

RBP - RNA-binding protein

RHA - RNA helicase A

RISC - RNA-induced silencing complex

RITA - RNA-induced transcriptional activation complex

RNAa - RNA activation

RNAi - RNA interference

RNAPII - RNA polymerase II

S - sense

saRNA - small activating RNA

SBMA - spinal and bulbar muscular atrophy

SCA - spinocerebellar ataxia

SCN5A - cardiac sodium channel

SEM - standard error of mean

SETDB1 - SET domain bifurcated histone lysine methyltransferase 1

siRNA - small interfering RNA

SNP - single nucleotide polymorphism

TALEN - transcription-activator-like effector nuclease

TNNT2 - cardiac troponin T2

TSS – transcription start site

UCSC - University of California, Santa Cruz

UTR - untranslated region

WT - wild type

ZFN - zinc finger nuclease

ZnF - zinc finger

I. INTRODUCTION

1. Myotonic dystrophy type I

Repeat expansion diseases are a group of pathological conditions caused by abnormally expanded repetitive DNA sequences, usually 3 to 6 nucleotides long, throughout certain genes. These excessive repeats may reside in promoters, 5' or 3' untranslated regions (UTRs), coding exons or in introns, subsequently disrupting the production or processing of RNA and proteins (1,2) (Figure 1). The vast majority of repeat expansion diseases primarily lead to neurodegenerative and neuromuscular diseases, including myotonic dystrophy (DM), C9ORF72 frontotemporal dementia and/or amyotrophic lateral sclerosis (C9ORF72-FTD/ALS), fragile X syndrome and fragile X tremor ataxia syndrome (FXS/FXTAS), Huntington's disease (HD), spinal and bulbar muscular atrophy (SBMA) and different types of spinocerebellar ataxia (SCA) like spinocerebellar ataxia type 3 (SCA3) (2–4).

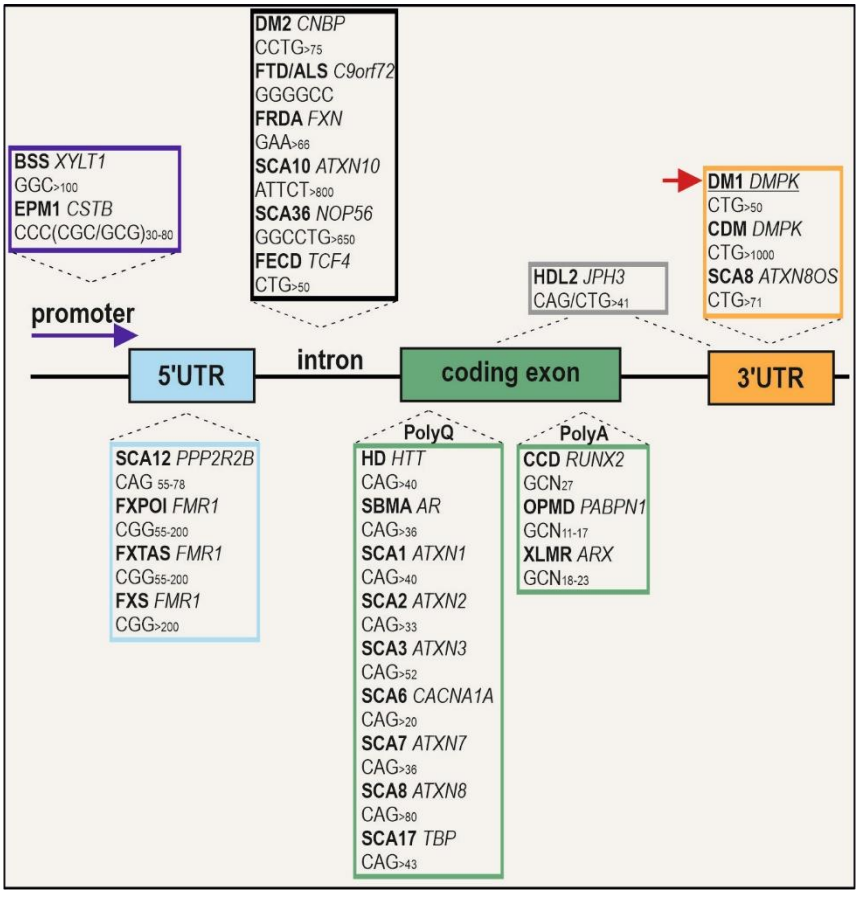

Figure 1. Selected examples of the repeat expansion diseases caused by expansions in the promoter (purple), 5' untranslated region (5'UTR) (blue), intron (black), coding exon (green) or 3' untranslated region (3'UTR) (orange). The figure shows genes with indicated nucleotide expansion and number of expansions. BSS - Baratela-Scott Syndrome; EPM1 - Progressive Myoclonus Epilepsy; SCA - Spinocerebellar Ataxia; FXPOI - Fragile X-Associated Primary Ovarian Insufficiency; FXTAS - Fragile X-Associated Tremor/Ataxia Syndrome; FXS - Fragile X Syndrome; DM2 – Myotonic Dystrophy Type 2; FTD/ALS - Frontotemporal

Dementia and/or Amyotrophic Lateral Sclerosis; FRDA - Friedrich's Ataxia; FECD - Fuchs Endothelial Corneal Dystrophy; HD - Huntington Disease; SBMA - Spinal and Bulbar Muscular Atrophy; CCD - Cleidocranial Dysplasia; OPMD - Oculopharyngeal Muscular Dystrophy; XLMR - X-linked Mental Retardation; HDL2 - Huntington Disease-Like 2; DM1 – Myotonic Dystrophy Type 1; CDM - Congenital Myotonic Dystrophy. Red arrow indicates DM1. Based on (1,2).

Myotonic dystrophy is a genetic disorder that affects multiple tissues and systems, including skeletal and heart muscles, brain, gastrointestinal tract, eyes, reproductive and endocrine system. There are two types of myotonic dystrophy: type I (DM1) and type II (DM2). Both share a common set of features, in particular muscle weakness, prolonged muscle contractions (myotonia), cataracts, and cardiac conduction abnormalities, but are caused by expansions in different genes and differ in clinical presentation and severity (5). DM1 is more common and typically more severe form of the disease. It is caused by an expansion of the CTG trinucleotide repeat within the 3'UTR of the dystrophia myotonica protein kinase gene (*DMPK*), located on chromosome 19 (6,7). In unaffected individuals, the length of the expansion is usually fewer than 37 repeats. In DM1, the number of repeats is directly linked to the severity of the disease and the age of onset, ranging from 50 to several thousand repeats (8). As a result, multiple tissues - especially skeletal and cardiac muscle - fail to function properly. Importantly, DM1 is highly variable in its clinical presentation. It can appear in infancy (congenital DM1), childhood or adulthood (5). Congenital DM1 is the most severe form and includes symptoms like hypotonia, respiratory difficulties at birth, and developmental delays. In adults, common symptoms include progressive muscle weakness and wasting (especially in the cranial, trunk, and distal limbs), myotonia, excessive daytime sleepiness, and endocrine problems such as insulin resistance and infertility. Cardiac issues, particularly arrhythmias, are a major cause of morbidity and mortality in DM1 (5,9). What is more, the CTG repeat length tends to increase throughout next generations during meiosis of mutated *DMPK* alleles, a phenomenon known as genetic anticipation. This is significant as children that inherit DM1 may have increasingly severe symptoms that appear at younger age due to larger CTG expansion. Interestingly, in DM1 patients CTG repeat length is highly variable among different cells due to somatic expansion (5,10).

DM2 is caused by a CCTG tetranucleotide repeats expansion in intron 1 of the cellular nucleic acid-binding protein gene (*CNBP*) on chromosome 3 (11). Unlike DM1, the size of the repeat expansion in DM2 may reach more than 10 000 and does not correlate strongly with disease severity, and anticipation is less pronounced compared to DM1 (12). Clinically, DM2 tends to have a later onset and milder course compared to DM1. Moreover,

unlike DM1, in DM2 muscle weakness commonly involves proximal muscles, and severe congenital forms have not been reported. Myotonia and multisystem involvement still occur but are less disabling (5,13).

2. MBNL family of proteins

Muscleblind-like proteins are a deeply conserved family of RNA-binding proteins that in humans are encoded by the following genes: *MBNL1*, *MBNL2* and *MBNL3* located on chromosomes 3q25, 13q32.2 and Xq26.2, respectively (14,15). They play significant roles in cellular RNA metabolism, with key molecular functions involving regulation of the alternative splicing (16), alternative polyadenylation (17), RNA stability (18) and localization (16) as well as microRNA biogenesis (19). MBNL proteins are highly conserved in both structure and function across multicellular organisms. Human MBNLs orthologs were described in e.g. *Drosophila melanogaster* (20), *Caenorhabditis elegans* (21), zebrafish (22) and mouse (23). Muscleblind proteins bind their RNA targets via N-terminal Cys(3)-His type (CCCH) zinc fingers (ZnF) arranged in one (invertebrates) or two (vertebrates) tandem zinc finger motifs which show high affinity towards consensus motif YGCY (where Y is a pyrimidine: C or U) (15,20,24). The sequence- and position-specific binding to pre-mRNA allows MBNLs to modulate AS events by controlling inclusion or exclusion of the targeted alternative exon. In general, MBNL binding within the alternative exon or upstream intronic sequences promotes exon exclusion. Conversely, binding to downstream intronic regions facilitates alternative exon inclusion (16,25). As a rule, MBNL family members promote splice isoforms characteristic of differentiated tissues while repressing alternative exons specific of embryonic stem cells (ESC) and fetal tissues (26–28). Likewise, expression of MBNL proteins is lower in undifferentiated cells then rises during their differentiation (26,28). Importantly, significant differences characterize the expression pattern of the three mammalian MBNL paralogs (14). Among the MBNL proteins, MBNL1 is the predominant and the most widely expressed family member, showing highest expression in muscle tissues e.g., skeletal (29) and cardiac muscle (26). MBNL2, in contrast, abounds within the central nervous system (mainly in hippocampus) (30). MBNL3 expression is primarily restricted to placenta (31), although recent studies implicate its transient role in adult skeletal muscle regeneration (32).

The compensatory mechanism between MBNL1 and MBNL2 is an important aspect of how cellular systems maintain essential functions in the face of genetic or environmental disruptions. Both MBNL1 and MBNL2 are co-expressed in a variety of tissues, target many

of the same pre-mRNAs and have overlapping binding preferences. Both can also compensate for each other's loss to a certain extent, ensuring that critical splicing patterns are preserved (16,33,34). For instance, in *Mbnl1* knockout (KO) mice, many splicing defects are observed, but these are often less severe than those seen in double knockouts (*Mbnl1/Mbnl2* KO), suggesting that *Mbnl2* can partially mitigate the loss of *Mbnl1* (33,35). Studies have shown that in the absence of MBNL1, MBNL2 expression can be upregulated at both the mRNA and protein levels, particularly in tissues where MBNL2 is normally expressed at lower levels (36,37). This upregulation appears to be a compensatory response aimed at maintaining proper splicing regulation. The most striking evidence of the compensatory relationship comes from studies involving double *Mbnl1* and *Mbnl2* knockout mice. These animals exhibit much more severe phenotypes compared to single knockouts, including widespread splicing abnormalities, developmental delays, and early postnatal lethality (33,38). This indicates that while each protein can buffer against the loss of the other to some degree, the simultaneous absence of both disrupts critical biological pathways beyond the threshold of compensation. Importantly, the compensation is partial and context-dependent, influenced by tissue type, developmental stage, and the expression patterns of the two MBNL proteins (36,37) as described further in details in Chapter III.

Despite the structural similarities among MBNL family members, alternative splicing of primary transcripts from the human *MBNL* genes gives rise to at least nine (MBNL1), three (MBNL2) and six (MBNL3) protein isoforms (14,15). Importantly, some exons are constitutive: e2, e4 and e10; while other are alternatively spliced (e1, e3, e5- 9) (28,36). MBNL proteins regulate the splicing of several alternative exons (e1, e3, e5, e7 and e8) within their own pre-mRNA through autoregulatory feedback mechanisms that ensures a tightly regulated homeostatic control of different isoforms expression in cells (28,36). For example, *MBNL1* exon 1 (the first coding exon, e1) autoregulation loop is controlled by all three MBNLs that bind to conserved motifs within UTR region of e1, promoting the exclusion of this exon. When MBNL1 protein level is high, MBNL1 binds to its pre-mRNA and tends to suppress the inclusion of exon 1, thereby reducing the production of full-length functional MBNL1 protein. E1-depleted *MBNL1* mRNAs are translated inefficiently and give rise to unstable and less active MBNL1 protein isoforms with decreased functionality due to loss of first two of four zinc fingers (ZnF1-2) that are essential for RNA target recognition and splicing. Importantly, ZnF1 is encoded by e1, while ZnF2 is encoded by both e1 and e2. Unstable MBNL1 isoforms are unable to further repress e1 inclusion, leading

to translation of a fully functional protein from e1-containing mRNAs. This e1-based autoregulatory feedback loop ensures appropriate MBNL1 protein level according to cellular demands. Importantly, *MBNL1* gene expression is driven by three promoters (P1, 2 and 3) associated with three transcription start sites (T1, 2 and 3). Each of the three transcription start sites is associated with a distinct exon constituting a part of 5'UTR (e5'UTR1, e5'UTR2 and e5'UTR3, respectively), which can be differentially spliced to e1. Only P2/T2-derived transcripts undergo MBNL-dependent regulation of e1 alternative splicing, while P1/T1- and P3/T3-derived mRNAs exhibit always skipped or included, respectively, exon 1 (36,39).

3. Pathomechanism of DM1

The molecular pathomechanism of myotonic dystrophy type I is associated with RNA toxicity. Briefly, CTG triplet repeat expansion within the 3′UTR of *DMPK* leads to production of mutant mRNA transcripts containing pathogenic CUG expansion (CUG^{exp}) which form thermodynamically stable hairpin-like structures accumulating in the nucleus (40,41). These toxic RNAs have high affinity to multiple RNA-binding proteins (RBPs), particularly members of the muscleblind-like (MBNL) family, leading to their sequestration in ribonuclear foci. This sequestration causes functional depletion of MBNL proteins from the nucleoplasm, leading to disruption of the alternative splicing (AltS) of their target pre-mRNAs (8,14,42,43) (Figure 2). In parallel to MBNLs sequestration, another splicing regulator, CUGBP, Elav-like family member 1 (CELF1), is abnormally upregulated in DM1 due to increased activity of the protein kinase C (PKC) signaling pathway that enhances CELF1 hyperphosphorylation and thus promotes its stability (44–46). Importantly, CELF1 may antagonize MBNL functions, e.g. while MBNL nuclear levels increase during development, CELF1 nuclear levels decrease. Further, MBNL1 and CELF1 antagonistically regulate alternative splicing of a large cohort of exons that reside in genes linked to development and cell differentiation regulation, that supports the model in which the level and localization of MBNL and CELF1 control a fetal to adult splicing transition, which is reversed in DM1 tissues (26). Importantly, MBNLs co-localize with toxic RNA foci (47), while CELF1 does not, as it binds to CUG^{exp} with lower affinity (48). As a result of MBNLs sequestration, many pre-mRNAs are mis-spliced in ways that are inappropriate for the cell's developmental stage or tissue type, e.g. adult cells start producing splice variants specific for fetal development, leading to production of fetal isoforms of proteins and exacerbating the disease phenotype (49,50). One of the most recognizable symptoms, myotonia (prolonged muscle contraction), is linked to mis-splicing of the chloride voltage-gated channel 1

(*CLCN1*), that controls muscle fibers relaxation after contraction. When *CLCN1* splicing is disrupted, a nonfunctional version of the channel is produced, reducing chloride conductance and making muscle fibers hyperexcitable. This leads to the characteristic delayed relaxation after gripping or other movements (51–53). Muscle weakness and wasting result from the mis-splicing of several muscle-related genes, including bridging integrator-1 (*BIN1*) (54) and myotubularin-related 1 (*MTMR1*) (55). These changes impair cellular structures like T-tubules and disrupt muscle metabolism, gradually weakening the muscle tissue over time (53–55). Cardiac conduction abnormalities stem from mis-splicing of genes such as cardiac troponin T2 (*TNNT2*) (44,56) and cardiac sodium channel (*SCN5A*) (57). These abnormalities alter the heart's conduction system signaling and can lead to arrhythmias or conduction blocks, increasing the risk of sudden cardiac events (9,56,57). Insulin resistance, which can progress to type 2 diabetes, is caused by mis-splicing of the insulin receptor (*INSR*) (53,58). This leads to an overproduction of the fetal form of the insulin receptor (*INSR-A*), which is less efficient at responding to insulin compared to the adult form (*INSR-B*). As a result, tissues fail to take up glucose effectively, even when insulin levels are normal (58). Cognitive symptoms and central nervous system involvement in DM1 are also driven by mis-splicing of MBNL-regulated neuronal genes, including NMDA receptor 1 (*NMDAR1*) (30,59), amyloid beta precursor protein (*APP*) (59), and microtubule-associated protein tau (*MAPT*) (60). These disruptions can impair synaptic function, learning, and progressive memory problems, and contribute to common symptoms like hypersomnia or behavioral changes (30,61). Recently, mis-splicing of autism spectrum disorder-risk (ASD) genes in DM1 during brain development was also demonstrated, supporting the model of myotonic dystrophy-associated autism (62).

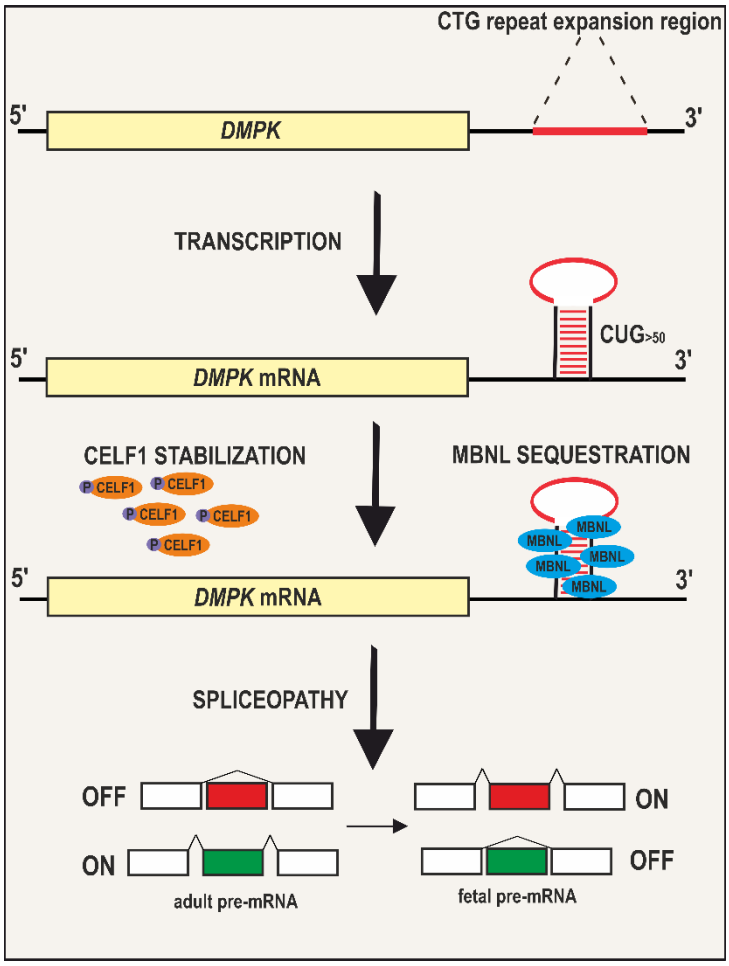

Figure 2. Schematic representation of DM1 patomechanism. DM1 is caused by a trinucleotide CTG repeat expansion in the 3'UTR (untranslated region) of *DMPK* gene (yellow boxes indicate *DMPK* coding sequence; black lines indicate 5' and 3'UTRs). Toxic *DMPK* mRNA transcripts containing $CUG_{>50}$ expansions are retained in the nucleus and sequester MBNL, forming nuclear foci. Phosphorylation/stabilization of CELF1 is caused by increased activity of the protein kinase C (PKC). Consequently, the MBNL loss-of-function and CELF1 gain-of-function, result in shift in aberrant alternative splicing pattern (spliceopathy) of their target pre-mRNAs from splice isoforms characteristic for adult towards those typical for fetal tissues . OFF indicates target alternative exons repressed by MBNL in healthy tissues; ON indicates target alternative exons promoted by MBNL in healthy tissues; P - phosphorylation.

3.1 MBNLs role in myotonic dystrophy

Apart from their role in development and differentiation, MBNL proteins play crucial roles in maintaining cellular homeostasis in an adult organism, as best illustrated in DM (8,14,16). In this RNA-dominant disease driven by the expansion of a C/CTG tri- or tetra-nucleotide repeat motif, dysregulation of the MBNL protein pool constitutes the central point of the pathological mechanism (8,14,42). Sequestration of MBNLs, particularly MBNL1 and MBNL2, on nuclear foci formed by expanded C/CUG RNAs triggers their functional depletion and imbalance, which shifts the alternative splicing pattern of hundreds of target RNAs from adult to fetal splice isoform (DM spliceopathy) (14,16,30). Importantly, it has been implied that altered microRNA (miRNA, miR) expression in DM1 patients is MBNL-

dependent, e.g. MBNL loss lead to downregulation of miR-1 in cardiac tissue (63) and skeletal muscle (64), and upregulation of miR-23b, miR-27b and miR-24-1 in skeletal muscle (64). This dysregulations may play a role in the development of cardiac and skeletal pathologies observed in patients with DM1.

Experimental studies support the central role of MBNL in disease pathogenesis. In animal models, genetic deletion of *Mbnl1* results in phenotypes similar to those observed in DM1 patients, including myotonia, muscle weakness and splicing abnormalities (33). Combined deficiency of *Mbnl* genes further exacerbate the phenotype, indicating partial redundancy among family members but also reinforcing their collective importance (35,65). What is more, microscopic analyses confirmed that MBNL proteins co-localize with CUG^{exp} RNA foci in the nuclei of DM1 patient cells (47,66). Additionally, cells from DM1 patients showed a nuclear depletion of freely diffusible MBNL1 protein, consistent with sequestration (67). Interestingly, MBNLs functions are disturbed in several other pathological conditions including distinct types of repeat expansion diseases, including Huntington's disease (68), SCA 3 (69) and ALS (70).

3. Therapeutic approaches in DM1

At present, no cure is available for DM1 and patients' therapy is limited to alleviating disease symptoms and providing supportive care. However, over the past two decades, various therapeutic strategies have emerged (71,72) that act on (i) *DMPK* gene expression (73,74); (ii) CUG^{exp} RNA (75–78) (iii) MBNL:CUG^{exp} interactions (79,80); (iv) MBNL1/2 expression regulation (81–85); (v) CELF1 expression and signaling pathways downstream of CUG^{exp} (86–88) (FIGURE 3).

Molecular therapies aimed at reducing or removing the expanded CTG repeat region within the *DMPK* gene target the main cause of DM1, hence could serve as the most effective strategy. However, such therapies will require changes at the molecular level in every diseased cell or modification of stem cells in DM1 patients, which is currently technically challenging. These approaches focus on induction of repeat contractions and transcription inhibition of the *DMPK* gene. Repeat contraction refers to the reduction of the number of CTG repeats within the expanded region of the *DMPK* gene via DNA damaging agents (e.g. UV light, X-rays, anticancer drug cisplatin (89), and cytosine arabinoside, ethidium bromide or 5-azacytidine (73)). Since the disease severity in DM1 correlates with repeat length, shrinking the repeat expansion could reverse or attenuate disease symptoms, however, tested

drugs are not therapeutically effective and have significant off-target effects (73,74,89). Another strategy for reducing the toxic RNA is to suppress transcription of the mutant *DMPK* allele using small molecules (e.g. pentamidine and colchicine), thereby decreasing or eliminating the production of CUG^{exp} RNA (74,90)). What is more, gene editing techniques offer intriguing strategies acting on *DMPK* gene via nucleases such as zinc-finger nucleases (ZFNs) (91), transcription-activator-like effector nucleases (TALENs) (92) or CRISPR (clustered regularly interspaced short palindromic repeats)/Cas9 (CRISPR-associated protein 9) (93,94), which can modify gene sequence by inducing CTG-repeat contractions or deletions (91,93,94), or by inserting premature polyadenylation signals (92).

Targeting the CUG^{exp} RNA in DM1 is a widely studied approach in disease-modifying therapy, as toxic RNA foci are the primary driving force of DM1 pathogenesis. Therapeutic approaches targeting CUG^{exp} RNA using nucleic-acid-based molecules aim to induce degradation of mutated *DMPK* mRNA (75,76,95) or block MBNL1 interaction (77,78,96,97) by binding to CUG^{exp} repeats, thereby restoring normal RNA processing. Additional strategy consists of therapeutics targeting a non-CUG sequence, downstream or upstream of the repeat region, to degrade *DMPK* mRNA (98,99). The major classes of RNA-targeting molecules include antisense oligonucleotides (ASOs) (75,77,97), small interfering RNAs (siRNAs) (76,100) or engineered human U7 small nuclear RNAs (hU7-snRNAs) (95). ASOs that bind to the CUG^{exp} repeated region in mutant *DMPK* transcripts, prevent the sequestration of MBNL proteins and promote their release from RNA foci (77,78,96,97), or induce mutant *DMPK* transcript degradation via RNase-H-dependent pathway (75). The first ASO identified and evaluated in a clinical trial for the treatment of DM1, IONIS-DMPKRx, developed by Ionis Pharmaceuticals, uses a gapmer design to target *DMPK* 3'UTR and degrade *DMPK* mRNA via RNase H-mediated cleavage (clinicaltrials.gov identifier NCT02312011). Despite promising preclinical results, it was discontinued in clinical trials due to limited muscle tissue uptake (101,102). RNA interference (RNAi) technologies have been tested for their ability to selectively target CUG^{exp} (76) or 3'UTR of *DMPK* mRNA to induce its degradation(72). RNAi mediated by intramuscular injection of siRNAs targeting CUG^{exp} RNA has achieved robust knockdown of toxic *DMPK* transcript in human α-skeletal muscle actin long-repeat (HSA^{LR}) mouse model of DM1 (76). Another approach showed that, delivered via rAAV vectors, miRNA-based RNAi hairpins targeting *HSA* mRNA with CUG^{exp} in the HSA^{LR} mouse model led to reduction of CUG^{exp} *HSA* transcript and improvement in the DM1 spliceopathy (100). Additionally, engineered hU7-

snRNAs containing a poly-CAG antisense sequence were used to induce the degradation of the CUG^{exp} repeats of mutant *DMPK* transcripts in DM1 patient-derived cells (95).

Disrupting of the MBNL:CUG interaction aims to release MBNL proteins from toxic RNA foci. As mentioned, MBNL:CUG interaction is central to DM1 pathogenesis as it leads to functional depletion of MBNL proteins, which in turn disrupts the RNA processing in cells (79,103). Therefore, inhibiting this toxic RNA-protein complex offers to restore the proper MBNL function, without necessarily eliminating the toxic RNA itself or modifying the genome. Several high-throughput screens have identified small molecules that bind CUG^{exp} RNA and prevent the formation of hairpin structures that sequester MBNL1 (103,104). One such compound is pentamidine, an FDA-approved antimicrobial agent that can bind to the CUG^{exp} repeats, reducing nuclear foci formation and restoring proper alternative splicing in DM1 cells and mouse models (105). Another tested small molecule, erythromycin, reduced nuclear foci and restored proper AltS of several MBNL-regulated exons, such as *INSR* and *CLCN1* (80).

DM1 pathogenesis is characterized not only by MBNL1 loss-of-function but also by gain-of-function of CELF1, which exacerbates splicing dysregulation (45). Therefore, targeting CELF1 expression via its phosphorylation pathways, particularly through inhibition of PKC (86) or glycogen synthase kinase-3β (GSK3β) (87), can restore splicing patterns and improve muscle function in DM1 models. These pharmacologic interventions are still in preclinical stages but suggest an interesting strategy to targeting toxic RNA.

Finally, modulation of MBNL expression may be a straightforward approach in DM1 therapy as the loss of functional MBNL activity is a major molecular pathomechanism leading to a plethora of defects in DM1. Exogenous overexpression of MBNL was firstly described for the DM1 mouse model, HSA^{LR} (83). This study proved that rAAV-mediated *Mbnl1* overexpression rescued disease-associated alternative splicing defects and muscle hyperexcitability (83). Subsequently, transgenic MBNL1-overexpression in mice confirmed that MBNL1 exogenous upregulation shifts AltS of MBNL1-regulated genes, and prevents myotonia and myopathy in DM1 mice (106). However, exogenous overexpression-based therapy approaches may lead to uncontrolled MBNL expression, hence induce toxicity in multiple tissues (107). What is more, exogenous MBNL delivery lead to production of only one MBNL1 isoform, which may disturb the balance of other - alternatively spliced - MBNL isoforms. To overcome limitations related to exogenous overexpression, endogenous

expression of MBNL1 was tuned by antisense reagents that block the miRNAs negatively regulating *MBNL* expression, e.g. by miRNA sponge constructs (108) or antagomiRs (84). Recently, another strategy was proposed to inhibit the microRNA binding within 3'UTR of *MBNL1* mRNA via peptide-linked blockmiR (109). Furthermore, to increase the functional pool of MBNL, endogenous enhancement of MBNLs has been achieved by different mechanisms of action, e.g. using nonsteroidal anti-inflammatory drugs phenylbutazone (PBZ), that suppresses DNA methylation, and ketoprofen (81), MBNL1 autophagy blocker chloroquine (82), and histone-deacetylase inhibitors (HDAC) such as ISOX and vorinostat (110). Modulation of *MBNL* expression is a powerful tool with direct mechanistic relevance to DM1. It offers the potential to bypass the need to eliminate toxic RNA and correct alternative splicing defects globally. rAAV vectors remains the most advanced delivery method in preclinical development for exogenous MBNL overexpression, while endogenous activation holds promise as a safer and potentially more durable strategy (72,111). However, drug delivery is one of the major challenges in developing therapies for DM1, as it is a multisystemic disease affecting muscle, heart, CNS, and other systems. Effective therapy often requires delivery of ASOs, siRNAs, or gene-editing tools broadly and specifically, whereas their cellular uptake is inefficient and may activate immune responses (71). DM1 requires long-term therapy, thus delivery platforms must be safe and sustainable for repeated administration (for oligonucleotides) or provide durable MBNLs expression without adverse effects (for viral vectors or gene editing).

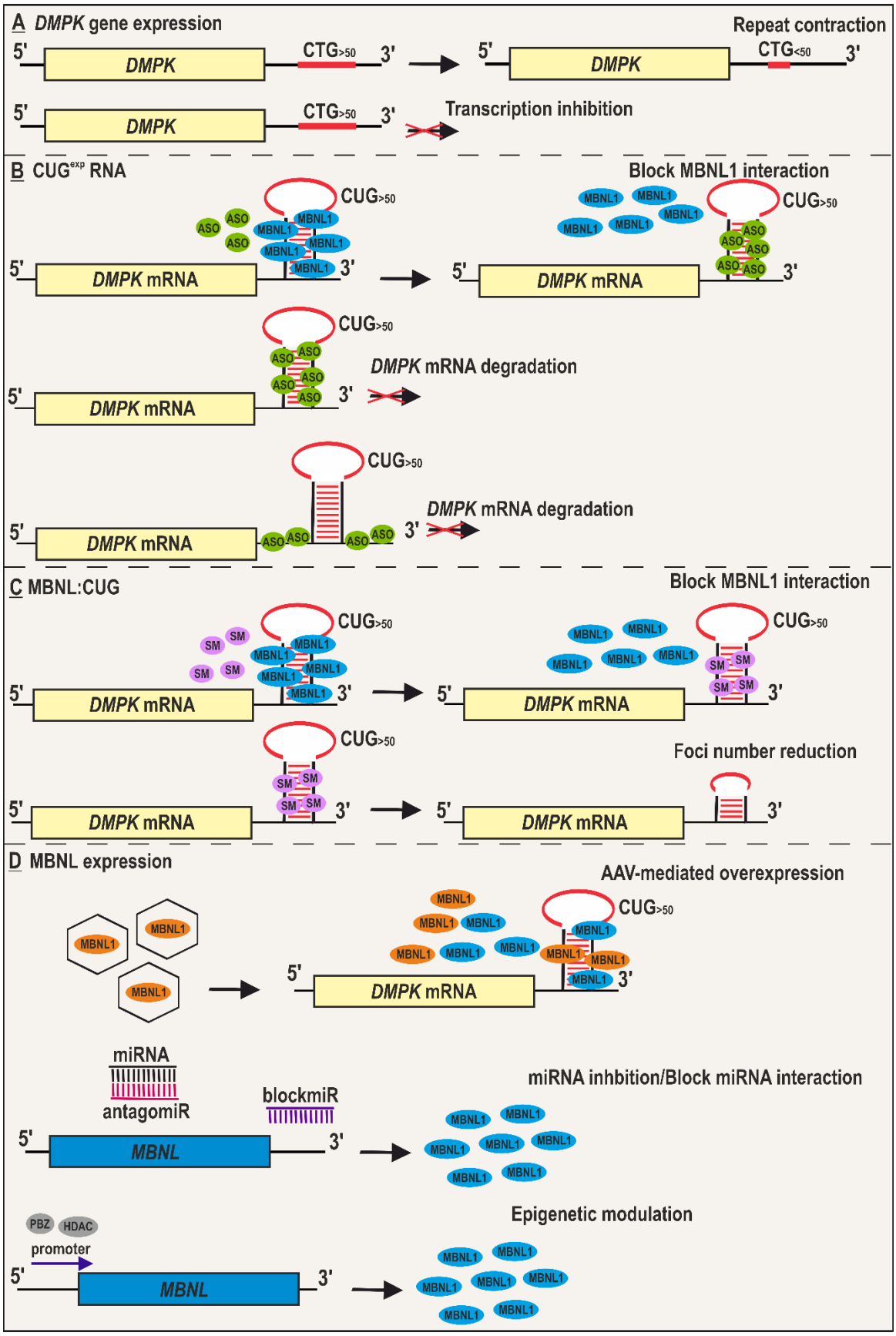

Figure 3. Selected examples of molecular therapies of DM1 at different pathogenetic levels. (A) At *DMPK* expression via repeat contraction induction or CTG-repeat transcription inhibition. **(B)** Targeting CUG^{exp} toxic

repeats via ASO (green) that block MBNL interaction with toxic RNA or degrade *DMPK* mRNA. **(C)**Disrupting MBNL:CUG interaction via small molecules (purple) that release MBNL from CUG^{exp} repeats and reduce foci number. **(D)** Modulating MBNL expression via exogenous rAAV-mediated MBNL (orange) delivery or endogenous tuning via antagomiRs (pink) that directly inhibit MBNL translational repressor (miRNA) (black) or by blockmiR (purple) that block miRNA target binding sites within the 3'UTR of MBNLs, or by epigenetic modulators affecting *MBNL* promoter region. rAAV - recombinant adeno-associated virus; ASO - antisense oligonucleotide; CUG^{exp} - CUG expansions; HDAC - histone-deacetylase inhibitor; miRNA - micro RNA; PBZ - phenylbutazone; SM - small molecule.

4. RNA activation

The groundbreaking finding described in early-2000s by two independent research groups, revealed an unexpected counterpart to RNAi: the RNA activation (RNAa) mechanism (112,113). In contrast to RNAi, RNAa involves the upregulation of gene expression through small double-stranded RNAs called small activating RNAs (saRNAs) (112,113). RNAa represents a powerful epigenetic and transcriptional gene regulation mechanism, where saRNAs specifically target promoter regions of genes to enhance transcription. This discovery not only expanded the functional landscape of non-coding RNAs but also opened up new possibilities for targeted gene modulation in basic research and therapeutic development (114,115).

4.1 Mechanism of RNA activation

RNAa mechanism consists of a series of molecular events involving saRNAs, Argonaute (AGO) proteins, chromatin remodeling, and specific transcription factors recruitment. Unlike cytoplasmic RNAi, RNAa occurs in the nucleus, however, detailed mechanism of how the saRNA enters the nucleus (free or AGO2 protein-loaded) and which proteins are responsible for their nuclear import remain largely unknown (116). saRNAs are typically 19 nucleotides in length with 3′ terminal dTdT overhangs, forming short double-stranded RNA duplexes (dsRNA). Unlike siRNAs, saRNAs are not designed to be complementary to mRNA but to sequences in the gene promoter region, located typically within 200-1000 bp upstream of the indicated transcription start site (TSS) (117). The specificity of saRNA targeting depends on the sequence complementarity between the saRNA and the promoter, and the location of the target site, ideally positioned within regulatory elements like transcription factor binding sites or enhancer regions (114–117). Interestingly, RNAa distinguishes from RNAi in effective concentration (picomolar and even femtomolar range) and kinetics, as saRNA require higher dose (typically 5-75 nM) and is characterized by delayed kinetics by 24-48 hours (with peak on day 4-5) compared to siRNA (118).

After entering the cell, saRNA duplex is incorporated into the RNA-induced transcriptional activation complex (RITA), primarily involving Argonaute 2 (AGO2). While AGO2 is well known for its role in RNAi (mediating mRNA cleavage), its function differently in RNAa (116,119,120). Here, AGO2 interacts with saRNA to cleave and discharge one of the two strands of the saRNA duplex – the passenger strand (the sense

strand, S), and facilitates complexing with the leading antisense strand (AS) – the guide strand. Mechanistically, AGO2 interaction with the guide strand in RNAa depends on the 5' terminal thermodynamic characteristics of the saRNA strand, i.e. guide strand has lower thermodynamic stability at its 5'-end than passenger strand (119). Therefore, the AGO2-loaded guide strand may vary between the sense or antisense strand in various saRNAs (119,121). Afterwards, AGO2 mediates nuclear import of the guide strand of the saRNA duplex, creating saRNA-AGO2 complex, where saRNA guides it to the genomic region of the target gene promoter, and facilitating the assembly of a RITA complex, that includes RNA helicase A (RHA) and RNA polymerase-associated protein CTR9 homolog (part of the PAF1 complex) among many other protein components. However, the precise mechanism of how the saRNA-AGO2 complex enters the nucleus remains to be fully elucidated (115,116). Next, formation of RITA complex induces transcriptional and epigenetic modifications that eventually lead to gene activation. In particular, RITA complex interacts with RNA polymerase II (RNAPII) to initiate transcription and to ensure productive elongation of the mRNA (116,120). Additionally, upon localization to the promoter, the saRNA-AGO2 complex does not cleave DNA or RNA but instead induces epigenetic modifications, such as reduction of acetylation at histones H3K9 and H3K14, increased di/trimethylation at histone H3K4, reduced dimethylation of H3K9, and monoubiquitination of H2B leading to an open chromatin structure that promotes transcription (113,116). This targeted promoter interaction enables precise and gene-specific activation, making saRNAs a powerful tool for modulating key regulatory genes in therapeutic contexts (Figure 4).

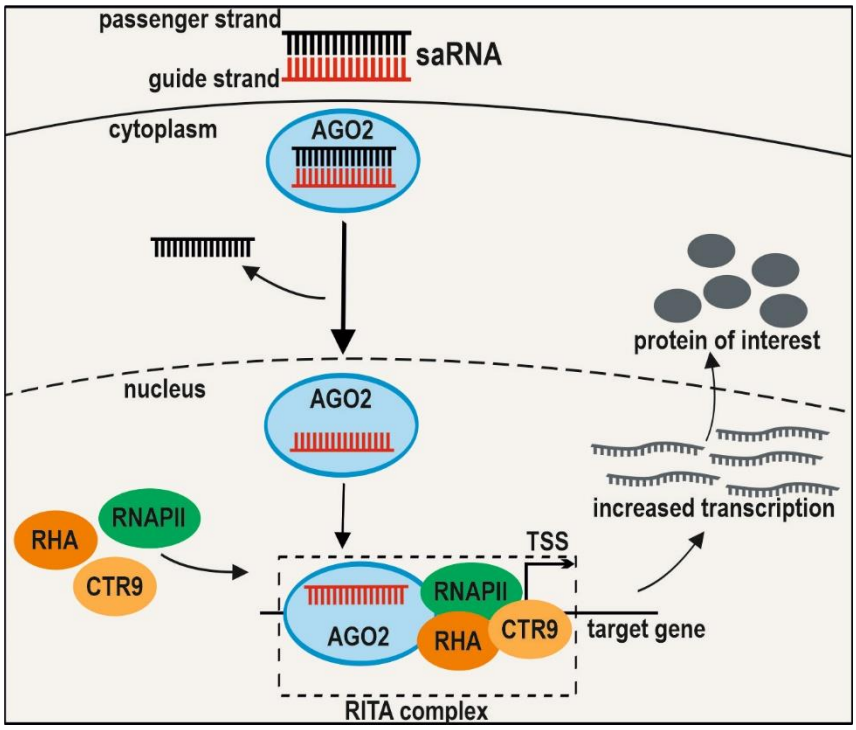

Figure 4. Schematic model of RNA activation mechanism. saRNA duplex enters the cell and interacts with AGO2 protein in the cytoplasm. Next, passenger strand is displaced from saRNA duplex, while guide strand-AGO2 complex enters the nucleus and docks to the targeted promoter sequence to recruit RNAa pathway components, e.g. RHA and CTR9, and promoter-specific factors, forming the RITA complex. RITA activates the transcription of the target gene by recruiting RNAPII thus leading to an increase in transcription and consequently, protein level. AGO2 - Argonaute 2; RHA - RNA helicase A; RNAPII - RNA polymerase II ; TSS-transcription start site.

There are four primary models for how saRNAs locate and interact with their target sequences: (1) direct DNA binding model (RNA:DNA hybrid); (2) long non-coding RNA (lncRNA) binding model (RNA:RNA); (3) nascent promoter-associated transcripts binding model (RNA:RNA); (4) triplex structure model (RNA:duplex DNA) (118). In RNA:DNA model, saRNAs guide the AGO2 complex to the promoter region of the target gene via base-pairing of the antisense or the sense strand of saRNA duplex onto complementary sequence within the genomic DNA (118,119). RNA:RNA models proposes that saRNAs bind to lncRNAs overlapping promoter region or to nascent short transcripts associated with promoter (in sense or antisense orientation) (118,121). In the RNA:duplex DNA model purine or pyrimidine-rich miRNAs directly bind to purine-rich duplex DNA via Hoogsteen or reverse Hoogsteen base-pairing, hence forming heterotriplex structure. This miRNA:DNA triplexes may contribute to RNAa by facilitating the recruitment of the triplex-specific binding proteins that alter the topography of promoter regions to enhance binding of transcription factors (118,122).

The mode of action for saRNA is dependent on their seed region, that is critically important for their ability to specifically recognize and bind to target sequences within gene promoters, which is essential for effective gene activation (112,114,115). The seed region refers to sequence of the first 6 to 7 nucleotides in positions 2 to 8 from the 5' end of the saRNA antisense (guide) strand. This region plays a dominant role in guiding the saRNA-AGO2 complex to the complementary target sequences near the gene promoter (112,114). Importantly, the seed region mediates the initial binding between the saRNA and the target sequence, hence perfect or near-perfect complementarity in the seed region is essential for the saRNA to specifically bind the target sequence and localize the RITA complex within target gene. Moreover, the accuracy of seed region base-pairing directly influences how effectively the antisense strand of the saRNA is incorporated into AGO2, which is crucial for guiding the complex to the target promoter and for recruiting epigenetic activators of chromatin remodeling to enhance transcription (114) Mismatches within the seed region can weaken binding affinity and reduce the ability of saRNA to localize at the promoter and activate transcription. Interestingly, some mismatches in the seed region may still lead to partial gene activation, but the efficiency usually drops significantly. This ensures high specificity of saRNA-mediated gene upregulation, however even a single nucleotide difference in the target sequence can impair RNAa mechanism (114,115).

Chemical modifications, such as 2'-O-methyl (2'-OMe), 2'-fluoro (2'-F), or locked nucleic acids (LNAs), play crucial roles in enhancing the stability and effectiveness of saRNAs (123–126). Unmodified saRNA molecules are highly susceptible to degradation by nucleases, which are abundant in the bloodstream and inside cells, while these modifications help protecting saRNAs and improve their bioavailability and therapeutic potential *in vivo* (124,126,127).

4.2 Therapeutic potential of RNA activation

RNAa has been demonstrated in various human and animal cell types, showing that it is a conserved and reproducible biological phenomenon (128). In the past two decades, a steadily increasing number of preclinical and clinical studies have been performed, using various saRNA-based experimental therapies for the treatment of a multitude of different diseases. Some well-characterized saRNAs include: (i) dsP21-322 targeting cyclin dependent kinase inhibitor 1A (*CDKN1A*; *p21*) (112,124); (ii) dsEcad-215 targeting E-cadherin (*CDH1)* (112,129); (iii) MTL-CEBPA targeting CCAAT/enhancer-binding protein

alpha (*C/EBPα*) (115); (iv) dsPAWR-435 targeting pro-apoptotic WT1 regulator (*PAWR*) (130); (v) dsKLF4-496 targeting Kruppel-Like Factor 4 (*KLF4*) (131).

Clinical trials using RNA activation are currently underway, primarily focusing on cancer therapies. One of the most advanced and first RNAa-based therapy is MTL-CEBPA, developed by MiNA Therapeutics (clinicaltrials.gov identifier NCT02716012) (132). This saRNA targets the *C/EBPα* gene, a tumor suppressor silenced in hepatocellular carcinoma (HCC). It is delivered using SMARTICLES® liposomal nanoparticles. These lipid-based particles encapsulate the saRNA, protect it from degradation in the bloodstream and facilitate its entry into cells through endocytosis. Phase I clinical trials in patients with advanced HCC have demonstrated that MTL-CEBPA is safe and can induce indicated gene expression in tumor (132).

Another promising RNAa therapy is RAG-01, developed by Ractigen Therapeutics, which targets the *p21* gene. This saRNA therapy is being tested in patients with non-muscle invasive bladder cancer (NMIBC), particularly those unresponsive to Bacillus Calmette-Guérin (BCG) treatment. The FDA has approved a Phase I clinical trial (clinicaltrials.gov identifier NCT06351904), and early clinical data presented in 2025 showed RNAa-mediated therapeutic responses, including complete tumor regression in some patients (133). RAG-01 is administrated via intravesical instillation, using lipid-conjugated oligonucleotide (LiCO™) delivery technology, that effectively delivers the saRNA directly to the urothelial cells. Therefore, it ensures a high concentration of the saRNA in the bladder, minimizing systemic exposure and potential side effects (133). Recently, Ractigen Therapeutics developed a new program for Duchenne muscular dystrophy (DMD) using saRNA (RAG-18) to increase utrophin (UTRN) expression in muscle cells. RAG-18 is delivered to muscle tissue by Ractigen's LiCO™ technology. Currently, Ractigen Therapeutics showed in preclinical data that RAG-18 ameliorated muscle damage *in vivo* in newly created mice model that carries human *UTRN* promoter in mouse *Utrn* gene (134).

Aforementioned trials are the first to apply saRNA-mediated gene activation in humans, representing a significant step in the field of RNAa therapeutics. While still in early phases, the results suggest that RNAa can be a viable strategy for reactivating tumor suppressor genes and treating cancers with limited treatment options. Challenges such as targeted delivery, avoiding off-target effects, and achieving durable responses remain important areas of ongoing research.

II. AIMS OF THE STUDY

The main hypothesis of the proposed project is that site-specific modulation of endogenous *MBNL1* expression using RNA activation mechanism in myotonic dystrophy type 1 cell models with functional depletion of MBNL1, will enhance the abundance of *MBNL*1 mRNAs, thus boosting cellular MBNL1 protein pool able to rescue disease-associated alternative splicing defects of MBNL1 target pre-mRNAs. Therefore, analyzed approach will offer brand new perspectives in DM1 therapeutic options as well as in MBNL expression regulation.

The main aim of the project was to upregulate *MBNL1* transcription via RNA activation mechanism using small activating RNA duplexes directed at specific sequences within two distinct *MBNL1* promoters, P2 and P3 to develop new experimental therapeutic strategy in myotonic dystrophy type 1.

Therefore, specific goals of the presented study were to:

1. Extensively analyze the feasibility of RNAa to upregulate the major paralog of the MBNL family, *MBNL1*, in DM1 cell models using variety of molecular and biochemical approaches.
2. Compare potential of saRNA-mediated *MBNL1* upregulation via targeting sequences within two distinct *MBNL1* promoters.
3. Investigate molecular mechanism underlying MBNL1 RNAa :
    a. Confirm whether saRNA-mediated *MBNL1* upregulation occurs at the transcriptional level.
    b. Identify transcription factors regulating *MBNL1* RNAa based on UCSC genome browser datasets.
    c. Verify the involvement of major RNAa factors in saRNA-mediated *MBNL1* upregulation.
    d. Dissect saRNA duplex strand involvement by using chemical modifications that either inhibits (5'-end biotin modification) or promotes (introduce mismatched base at the 3'-end of the opposite strand) the selection of each strand by AGO.
    e. Verify potential role of lncRNA *MBNL1-AS1* in *MBNL1* expression regulation in the context of *MBNL1* RNAa.

4. Investigate *MBNL1* RNAa as novel molecular therapy of DM1 by analyzing the alternative splicing of multiple MBNL1 target pre-mRNAs in DM1 cell models.
5. Verify potential changes in CUG^{exp} foci number or size in saRNA-treated DM1 patients' cells.
6. Analyze the feasibility of RNAa to upregulate murine *Mbnl1* in mouse cell models to test *in vivo* the therapeutic potential of RNAa in mouse models.

The PhD thesis consists of two parts (Chapter III RESULTS – MANUSCRIPT IN REVISION AND PUBLISHED ORIGINAL ARTICLE; Chapter IV RESULTS AND DISCUSSION - UNPUBLISHED DATA). Chapter III comprises two articles. The first one is a comprehensive literature review entitled "***MBNL proteins in health, disease and therapeutic applications***" authored by Musiała-Kierklo N.*, Konieczny P., Plewka P., Jasiok A., Stępniak-Konieczna E*,# (*equal contribution in writing; #corresponding author). This review is an all author-approved version of the manuscript, currently under peer-review. Second article entitled "***Promoter-targeted small RNA duplexes increase MBNL1 transcription and mitigate myotonic dystrophy-associated spliceopathy***." is a work published in Nucleic Acids Research as a Breakthrough Article, authored by Musiała-Kierklo N., Plewka P., Jasiok A., Stępniak-Konieczna E.# (corresponding author), doi: 10.1093/nar/gkaf756.

Chapter IV constitutes unpublished results that detail additional molecular insights into the *MBNL1* RNAa mechanism and investigate RNAa feasibility in modulation of *Mbnl1* expression in mouse cell models.

III. RESULTS – MANUSCRIPT IN REVISION AND PUBLISHED ORIGINAL ARTICLE

3.1 THE LITERATURE REVIEW

This PhD dissertation section provides an overview of MBNL biology in health and disease. It outlines structural and organizational features of MBNL genes and proteins, summarizes lessons from animal models, and highlights paralog-specific functions in physiological processes. Particular focus is placed on disorders linked to MBNL deficiency, especially myotonic dystrophy, and on cancers where deregulated MBNL expression reshapes transcriptomes. Finally, emerging therapeutic strategies targeting endogenous *MBNL* expression are discussed, with DM1 serving as a model for exploring their potential as therapeutic targets. The main assumptions of the literature review are summarized below.

The Muscleblind-like (MBNL) family comprises highly conserved RNA-binding proteins (RBPs) that recognize target pre-mRNA transcripts through zinc-finger (ZnF) domains. In mammals, three paralogs - MBNL1, MBNL2, and MBNL3 - act as master regulators of RNA metabolism, with their most prominent role being the control of alternative splicing (AS). By repressing embryonic splicing patterns and promoting adult isoforms, MBNLs regulate “fetal-to-adult” transition, crucial in regulating gene expression. This developmental switch underlies normal differentiation and tissue homeostasis, and its disruption has been implicated in the pathogenesis of diverse human diseases.

Despite their shared structural features, MBNL paralogs differ significantly in expression patterns and physiological functions. MBNL1 is broadly expressed and plays a dominant role in skeletal and cardiac muscle differentiation, whereas MBNL2 is enriched in the brain and supports developmental splicing programs in the central nervous system. In contrast, MBNL3 is mainly active during embryonic stages, particularly in the placenta, and in regenerating muscle, where it often antagonizes the differentiation-promoting effects of MBNL1 and MBNL2.

Dysregulation of MBNL-mediated splicing has been identified as a pathogenic mechanism in wide range of diseases. In nucleotide repeat expansion disorders, most notably myotonic dystrophy (DM), MBNL proteins become sequestered on toxic RNA repeats, leading to their functional depletion and a reversion to fetal-like splicing patterns across multiple tissues. In cancers, misregulation of MBNL expression contributes to transcriptomic reprogramming toward stem cell–like states. While often tumor-suppressive,

MBNLs can also exert pro-oncogenic effects depending on the cellular and tissue context, highlighting their dual role in tumorigenesis.

Animal models of MBNL deficiency unraveled paralog-specific functions and compensatory mechanisms. Single knockouts of *Mbnl1* or *Mbnl2* in mice reveal tissue-specific functions of *Mbnls*, e.g. MBNL1 role in muscle and thymus development, and MBNL2 role in hippocampal function and synaptic plasticity. Importantly, numerous Mbnl3-deficient models demonstrate its unique role in placental growth restriction and muscle regeneration. Combined knockouts exacerbate disease-like phenotypes, confirming overlapping functions of MBNL1 and MBNL2, and providing insight into the molecular basis of DM. Studies in zebrafish, nematodes, and fruit flies further corroborate the evolutionary conservation of MBNL roles in RNA metabolism and development regulation.

Importantly, MBNL proteins regulate a wide range of physiological processes, including myogenesis, cardiac and neuronal maturation, hematopoiesis, and stem cell differentiation. Conversely, altered MBNL expression or function contribute to a variety of pathological processes, ranging from muscular dystrophies to cancer, underscoring their clinical relevance as potential therapeutic targets.

MBNL proteins in health, disease and therapeutic applications

Nikola Musiała-Kierklo[1,2,†], Patryk Konieczny[3], Patrycja Plewka[1], Adam Jasiok[1,4] and Ewa Stępniak-Konieczna[1,†,*]

[1]Laboratory of RNA Biology, Department of Biochemistry and Biotechnology, Poznan University of Life Sciences, Dojazd 11, 60-632 Poznan, Poland

[2]Doctoral School of Natural Sciences, Adam Mickiewicz University, Uniwersytetu Poznanskiego 2, 61-614 Poznan, Poland

[3]Institute of Human Biology and Evolution, Adam Mickiewicz University, Uniwersytetu Poznanskiego 6, 61-614 Poznan, Poland

[4]Poznan University of Life Sciences Doctoral School, Collegium Maximum, Wojska Polskiego 28, 60-637 Poznan, Poland

[†] These authors contributed equally to writing of this manuscript

[*]Corresponding author:
ewa.stepniak-konieczna@up.poznan.pl
ORCID 0000-0002-7387-1013

Abstract

The Muscleblind-like (MBNL) family comprises evolutionarily conserved RNA binding proteins (RBPs) interacting with target RNAs via zinc finger (ZnF) domains. MBNLs are the prime regulators of alternative splicing (AS) and support a developmental 'fetal-to-adult' switch in the use of defined cassette exons in multiple target precursor mRNAs. This transition is a cornerstone in the process of MBNL-maintained cellular homeostasis and fails in a plethora of pathological conditions associated with deregulated expression or function of specific MBNL paralogs. This review synopsizes the current knowledge on *MBNL* genes and proteins in health and disease conditions. We recall key lessons from animal models of *MBNL* genes deficiency and highlight selective versus compensatory roles of individual MBNL paralogs in normal physiological processes. To portray the roles of MBNLs in disease, we outline nucleotide expansion disorders characterized by functional depletion of these proteins, focusing primarily on myotonic dystrophy (DM). Distinct cancer studies are discussed to delineate double-edged roles of MBNLs in tumorigenesis, pro-oncogenic and tumor suppressive. Finally, using DM as an example, we thoroughly examine pivotal works supporting therapeutic potential of endogenous modulation of *MBNL* genes. We argue that similar strategies could be tailored to balance *MBNL* expression in other diseases associated with their deregulation.

Introduction

The Muscleblind-like (MBNL) family comprises a group of highly conserved RNA binding proteins (RBPs) which interact with target RNAs via zinc finger (ZnFs) domains. Mammalian MBNL family is composed of three paralogs (MBNL1, 2 and 3) which, in essence, function as master regulators of cellular RNA metabolism and homeostasis. Among their multiangled roles in the control of alternative polyadenylation, RNA stability and localization as well as microRNA biogenesis and circular RNA generation, MBNLs are primarily involved in the regulation of the alternative splicing (AS) [1]. Principally, they operate as developmental sensors that govern a key switch in the alternative use of defined cassette exons within pre-mRNA: while repressing embryonic and/or fetal splicing patterns, they promote splice isoforms characteristic of adult and differentiated tissues.

The three mammalian MBNL paralogs share structural similarities but differ largely in functional specialization and expression pattern throughout embryonic and postnatal development. The abundance of MBNL1 and MBNL2 is low in fetal tissues and undifferentiated cells but rises significantly throughout the process of differentiation and development, with widespread expression pattern in diverse adult tissue types, particularly high in muscle [2-4]. While both MBNL1 and 2 are largely co-expressed in many tissues and share compensatory roles, MBNL1 constitutes the most prominently expressed family member and serves major roles in promotion of muscle differentiation and AS transition [4, 5]. The expression of MBNL2 paralog predominates in the brain where it governs major developmental splicing program [6]. In contrast, MBNL3 is mostly expressed at early developmental stages in the placenta and only transiently in the adult regenerating muscle tissue [7]. Strikingly, while MBNL1 and 2 promote muscle formation, MBNL3 appears to function in an opposing manner to the other two paralogs and antagonizes muscle differentiation [8].

MBNL-regulated AS transition fails in a number of pathological processes. This can be either due to sequestration and functional inhibition of MBNL proteins or mis-regulated expression of *MBNL* genes. The former scenario is best illustrated in many nucleotide repeat-expansion disorders, including the most extensively studied myotonic dystrophy (DM) – a multisystem disease characterized by sequestration of MBNLs on toxic RNA repeats, their functional depletion and subsequent shift in the AS pattern towards fetal-like splicing in multiple tissues. The latter scenario often occurs in several common cancer types, where low *MBNL* expression levels may promote transcriptomic alterations resembling those observed in a stem-cell like state, at the level of both, gene expression and AS [9-12]. By default, MBNL proteins repress a program of alternative exons specific of embryonic stem cells and fetal tissues in favor of splice isoforms characteristic of differentiated tissues, which supports their tumor suppressive roles (e.g.[9-11]). Strikingly, however, MBNLs may serve a dual and context-dependent role in tumorigenesis by acting also as tumor promoters (e.g.[13, 14]). As outlined in the following chapters, these roles are strictly cell-, tissue- and cancer-type dependent and often rely on the expression of a specific MBNL isoform [13]. Thus, the emerging roles of MBNL proteins in both physiological as well as multiple pathological conditions necessitate research on their expression modifiers and highlight the importance of developing targeted strategies to precisely tune MBNL expression for a therapeutic benefit.

This review focuses primarily on the principal role of MBNLs in AS regulation, which we discuss in the context of major physiological processes governed by MBNLs as well as pathological conditions characterized by their functional deficiency or deregulated expression. We synopsize main organizational and structural features of *MBNL* genes and proteins, as well as their mechanisms of splicing control. Key lessons from distinct animal models of *MBNL*

genes deficiency are summarized to portray major physiological tissue-specific functions of individual MBNL paralogs and delineate their selective versus compensatory roles. The importance of MBNLs in pathophysiology is discussed primarily in the context of DM, the most extensively studied disease associated with MBNL insufficiency, but also in other types of nucleotide expansion disorders characterized by functional depletion of MBNLs. Further, dual pro-oncogenic and tumor suppressive roles of MBNL paralogs are illustrated in selected cancer types associated with their aberrant level or function. Finally, using DM as an example, we highlight seminal works demonstrating that endogenous modulation of *MBNL* genes poses a viable therapeutic option to balance their cellular roles. We also spotlight novel emerging strategies to control *MBNL* expression in DM. Based on available data, we argue that *MBNLs* are feasible therapeutic targets and gene tuning strategies could be carefully tailored to other conditions associated with their deregulated expression.

MBNL genes

MBNLs share a high degree of functional and structural conservation across multicellular organisms. Human orthologs of *MBNL* genes exist in diverse species including *Drosophila melanogaster* [15, 16], *Caenorhabditis elegans* [17], *Danio rerio* [18, 19] as well as higher vertebrates and mammals including *Mus musculus* [20]. Historically, *muscleblind* was identified as a protein essential for photoreceptor and muscle differentiation in *Drosophila melanogaster* (*Mbl*) [15, 16], while mammalian homologue of *Mbl* was first cloned as a polypeptide binding the CUG repeat expanded RNA underlying the genetic multiorgan disorder myotonic dystrophy (DM) [3, 21-23]. Subsequent studies identified three distinct homologous mammalian genes including *MBNL1* (formerly *MBNL/EXP*), *MBNL2* (formerly *MBLL/MPL1*) and *MBNL3* (formerly *MBXL/CHCR*) mapped to chromosomes 3, 13 and X, respectively [3, 4, 24], and demonstrated their role as alternative splicing regulators [25]. In contrast to invertebrates, which only have a single *muscleblind* gene, the three homologs present in most vertebrate species arose likely as a consequence of gene duplication of a common ancestor [26]. All human *MBNL* genes share structural similarities. The coding sequence (CDS) of the major paralog *MBNL1* is composed of three constitutive (e2, e4 and e10) and seven alternatively spliced exons (e1, e3 and e5-e9). Alternative 5' untranslated (UTR) initiation exons (e5'UTRs) comprise important regulatory elements [27-29] while 3'UTR exon (e3'UTR) have critical roles in *MBNL* translation and stability [30] (**Figure 1A).**

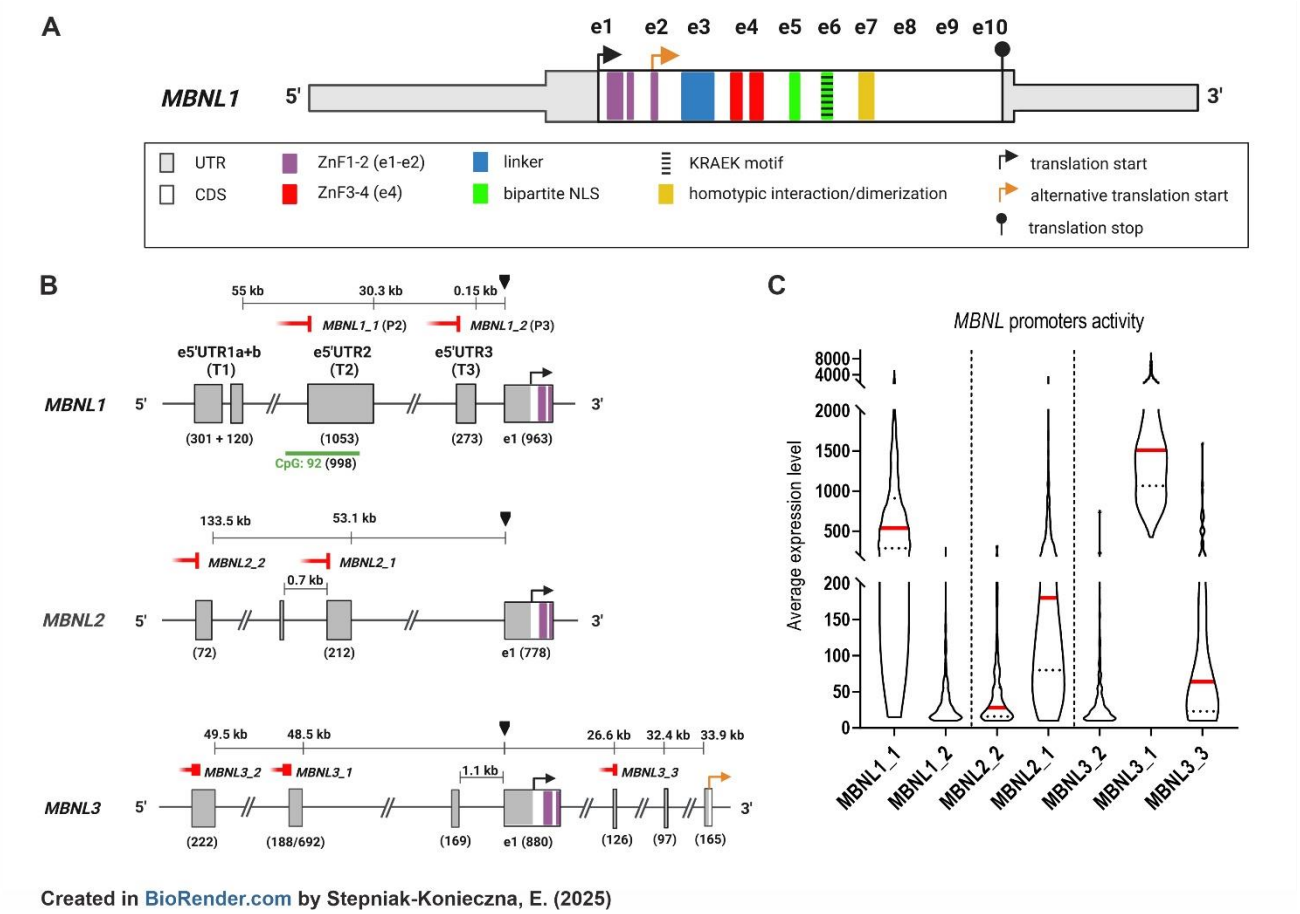

FIGURE 1. Genomic organization of human *MBNL* genes and promoters. (A) Schematic (not to scale) of genomic organization of *MBNL* genes exemplified by the major paralog *MBNL1,* with key features indicated in the legend. **(B)** Schematic of Eukaryotic Promoter Database (EPD) and UCSC Genome Browser annotated promoters of *MBNL1* (*MBNL1_1*,

MBNL1_2), *MBNL2* (*MBNL2_2*, *MBNL2_1*) and *MBNL3* (*MBNL3_2*, *MBNL3_1* and *MBNL3_3*) (not to scale). Promoters P1, P2, P3 (e5'UTR1-e5'UTR3) and their corresponding transcription initiation sites in *MBNL1* are depicted based on published data [29]. Numbers in parentheses denote nucleotide lengths. Approximate distances (kb) relative to the beginning of the first coding exon (inverted arrowhead) of respective *MBNL* genes are marked. Marked features are indicated in the legend. Promoter regions are marked red with the thin horizontal line representing ~50 bp upstream of the annotated transcription start site (TSS) and the red vertical line indicating the TSS. The relative position of the horizontal and vertical line defines the orientation of the promoter. (A-B) **Created in BioRender. Stepniak-Konieczna, E. (2025)** https://BioRender.com/38g5t79. **(C)** Meta-analysis of EPD deposited data on the overall activity of the annotated *MBNL1, 2* and *3* promoters. Violin plot represents average expression level of promoter-specific *MBNL1*, *2* and *3* transcripts in all samples in which these promoters are active (n=1051 for *MBNL1_1*; n=371 for *MBNL1_2;* n=169 for *MBNL2_2;* n=1029 for *MBNL2_1*; n=314 for *MBNL3_2*; n=928 for *MBNL3_1*; n=62 for *MBNL3_3*). Average expression represents the number of tags in a 100-bp region centered on the EPD-annotated respective TSS and normalized to 10M total tags. Red horizontal lines mark average expression represented by number of tags per 10M tags; grey dashed lines indicate quartiles.

Promoters and regulatory regions of *MBNL* genes

Tissue-specific expression of distinct *MBNL* isoforms is determined by alternative usage of *MBNL* promoters and upstream regulatory regions. In human *MBNL1,* these include three promoters (P1-3; listed in order from the most upstream relative to the first coding exon) and corresponding transcription initiation sites (T1-3) associated with the usage of three alternative 5'UTR exons (e5'UTR1-3) (based on FasterDB, UCSC RefSeq available data, Eukaryotic Promoter Database (EPD) deposited data and [2, 26, 29]) (**Figure 1B**). Among these, P2/TSS2 (annotated as *MBNL1_1* in EPD) shows the highest activity in majority of tissues including fetal as well as adult heart and skeletal muscle, while P3/TSS3 (annotated as *MBNL1_2* in EPD) plays a secondary role to P2/TSS2 [5, 29] (**Figure 1C**). P1/T1 displays marginal activity compared to the other two promoters and *MBNL1* transcripts originating from P1/T1 are detectable mainly in fetal and adult liver as well as fetal spleen and thymus [29].

Furthermore, EPD and UCSC RefSeq data annotate two promoters for *MBNL2* (*MBNL2_2* and *MBNL2_1*; listed in order from the most upstream relative to the first coding exon) and three promoters for *MBNL3* genes (*MBNL3_2, MBNL3_1* listed in order from the most upstream relative to the first coding exon, and *MBNL3_3* associated with alternative first coding exon) (**Figure 1B**). The significance of alternative promoter usage is crucial for defining tissue-specific expression of *MBNLs* as well as their functionality. The latter was shown for *MBNL1*, whose alternative splicing of the first coding exon, critical for protein turnover and splicing activity, occurs specifically in transcripts derived from P2/T2 [29]. The former is exemplified in *MBNL3,* whose truncated protein isoform with only single ZnF pair (ZnF3-4), generated via the use of a novel eutherian-specific promoter, occurs specifically in placental tissue [31]. This novel TSS lies in a proximity of two eutherian-specific transposable elements of the MER53 and MER103c families, prompting speculations that their insertion in eutherian ancestors may be linked to the origin of the short MBNL3 isoform in placenta. Similarly truncated MBNL3 protein isoform can also be generated from alternatively spliced transcripts that initiate from the ancestral TSS but skip exon 2 encoding the canonical start codon.

Despite therapeutic relevance, little is known about transcription factors (TF) contributing to promoter-differential expression of *MBNL* genes. A candidate approach in *Drosophila muscleblind* (*Mbl*) identified two putative promoter regions, P1 and P2 located in exon 1 and 2, respectively, that were able to initiate transcription [27]. ChIP-on-chip data showed that multiple *cis*-regulatory modules around those regions bound Myocyte enhancer factor 2 (Mef2) as well as muscle organizing factors Biniou (Bin), Tinman (Tin) and Twist. Moreover, a crucial muscle enhancer (ME) of *Mbl* expression in embryonic somatic musculature was narrowed down to genomic region downstream of P2, while sequences farther downstream, harboring additional binding sites for TFs essential in central nervous system (CNS) development, were indicated as neural-specific *Mbl* enhancer (NE). Importantly, the same study pointed out functionally conserved human *MBNL1* promoter regions, Hsa-P1 and Hsa-P2 [27] in the proximity of the human *Muscleblind* e5'UTR2/P2 and e5'UTR3/P3, respectively [29]. Noteworthy, *Drosophila* ME drove the expression of a reporter gene in embryonic musculature only when fused to Hsa-P1, but not Hsa-P2, indicating the relevance of this promoter in muscle-specific *muscleblind* expression [27].

Murine *Mbnl1* harbors important enhancer activity within methylated region 2 (MeR2) located in the intron preceding the first coding exon [32], corresponding to e5'UTR3/P3 region directly preceding the first coding exon in human *MBNL1*. While MeR2 is methylated during myogenic differentiation, data shows that pharmacological suppression of methylation dramatically increases RNAPII occupancy around this region and enhances *Mbnl1* transcription starting at the upstream exon, suggesting enhancer activity within MeR2 [32]. Considering that similar enhancer regions in intron 1 were identified in several muscle specific genes, e.g. *Dmd* [33] or *Ache* [34], MeR2 as well as corresponding e5'UTR3/P3 region in human may be critical for muscle-specific *Muscleblind* expression [32].

Functional features encoded by *MBNL* exons

MBNL exons e1-e2 (with e1 referring to the first coding exon) and e4 encode the key structural and functional protein domains essential for target recognition, binding and splicing activity - the four ZnF domains arranged in tandem motifs ZnF1-2 and ZnF3-4. While ZnF1 and ZnF3-4 are encoded entirely by e1 and e4, respectively, the CDS of ZnF2 is split between e1 and e2, such that the latter covers its major part [2] (**Figure 1A**). Both ZnF pairs are juxtaposed and joined via flexible and unstructured linker encoded by e3, which connects ZnF2 and ZnF3 domains and is essential for splicing regulatory activity [35-37]. Moreover, sequences within e2, e3 and e6 of *MBNL1* contain proline-rich motifs (PRM) which enable interactions with the Src-homology 3 (SH3) domains present in many signaling proteins, including the tyrosine (Tyr) kinases of the Src family, suggesting MBNLs' involvement in signaling cascade mediated by Tyr phosphorylation [38]. Exon 5 and the highly conserved five amino-acid KRAEK motif in e6 encode a bipartite nuclear localization signal (NLS) [36, 39]. While the KRAEK motif alone is sufficient for nuclear redistribution of *Drosophila Muscleblind* [39], extensive analyses of human MBNL1 truncation mutants demonstrated that in fact both e5 and e6 are required for exclusive nuclear retention [36]. While alternative e5 is found in all *Mbnl1* and *Mbnl2* paralogs and in most non-eutherian *Mbnl3* genes, it is lost in eutherian *Mbnl3* hence promoting *Mbnl3* cytoplasmic localization [31]. The C-terminus, particularly sequences encoded by e7, determine homotypic MBNL-MBNL interactions and dimerization as well as improved binding of the protein to the CUG repeated region [36]. As in the case of e5, the cassette exon e7 is preferentially included when MBNL protein abundance is low, i.e. in fetal tissues including muscle and brain, in early differentiation stages or adult DM tissues [36, 40, 41] as well as in distinct cancerous tissues and cell lines [13].

A considerable amount of data indicates that sequences within the 3'UTR exons of all *MBNL* paralogs harbor binding sites for several micro RNAs (miRNA) regulators of *MBNL* transcripts [30, 42]. For example, the miR-30-5p family involved in inhibition of muscle differentiation may inhibit *MBNL* expression via direct transcript binding within its 3'UTR [42]. Further, negative regulation of *MBNL1* and *2* transcripts by miR-23b and miR-218 has recently been exploited in an experimental therapy against DM using designed antisense oligonucleotides targeting either these miRNAs directly (antagomiRs) or their binding sites within the 3'UTR of *MBNL1* RNA (blockmiRs), thus preventing translational repression of *MBNL1* and boosting the protein availability [30, 43-45].

Structural features of MBNL proteins essential for target recognition and splicing control

MBNL proteins recognize and bind RNA targets via highly conserved N-terminal CCCH-type (three cysteines followed by one histidine) ZnFs arranged in one (invertebrates) or two (vertebrates) tandem motifs. Remarkably, vertebrate MBNL proteins share 99% identity within the ZnF domains architecture and structure [46]. The individual ZnF domains are folded into similar compact pairs (tandems), with ZnF1-2 positioned towards the N-terminal end of the protein and ZnF3-4 arranged within its middle part. Both tandems as well as each individual ZnF are separated from each other by amino acid linkers. While the aminoacid linker connecting the two individual ZnFs within each tandem orients their RNA-binding surfaces in a back-to-back position enforcing an antiparallel alignment of bound RNA strands ([46] and reviewed in [2]), the e3-encoded unstructured linker separating the two tandems supports the protein flexibility and facilitates a wide array of interactions with differentially structured RNAs [35, 36, 46, 47]. Consistently, its' loss dramatically decreases MBNL affinity towards target sequences [36, 37].

MBNLs recognize a consensus GC motif embedded in pyrimidines (YGCY motif, where Y is a pyrimidine C or U) [15, 24, 48, 49]. Particularly, CUG and CCUG repeated sequences expanded in mutated transcripts found in DM type 1 and 2, respectively, constitute high-affinity binding sites for MBNLs [2, 50]. Target recognition mechanisms via ZnFs are highly conserved; *Drosophila Muscleblind* ZnFs are able to bind human MBNL1 targets [51] and even regulate the alternative splicing of murine *cTnT* and *Tnnt3* in minigene assays [52]. Although all mammalian MBNL paralogs recognize and bind the same RNA motifs, they do so with different affinities and may affect the splicing of the same exons with different strength, with MBNL1 possessing the strongest and MBNL3 the weakest splicing activity [53]. Variations in nucleoplasmic and cytoplasmic distribution of particular paralogs as well as the structural context of targeted RNA sequences and motif distribution likely contribute to these differences [36, 53-55].

Mutagenic studies of ZnFs revealed that while disruption of either individual or tandem ZnF only marginally affected MBNL1 splicing activity, it almost completely abrogated it when combined and arranged pairwise to affect both ZnF pairs [56]. Although this supports a model in which either ZnF tandem is sufficient for splicing regulation, mutations ablating specific RNA interactions via particular ZnFs showed that the splicing activities of ZnF1-2 and ZnF3-4 were not equivalent for all classes of splicing events. While their redundancy was observed for some pre-mRNA targets, a subset of MBNL1-regulated events required a functional ZnF1-2 for effective splicing regulation [56]. Studies with chimeric MBNL proteins carrying duplicate ZnF1–2 or ZnF3–4 demonstrated that duplication of the former tandem strikingly increased splicing activity compared to canonical arrangement, while duplication of the latter markedly decreased it due to partially lost ability to recognize canonical YGCY motifs [57]. A model that emerged from these works proposed that both domains act as independent units;

while ZnF1–2 confers specific sequence recognition, ZnF3–4 acts as a more general RNA binding domain [57]. In agreement, targeted point mutations interfering with the RNA binding of MBNL1 ZnF1-2 were more detrimental for splicing activation, repression and RNA binding than those in ZnF3-4 [47].

Positional model for MBNL splicing activity

MBNLs modulate AS events by promoting or suppressing exon inclusion into mature transcript via sequence- and position-dependent binding to cognate motifs within target pre-mRNAs, relative to the regulated exon [6, 48, 49, 58, 59]. As a general rule, MBNLs suppress exon inclusion when bound near the upstream intron/exon boundary of the regulated exon (defining the 3′ splice site) or within the regulated exon, and enhance exon inclusion by binding near the downstream exon/intron junction (defining the 5′ splice site) ([48, 49, 58] and reviewed in [2, 59]) (**Figure 2A**). This positional mode of action resembles splicing regulation by other splicing factors including CELF [60], FOX [61, 62], NOVA [63, 64], PTB [65, 66] or SR and hnRNPL [67] (reviewed in [68]).

Mechanistically, promotion of exon inclusion may follow MBNL-dependent activation of intronic splicing enhancers (ISE) or blocking of intronic or exonic splicing silencers (ISS and ESS, respectively), the latter usually located within the proximity of the 3’ end of an exon. Furter, enhanced recognition of 5’ splice-site (5’ss) by spliceosome or MBNLs competition with trans-acting splicing silencers may also enhance MBNL-dependent exon inclusion. Conversely, MBNL-mediated splicing inhibition may result from blocking of cis-acting sequence motifs including 3’ splice sites (3’ss), polypyrimidine tracts (pY tract) or intronic branch site elements as well as exonic splicing enhancers (ESE) located within the 5’end of an exon. Alternative exon repression may also result from a direct competition with essential splicing factors. [69, 70] (**Figure 2B**).

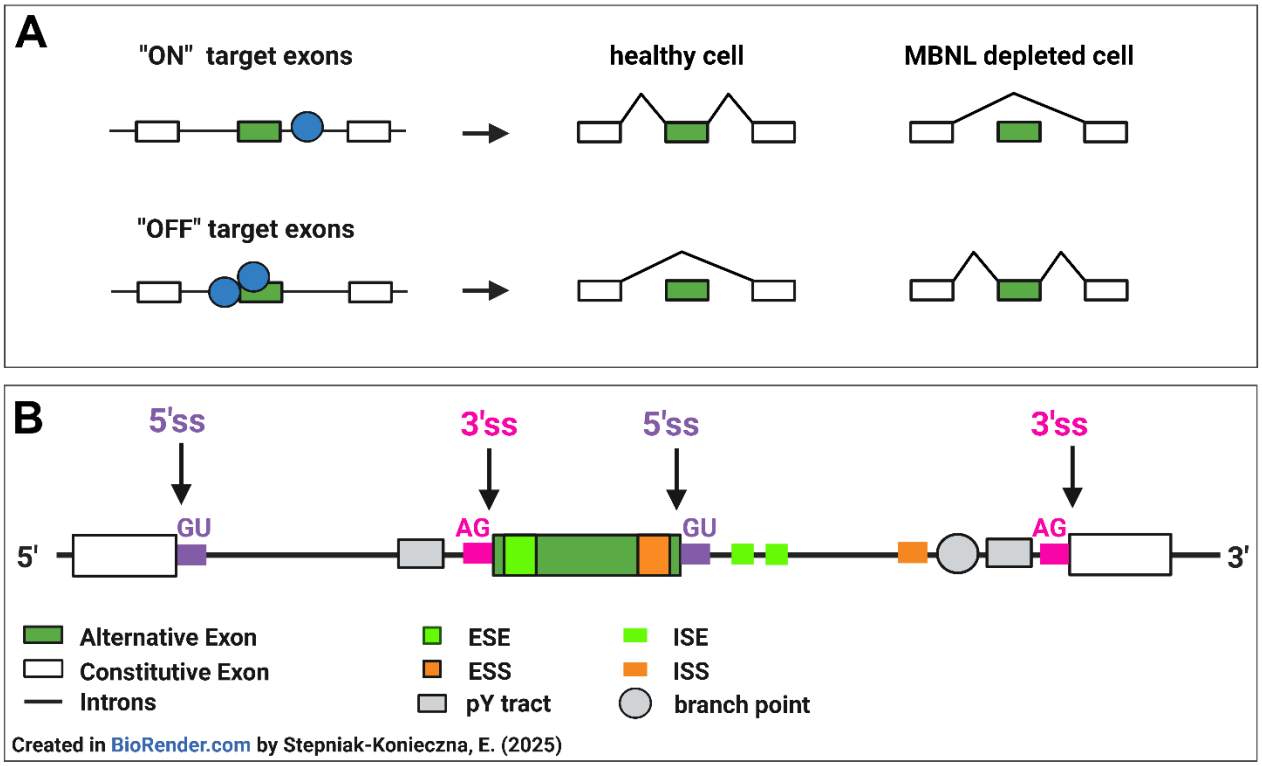

FIGURE 2. Schematic of the positional model of MBNL-dependent alternative splicing regulation. Sequence and position-dependent binding of MBNL proteins to their cognate motifs determines the outcome of an alternatively spliced event. **(A)** MBNL binding downstream of the regulated exon promotes its inclusion into mature mRNA, while binding upstream or within the regulated exon represses its inclusion into mature transcript. This pattern is reversed in cells with functionally depleted MBNL proteins, such as myotonic dystrophy cells. **(B)** Major mechanisms involved in MBNL-mediated exon inclusion or repression which are detailed in main text. Abbreviations: ESE-exonic splicing enhancer; ESS-exonic splicing silencer; ISE-intronic splicing enhancer; ISS-intronic splicing silencer. **Created in BioRender. Stepniak-Konieczna, E. (2025)** https://BioRender.com/2df1lx8.

Autoregulatory splicing of MBNL exons

MBNL proteins possess a unique feature allowing them to switch isoforms via autoregulatory splicing of several alternative exons within their own pre-mRNAs. Negative feedback mechanisms based on MBNL-dependent repression of own exons have been observed for *MBNL* e1, e3, e5, e7 and e8 [28, 29, 71]. These mechanisms have been extensively reviewed [28] and here we highlight only one selected example including e1, whose presence is crucial for MBNL protein stability and splicing activity.

Repression of e1 is mediated by MBNLs via binding to cognate motifs within the untranslated region of e1. Loss of e1 shifts the translation start to e2, thus depriving the protein of ZnF1-2 domain and consequently decreasing its RNA binding and splicing activity, as well as the overall protein stability [28, 29]. This in turn relieves repression of e1, allowing translation of the fully functional MBNL1 isoform from pre-mRNAs containing e1. This self-limiting feedback loop is an important element in buffering of the overall cellular level of MBNL1. Intriguingly, it was demonstrated that only P2-driven *MBNL1* pre-mRNAs undergo alternative splicing of e1 [28, 29]. Transcripts driven by the two less active promoters P1 and P3, by default lack or include e1, respectively, regardless of the presence of MBNL proteins. This is likely due to exceptionally large (~55 kb for P1) and small (~0.15 kb for P3), respectively, distance between the specific transcription initiation site and e1 [29]. In addition, published data as well as UCSC and RefSeq annotated sequences indicate that e1 may be spliced to alternative e1a generating a small 83 amino acid protein isoform with only one ZnF and an unconserved C-terminus, an isoform identical to fruit fly MblD [26]. Moreover, the use of alternative exons e1b and e1c in the absence of e1 results in N-terminally truncated isoforms lacking ZnF1-2 domain. While short isoforms devoid of e1 were described for human *MBNL1* and murine *Mbnl1* as well as for *Mbnl2*, they are poorly translated and give rise to highly unstable proteins [6, 28, 29, 72]. This is possibly due to inefficient loading of the mRNA lacking e1 on polysomes [29]. Conversely, production of a stable isoform lacking e1 may be unique to eutherian-specific MBNL3 paralog [7, 31, 73]. Notably, the e1-dependent autoregulatory loop is active in DM, where it serves a protecting role against sequestration and functional scarcity of MBNLs caused by toxic expanded RNAs, though becomes exhausted with increasing expansion size as the disease progresses [29].

Factors affecting MBNL splicing outcome

The overall amount of available MBNL largely determines the strength of exon exclusion versus inclusion. Studies in human myoblasts with siRNA-mediated incremental depletion of MBNL pool clearly demonstrated dose-dependent effect on the number as well as the severity of the AS defects [74]. Further, precise tuning of the protein concentration in a

cellular model revealed that splicing events exhibit different responses depending on the available MBNL amount, and indicated critical role of MBNL1 binding site number, location and affinity [75]. In addition, inducible expression of exogenous MBNL1 in an engineered cell line revealed that MBNL1-regulated exclusion events may require higher concentrations of the protein to properly regulate AS outcomes compared to inclusion events [76]. Considering that MBNL dose variations have an important impact on DM variability, these dose-dependent MBNL-regulated AS events are excellent biomarkers of the disease severity and response to therapeutics [75, 77].

Alternative splicing of pre-mRNAs is frequently controlled by combinatorial or competitive effects of both activators and inhibitors [68], hence the amount of MBNL relative to other splicing factors e.g., CELF [78], RBFOX [76], hnRNP H [79] plays a significant role in determining both, the direction and the strength of the splicing response. One example involves a functional antagonism between MBNL1 and CELF1 in AS control as well as mRNA expression regulation [78]. As more than two hundred exons were shown to be oppositely regulated by both proteins [78], this antagonism is particularly important in DM pathogenesis, where MBNLs are depleted and the steady-state levels of CELF1 are increased due to enhanced stability elicited by hyperphosphorylation via excessively active protein kinase C (PKC) [80].

Animal models of MBNL deficiency

Mbnl loss-of-function mutant mice

Genetically modified animal models have been invaluable for deciphering the roles of individual MBNL proteins in physiological and molecular processes. We synopsize key lessons from these models focusing primarily on murine *Mbnl* loss-of-function (LOF) mutants (**Table 1**) and non-mammalian vertebrate model zebrafish *zmbl* mutants. We also highlight selected studies in invertebrates including nematode and fruit fly.

Mbnl1 isoform knockout (KO) mice with genetic ablation of the first coding exon (*Mbnl1*$^{\Delta E3/\Delta E3}$) recapitulated DM phenotype including myotonia, myopathy, cataracts and aberrant alternative splicing [72], but failed to develop muscle weakness [72] [6, 58, 81] or AS dysregulation in the brain [82]. Further studies in this model, but on a different genetic background, showed additionally the requirement for MBNL1 in normal thymus development and function, as loss of MBNL1 resulted in thymic hyperplasia and thymocyte accumulation associated with misprocessing of developmental AS events critical for T lymphocyte maturation [83].

Gene trap (GT) studies provided contradictory data on the effects of *Mbnl2* deficiency. The first described *Mbnl2* mutant mice, generated by β-geo GT insertion into intron 4 of *Mbnl2* (*Mbnl2*$^{GT4/GT4}$ mice), displayed no apparent change in muscle structure and function and no AS alterations compared to the *HSA*^{LR} (Human Skeletal Actin Long Repeats) mouse model of DM carrying ~250 CTG repeats, or to *Mbnl1* KO mice [40]. No effects on the development of DM features including myotonia were observed [40]. However, the same GT inserted in intron 2 of *Mbnl2* (*Mbnl2*$^{GT2/GT2}$ mice) led to myotonia, skeletal myopathy and altered chloride channel expression characteristic of DM [84]. These striking differences stem likely from GT insertion sites; while the former mutant contains additional coding regions thus yielding a truncated protein containing two ZnFs, the latter leads to production of a molecule encoded by the first coding exon of *Mbnl2* fused in-frame to a β-geo reporter, yielding a truncated protein with only one complete ZnF. Moreover, the late onset myotonia phenotype observed in *Mbnl2*$^{GT2/GT2}$ mice [84] is consistent with the adult onset phenotype often observed in DM patients, indicating that perhaps MBNL2 has an independent role in mature or remodeling skeletal muscle that is not completely compensated by the presence of MBNL1 [84]. To address these inconsistencies, loss-of-function *Mbnl2* mutant mice, lacking exon 2 encoding the initiation codon for the full-length MBNL2 protein (*Mbnl2*$^{\Delta E2/\Delta E2}$), were generated by homologous recombination [6]. Removal of the first coding exon led to ablation of the full-length mRNA expression and a complete absence of MBNL2 protein, indicating that these mutants were true functional nulls. Strikingly, *Mbnl2*$^{\Delta E2/\Delta E2}$ mice did not develop any apparent skeletal muscle pathology or motor deficits but instead exhibited phenotypes consistent with pathologies observed in the CNS of DM patients, including widespread splicing abnormalities in the brain, increased REM (Rapid Eye Movement) sleep propensity and seizure susceptibility as well as deficits in spatial memory [6]. The expression of MBNL2 is prominent in the hippocampus and concomitantly, *Mbnl2*$^{\Delta E2/\Delta E2}$ KO animals exhibited impaired hippocampal synaptic plasticity associated with a decrease in N-methyl-D-aspartate receptor (NMDAR) synaptic transmission. In all, these data suggest that while MBNL2 alone does not significantly contribute to DM skeletal muscle pathology, it plays a major role during postnatal brain development [6].

Analyses of spatial and temporal pattern of *Mbnl3* expression during murine development indicated that it peaks early during the embryonic period and is largely absent or low in adult tissues [7, 85]. In contrast to *Mbnl1* and *Mbnl2* isoform knockouts, *Mbnl3* mutants

generated by homologous recombination of exon 2 (*Mbnl3*$^{\Delta E2/\Delta E2}$), which results in the absence of the full length MBNL3 protein but retains shorter isoform with ZnF3-4, fail to develop overt muscle- or CNS-related phenotypes during postnatal development [7, 73]. Instead, a progressive decline in skeletal muscle regenerative capacity, manifested as age-dependent delay in myotoxin-induced muscle injury/regeneration, has been demonstrated in these mice [7]. Apart from impairing muscle regeneration, MBNL3 deficiency accelerated the onset of a subset of age-associated DM-like pathologies including glucose intolerance and elevated insulin levels, cardiac dysfunctions and cataracts [73]. Intriguingly, these changes were accompanied by minimal AS alterations, suggesting that mechanisms distinct from embryonic splice isoforms retention may contribute to the onset of age-associated phenotypes in DM [7, 73]. To ablate both long and short *Mbnl3* isoforms, conditional mouse mutants were generated by removal of loxP-flanked exons 2 and 7c [86]. Multiple transcriptome abnormalities accompanied MBNL3 deficiency, including precocious expression of muscle-specific transcripts in knockout myoblasts as well as preferential inclusion of adult pattern exons in many misregulated AS events. In another study, these mutants displayed significantly increased placental weight throughout embryonic development, pointing to MBNL3 role in restricting placental growth [31]. Consistently with an increase in cell proliferation, upregulation of *Myc* and its associated regulatory network was found in these animals. Although MBNL3 may bind the 3'UTR sequences of target transcripts, no direct interaction between *Myc* and MBNL3 was demonstrated [31].

TABLE 1. Murine *MBNL* LOF mutants (selected examples). Abbreviations: KO – knockout; GT – gene trap; DKO – double knockout; TKO – triple knockout; Cond. – conditional; WL – whole locus; Cond. KO – conditional KO; AS – alternative splicing; CNS-central nervous system; Ref. – reference publication.

***Mbnl* gene mutant**	**Mouse model**	**RNA and protein expression**	**Key phenotype features & findings**	**Ref.**
***Mbnl1* KO**	*Mbnl1*$^{\Delta E3/\Delta E3}$ (deletion of the first coding exon by homologous recombination)	-Partial decrease of *Mbnl1* mRNA (some isoforms present); -No expression of MBNL1 41- to 42-kDa proteins	-Myotonia, myopathy, cataracts, aberrant AS, postnatal thymic hyperplasia; -No muscle weakness; -No AS dysregulation in the brain	[72]
***Mbnl2* GT**	*Mbnl2*$^{GT4/GT4}$ (GT insertion in intron 4)	-90% reduction of *Mbnl2* mRNA; -Mutant encodes a truncated protein with two ZnFs	-No DM phenotype; -No apparent contribution of MBNL2 loss to DM muscle pathology; -No AS alterations	[40]
***Mbnl2* GT**	*Mbnl2*$^{GT2/GT2}$ (GT insertion in intron 2)	-*Mbnl2* RNA significantly decreased; -Truncated MBNL2 protein with only one complete ZnF detected (a fusion molecule encoded by the first coding exon fused in-frame to a neo-reistance / βgeo-reporter)	-Independent role of MBNL2 in mature skeletal muscle; -Skeletal muscle pathology (decrease myofiber size, central nuclei, fibrosis); -Myopathy; -AS defect of calcium chloride channel but no alterations in splicing of other genes; -Late onset myotonia	[84]

***Mbnl2* KO**	*Mbnl2*$^{\Delta E2/\Delta E2}$ (removal of the first coding exon by homologous recombination)	-Ablation of full length *Mbnl2* mRNA and absence of protein; true functional null mutants	-No overt skeletal muscle pathology or myotonia; -Essential role of MBNL2 in brain development and hippocampal synaptic plasticity; -CNS pathologies with widespread AS defects in the KO brain; -REM sleep propensity, seizures and spatial memory deficits	[6]
***Mbnl2* Cond. KO**	In utero electroporation of Cre recombinase into the developing cortex of *Mbnl2*$^{f/f}$ mice [6]	-Ablation of *Mbnl2* expression in cortical neurons	-Decreased dendritic spine density and dynamics in adolescent mice; -*Add1* isoform switch from adult to fetal produced truncated ADD1 which failed to interact with SPTAN1, a critical protein for spinogenesis	[87]
***Mbnl3* KO**	*Mbnl3*$^{\Delta E2/\Delta E2}$ (removal of the first coding exon by homologous recombination)	-Absence of the full length MBNL3 protein; -Retains short MBNL3 isoform with ZnF3-4 only, predominantly cytoplasmic	-No overt muscle/CNS defects and minimal AS alterations; -Glucose intolerance, elevated insulin levels, cardiac dysfunction and cataracts; -Delayed and impaired injury-induced skeletal muscle regeneration; -Accelerated inset of age related pathologies	[7, 73]
***Mbnl3* Cond. KO**	*Mbnl3*^{condWL} (Cond. null allele of *Mbnl3* with loxP sites flanking e2 and e7c); *CMV-Cre*	Complete absence of *Mbnl3* RNA and protein (both long and short isoforms)	-Defective myoblast differentiation in culture and precocious expression of muscle-specific transcripts; -Prominent AS dysregulation in cultured myoblast characterized by inclusion of adult pattern exons	[86]
***Mbnl3* Cond. KO**	*Mbnl3*^{condWL}; *CMV-Cre* ([86])	Complete absence of *Mbnl3* RNA and protein (both long and short isoforms)	-MBNL3 restricts placental growth: larger placentas in the absence of *Mbnl3* due to increased cell proliferation and upregulation of *Myc* and its associated regulatory network	[31]
***Mbnl1/2* Combined DKO**	*Mbnl1*$^{\Delta E3/\Delta E3}$ / *Mbnl2*$^{+/\Delta E2}$ (DKO)	-Homozygous DKO (*Mbnl1*$^{\Delta E3/\Delta E3}$; *Mbnl 2*$^{\Delta E2/\Delta E2}$) are lethal - DKO heterozygous for *Mbnl2* (*Mbnl1*$^{\Delta E3/\Delta E3}$; *Mbnl2*$^{+/\Delta E2}$) show partial decrease of *Mbnl1* mRNA; no expression of MBNL1 41- to 42-kD protein and compensatory increase of *Mbnl2* (RNA, protein) in the absence of *Mbnl1*	-Dual depletion worsens splicing defects and aggravates DM phenotype; -Severely reduced lifespan; -Muscle weakness/wasting, cardiac arrhythmia, severe AS defects	[81]

***Mbnl1/2* Combined DKO (Cond.)**	*Mbnl1*$^{\Delta E3/\Delta E3}$ (KO) / *Mbnl2*$^{c/c}$; *Hb9-Cre-MN* (Cond. KO of *Mbnl2*)	-Full KO of *Mbnl1*; no expression of 41- to 42-kDa proteins; -Neuromuscular junction-specific ablation of *Mbnl2*	-Conditional mice develop gait coordination deficits associated with structural and ultrastructural defects in the neuromuscular junction; -AS aberrations in genes associated with synaptic transmission and neuromuscular junction homeostasis	[88]
***Mbnl1/2* Combined DKO (Cond.)**	*Mbnl1*$^{\Delta E3/\Delta E3}$ (KO) / *Mbnl2*$^{c/c}$; *Myo-Cre* (Cond. KO of *Mbnl2*)	-Full KO of *Mbnl1*; no expression of 41- to 42-kDa proteins; -Muscle-specific ablation of *Mbnl2*	-Profound deficiency of adult skeletal muscle; -Severe muscle pathology; -Aggravation of splicing defects	[81]
***Mbnl1/2* Combined DKO (Cond.)**	*Mbnl1*$^{\Delta E3/\Delta E3}$ (KO) / *Mbnl2*$^{c/c}$; *Myh6-Cre* (Cond. KO of *Mbnl2*)	-Full KO of *Mbnl1*; no expression of 41- to 42-kD protein; -Cardiomyocyte specific ablation of *Mbnl2*	-Sudden death due to lethal cardiac rhythms; -Reduced lifespan; -Dilated fibrotic hearts; -Gene expression and AS changes recapitulating DM heart spliceopathy	[89]
***Mbnl2/3* Combined DKO**	*Mbnl2*$^{\Delta E2/\Delta E2}$ (KO) / *Mbnl3*^{condWL}; *CMV-Cre* (Cond. KO of *Mbnl3*) ([6] , [86])	-Absence of full length *Mbnl2* mRNA and absence of protein; -Absence of *Mbnl3* RNA and protein (both long and short isoforms)	-Severe intrauterine growth restriction of DKO embryos; -Maturation defect in DKO placentas; -Large splicing changes in DKO placentas – *Mbnl*2/3 coregulate placental AS and polyadenylation	[31]
***Mbnl1,2,3* Combined TKO (Cond.)**	*Mbnl1*$^{\Delta E3/\Delta E3}$ (KO) /*Mbnl2*$^{c/c}$; *Mbnl3*^{condWL}; *Myog-Cre* (Cond. KO of *Mbnl2,3*)	-No expression of MBNL1 41- to 42-kDa proteins; -Muscle-specific ablation of *Mbnl2/3*	-TKO exacerbates DM-like defects; -Severe myopathy and presence of congenital DM features	[86]

Compound loss of mammalian *Mbnl* genes

Combined *Mbnl* KO mutant mice display more severe phenotypes than single KO, implying that MBNL proteins can functionally compensate for each other. While *Mbnl1* and *Mbnl2* double KO (DKO) homozygous mutant mice (*Mbnl1*$^{\Delta E3/\Delta E}$; *Mbnl2*$^{\Delta E2/\Delta E2}$) were embryonic lethal, inactivation of both alleles of *Mbnl1* and only one copy of *Mbnl2* (heterozygous *Mbnl1*$^{\Delta E3/\Delta E3}$; *Mbnl2*$^{+/\Delta E2}$ mutant mice) was compatible with survival but dramatically reduced lifespan and led to decreased body weight, severe progressive muscle weakness and wasting, cardiac arrythmia and DM-like splicing defects [81]. Dual depletion of *Mbnl1* and *2* also exacerbated splicing alterations observed in *Mbnl1* KO animals [81]. Likewise, conditional DKO mice with *Myo-Cre*-mediated muscle-specific elimination of *Mbnl2* in a *Mbnl1* KO background showed dramatic neonatal lethality and body weight reduction at birth, along with a profound deficiency of adult skeletal muscle and severe muscle pathology [81]. Also, these conditional DKOs displayed more pronounced AS defects compared to those observed in *Mbnl1* KO alone. Most recently, *Myh6-Cre*-mediated conditional deletion of *Mbnl2* in cardiomyocytes in a *Mbnl1* KO background resulted in sudden deaths due to spontaneous lethal cardiac rhythms [89]. Studies with muscle-specific double (*Mbnl1* and *2*) as well as triple (*Mbnl1*, *2* and *3*) conditional KO mouse models demonstrated that compound deficiency of MBNLs aggravated these defects and recapitulated many of the

phenotypes associated with congenital form of DM including myopathy and associated widespread mis-splicing events [86].

The phenotypes observed in single *Mbnl1* and *Mbnl2* KO mice, even though severe, fail to model the full spectrum of DM. The reason may be that apart from specific functions, MBNL paralogs may share overlapping or compensatory roles and loss of one paralog is counterbalanced by increased expression of the remaining one. Indeed, elevated levels of MBNL2 protein were detected in *Mbnl1* KO mice [72, 81, 86, 90, 91] and shown to regulate MBNL1-target exons [81]. However, single *Mbnl1* or *Mbnl2* KO mice showed no change in mRNA levels of *Mbnl2* or *Mbnl1*, respectively [91]. Recent work shed more light on the mechanism of compensatory MBNL2 upregulation demonstrating that loss of MBNL1 led to the inclusion of alternative e9 in *Mbnl2* mRNA, shifting the reading frame to an alternative C-terminus lacking the PEST domain required for proteasomal degradation [92]. Compensatory mechanisms between MBNL paralogs were also observed in human cells, e.g. in DM-patient's derived fibroblasts, in which knockdown of *MBNL1* increased *MBNL2* mRNA levels, but not vice versa [28] (**Figure 3**). Conversely, CRISPR-mediated KO of specific *MBNL* genes in human induced pluripotent stem cells (hiPSC) differentiated into skeletal muscle cells demonstrated a compensatory increase in MBNL1 or MBNL2 expression in *MBNL2* and *MBNL1* edited cells, respectively, while MBNL3 was unaffected by loss of either of these paralogs [93]. Such mutual compensatory increase was also reported in C2C12 muscle cells with shRNA-mediated knockdown of either paralog [49]. Overall, those data suggest that the mutual compensatory mechanisms between MBNL1 and 2 might be cell context-dependent.

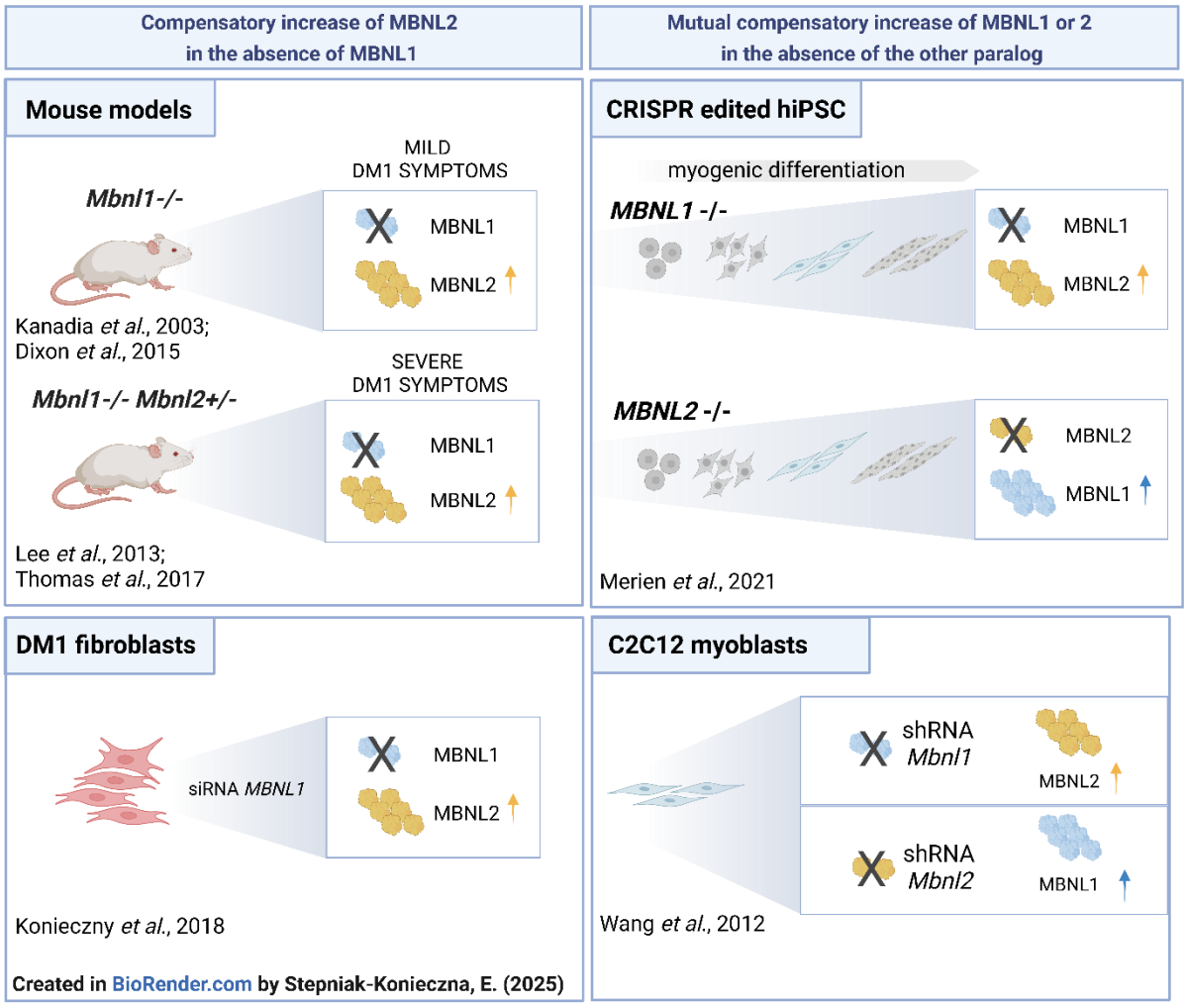

FIGURE 3. Compensatory increase of MBNL1 and MBNL2 paralogs. Left panel: Compensatory upregulation of MBNL2 in the absence of MBNL1 paralog was reported in *Mbnl1* KO mouse model [72, 90] and DM1 patients'-derived fibroblasts with siRNA-mediated knockdown of *MBNL1* [28]. Notably, *Mbnl1* null mice deficient in only one allele of *Mbnl2* displayed much more severe DM1 symptoms compared to *Mbnl1* KO mice, suggesting that MBNL2 may be involved in modifying DM1 severity [81, 86]. These mice also show MBNL2 protein levels elevated over WT mice [81]. **Right panel**: Mutual compensatory increase in either MBNL1 or MBNL2 protein levels in the absence of the other paralog, respectively, was reported in human induced pluripotent stem cells (hiPSC) which were CRISPR-edited to lack either *MBNL1* or *MBNL2* and subjected to myogenic differentiation [93] as well as in C2C12 myoblasts with shRNA mediated knockdown of *Mbnl1* or *Mbnl2* [49]. Further details in the main text. **Created in BioRender. Stepniak-Konieczna, E. (2025)** https://BioRender.com/ej75chg.

Non-mammalian vertebrate models of *muscleblind* deficiency

Three *muscleblind-like* genes (*zmbnl1, zmbnl2, zmbnl3*) have been identified in the zebrafish genome [18]. Although all of them have a very similar genomic organization and give rise to primary transcripts undergoing extensive splicing, comparable to human *MBNL* genes, there are several key differences between zebrafish and mammalian *muscleblind* orthologs. First, AS of the first three exons in *zmbnl2* generates mRNAs translated into a protein lacking the first ZnF pair. Such protein isoforms with a single ZnF pair have been detected for human MBNL1 and MBNL3, but not for MBNL2 or zebrafish *zmbnl1* and *zmbnl3* [4, 18, 94]. Second, all *zmbnl* genes including *zmbnl3* are expressed in adult zebrafish tissues, which is in a stark contrast to orthologs from higher vertebrates like mice and humans, in which *MBNL3* is expressed at a very low level in most adult tissues [18]. Third, unlike in mammals, zebrafish *zmbnl1* does not show predominant expression in skeletal muscle and heart. While *zmbnl1* is expressed in most adult tissues, *zmbnl2* is found mainly in heart and muscle whereas *zmbnl3* in eye, muscle, heart and testis [18]. The first comprehensive zebrafish model of DM-associated MBNL depletion was generated through LOF mutation of the three zebrafish z*mbnl* genes [19]. Homozygous zebrafish single, double as well as triple z*mbnl* LOF mutants were viable to adulthood which is clearly different from the phenotype observed in mouse mutants, in which combined loss of *Mbnls* in a homozygous state is incompatible with survival [81, 86]. Triple *zmbnl* zebrafish mutants exhibited phenotypes that are accurate to those observed in DM patients, e.g., decreased body size, altered motor function as well as widespread changes in AS events [19].

Invertebrate models of *muscleblind* deficiency

A nematode *Caenorhabditis elegans* contains a single *muscleblind* (*mbl-1*) gene orthologous to mammalian MBNL [95]. *Mbl-1* transcript was initially shown to generate two isoforms, *CeMbl-a* and *CeMbl-b,* respectively [17, 26]. In contrast to mammalian MBNLs characterized by four ZnF domains, CeMBL-A and CeMBL-B proteins contain only two ZnFs with distinguishable CCCH domain [17, 95], highly homologous to Cys(3)-His ZnF found in human MBNL1 [95]. Although both *mbl-1* transcripts are detectable in larval and adult stages, they seem to play major roles in an adult organism [17]. In early studies, a full-genome RNA interference (RNAi) knockdown of the predicted *C. elegans muscleblind* gene did not affect embryogenesis at all, suggesting MBL-1 redundancy in early embryogenesis and larval development [96]. In agreement, RNAi targeted to *mbl-1* transcripts affected only muscle structure and function in adult worms [17]. Essential roles of MBL-1 were also demonstrated in proper formation of neuromuscular junction synapses in neurons and dendrite

morphogenesis [97, 98] and in nematode lifespan control [99, 100]. In the latter case, interaction between nematode MBL-1 and the ELAV homologue exc-7 strikingly decreased the lifespan, as shown in *exc7;mbl-1* double LOF mutant worms. Additionally, the *CeMbl* mutant with deletion of e3 and flanking introns (resulting in a protein that lacks the ability to bind RNA) exhibited a reduced lifespan similarly to *exc7;mbl-1* double mutant [95]. More recent analyses of the reduced lifespan phenotype indicated that *Mbl-1* deficiency in *CeMbl* mutant worms reduced the activity of the p38 mitogen-activated protein kinase (MAPK; PMK-1 in *C. elegans*) and its downstream target genes *ATF-7* and *SKN-1* [101].

In a fruit fly *Drosophila melanogaster*, a single muscleblind gene (*mbl*) gives rise to primary transcript undergoing complex AS to generate seven mature canonical transcripts encoding protein isoforms MblA-G [59, 102]. Isoforms *mblA-D* have been most extensively studied; while *mblA-C* are translated into proteins with two complete CCCH-type ZnFs, *mblD* generates a smaller protein with only one complete ZnF [15, 26]. Because of this, it was proposed that *MblD* could potentially bind to RNA in an unproductive way and thus exert regulatory functions [26]. Profiling of *mbl* isoforms during fruit fly development revealed that they are functionally distinct, with *mblC* being the most widely expressed as well as the most ancient isoform [52, 103]. During development, *mbl* expression is tissue-specific, e.g., in photoreceptor differentiation [15], embryonic CNS and somatic muscles differentiation [16] as well as in development of neural substrates that regulate female sexual receptivity [104]. Data from cultured *Drosophila* S2 cells transiently transfected with *muscleblind* expression plasmids shows that different protein isoforms localize to the peri-plasma membrane (MblA), cytoplasm (MblB), or both, the nuclear as well as the cytoplasmic compartment (MblC and MblD) [39].

First described *Drosophila* LOF lethal mutants lacked normally differentiated photoreceptors within mutant tissue, indicative of *mbl* requirement in this developmental process [15]. Further work revealed that *mbl* loss-of-function lethal mutants die as late embryos exhibiting a clear musculature phenotype that involves disruption of sarcomeric Z bands and lack of extracellular matrix at indirect muscle attachment sites [16]. Muscle defects in *mbl* mutants are apparently caused by AS alterations in multiple muscle-specific transcripts including e.g. alpha-actinin [103, 105], Z-band associated transcript CG30084 (a homolog of human *ZASP/LDB3* mis-spliced in DM muscle) [105], troponin T [52] and calcium pump dSERCA [106]. In addition, silencing of *mbl* induced a subcellular redistribution in the muscle of two RBP proteins identified as key modifiers of the DM phenotype in a *Drosophila* DM model expressing 480 interrupted CTG repeats [i(CTG)480] [107], that is BSF (Bicoid stability factor; homolog of human LRPPRC) involved in cytoskeletal organization and vesicular transport, and TBPH (homolog of human TDP-43) implicated in a number of inherited neurodegenerative diseases [108]. This redistribution induced by Mbl depletion mimicked the effect induced by CTG repeats expression in i(CTG)480 flies. Moreover, BSF and TBPH localization to the muscle sarcomere was regulated by Mbl, but not vice versa, indicating that both proteins are downstream of Mbl and pointing to a novel cytoplasmic role of Mbl, different from its established activity as a AS regulator [108]. Worth adding, among all isoforms only MblC overexpression (OE) was able to rescue most of the *mbl* LOF lethal mutant embryos [103]. Remarkably, expression of human MBNL1 in *Drosophila muscleblind* embryos also rescued embryonic lethality [109] and suppressed both the somatic muscle and rough eye phenotypes in the i(CTG)480 model [107, 108], indicating functional conservation between human and fly proteins. Conversely, reduction of muscleblind levels by heterozygous LOF mutation in *mbl* aggravated the i(CTG)480 eye phenotype [107]. Notably, while the degree of i(CTG)480 phenotype suppression was dependent on MBNL1 OE level, transgenic lines expressing high levels of MBNL1 exhibited a muscle phenotype on their own, even in the

absence of i(CTG)480[107], altogether pointing to the importance of the steady-state levels of the protein.

MBNLs in physiological processes

As developmental sensors, MBNL proteins are crucial for differentiation and function of various tissues and have been implicated in multiple physiological processes including cellular reprogramming, skeletal muscle and heart function, structural integrity and plasticity of the nervous system as well as hematopoiesis and myeloid lineage commitment, among others (**Figure 4**).

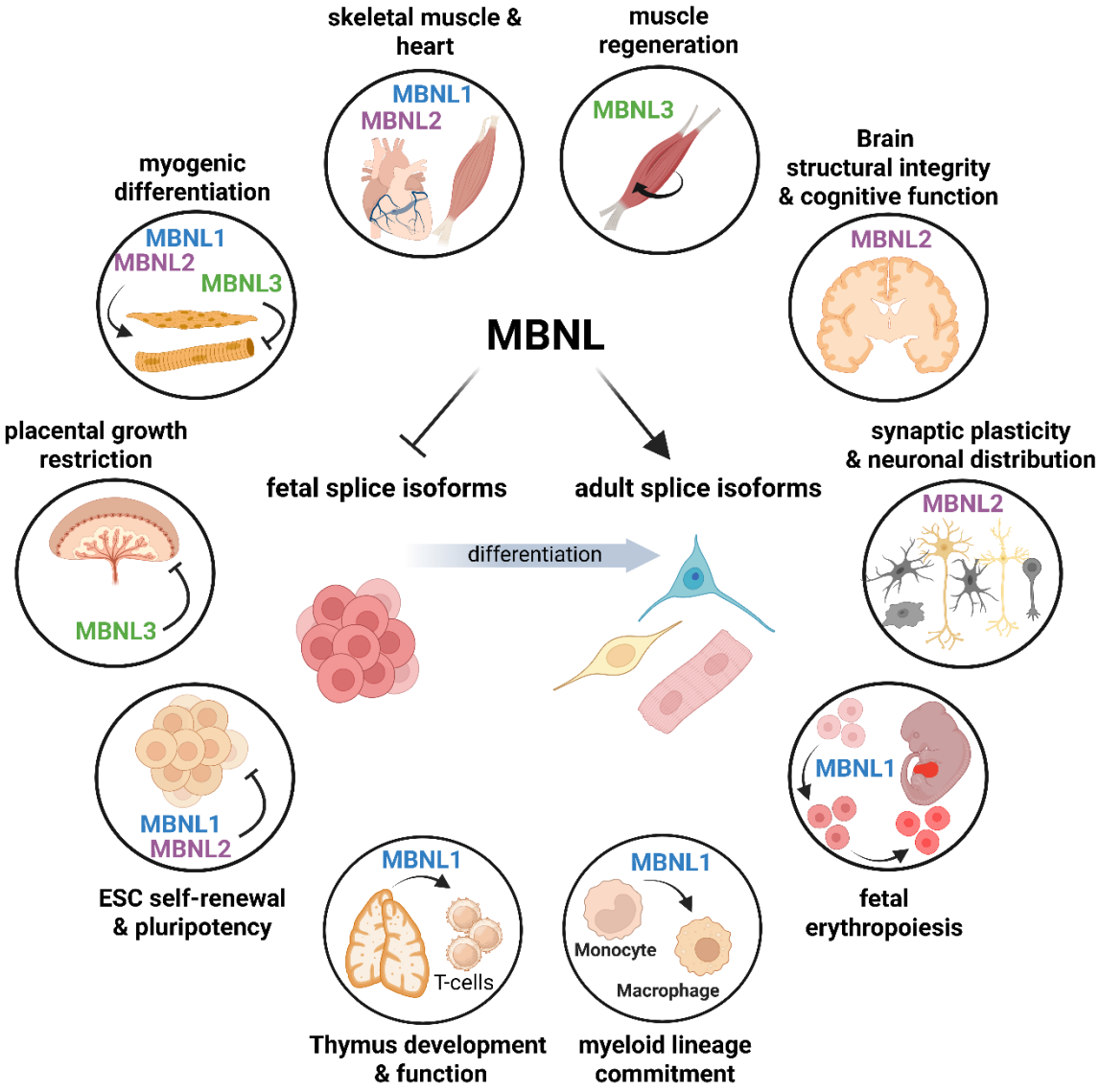

FIGURE 4. Main physiological roles of MBNL proteins. MBNL proteins promote cellular differentiation by repressing fetal splicing patterns and supporting splicing pattern typical of adult tissues. As such, MBNLs are critically involved in differentiation and maintenance of many tissues and organs including muscle, nervous system and the brain as well as hematopoietic and the immune system. The specific roles of MBNL paralogs in these processes can be mutual or opposing, compensatory or redundant, as detailed in in the main text. **Created in BioRender. Stepniak-Konieczna, E. (2025)** https://BioRender.com/kaumxto.

Embryonic stem cell differentiation

In human and mouse, motifs corresponding to consensus binding sites of MBNL proteins are strongly associated with embryonic stem cells (ESCs) differential AS, as revealed by RNA-seq analyses of alternative exons differentially spliced between ESCs, iPSCs and diverse differentiated cells and tissues [12]. In particular, MBNL1 and MBNL2 paralogs were found to be direct negative regulators of a large program of cassette exon AS events that are characteristic of ESCs. MBNLs' expression is at minimal levels in ESCs compared to differentiated cell types, and in the latter they may repress ESC-differential exons and/or activate the inclusion of exons that are skipped in ESCs [12]. For instance, a conserved and partially redundant roles of MBNL1 and MBNL2 proteins were demonstrated in the negative regulation of ESC-specific FOXP1/Foxp1 exon 18b/16b inclusion in human and mouse, respectively. The presence of this exon is crucial for maintaining ESC self-renewal and pluripotency, as it affects DNA binding properties of FOXP1 transcription factor to promote the expression of core pluripotency genes including *OCT4*, *NANOG*, and *SOX2* [12, 110]. Consistently, OE of MBNL1 proteins in ESCs triggered silencing of those pluripotency factors upon differentiation and promoted the expression of specific lineage markers representative of all three germ layers, while knockdown of *MBNL1* in differentiated cells enhanced somatic cell reprogramming leading to ESC-like AS pattern [12]. Additional analyses of AS changes during induction of fibroblasts into iPSCs and their subsequent re-differentiation indicated that stem-cell specific AS pattern mirrors knockdown of *MBNL1* [111]. The *in vivo* significance of MBNL-regulated AS in ESC biology was demonstrated in a planarian flatworm model, where knockdown of MBNL or CELF orthologs revealed their direct antagonistic effects on planarian regeneration *in vivo* by affecting the stem cell-specific transcriptome [112]. Specifically, negative regulation of stem-cell characteristic AS by MBNLs was counteracted via positive effect of CELF [112]. Thus, the functional interplay between MBNL and CELF may form an ancestral developmental regulatory switch module that controls pluripotent vs differentiated transcriptome. Strikingly, these findings may have profound consequences for carcinogenesis, as cancer cells often possess low MBNL expression profile that could facilitate reversion to an embryonic AS pattern and promote malignant reprogramming by enhancing survival and self-renewal.

Placenta development

Among splicing factor genes differentially expressed between trophoblastic and embryonic mouse tissues, *Mbnl3* displays the strongest placenta-specific enrichment alongside very low levels of expression in nonplacental tissues [31]. *Mbnl2* is also expressed in placenta and both *Mbnl2* and *Mbnl3* coregulate AS and polyadenylation during placenta development and embryo growth. However, while both *Mbnl2* and *Mbnl3* appear to have been recruited to the placenta early in eutherian evolution, concomitant loss of expression from other tissues was found only for *Mbnl3*, but not for *Mbnl2* [31]. This is likely associated with the evolution of a novel promoter and the emergence of a short isoform lacking the first ZnF pair [31] as well as genomic localization of *Mbnl3* on the X chromosome.

Moreover, MBNL3 was found to restrict placental growth in mouse development via inhibitory effect on cell proliferation through *Myc*-dependent pathway [31]. RNA-seq analyses in *Mbnl3* KO placentas revealed upregulation of *Myc* and its associated regulatory network, consistent with an increase in proliferation contributing to the larger placentas observed in mutant mice. The association between MBNL3 and Myc seems to be indirect, as no evidence for MBNL3 binding directly to *Myc* transcripts was found so far [7, 31, 113].

Skeletal muscle biology

MBNL proteins are required for myogenic differentiation throughout development as well as for normal muscle function in the adult organism, including postnatal muscle remodeling. The overall increase in MBNL protein level during muscle differentiation coincides with the fetal-to-adult splicing transition of hundreds of their target RNAs [49]. The expression level of individual *MBNL* genes and specific functions of MBNL proteins differ largely during these processes [114]. While *MBNL1* governs the majority of functions in developing and adult skeletal muscle biology [2, 114], *MBNL2* is downregulated during myogenic differentiation [114, 115] and kept at low levels in adult muscle tissue [6]. Specifically, direct comparison experiments showed a marked increase in *MBNL1* expression during muscle differentiation, approximately 10-fold lower level of *MBNL2* and hardly any *MBNL3* in the adult muscle, with a transient *MBNL3* activation during the early stages of regeneration [2, 3, 6, 28, 114-116]. The dominance of the MBNL1 paralog in the mature striated muscle explains why ablation of the mouse *Mbnl1* gene alone is sufficient to cause myotonic dystrophy features [72], while mice deficient in *Mbnl2* fail to show an obvious muscular phenotype [6]. Intriguingly, compound loss of both paralogs in mice is crucial for increasing the severity of muscle-related hallmarks in DM [81].

In stark contrasts to MBNL1 and 2, the MBNL3 paralog acts as an inhibitor of myogenic differentiation [7, 24]. This antagonizing effect is exerted via multiple mechanisms which include, e.g.: (i) suppression of early differentiation marker myogenin and inhibition of sarcomeric myosin heavy chain (MyHC) induction [24], (ii) inhibition of myogenic differentiation 1 gene (MyoD)-dependent myogenic genes transcription [8], (iii) repression of the alternatively spliced β-exon of myocyte enhancer factor 2D (*Mef2D)* to suppress its expression [117], while at the same time (iv) promotion of myoblast proliferation [7, 24, 118]. MBNL3 is expressed mainly in embryonic development and consistent with its inhibitory function during muscle differentiation, the levels of MBNL3 are low in adult cardiac and skeletal muscle and also decrease in C2C12 muscle cells undergoing differentiation [118]. However, MBNL3 is essential for normal adult muscle satellite cell activation and myoblast function as well as for adult muscle tissue remodeling [7]. Loss of *Mbnl3* delayed injury-induced muscle regeneration and impaired muscle function [7]. In contrast, the regenerative capacity and satellite cell numbers were not affected by the deletion of *Mbnl1* or *Mbnl2* alone [91], despite earlier reports showing that MBNL2 expression remains high in regenerating muscle fibers implying its role in muscle tissue remodeling [119],

MBNL1 and MBNL2 regulate also the microtranscriptome dynamics during postnatal development of skeletal muscle by affecting miRNA levels and biogenesis, the latter through the control of the alternative splicing of primary miRNA transcripts. [120]. Notably, MBNL1 had a greater impact on miRNA biogenesis than MBNL2, consistent with its predominant splicing activity in skeletal muscle tissue. These findings suggest that MBNL sequestration in DM may be partially responsible for altered miRNA activity observed in patients' tissues.

Cardiac muscle biology

Similarly to the skeletal muscle tissue, *MBNL1* is also the dominant paralog in the heart, both embryonic and adult [2, 121, 122] with markedly lower *MBNL2* levels and very low *MBNL3* amounts [2]. During development, a shift in the splicing of *MBNL* alternative exons is observed in cardiac tissue akin to the one observed in the skeletal muscle [2, 53] with reduced percentages of transcripts containing e5 and e8. MBNL1 is also the major driver of fetal-to-

adult AS transitions of cardiac transcripts during late fetal and postnatal heart development in mammals [121].

While *Mbnl1* KO mice revealed heart conductive abnormalities and fibrosis [90], other murine models of DM characterized by functional depletion of MBNL proteins also display cardiac phenotypes. These include the DM200 transgenic mice expressing the *DMPK* 3' UTR [123] and the HSA^{LR} transgenic mice expressing a human skeletal actin gene carrying a CTG repeat expansion [124, 125], which reproduce cardiac conduction defects, heart block and sudden death. Furthermore, consistently with the results from skeletal muscle, *Mbnl1*-deficient mice with conditionally deleted *Mbnl2* gene in the heart show a more severe pathogenesis and spontaneous lethal cardiac phenotype, mirroring the phenotype observed in DM patients [89]. This severe cardiac pathology could be explained by splicing alterations in specific mRNA targets as well as changes in gene expression and the resultant protein synthesis [89, 126, 127]. A well-studied example includes cardiac isoform of troponin encoded by the *TNNT2* gene, one of the major targets of MBNL1 within cardiac tissue that determines calcium sensitivity of the muscle fibre [69, 128]. Depletion of MBNL1 causes *TNNT2* mis-splicing and production of an e5-included isoform, giving rise to a protein conferring different calcium sensitivity to the myofilament, which ultimately negatively affects the contractile properties of cardiomyocytes and reduces myocardial function [69, 128].

During cardiomyocyte development MBNLs are essential regulators of AS of transcripts important in vesicular trafficking, mechano-sensing, formation of cardiomyofibral structures as well as maintaining of the overall mitochondrial homeostasis [89]. Loss of both *Mbnl1* and *Mbnl2* triggered spliceopathy of mRNAs encoding proteins involved in these processes, including, e.g.: *Nexn*, *Ttn* (involved in mechano-sensing, myofibril elasticity and structural integrity), *Plekhm2, Prune 2*, *Aplp2* (involved in vesicular/post-endocytic trafficking) and *Mff* (involved in mitophagy/endocytic pathway) [89]. Also, the mis-regulation of several transcripts encoding ion channel proteins, including *Scn5a, Kcnip2*, *Ryr2* and *Camk2d*, suggests a critical role for MBNL1 and 2 in DM cardiac pathogenesis via control of ion channel trafficking [89]. Loss of both paralogs affected also gene expression, causing, e.g., downregulation of genes critical for mitochondrial respiratory chain biogenesis, or upregulation of proteins crucial for calcium buffering [89]. In particular, increased amounts of *Casq1* mRNA, encoding a protein that regulates calcium release from sarcoplasmic reticulum in skeletal muscle, may - in the absence of MBNLs - substantially affect excitation-contraction coupling and signaling pathways that are essential for maintaining normal cardiac function [89]. MBNL1 regulates also the AS of a network of cardiac transcripts encoding proteins crucial for intra- and intercellular transport (e.g., *Atp2a1*, *Junctin*, *Cacna1s*, *Ryr2*), cell survival (e.g., *Capn3*, *Sirt2*), sarcomere and cytoskeleton organization (e.g., *Trim55*, *Mapt*, *Pdlim3*, *Sorbs1*, *Fhod1*) and structural components of the sarcomere (e.g., *Myom1*, *Tnnt2*, *Zasp*) [90]. Consistently, MBNL1 depletion results in the persistence of embryonic splice isoforms of these mRNAs, initiating cardiac pathology and ultimately leading to the development of DM cardiac disease.

Nervous system development and function

While both MBNL1 and 2 play important roles in AS regulation during formation and maintenance of synaptic architecture, neuronal distribution and dendritic morphology in the developing brain [129], MBNL2 is the most predominantly expressed paralog in brain tissue and its loss leads to widespread splicing abnormalities [6, 49]. Key examples of MBNL2-regulated events include the AS of the N-methyl-D-aspartate receptor 1 (*Nmdar1*) gene, a crucial component of the synaptic machinery involved in long-term potentiation process

underlying learning and memory, also involved in synaptic function and plasticity [6]. Likewise, the survival, differentiation and growth of neurons is controlled by MBNL2-dependent AS of the brain-derived neurotrophic factor (*Bdnf*) gene, while signaling of the neurotransmitter dopamine via AS of the dopamine receptor D2 (*Drd2*) gene [130]. Through regulation of numerous alternative exons during brain development, MBNL2 also affects transcripts localization and translation [6]. MBNL2 also promotes adult splicing events during dendritic spine development via AS of transcript encoding synaptic protein adducin 1 (ADD1), an essential factor in spinogenesis through interaction with alpha-II spectrin (SPTAN1) [87]. MBNL2-dependent AS alterations were also reported during choroid plexus development, affecting ion homeostasis, secretory output and cerebrospinal fluid composition [131].

Additionally, both MBNL1 and 2 regulate brain structural integrity including brain and ventricle volume, white matter and anterior commissure structure as well as gray matter structure (isocortex, hippocampus, inter-/midbrain, hindbrain) [132], while polyubiquitinated cytoplasmic MBNL1 enhances neurite outgrowth and morphogenesis, and reverses defects in neurite morphogenesis caused by expanded RNA in DM [133]. Both MBNL1 and 2 control brain development by combined regulation of the AS of *MAPT* transcript encoding the microtubule-associated protein Tau [134] and may also affect behavioral changes [132], while only MBNL2 regulates REM sleep and cognitive functions [6]. Recent study also highlighted the complex roles of MBNL proteins in neuromuscular junction maintenance in motor neurons essential for muscle function and locomotion. It appears that MBNL1 and 2 regulate neurotransmission in motor neurons by targeting diverse transcripts which encode for proteins involved in synaptic vesicle homeostasis, neurotransmitter release and RNA localization (e.g., *Dvl1* e14b, *Claps1* e26, *Tanc2* e23 and *Cacna1d* e12) [88]. Finally, disruptions in MBNL function have been linked to neurodevelopmental disorders, including certain forms of autism spectrum disorders, as shown by a recent study which revealed that MBNL loss triggered developmental mis-splicing of autism-risk genes, along with social behavioral deficits and altered responses to novelty [135].

Hematopoiesis and the immune system

During mammalian development, fetal liver serves as an important center of hematopoiesis, a layered and multistep process of commitment into erythrocytes, lymphoid and myeloid lineage cells. Although loss of neither MBNL paralog is associated with developmental liver defects, MBNL1 plays essential role in fetal erythropoiesis [136]. Among the three family genes, only *Mbnl1* expression was found in both fetal and adult stage of erythropoiesis, while *Mbnl2* was expressed only in adult, and *Mbnl3* in neither erythropoietic stage (The Erythron Database ([137]) and [136]). Knockdown of *Mbnl1* in cultured murine fetal liver cells disrupted the developmentally regulated exon skipping in *Ndel1* transcript, normally bound by MBNL1, and adversely affected hematopoiesis by impairing terminal proliferation and differentiation of liver erythroid progenitors [136]. Ndel1 protein is essential in mitosis and neurogenesis, constitutes a key component of cytoskeletal organization and dynamics and may serve as a docking platform for several regulatory and signaling proteins. During terminal erythropoiesis both, the nuclear *MBNL1* e5-included as well as the cytoplasmic *MBNL1* e5-excluded mRNA isoforms, are expressed. However, knockdown of both subcellular isoforms simultaneously or only e5-included isoform alone was able to maintain erythroblasts in an undifferentiated stage by affecting *Ndel1* splicing. This indicated the critical role of the nuclear e5-included isoform in erythroid differentiation and supported the essential role of MBNL1 in terminal erythropoiesis [136].

Conversely, another study demonstrated only modest effect of *Mbnl1* loss on normal human hematopoiesis. At both, steady-state as well as stress conditions induced by a sublethal dose of 5-Fluorouracil, *Mbnl1* KO and WT mice displayed no differences in peripheral blood counts, bone marrow cellularity, progenitor and stem cell counts and time to recovery of red and white blood cells and platelets [14]. Likewise, bone marrow repopulation upon lethal irradiation remained unaffected regardless of MBNL1 presence [14]. In stark contrast, loss of MBNL1 significantly impaired development and propagation of murine and human mixed lineage leukemia (MLL)-rearranged leukemia *in vitro* and *in vivo*, indicating that while under steady-state conditions murine hematopoietic system functions normally without MBNL1, this splicing factor is essential for survival and propagation of transformed hematopoietic cells [14].

Mbnl1 is highly expressed in murine thymus [20] and promotes its development and function [83]. Loss of *Mbnl1* led to aberrant thymic gene expression, pre-mRNA misprocessing and mis-splicing of factors regulating thymocyte/T-cell development, including transcription factors of the TCF/Lef family (e.g. *LEF1* e6). Ultimately, these events triggered postnatal thymic hyperplasia with thymocyte accumulation and pointed to MBNL1 role in the immune system [83].

High-depth RNA-seq profiling of human primary monocytes differentiated into macrophages demonstrated that MBNL proteins are critical regulators of myeloid lineage commitment [138]. Differentiation of monocytes into macrophages was accompanied by major changes in gene expression and AS, particularly in events characterized by net increase in exon inclusion. MBNL1 was significantly downregulated during this process, while MBNL2 expression remained unchanged and MBNL3 was only slightly downregulated. Multiple differential AS events during monocytes to macrophages differentiation were largely recapitulated by knockdown of *MBNL1* in undifferentiated cultured monocytes [138] as well as other cell models [12]. Surprisingly, *MBNL1* knockdown strongly impaired phorbol ester induced differentiation and activation of primary monocytes, indicating that apart from MBNL1-mediated regulation of AS, other processes such as mRNA localization may be essential for myeloid lineage commitment [138]. In all, this may have pronounced physiological consequences in processes involving inflammation and wound healing like infection, tissue damage or regeneration, when blood monocytes migrate into tissues and differentiate into macrophages to directly combat infection via pro-inflammatory response and clearing off cellular debris, or via anti-inflammatory wound healing response. Conversely, excessive monocyte differentiation into macrophages and their activation could trigger autoimmunity, inflammation and sepsis as well as metastasis promotion in certain cancers. In all, this exemplifies central roles of MBNL1-dependent AS in the immune system.

Multifaceted roles of MBNLs in pathological conditions

MBNLs dysfunction in Myotonic Dystrophy

Myotonic dystrophy (DM), a highly variable multisystem disorder manifested mainly by muscle hyperexcitability (myotonia) and overall muscular weakness and atrophy, is the most common form of muscular dystrophy in adulthood. DM patients suffer also from heart conductions disturbances, arrythmia, dilated cardiomyopathy and heart failure, with males showing more severe phenotype than affected women [139]. Common features involve insulin-resistance and cataracts [21] while post mortem studies revealed fibrosis and fatty infiltration in patients' hearts [140].

The two genetically distinct types of the disease, the DM type 1 (DM1; OMIM #160900) and DM type 2 (DM2; OMIM #602668), are caused by nucleotide repeat expansion within noncoding regions of two unrelated genes: a (CTG)n triplet expansion within the 3′ untranslated region (3′UTR) of *dystrophia myotonica protein kinase* (*DMPK*) gene [21-23] and a (CCTG)n tetranucleotide repeat expansion within intron 1 of *cellular nucleic acid binding protein* (*CNBP*) gene [141-146], respectively. While the size of DM1 expansion strongly correlates with the disease severity, likely due to efficiency of MBNL sequestration on expanded repeats [3], no such correlation was demonstrated for DM2 [147] which also lacks the congenital form observed in DM1. The DM1 expansion size is highly variable between distinct tissues of distinct patients or even within the same tissue of a single patient. Factors contributing to this heterogeneity include germline variation that affect intergenerational differences, as well as substantial somatic expansion and mosaicism [21, 148-151]. In DM1, notably, the skeletal muscle and the heart in particular show larger CTG expansion compared to other tissues, e.g., blood [152]. Intriguingly, while gene mutation constitutes the underlying cause of DM, the disease pathology itself is not related to DMPK or CNBP protein deficiency, but stems from toxic RNA transcribed from those genes.

Mutant transcripts carrying pathogenic C/CUG expansions (C/CUG^{exp}) assemble thermodynamically stable double-stranded RNA hairpin structures which accumulate in the cell nuclei as discrete foci (inclusions) that attract and sequester distinct poly(CUG) RBPs [153-158]. Although multiple mechanisms and pathways contribute to disease hallmarks downstream of nucleotide expansions, in this review we focus specifically on those pertaining specifically to MBNL proteins, the key players in DM pathogenesis. The findings that all three mammalian MBNL paralogs colocalize with nuclear foci of CUG^{exp}/CCUG^{exp} RNA [3, 4, 116] and that this binding correlates with repeat length [3], shaped the initial hypothesis on a direct link between MBNL deficiency and a pathogenic process and provided first glimpse into molecular mechanism underlying DM. Notably, MBNL proteins are not merely trapped in foci, but assemble labile nuclear aggregates with constantly forming and disaggregating structures, causing free versus sequestered pools of MBNL to be very dynamic [53, 159]. Data indicates that when CUG^{exp} foci are saturated with MBNLs (e.g., when expansions are relatively small), the proteins may freely dissociate from these structures and are rapidly exchanged by nucleoplasmic MBNL proteins. Conversely, when unoccupied binding sites are still available within longer expansions, MBNL proteins circulate within RNA foci continuously changing the intra-foci binding sites on CUG^{exp} transcripts [53]. The latter, unsaturated model, takes into account the stoichiometry of MBNL and its binding sites thus partly explaining the mechanism underlying increasing sequestration and splicing deregulation as the disease progresses [53]. The repeat-imposed sequestration depletes the cellular pool of active MBNLs causing their functional imbalance and consequently hampering AS of hundreds of target pre-mRNAs. As a result of this imbalance, a shift in the splicing pattern occurs, mimicking the one observed in

fetal and neonatal tissues (DM spliceopathy) (**Figure 5**). Cumulatively, these splicing alterations lead to translation of protein isoforms unfitted to perform their function in an adult organism, ultimately driving pathological changes in multiple tissues, particularly muscle.

While detailed spectrum of AS alterations in adult DM1 muscle has been reviewed extensively [160, 161], we highlight a few selected MBNL-dependent AS events disrupted in muscle and causal to DM1 hallmarks - myotonia, muscle weakness and wasting (**Figure 5**). The muscle-specific chloride voltage-gated channel 1 protein (CLCN1), which controls proper muscle contraction and relaxation, is encoded by *CLCN1* - one of the best studied MBNL1 targets. Reversal to fetal splice pattern of *CLCN1* in MBNL-depleted DM1 skeletal muscle causes a failure to express the adult isoform of the CLCN1 protein, leading to prolonged muscle contractions and delayed relaxation due to defective ion conductance and excitability, defined as myotonia [162, 163]. Specifically, MBNL1 exhaustion triggers an in-frame inclusion of intron 2 and exon 7a of *CLCN1*, generating a pre-mature stop codon. Truncated CLCN1 protein cannot localize within the membrane, leading to its hyperexcitability [121, 164-166]. Similarly, proper calcium-dependent contraction/relaxation cycle within the muscle depends on MBNL1-regulated AS of three main transcripts that encode proteins involved in this process, including calcium channel CaV1.1 (CACNA1S), ryanodine receptor 1 (RYR1) and sarcoplasmic/endoplasmic reticulum Ca^{2+}-ATPase SERCA1 (ATP2A1) [167] [168]. Depletion of MBNL1 in DM1-muscles promotes neonatal splicing isoforms of these transcripts, such that they lack e29, e70 or e22, respectively, thus contributing to muscle weakness via altered excitation–contraction coupling (*CACNA1S*), decreased muscle contraction (*RYR1)* as well as muscle degeneration due to impaired intracellular calcium homeostasis *(ATP2A1).* Further, proper tubular invaginations of muscle membranes and the biogenesis of muscle T tubules are regulated via MBNL1-dependent AS of transcripts encoding bridging integrator-1 protein (BIN1). Loss of functional MBNL1 in DM promotes *BIN1* isoforms lacking exon 11 and the expression of an inactive form of BIN1 protein, leading to muscle weakness due to altered excitation–contraction coupling [169]. Similarly, increased exclusion of *dystrophin* (*DMD*) exons 71 and 78 in the absence of MBNL1 compromises muscle membrane integrity leading to muscle weakness [170, 171]. Notably, titration of MBNL activity revealed that distinct splicing events respond with different strength depending on the concentrations of free MBNLs, hence even small fluctuations may affect the AS outcome and the severity of the disease manifestations, particularly in muscle tissue [75].

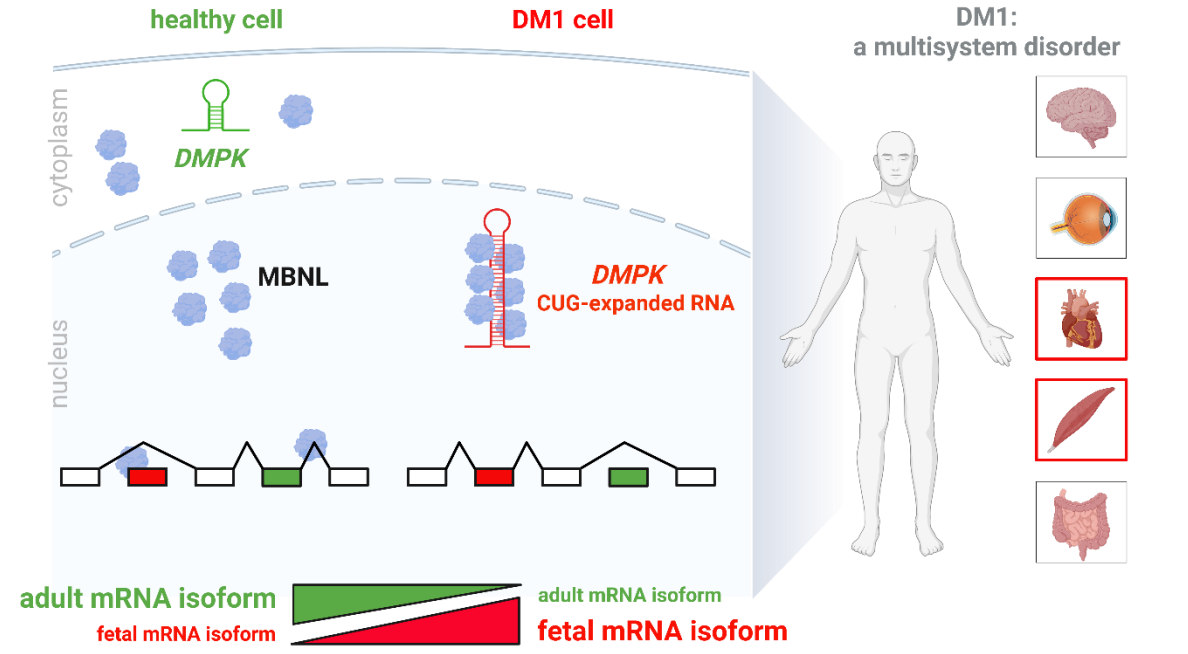

CLCN1	-e7a	+e7a	loss of chloride channel function hyperactivity of the muscle cell membrane	MUSCLE MYOTONIA
DMD	+e71 +e78	-e71 -e78	cell membrane damage in muscle cells	MUSCLE WEAKNESS & WASTING
BIN1	+e11	-e11	disrupted biogenesis of muscle T tubules altered excitation–contraction coupling	
ATP2A1	+e22	-e22	disturbed calcium ion homeostasis	MUSCLE DEGENERATION

Created in BioRender.com by Stepniak-Konieczna, E. (2025)

FIGURE 5. Myotonic dystrophy type 1 results from a functional depletion of MBNL proteins. In healthy cell, balanced cellular pool of MBNL proteins controls alternative exon inclusion and exclusion, promoting adult splicing patterns. In DM1 cells, toxic *DMPK* transcripts carrying stretches of expanded CUG repeats sequester multiple RBPs including MBNL proteins, within ribonuclear foci. Functional depletion of MBNLs from the nucleoplasm alters the AS pattern leading to generation of predominantly fetal-like mRNA isoforms. These transcripts give rise to proteins inapt to perform in adult tissues, leading to multiple disorders in distinct tissues of DM patients including brain, eyes, skeletal muscle and heart as well as gastrointestinal tract, among others. In particular, muscle dysfunction is directly caused by aberrant AS of *CLCN1* [77, 165], *DMD* [170, 171], *BIN1* [169] and *ATP2A1* [168], among many other altered splicing events, as detailed in main text. **Created in BioRender. Stepniak-Konieczna, E. (2025)** https://BioRender.com/r4mscbl.

Dysfunction of MBNLs in other nucleotide repeat-expansion disorders

Pathogenicity of abnormal MBNL localization and function was implicated in a subset of rare neurodegenerative diseases caused by exonic CAG trinucleotide repeat expansions that are translated into abnormally long polyglutamine (polyQ) tracts, including Huntington's disease-like 2 (HDL2; [172]), Huntington's disease (HD; [173]) and spinocerebellar ataxia type

3 (SCA3; [174]) and 8 (SCA8;[175]). Other tandem repeat disorders including fragile X-associated tremor/ataxia syndrome (FXTAS; [176]) and amyotrophic lateral sclerosis (ALS; [177]) are also associated with MBNL aberrations.

While HD is caused by a CAG repeat expansion in the huntingtin (*HTT*) gene, HDL2 develops as a consequence of a CTG/CAG triplet expansion in the *JPH3* locus [172]. Apart from pathogenic pathway including transcription of CAG transcripts and their translation to polyQ proteins forming toxic ubiquitin-positive inclusions, important pathogenic route in both diseases involves the toxic effect of MBNL sequestration on expanded RNAs. Mutant *JPH3* mRNA inclusions with MBNL1 and consequent alterations in splicing of *MAPT* and *APP* in HDL2 frontal cortex were reported [178]. Notably, the CUG foci and the ubiquitin-positive inclusions did not frequently co-localize within the neuronal nuclei, indicating that they are distinct pathogenic entities [172, 179]. Expanded CAG RNAs were also shown to sequester MBNL1 in cell and mouse models of HD [173, 180], indicating that dysfunction of MBNLs might be a common cause of mRNA splicing misregulation in polyQ diseases.

SCA3, the most common spinocerebellar ataxia, is caused by abnormal CAG repeat expansion in exon 10 of *ATXN3* gene, leading to the expression of aberrant protein with an expanded polyQ stretch that easily aggregates and deposits in the neurons of the cerebellum and brainstem [181]. Intriguingly, OE-based screen in a *Drosophila* model of ataxin-3 for modifiers of polyQ-induced eye degeneration identified insertional mutation in the promoter region of *mbl* gene [174]. This mutation led to upregulated *mbl* gene expression which dramatically enhanced toxicity, causing severe pigmentation loss and striking collapse of the retina, but had no effect on its own when directed to the eye. Notably, Mbl increased the level of the polyQ RNA as well as protein, accelerating inclusion formation. The Mbl association with polyQ toxicity is conserved, as flies co-expressing human MBNL1 isoform 40 with pathogenic SCA3 also displayed dramatically enhanced toxicity [174]. Of note, transgenic flies expressing human MBNL1 35, an isoform lacking e4 critical for optimal CUG repeat binding and conserved in *Drosophila* Mbl, exhibited only mild enhancement of the toxic phenotype. In all, these data indicate that MBNL1 modulates polyQ toxicity by acting at the RNA, while other contributing mechanisms remain to be identified [174].

SCA8 is a slowly progressing ataxia caused by a CTG/CAG expansion in the SCA8 locus [175, 182]. Two transcripts with expanded repeats are generated from two overlapping genes, with *ATXN8OS* lying on the plus strand and *ATXN8* on the minus strand, respectively. The CAG expanded transcript, derived from *ATXN8*, is translated in different reading frames resulting in, among others, a polyQ protein [183, 184] forming ubiquitinated neuronal nuclear inclusions [185]. The CUG expanded transcript derived from *ATXN8OS*, on the other hand, does not generate protein and accumulates in the nucleus sequestering MBNL [186], similarly to the phenotype observed in DM1 and HDL2. These expansions contribute to a toxic gain-of-function at both the RNA and protein levels. Importantly, targeted genetic screen in *Drosophila* overexpressing SCA8 with a CTG expansion identified *muscleblind* as one of the key dominant modifiers and enhancers of SCA8-induced late-onset progressive neurodegeneration in the retina [187]. This interaction was likely synergistic, as the modifier did not exhibit dominant eye phenotype on its own. Moreover, MBNL sequestration in post-mortem brain tissue samples correlated with splicing alterations and upregulation of the GABA-A transporter 4 (*GAT4*) mRNA that in turn might indicate loss of the GABAergic inhibition in the cerebellum. Interestingly, splicing of the *GAT4* mRNA is unaltered in DM1, which might be due to the distinctive expression patterns of *DMPK* and *ATXN4* in the brain [186].

FXTAS is a neurodegenerative disorder caused by a limited expansion of CGG trinucleotides in the 5' untranslated region of the *FMR1* gene and manifested at the molecular level in slightly elevated *FMR1* mRNA and decreased FMRP protein, respectively [188-194]. Larger expansions above 200 repeats cause fragile X syndrome (FXS), an early-onset disorder in which no mRNA and no protein is generated due to the hypermethylation of the *FMR1* promoter and transcriptional silencing [176, 195]. Degeneration of neurons, a key FXTAS hallmark, could be attributed to sequestration of a number of proteins on the mutated *FMR1* mRNA [196-200] as well as toxicity of polyglycine protein translated from the mutated mRNA upstream to the CGG repeats [201-205]. While MBNL was found in both ubiquitin-positive inclusions and CGG aggregates [196, 198], MBNL mis-localization, although significant, appears to be only a secondary event and its splicing function is largely unaltered in FXTAS patients, likely because it is not immobilized in the FXTAS-associated inclusions and may still perform its roles [196]. Recently, however, a study with *Fmr1* deficient mice challenged this view by demonstrating widespread mis-splicing events (mostly exon skipping) in all brain regions and peripheral tissues of the mutant animals, which were in major part contributed to upregulated activity of MBNL1 and MBNL2 [206]. The study showed that in a healthy tissue, *Mbnl1/2* transcripts are translationally inhibited by a direct interaction with FMRP and in the absence of the latter, an increase in *Mbnl1* and *Mbnl2* translation results in a frequent autoregulatory skipping of NLS-containing exon 5 from their pre-mRNAs. This in turn alters MBNLs nucleus-cytoplasm distribution and affects the splicing decisions on target mRNAs, contributing to the overall pathology in FXTAS [206].

Finally, MBNL proteins affect FUS (*fused in sarcoma*)-associated ALS. Mutations in *FUS* gene contribute to the familial and sporadic ALS [207], a devastating neurodegenerative disease, in which degeneration of motor neurons induces progressive denervation of voluntary muscles [177]. FUS is mostly a nuclear protein interacting with both DNA and RNA [208] and plays essential roles in various stages of RNA processing including transcription, AS and RNA trafficking and in the maintenance of the genome integrity [209]. Accumulation of mutated FUS in stress granules perturbs their dynamics and results in dysregulation of mRNA processing and cellular toxicity [210, 211]. Interestingly, knockdown of MBNL1 in *FUS*-mutated neurons ameliorated defects in dendrite morphology and cellular toxicity by releasing FUS from stress granules indirectly via restoration of survival motor neuron (SMN) protein localization [210]. In contrast, downregulation of MBNL did not suppress toxicity of other proteins linked to ALS, such as TDP-43, also shown to localize to stress granules [210, 212]. Cumulatively, this data indicates that the therapeutic rescue effect of MBNL-depletion is only specific for FUS-associated ALS.

Dual roles of MBNLs in cancer

Essential genes associated with cellular proliferation, apoptosis, invasion and metastasis undergo aberrant AS in cancerous cells, thus not surprisingly MBNLs have been implicated in tumorigenesis. Emerging evidence shows that MBNL proteins may act as a double-edged sword in tumorigenesis serving either tumor suppressive or pro-oncogenic functions. We review selected examples of these dual roles, emphasizing that they are cell, tissue type- and context-dependent. Mechanistically, these roles are controlled by MBNLs via AS of target RNAs implicated in cancer-associated networks, impact on cancer-related transcripts stability or direct effect on multiple circRNAs and lncRNAs implicated in tumorigenesis. Moreover, these roles are often determined by *MBNL* isoform switch. Numerous evidence shows that through these basic mechanisms MBNLs may modulate virtually all cancer hallmarks, from cell cycle checkpoints and signaling pathways crucial for

cancer cell survival, proliferation and replicative immortality, to angiogenesis, invasion and metastasis (**Figure 6**).

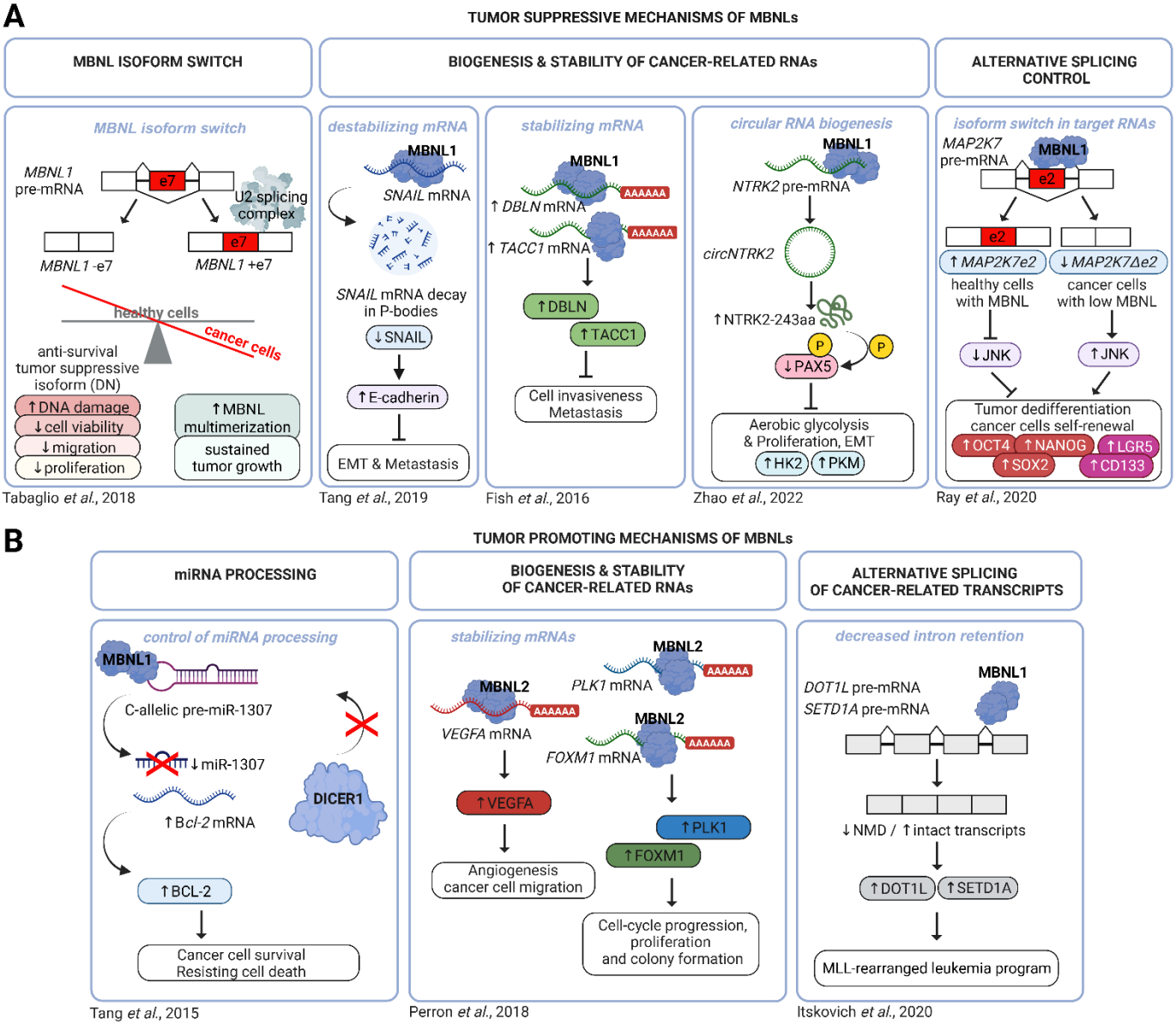

FIGURE 6. Duplicity of MBNLs in cancer. MBNLs may affect virtually all cancer hallmarks through several basic molecular mechanisms involving isoform switch [13], RNA biogenesis, processing and stability [213-217] as well as alternative splicing control of cancer-related transcript networks [11, 14]. From cell cycle checkpoint and progression through signaling pathways crucial for cancer cell survival, proliferation and replicative immortality, to angiogenesis, invasion and metastasis - all these effects are context-, cell- and cancer-type dependent, ultimately leading to tumor suppression **(A)** or promotion **(B)**. Detailed description in the main text. **Created in BioRender. Stepniak-Konieczna, E. (2025)** https://BioRender.com/vqjpt0j.

A simple isoform switch controls tumor suppressive vs pro-oncogenic roles of MBNL1. For example, e7 of *MBNL1* transcript, fundamental for protein homodimerization, is the most differentially included exon in cancer despite the overall downregulation of *MBNL1* expression in cancerous samples [13]. Exon 7-deficient MBNL1 proteins are anti-survival factors with a defined tumor suppressive role that cancer cells tend to downregulate in favor of e7 containing isoforms (**Figure 6A**). This is because e7-depleted *MBNL1* isoforms give rise to proteins acting in a dominant-negative manner through their effect on the expression and/or splicing of genes involved in proliferation, apoptosis, cell cycle checkpoints and chromosome segregation, ultimately resulting in DNA damage and inhibition of cancer cell survival and migration [13]. In contrast, e7-included MBNL1 isoforms, contributed by components associated to the U2 splicing complex, promote cancer cell survival and migration, particularly in prostate cancer [13]. Similarly, prooncogenic e5- and e7-included *MBNL1* transcripts are often found in colorectal carcinoma (CRC) due to upregulated levels of SRSF3, a splicing factor antagonizing the autoregulatory repression of these exons by MBNL1 itself [218]. This isoform drives prooncogenic AS changes in the pro-apoptotic *ACIN1* transcript from the *ACIN1-S* to the *ACIN1-L* isoform, leading to diminished DNA fragmentation in cultured CRC cells [218]. Further, inactivation of MBNL1 splicing activity by hypoxic tumor microenvironment in aggressive brain cancer glioblastoma (GBM), via simple isoform switch from e5-containing to e5-lacking *MBNL1* mRNAs, promotes rapid nuclear export of MBNL1 protein facilitating expression of numerous gene isoforms associated with an embryonic stem cell-like state [219]. This is consistent with reports on the key role of MBNL1 in inhibition of stem cell-specific AS program and promotion of stem cells differentiation [12, 111]. In all, MBNL isoform switch determines the abundance and splicing of key genes involved in cell migration, DNA repair, and cell division during cancer development.

Dual roles of MBNLs in cancer are largely determined by their functions in RNA processing and stability as well as AS regulation, which in turn impact hallmark cancer processes including metastasis (**Figure 6A**). For example, MBNL1 suppresses CRC by direct binding to *Snail* transcript and destabilizing it, which in turn promotes upregulation of adhesion protein E-cadherin, ultimately inhibiting epithelial-to-mesenchymal transition (EMT), the major hallmark of metastasis [213]. Mechanistically, MBNL1 induces *Snail* mRNA degradation by promoting its intensified recruitment to processing bodies (P-bodies), in turn suppressing *Snail* translation and blocking its downregulatory impact on E-cadherin whose expression is essential in preventing metastasis [213]. Conversely, in breast cancer MBNL1 stabilizes transcripts implicated as metastasis suppressors, *DBLN* and *TACC1*, by directly binding to their 3'UTRs [214]. Consequently, upregulation of MBNL1 in both types of cancer is linked to reduced invasiveness and metastasis, while downregulation to increased cancer progression, metastases and poor prognosis [213, 214]. Apart from the effect on RNA stability, MBNLs may reduce tumorigenicity through their role in RNA biogenesis (**Figure 6A**). Such is the case in esophageal squamous cell carcinoma, where downregulation of MBNL1 causes extensive downstream alterations in the expression of numerous circRNAs, lncRNAs and mRNAs associated with tumor progression [220]. Similar mechanisms operate in GBM, where MBNL1 reduction promotes aerobic glycolysis, a hallmark process of tumor development and malignancy [215]. Mechanistically, MBNL1 exerts antitumor activity in GBM by directly binding *NTRK2* pre-mRNA to promote its circularization (circNTRK2) and expression of encoded NTRK2-243aa, which in turn reduces the half-life of PAX5 by phosphorylation, ultimately inhibiting the expression of PAX5-dependent glycolysis-related genes [215]. In CRC, in contrast, MBNL1 promotes cancer initiation by directly binding 'UGCUGC' motif in the stem-loop of a C-allelic pre-miR-1307, prevalent in CRC patients, thus antagonizing its processing by DICER1 and ultimately leading to a lower level of miR-1307. This in turn elevates the expression of its direct target, a pro-survival and antiapoptotic protein BCL2,

which protects cancer cells [217] (**Figure 6B**). Further, analyses of rearranged signatures within the reciprocal chromosomal translocations of the mixed lineage leukemia (*MLL*) gene revealed that *MBNL1* is one of the most consistently overexpressed genes in MLL-rearranged leukemia compared to other leukemia types [14]. Intriguingly, ChIP-seq data indicated that MBNL1 upregulation was caused by direct stimulation of *MBNL1* promoter by MLL-fusion protein. Excessive MBNL1 directly interacted with and stabilized the transcripts of multiple leukemogenic genes (mostly through decreased intron retention), including histone methyltransferases *DOT1L* and *SETD1A*, which subsequently supported transcriptional activation of downstream targets of the MLL-fusion protein, including activation of *MBNL1* promoter itself [14]. This positive feedback loop ultimately drove changes in the AS of target RNA transcripts, promoting cancer cell survival. In all, this shows that MBNL1-mediated RNA splicing is causal to the pathogenesis of MLL-rearranged leukemias.

Consistently with the reports that MBNL proteins repress stem cell-specific AS program and promote stem cells differentiation [12, 111], MBNL1-low cancers and embryonic stem cells share a discrete set of common AS events [10-12]. A fair amount of data indicates that MBNLs promote AS events that suppress tumor dedifferentiation, and their loss or down-regulation correlates with increased stemness phenotype of cancer cells [10-12] (**Figure 6A**). Specifically, MBNL1 promotes the inclusion of e2 within *MAP2K7* pre-mRNA in healthy cells, while low levels of MBNL1 in cancer allow its skipping. Resultant *MAP2K7*Δe2 splice variant increased stem- and progenitor-like properties of cancer cells via c-Jun N-terminal Kinase (JNK) activation and signaling [11]. Consistently, increased tumorigenic properties of normal and cancer cells with MBNL1 knockdown are accompanied by upregulation of cancer stem cells markers (*CD133* and *LGR5*) and pluripotency markers (*OCT4*, *NANOG*, and *SOX2*) [11]. Interestingly, cooperation of MBNL1 with the splicing factor RBFOX2 seems to be crucial in switching the AS network that drives stem cell differentiation [111].

Similarly to MBNL1, the expression of MBNL2 paralog in breast, prostate and lung carcinoma tumor tissues is significantly lower compared to healthy tissues [221, 222]. Enhancing its expression with a natural plant-derived compound neobractatin inhibited cancer cell motility and metastasis, though the molecular mechanism is yet unknown [221]. Deep RNA-seq analyses of the transcriptomes of epithelial and mesenchymal cells demonstrated that MBNL2 and MBNL3 are among the key factors altering the splicing of EMT-associated regulators in breast cancer and are downregulated during EMT [223]. Similarly, MBNL2 suppressed cell proliferation and migration in hepatocellular carcinoma (HCC) *in vivo*, while its knockdown was associated with a more aggressive phenotype of HCC cells [224]. Interestingly, both upregulation of miR-182 and high levels of *MBNL2* promoter methylation contributed to the downregulation of MBNL2 in breast, liver and lung cancer tissues [225]. Also, downregulation of *MBNL2* mRNA level in prostate cancer promoted cancer cell migration, invasion and EMT process, and inversely correlated with *MBNL2* methylation status implying that it may be a methylation-driven gene [225].

In clear cell renal cell carcinoma (ccRCC), in contrast, MBNL2 appears to be an essential post-transcriptional regulator of the ccRCC transcriptome and significantly upregulated MBNL2 expression in this cancer type is associated with increased tumorigenicity [216]. By positive modulation of mRNA stability and abundance of transcripts involved in HIF-α and FOXM1 networks as well as in PLK1 signaling, MBNL2 promoted cell cycle progression, proliferation and colony-forming ability of ccRCC cells [216] (**Figure 6B**). For example, MBNL2 directly bound the 3'UTR of *VEGFA* mRNA, stabilizing it and leading to increased expression of VEGFA protein, a well-known angiogenic factor of the HIF-α network with major role in the hypoxic response of tumors [216]. Consistently, MBNL2 was

specifically induced in tumor cells upon hypoxic conditions and was critical for hypoxia adaptation by controlling the transcript abundance of hypoxia response genes, such as *VEGFA* [226].

Likewise, the expression of MBNL3 paralog is also dysregulated in diversified cancers and in general, associated with poor prognosis and therapy resistance [227-231]. For example, *MBNL3* expression is activated in HCC by the stem cell transcription factors NANOG, OCT4 and SOX2, and in turn modulates the isoform switch in the long noncoding RNA-PXN antisense transcript 1 (*lncRNA-PXN-AS1*) to protect its sense counterpart, *PXN* mRNA, from degradation, ultimately leading to paxillin upregulation and promotion of tumorigenesis [227]. Similarly, TBP-mediated transactivation and enhanced *MBNL3* expression stimulated isoform switch in *lncRNA-PXN-AS1* and upregulated *PXN*, thus promoting EMT and HCC progression [228]. Furthermore, MBNL3 aggravated gastric adenocarcinoma (GAC) progression through promotion of proliferation, invasion, and angiogenesis [229]. Interestingly, miR-302e directly repressed *MBNL3* expression and lower levels of miR-302e in tested GAC cell models facilitated MBNL3 upregulation and subsequent stimulation of the pro-survival AKT/VEGFA pathway to promote cancer progression [229]. Consistently with these finding, high expression of miR-302a led to MBNL3 downregulation hence promoting sensitivity response of non-small cell lung cancer (NSCLC) to radiotherapy and reducing tumor growth *in vivo* [232].

Summarizing, all these examples allow to conclude context-dependent functions of MBNLs in cancer, reflecting differences in tumor type, stage and cellular environment. In some contexts, MBNLs act as tumor suppressors by maintaining normal splicing patterns and preventing EMT, while in others, their activity supports tumor progression by stabilizing oncogenic transcripts and enhancing cell plasticity. Understanding these dual roles is crucial for exploring MBNL proteins as potential therapeutic targets in oncology.

MBNLs as therapeutic targets in myotonic dystrophy

No effective cure is available to fundamentally improve the course of DM and patients' therapy is limited to symptomatic treatment and supportive care. Numerous strategies have been designed with the aim to: (i) remove the prime culprit, i.e., the expanded repeats, by e.g., repeat contraction, transcription blocking or DNA editing (reviewed in [233, 234]), (ii) alleviate the disease symptoms by either removing the toxic RNA (e.g., by antisense reagents-mediated degradation) or inhibiting its interaction with MBNL proteins to prevent their sequestration (e.g., by small-molecule compounds or antisense reagents; reviewed in [234, 235]), or (iii) modulate MBNL expression to restore the pool of functional protein. In this review, we outline selected MBNL-directed approaches grounded either on OE of various exogenous MBNL isoforms to compensate for endogenous protein deficiency, or modulation of the endogenous *MBNL1* to increase the cellular pool of the protein and counteract the effect of toxic RNA-imposed sequestration (**Figure 7 and Table 2**).

MBNL gene replacement strategies in DM

The seminal study by Kanadia and coworkers, who used localized AAV2-mediated OE of a single *Mbnl1* isoform (Mbnl1/41; lacking e5) in *tibialis anterior* muscle of the HSA^{LR} mouse model of DM1 ([124]), provided evidence that even a small boost in MBNL1 protein levels is a viable option to alleviate DM1 symptoms [236]. Although relatively low levels of MBNL1 protein upregulation were achieved (only a 2-fold increase compared to endogenous expression), they were sufficient to rescue myotonia and mis-splicing of several AS events in HSA^{LR} muscles, including chloride channel *Clcn1* e7a directly underlying DM-associated myotonia [162, 164-166]. Normal myofiber structure was not restored, however, possibly because the *Mbnl1* 41-kDa isoform, which is expressed mainly in neonatal but not adult skeletal muscle, was insufficient to fully rescue the DM1 phenotype. In support, constitutive multisystemic OE of a transgene carrying humanized version of the major isoform found in adult skeletal muscles, the *MBNL1* 40 kDa isoform (lacking e7 and e9), corrected not only spliceopathy and myotonia but also myopathy to some extent, in the background of the same HSA^{LR} model [237]. However, the expression levels of the recombinant protein in these transgenic mice were much higher than those achieved with viral transduction (up to 17-fold in comparison to 2-fold). Such high expression contributed to premature fetal-to-adult AS transition of MBNL1 targets in skeletal muscle early in embryonic development. Even with this premature transition, the skeletal muscle developed and functioned normally suggesting a compensatory mechanism allowing muscle development despite the expression of adult isoforms of MBNL1 target transcripts [237]. Intriguingly, AAV9-mediated delivery of *Mbnl2* 40-kDa isoform in HSA^{LR} model partially reversed fetal splicing pattern of several DM1 biomarker exons, particularly in paraspinal muscles [238]. This implies that while re-expression of either of the paralogs alone may fail to fully rescue the spectrum of DM1 pathologies, combined therapies based on OE of both paralogs may be more beneficial. This is corroborated by findings that compound loss of *Mbnl1* and *2* paralogs in mice leads to a much more severe DM1phenotype [81, 239].

While viral delivery of artificial constructs or random transgenesis may offer robust OE with some therapeutic advantages, it has inherent drawbacks such as unopposed and uncontrolled expression of the protein, exclusion of sequences important for gene function or potential insertional mutagenesis associated with the use of viral vectors which may altogether drive deleterious effects. This is important in light of findings showing that OE of MBNL1 in mouse embryonic fibroblasts led to damaging consequences including myofibroblasts

transformation, while inducible expression of a conditional human *MBNL1* transgene in quiescent fibroblasts in mice elicited a fibrotic response in multiple tissues and organs that progressed with age [240]. These data necessitate controlled, context-dependent MBNL OE in therapeutic strategies, but also indicate that therapeutic impact may strictly depend on the mouse model used. For example, when transgenic mice overexpressing *MBNL1* 40 kDa isoform [237] were crossed to DM200^{+} mice expressing *DMPK* 3'UTR with toxic CUG repeat (~200) as a part of an inducible RNA transcript encoding GFP [123], no therapeutic effect on myotonia or skeletal muscle function was observed [241]. Conversely, MBNL1 OE in this context impaired cardiac function while DM1 splicing abnormalities persisted regardless of MBNL1 upregulation. The genetic context of the expanded CTG repeated region may be crucial, as significant therapeutic effect of MBNL1 OE was observed in the *HSA*^{LR} mouse, where CTG repeats are incorporated in the 3'UTR of the human skeletal actin gene [236]. Finally, recent work with OE of truncated MBNL1 containing both ZnF domains but lacking C-terminal domain (MBNL1Δ-decoy), demonstrated its' potential as a therapeutic decoy for CUG^{exp} repeats, resulting in the release of endogenous MBNL1 from sequestration [242]. This decoy interfered with foci dynamics and competed with endogenous MBNL1 for CUG^{exp} binding. It also formed less stable aggregates with expanded repeats than MBNL1. Notably, AAV-delivered MBNL1Δ-decoy induced prolonged therapeutic effect in *HSA*^{LR} DM1 mouse model, reversing the spliceopathy in skeletal muscle and ameliorating disease pathology.

Expression of autoregulatory MBNL proteins in DM

MBNL1 autoregulation is an appealing concept that could be explored in therapeutic designs to eliminate unwanted effects associated with protein excess, which poses the risk of detrimental effect (as shown e.g. in [240]). Controlled expression by adopting self-buffering and tuning mechanisms may be beneficial in developing safe and effective DM1 therapy. This idea was tested using OE of hybrid constructs carrying MBNL1 CDS separated between e2 and e3 by MBNL-sensitive *ATP2A1* exon 22 (e22) with an in-frame stop codon, thus allowing for MBNL-dependent shutting off of the protein production via promotion of e22 inclusion [243]. In cells with low levels of functional MBNLs, as in DM1, e22 exclusion allowed translation of a fully functional MBNL1 protein. Conversely, MBNL abundance triggered e22 inclusion resulting in the assembly of inactive, truncated MBNL1 due to the presence of the in-frame stop codon. Such self-buffering enabled efficient correction of AS abnormalities in a cellular DM1 model, signifying therapeutic potential of tunable MBNL1 proteins.

Modulation of endogenous *MBNL* expression in DM

Whereas artificial OE concerns usually only a single cDNA variant, endogenous modulation enables correct stoichiometric expression of a balanced splice isoforms diversity. We summarize several examples of compounds, including pharmacological modulators of the epigenome as well as antisense-based reagents, that were reported to increase endogenous MBNL expression by distinct mechanisms, sufficiently to trigger therapeutic benefits in DM1 (**Figures 7** and **Table 2**).

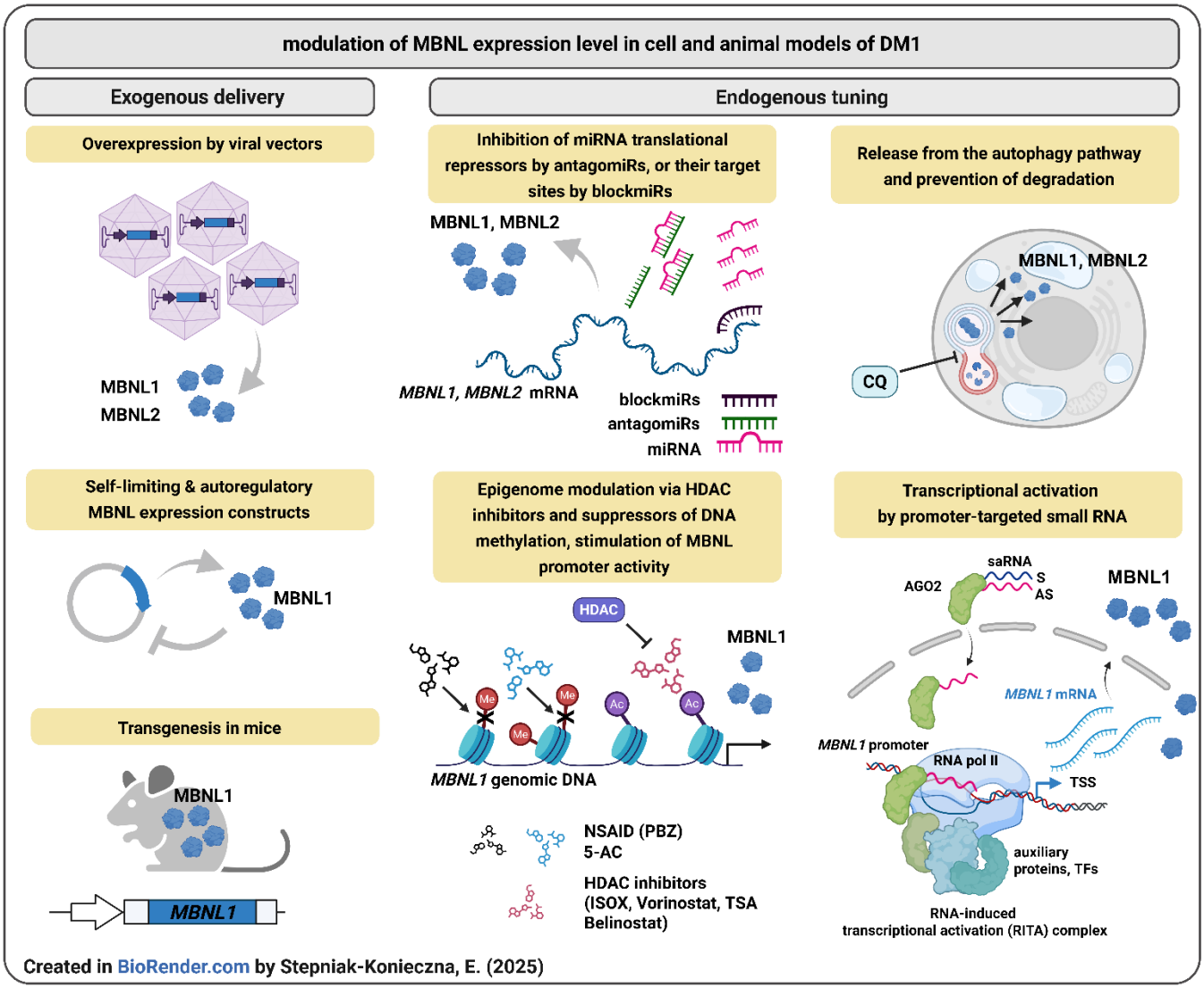

FIGURE 7. Examples of MBNL-targeted approaches to alleviate DM1 pathogenesis. DM1 hallmarks may be reversed either by exogenously delivered MBNL as well as endogenous enhancement of its expression. The first category includes MBNL1 or MBNL2 overexpression by viral vectors (e.g. [236, 238, 244]), delivery of self-buffering MBNL1 expression constructs (e.g. [243]) or transgenesis in mice (e.g. [237]). The second category comprises approaches grounded on the use of autophagy blockers to prevent MBNL1 and MBNL2 degradation [245], the use of antisense oligonucleotides to directly inhibit translational repressors of *MBNL1* and *MBNL2* (antagomiRs; e.g. [30, 43, 44]) or block their target binding sites within the 3'UTRs (blockmiRs; e.g. [45, 246]), as well as small-molecule compounds enhancing the expression of endogenous *MBNL1* including epigenome modulators - histone deacetylase (HDAC) inhibitors (e.g. [247, 248]), non-steroidal anti-inflammatory drugs (NSAID) or global demethylating agents (e.g. [32]). In addition, natural endogenous pathway of RNA activation (RNAa) via duplex RNAs targeted to *MBNL1* gene promoter may be leveraged to stimulate its transcription [249]. **Created in BioRender. Stepniak-Konieczna, E. (2025)** https://BioRender.com/ykj65so.

Table 2. Selected modulators of the endogenous MBNL expression. Abbreviations: HDAC – histone deacetylases; NSAID - nonsteroidal anti-inflammatory drug; MOA – mechanism of action; Ref. – reference publication.

Name	Compound type	Effect on endogenous MBNL / MOA	Ref.
ISOX	generic HDAC inhibitor	~1.5-fold increase in MBNL1 protein expression in DM1 patient-derived fibroblasts MOA: unknown	[247]
Vorinostat	pan-HDAC inhibitor	up to ~2-fold [247] and up to ~1.5-fold [248] increase in MBNL1 protein expression in DM1 patient-derived fibroblasts and myoblasts, respectively MOA: presumably post-transcriptional, precise mechanism unknown	[247, 248]
5-aza(deoxy)cytidine	global DNA methylation inhibitor	~2-fold *Mbnl1* mRNA upregulation in C2C12 cells MOA: presumably suppression of DNA methylation	[32]
Phenylbutazone	NSAID	~1.3-1.9-fold increase in *Mbnl1* mRNA and protein expression in C2C12 cells; ~2-6-fold increase in *Mbnl1* mRNA level in HSA^{LR} mouse model MOA: suppression of methylation of MeR2 region in *Mbnl1* genomic DNA	[32]
Ketoprofen	NSAID	~1.2-fold increase in *Mbnl1* mRNA level in C2C12 cells MOA unknown	[32]
Furamidine	Small molecule binding CTG/CAG repeat DNA	~up to 2-fold increase in MBNL1/2 transcript and protein MOA: unknown, speculations include interactions with DNA in the *MBNL1/2* genes, altered transcription factor binding or interaction directly with the *MBNL1/2* transcripts and their stabilization	[250]
Calcitriol	active form of vitamin D3	~2-fold increase in *Mbnl1* mRNA and protein expression in C2C12 cells and HSA^{LR} mouse model MOA: activates *Mbnl1* promoter, precise mechanism unknown	[251]
Chloroquine (CQ)	Autophagy blocker	~3-fold increase in *Mbl* mRNA and protein expression in a *Drosophila* model; ~2-fold increase in MBNL1 protein expression in patient-derived myoblasts MOA: blocks autophagosome fusion with lysosomes and promotes MBNL release from the autophagic pathway hyperactivated in DM, thus preventing its degradation;	[245]
AntagomiRs / antimiRs	Antisense oligomer	~1.5-4-fold increase in *MBNL1* mRNA and protein expression in DM1 cells and HSA^{LR} mouse model MOA: antisense blocking of miRNA translational inhibitors of *MBNL1* (miR-23b and miR-218)	[30, 43, 44, 252]

BlockmiRs	Antisense oligomer	~1.5-4-fold increase in *MBNL1* mRNA and protein expression in DM1 cells and *HSA*^{LR} mouse model MOA: antisense blocking of miR-23b and miR-218 target binding sites within *MBNL1* 3'UTR	[45, 246]
saMB1_1 and saMB1_2	Small activating RNA (saRNA) duplexes	~ up to 2-3-fold increase in MBNL1 mRNA and protein level in DM1 cells MOA: direct on-site effect of saRNA's antisense strand on *MBNL1* promoter – AGO2 mediated loading of the antisense strand onto target sequence, recruitment of RITA components and auxiliary proteins stimulating transcription	[249]

Epigenetic modifications of *MBNL* expression

ISOX and vorinostat, two small molecule histone deacetylase (HDAC) inhibitors, increased endogenous MBNL1 expression in DM1 fibroblasts by two-fold and significantly corrected the splicing of several MBNL1-target transcripts, corroborating therapeutic potential and a regulatory role of specific epigenome modifications in MBNL expression, although the molecular mechanism has not been studied in detail [247]. More recently, a high-throughput screening of FDA-approved compounds indicated vorinostat as a strong inhibitor of CUG foci formation in DM1 myoblasts [248]. Vorinostat elevated MBNL1 protein in a dose-dependent manner by up to two-fold, but at the same time decreased *MBNL1* mRNA, suggesting mechanism other than transcription stimulation, e.g., increased bioavailability of MBNL1 protein due to release from foci and/or reduced foci formation. Several other pan-HDAC inhibitors including trichostatin A (TSA) and belinostat also alleviated pathogenic DM1 features similarly to vorinostat [248]. On the downside, neither of these compounds is selective and despite therapeutic effect in DM1 cells, broad-acting compounds pose the risk of collateral damage including global alterations in gene transcription and unwanted cellular effects.

Other epigenetic modifications, including DNA methylation marks around promoter regions that affect its general accessibility and transcription, can profoundly influence endogenous *MBNL1* expression level. The suppressive role of DNA methylation on *Mbnl1* expression was demonstrated using a global suppressor of DNA methylation, 5-aza(deoxy)cytidine (5-AC), which boosted *Mbnl1* mRNA by more than 2-fold in C2C12 cells [32]. Detailed analyses identified three distinct methylated regions (MeR) around murine *Mbnl1* locus including MeR1, 2 and 3 located upstream of exon 1 (UTR exon preceding the first coding exon), in intron 1 (intron directly upstream of the first coding exon), and in exon 2 (the first coding exon), respectively. However, only MeR2 was methylated during myogenic differentiation, a program governed in major part by MBNL. Further, drug repositioning-based screening strategy identified a nonsteroidal anti-inflammatory drug (NSAID) phenylbutazone (PBZ), which pharmacologically suppressed methylation at MeR2 and triggered upregulation of *Mbnl1* transcription starting at the upstream UTR exon, indicating an important enhancer activity within this genomic region. PBZ increased *Mbnl1* expression from 1.3-fold up to 1.9-fold both *in vitro* (C2C12) and from 2-fold up to 6-fold *in vivo* (*HSA*^{LR} mouse model), resulting in a partial rescue of the aberrant splicing phenotype and a decrease in the number of abnormal central nuclei in muscle fibers [32]. Noteworthy, PBZ is a non-selective cyclooxygenase (COX) inhibitor and in a more recent study, knockdown of COX-1 isoform in C2C12 myoblasts and myotubes led to ~1.5-fold increase in MBNL1 protein level [253]. In agreement,

bisulfite sequencing confirmed that COX-1-knockdown, just like PBZ treatment, suppressed methylation of MeR2, indicating that COX-1-mediated pathway inhibition may be one of the key triggers in *Mbnl1* transcriptional regulation. Another NSAID, ketoprofen, identified as a chemical modifier and a suppressor of CUG-induced toxicity in a *Drosophila* model of DM [254], also upregulated the expression of *Mbnl1* in C2C12 cells (albeit at a slightly lower level compared to PBZ) which suggests that NSAID may have a general beneficial effect in DM [32]. The exact molecular mechanism of action on MBNL modulation, however, remains unresolved.

Other small molecules affecting *MBNL* expression

A more recent study demonstrated that calcitriol, an active form of vitamin D, increased *Mbnl1* mRNA and protein expression up to ~2-fold in C2C12 myoblasts and HSA^{LR} mice by stimulating *Mbnl1* promoter activity, ultimately leading to partial reversal of AS changes in several mis-regulated targets, correction of muscle pathology and improved muscle strength [251]. Although the mechanism remains unknown, multiple predicted MEF2 binding sites within *Mbnl1* promoter were implied as candidates for further analyses. Notably, vitamin D deficiency was shown to affect the phenotype severity in DM1 patients [255], consistently with its putative role in MBNL1 expression regulation.

Furamidine, a small molecule binding CTG/CAG repeat DNA with nanomolar affinity, was show to reduce CUG^{exp} foci and rescue missplicing in mouse and cell models of DM1 [250]. Interestingly, furamidine upregulated endogenous *MBNL1* and *MBNL2* transcripts and protein levels by up to 2-fold [250]. Although the mechanism has not been precisely elucidated, interactions with DNA in the *MBNL1* and *MBNL2* genes, altered transcription factor binding or interaction directly with the *MBNL1 and MBNL2* transcripts and their stabilization have been speculated.

Control of MBNL protein turnover

Prevention of MBNL protein turnover by releasing it from the autophagic pathway was achieved by administration of autophagy blocker chloroquine (CQ) in a DM1 *Drosophila* model [245]. This approach corrected AS of several Mbl target exons, reduced muscle degeneration, improved muscle function and prolonged lifespan [245]. When added to immortalized patient-derived myoblasts, the same compound increased MBNL1 and MBNL2 levels and mitigated splicing abnormalities. Importantly, CQ improved both histological and functional phenotypes in muscles of HSA^{LR} mice, however, the degree of spliceopathy reversal varied depending on the MBNL target gene as well as treated muscle.

Inhibition of *MBNL*s' translational repressors

Increase of endogenous MBNL protein pool was achieved by eliminating direct translational repressors of *MBNL1* and *MBNL2*, that is miRNA-23b (miR-23b) and miRNA-218 (miR-218) capable of binding *MBNL1* and *MBNL2* 3'UTRs, respectively [30]. Direct blocking of miR-23b and miR-218 activity via complementary antisense oligonucleotides (antagomiRs or antimiRs), enhanced MBNL1 expression, restored its cellular distribution and mitigated AS alterations in DM1 myoblasts and HSA^{LR} mice [30]. *In vivo* administration of antimiRs displayed low toxicity, high efficacy and induced long-lasting biological effects at the molecular and functional levels [43, 44]. Recently, improved versions of antimiRs that incorporated a combination of 2′-OMe, 2′-*O*-methoxyethyl (MOE) and locked nucleic acid (LNA) residues throughout their sequences, were additionally conjugated with fatty acid to

enhance their biodistribution and tested in a cohort of primary DM1 muscle cell lines [252]. These analyses demonstrated therapeutic potential of antimiRs across unrelated genetic backgrounds, in cells with a wide range of repeats, thus strengthening their potential for treating multiple clinical forms of the disease. As MBNL1-3 are targets of other miRNAs, antimiRs hold great potential in DM treatment. The caveat, however, is that miRNAs may act as e.g., tumor suppressors, therefore their direct blocking could trigger unwanted adverse effects or contribute to tumorigenicity by affecting multiple targets apart from the intended ones [44]. Refinement of this strategy based on targeting miRNAs binding sites within *MBNL1* transcripts with so-called blockmiRs, rather than blocking miRNAs themselves by antimiRs, was recently pioneered as a safer therapeutic option [45, 246]. Such site-specific blocking was evaluated in a DM1 muscle cell model as well as in *HSA*^{LR} mice using blockmiRs against miR-23b and miR-218 binding to *MBNL1* 3'UTR [45, 246]. When fused with Pip9b2 cell penetrating peptide for efficient delivery, blockmiRs increased *MBNL1* and *MBNL2* expression in DM1 cells and elevated MBNL1 protein level in *HSA*^{LR} mice. Ultimately, this led to decreased alternative splicing abnormalities thus strengthening blockmiRs potential as DM1 therapeutics [246].

Direct transcriptional stimulation of *MBNL* promoter by small RNAs

Recently, we demonstrated site-specific transcriptional enhancement of *MBNL1* gene by RNA activation (RNAa) [249] (**Figure 7**), a conserved endogenous mechanism of gene activation operating within the nucleus and mediated by short, promoter-directed double-stranded RNAs termed small activating RNAs (saRNAs) [256, 257]. The efficacy of canonical RNAa is critically dependent upon Argonaute 2 protein (AGO2), which incorporates the duplex, discards the passenger (sense) strand and forms an active complex with the guide (antisense) strand complementary to the target promoter sequence [256, 258, 259]. Upon nuclear translocation, saRNA-directed AGO2 binds to the promoter target site serving as a recruitment platform for the assembly of the RNA-induced transcriptional activation (RITA) complex. RITA interacts with RNA polymerase II (RNAPII) to initiate and sustain transcriptional elongation [259].

Broad screening of RNA duplexes targeting distinct *MBNL1* promoters resulted in the identification of two saRNAs, saMB1_1 and saMB1_2, which enhanced endogenous *MBNL1* expression in multiple cell lines including those originating from DM1-affected patients. More importantly, the resulting saRNA-induced increase in MBNL1 protein content (up to 2-3-fold) effectively compensated MBNL insufficiency as evidenced by remarkable rescue of disease-associated AS defects in DM1 patient-derived fibroblasts and myoblasts. At the same time, this moderate upregulation did not cause an undesired enhancement in CUG^{exp} foci formation or toxic cellular effects in DM1 cells, potentially circumventing the issues of OE-based gene therapy tools and thus opening exciting therapeutic possibilities of RNAa effectors in DM1 treatment. As good understanding of the mechanism of action of a new therapy may provide tangible benefits during commercialization process, molecular details of saRNAs action at the *MBNL1* promoter were thoroughly dissected using CUT&RUN scanning across saRNA target sites, *MBNL1* promoter-luciferase reporter assays as well as distinct biochemical methods including chemical modifications of saRNAs. Specifically, saRNA duplexes were shown to directly stimulate the transcription initiation and elongation *via* an on-site process involving AGO2-mediated loading of the antisense strands onto the target sequences (**Figure 7**). This was followed by the recruitment of RNAPII, canonical RNAa pathway components (i.e., CTR9 and RHA) and auxiliary transcription factors specific to the targeted region. Consistently with antisense strand engagement, the activity of the sense strand of saRNA duplex as well as the lncRNA *MBNL1-AS1* overlapping *MBNL1* P2 turned out to be dispensable for RNAa of

MBNL1. Likewise, promoter-associated cryptic transcripts in sense orientation were not involved in this process, proving that the coding DNA strand serves as the docking site for the antisense saRNA strand and RITA complex assembly. Moreover, integrated computational and experimental approaches identified two new trans-acting components of RNAa effector complex at the *MBNL1* promoter, transcription factors MEIS1 and MEIS2, which were essential for *MBNL1* induction mediated by saMB1_1.

One of the major caveats in the application of RNA-based therapeutics concerns their on-site versus off-target effects. The unexpected and AGO2-independent downregulation of the lncRNA *MBNL1-AS1,* caused partially by the sense strand of saRNA duplex, could be eliminated by biotin conjugation to the 5'-end of saRNA's sense strand and hampering its activity. This chemical modification was sufficient to inhibit the microRNA-like effect of the sense strand, thus excluding the risk of posttranscriptional regulation of unintended transcripts and enhancing the safety of the saRNA therapeutics without affecting their promising curative effectiveness.

A notable observation is that saRNAs targeting distinct sites located within a proximity were unable to trigger *MBNL1* RNAa, likely due to the steric hindrance between two transcription complexes assembling and/or transcribing within a relatively small distance. This is contrary to RNAi technology that often employes multiple siRNA duplexes targeting different regions of gene transcripts to improve silencing efficiency. However, saRNA-mediated transcriptional stimulation was unaffected when two genes located on different chromosomes (*MBNL1* and $p21^{WAF1/CIP1}$) were subjected to RNAa, demonstrating the feasibility of this technology for the parallel stimulation of *MBNL* paralogs, which in future could significantly improve the therapeutic outcome in DM1. One additional benefit of saRNA-based approach includes the possibility to achieve therapeutic effects with significantly lower levels of gene upregulation compared to exogenous overexpression, thereby reducing the likelihood of adverse effects. It is tempting to speculate that co-administration of saRNAs targeting distinct MBNL paralogs or their use in conjunction with other drugs stimulating MBNL, could leverage synergistic effects in disease conditions characterized by MBNL insufficiency. Altogether, these new findings warrant further studies on RNAa of *MBNLs* and on efficient drug-delivery systems for these therapeutic small RNAs.

Conclusions

In this review, we summarized the current knowledge on MBNL genes and proteins and portrayed their key roles in a wide range of physiological and pathological conditions. These highly versatile proteins exhibit different expression patterns, tissue-specific effects and functional diversity, underscoring the complexity of their regulatory mechanisms across cellular contexts. Accumulating evidence indicates that these essential regulators of RNA metabolism may be ample therapeutic targets in multiple pathological conditions associated with imbalance in their protein level, but with no underlying gene mutation. In myotonic dystrophy, for example, precise regulation of MBNLs expression can be achieved through targeted endogenous modulation of the promoter activity, as exemplified by application of RNAa technology. Such tailored augmentation may help to avoid current limitations related to unintended consequences associated with excessive activity of MBNLs. In all, although current knowledge regarding the physiology as well as pathophysiology of *MBNL* genes and proteins is relatively broad, elucidating their expression regulators and developing strategies to harness their activity may facilitate the development of novel therapeutic targets across diverse fields, including neuromuscular diseases and cancer.

AUTHOR CONTRIBUTION

Conceptualization and funding acquisition: E.S-K.; **Original draft of the manuscript:** lead contribution: E.S-K. and N.M-K., supporting contribution: P.K., P.P., A.J.; **Manuscript revision, editing and proofreading:** E.S-K., P.K., P.P.; **Preparation of Figures:** E.S-K. (F1-F7), N.M-K. (contribution to F6); **Preparation of Tables:** E.S-K. (lead) and N.M-K. (supporting).

FUNDING

This work was supported by grants from the **National Science Centre, Poland**: **2022/46/E/NZ5/00088** [to E.S-K.]; **2020/37/B/NZ5/01263** [to E.S-K.]; **2021/43/B/NZ5/00723** [to P.K.]; **2018/30/E/NZ5/00065** [to P.K.]. Funding to pay the Open Access publication charges for this article was provided by the grant from the National Science Centre, Poland: **2022/46/E/NZ5/00088** [to E.S-K.].

CONFLICT OF INTEREST

None declared

REFERENCES

REFERENCES

1. Sznajder, L.J. and M.S. Swanson, *Short Tandem Repeat Expansions and RNA-Mediated Pathogenesis in Myotonic Dystrophy.* International Journal of Molecular Sciences, 2019. **20**(13).
2. Konieczny, P., E. Stepniak-Konieczna, and K. Sobczak, *MBNL proteins and their target RNAs, interaction and splicing regulation.* Nucleic Acids Research, 2014. **42**(17): p. 10873-10887.
3. Miller, J.W., et al., *Recruitment of human muscleblind proteins to (CUG)n expansions associated with myotonic dystrophy.* The EMBO Journal, 2000. **19**(17): p. 4439-4448.
4. Fardaei, M., et al., *Three proteins, MBNL, MBLL and MBXL, co-localize in vivo with nuclear foci of expanded-repeat transcripts in DM1 and DM2 cells.* Human Molecular Genetics, 2002. **11**(7): p. 805-814.
5. *mbl-1 (gene) - WormBase : Nematode Information Resource*.
6. Charizanis, K., et al., *Muscleblind-Like 2 Mediated Alternative Splicing in the Developing Brain and Dysregulation in Myotonic Dystrophy.* Neuron, 2012. **75**(3): p. 437-450.
7. Poulos, M.G., et al., *Progressive impairment of muscle regeneration in muscleblind-like 3 isoform knockout mice.* Human Molecular Genetics, 2013. **22**(17): p. 3547-3558.
8. Lee, K.-S., et al., *MBNL3/CHCR prevents myogenic differentiation by inhibiting MyoD-dependent gene transcription.* Differentiation; Research in Biological Diversity, 2008. **76**(3): p. 299-309.
9. Sebestyén, E., et al., *Large-scale analysis of genome and transcriptome alterations in multiple tumors unveils novel cancer-relevant splicing networks.* Genome Research, 2016. **26**(6): p. 732-744.
10. Ray, D. and D.M. Epstein, *Tumorigenic de-differentiation: the alternative splicing way.* Molecular & Cellular Oncology, 2020. **7**(6).

11. Ray, D., et al., *A tumor-associated splice-isoform of MAP2K7 drives dedifferentiation in MBNL1-low cancers via JNK activation.* Proceedings of the National Academy of Sciences, 2020. **117**(28): p. 16391-16400.
12. Han, H., et al., *MBNL proteins repress embryonic stem cell-specific alternative splicing and reprogramming.* Nature, 2013. **498**(7453): p. 241-245.
13. Tabaglio, T., et al., *MBNL1 alternative splicing isoforms play opposing roles in cancer.* Life Science Alliance, 2018. **1**(5): p. e201800157.
14. Itskovich, S.S., et al., *MBNL1 regulates essential alternative RNA splicing patterns in MLL-rearranged leukemia.* Nature Communications, 2020. **11**: p. 2369.
15. Begemann, G., et al., *muscleblind, a gene required for photoreceptor differentiation in Drosophila, encodes novel nuclear Cys3His-type zinc-finger-containing proteins.* Development (Cambridge, England), 1997. **124**(21): p. 4321-4331.
16. Artero, R., et al., *The muscleblind gene participates in the organization of Z-bands and epidermal attachments of Drosophila muscles and is regulated by Dmef2.* Developmental Biology, 1998. **195**(2): p. 131-143.
17. Wang, L.-C., et al., *Growth-dependent effect of muscleblind knockdown on Caenorhabditis elegans.* Biochemical and Biophysical Research Communications, 2008. **366**(3): p. 705-709.
18. Liu, Y.-F., et al., *Zebrafish muscleblind-like genes: identification, structural features and expression.* Comparative Biochemistry and Physiology. Part B, Biochemistry & Molecular Biology, 2008. **151**(1): p. 118-124.
19. Hinman, M.N., et al., *Zebrafish mbnl mutants model physical and molecular phenotypes of myotonic dystrophy.* Disease Models & Mechanisms, 2021. **14**(6): p. dmm045773.
20. Kanadia, R.N., et al., *Developmental expression of mouse muscleblind genes Mbnl1, Mbnl2 and Mbnl3.* Gene expression patterns: GEP, 2003. **3**(4): p. 459-462.
21. Brook, J.D., et al., *Molecular basis of myotonic dystrophy: expansion of a trinucleotide (CTG) repeat at the 3' end of a transcript encoding a protein kinase family member.* Cell, 1992. **68**(4): p. 799-808.
22. Fu, Y.H., et al., *An Unstable Triplet Repeat in a Gene Related to Myotonic Muscular-Dystrophy.* Science, 1992. **255**(5049): p. 1256-1258.
23. Mahadevan, M., et al., *Myotonic-Dystrophy Mutation - an Unstable Ctg Repeat in the 3' Untranslated Region of the Gene.* Science, 1992. **255**(5049): p. 1253-1255.
24. Squillace, R.M., D.M. Chenault, and E.H. Wang, *Inhibition of muscle differentiation by the novel muscleblind-related protein CHCR.* Developmental Biology, 2002. **250**(1): p. 218-230.
25. Ho, T.H., et al., *Muscleblind proteins regulate alternative splicing.* The EMBO Journal, 2004. **23**(15): p. 3103-3112.
26. Pascual, M., et al., *The Muscleblind family of proteins: an emerging class of regulators of developmentally programmed alternative splicing.* Differentiation, 2006. **74**(2-3): p. 65-80.
27. Bargiela, A., et al., *Two Enhancers Control Transcription of Drosophila muscleblind in the Embryonic Somatic Musculature and in the Central Nervous System.* PLoS ONE, 2014. **9**(3): p. e93125.
28. Konieczny, P., E. Stepniak-Konieczna, and K. Sobczak, *MBNL expression in autoregulatory feedback loops.* RNA Biology, 2018. **15**(1): p. 1-8.
29. Konieczny, P., et al., *Autoregulation of MBNL1 function by exon 1 exclusion from MBNL1 transcript.* Nucleic Acids Research, 2017. **45**(4): p. 1760-1775.
30. Cerro-Herreros, E., et al., *miR-23b and miR-218 silencing increase Muscleblind-like expression and alleviate myotonic dystrophy phenotypes in mammalian models.* Nature Communications, 2018. **9**: p. 2482.

31. Spruce, T., et al., *The X-linked splicing regulator MBNL3 has been co-opted to restrict placental growth in eutherians.* Plos Biology, 2022. **20**(4).
32. Chen, G.Y., et al., *Phenylbutazone induces expression of MBNL1 and suppresses formation of MBNL1-CUG RNA foci in a mouse model of myotonic dystrophy.* Scientific Reports, 2016. **6**.
33. Klamut, H.J., et al., *Identification of a transcriptional enhancer within muscle intron 1 of the human dystrophin gene.* Hum Mol Genet, 1996. **5**(10): p. 1599-606.
34. Camp, S., et al., *Acetylcholinesterase expression in muscle is specifically controlled by a promoter-selective enhancesome in the first intron.* J Neurosci, 2008. **28**(10): p. 2459-70.
35. Cass, D., et al., *The four Zn fingers of MBNL1 provide a flexible platform for recognition of its RNA binding elements.* BMC Molecular Biology, 2011. **12**: p. 20.
36. Tran, H., et al., *Analysis of Exonic Regions Involved in Nuclear Localization, Splicing Activity, and Dimerization of Muscleblind-like-1 Isoforms.* The Journal of Biological Chemistry, 2011. **286**(18): p. 16435-16446.
37. Rehman, S., et al., *Development of an AP-FRET Based Analysis for Characterizing RNA-Protein Interactions in Myotonic Dystrophy (DM1).* Plos One, 2014. **9**(4).
38. Botta, A., et al., *MBNL142 and MBNL143 gene isoforms, overexpressed in DM1-patient muscle, encode for nuclear proteins interacting with Src family kinases.* Cell Death Dis, 2013. **4**(8): p. e770.
39. Fernandez-Costa, J.M. and R. Artero, *A conserved motif controls nuclear localization of Drosophila Muscleblind.* Mol Cells, 2010. **30**(1): p. 65-70.
40. Lin, X., et al., *Failure of MBNL1-dependent post-natal splicing transitions in myotonic dystrophy.* Human Molecular Genetics, 2006. **15**(13): p. 2087-2097.
41. Dhaenens, C.M., et al., *Overexpression of MBNL1 fetal isoforms and modified splicing of Tau in the DMI brain: Two individual consequences of CUG trinucleotide repeats.* Experimental Neurology, 2008. **210**(2): p. 467-478.
42. Zhang, B.-W., et al., *miR-30-5p Regulates Muscle Differentiation and Alternative Splicing of Muscle-Related Genes by Targeting MBNL.* International Journal of Molecular Sciences, 2016. **17**(2): p. 182.
43. Cerro-Herreros, E., et al., *Therapeutic Potential of AntagomiR-23b for Treating Myotonic Dystrophy.* Molecular Therapy. Nucleic Acids, 2020. **21**: p. 837-849.
44. Cerro-Herreros, E., et al., *Preclinical characterization of antagomiR-218 as a potential treatment for myotonic dystrophy.* Molecular Therapy. Nucleic Acids, 2021. **26**: p. 174-191.
45. Overby, S.J., et al., *BlockmiR AONs as Site-Specific Therapeutic MBNL Modulation in Myotonic Dystrophy 2D and 3D Muscle Cells and HSA(LR) Mice.* Pharmaceutics, 2023. **15**(4).
46. Teplova, M. and D.J. Patel, *Structural insights into RNA recognition by the alternative-splicing regulator muscleblind-like MBNL1.* Nature structural & molecular biology, 2008. **15**(12): p. 1343-1351.
47. Edge, C., C. Gooding, and C.W.J. Smith, *Dissecting domains necessary for activation and repression of splicing by muscleblind-like protein 1.* Bmc Molecular Biology, 2013. **14**.
48. Goers, E.S., et al., *MBNL1 binds GC motifs embedded in pyrimidines to regulate alternative splicing.* Nucleic Acids Research, 2010. **38**(7): p. 2467-2484.
49. Wang, E.T., et al., *Transcriptome-wide Regulation of Pre-mRNA Splicing and mRNA Localization by Muscleblind Proteins.* Cell, 2012. **150**(4): p. 710-724.
50. Warf, M.B. and J.A. Berglund, *MBNL binds similar RNA structures in the CUG repeats of myotonic dystrophy and its pre-mRNA substrate cardiac troponin T.* RNA, 2007. **13**(12): p. 2238-2251.

51. Goers, E.S., et al., *RNA Binding Specificity of Drosophila Muscleblind.* Biochemistry, 2008. **47**(27): p. 7284-7294.
52. Vicente-Crespo, M., et al., *Drosophila Muscleblind Is Involved in troponin T Alternative Splicing and Apoptosis.* PLoS ONE, 2008. **3**(2): p. e1613.
53. Sznajder, Ł.J., et al., *Mechanistic determinants of MBNL activity.* Nucleic Acids Research, 2016. **44**(21): p. 10326-10342.
54. Grammatikakis, I., et al., *Identification of MBNL1 and MBNL3 domains required for splicing activation and repression.* Nucleic Acids Res, 2011. **39**(7): p. 2769-80.
55. Taylor, K., et al., *MBNL splicing activity depends on RNA binding site structural context.* Nucleic Acids Research, 2018. **46**(17): p. 9119-9133.
56. Purcell, J., et al., *Combinatorial Mutagenesis of MBNL1 Zinc Fingers Elucidates Distinct Classes of Regulatory Events.* Molecular and Cellular Biology, 2012. **32**(20): p. 4155-4167.
57. Hale, M.A., et al., *An engineered RNA binding protein with improved splicing regulation.* Nucleic Acids Research, 2018. **46**(6): p. 3152-3168.
58. Du, H., et al., *Aberrant alternative splicing and extracellular matrix gene expression in mouse models of myotonic dystrophy.* Nature structural & molecular biology, 2010. **17**(2): p. 187-193.
59. Fernandez-Costa, J.M., et al., *Alternative splicing regulation by Muscleblind proteins: from development to disease.* Biol Rev Camb Philos Soc, 2011. **86**(4): p. 947-58.
60. Han, J. and T.A. Cooper, *Identification of CELF splicing activation and repression domains in vivo.* Nucleic Acids Research, 2005. **33**(9): p. 2769-2780.
61. Yeo, G.W., et al., *An RNA code for the FOX2 splicing regulator revealed by mapping RNA-protein interactions in stem cells.* Nature Structural & Molecular Biology, 2009. **16**(2): p. 130-137.
62. Zhang, C.L., et al., *Defining the regulatory network of the tissue-specific splicing factors Fox-1 and Fox-2.* Genes & Development, 2008. **22**(18): p. 2550-2563.
63. Licatalosi, D.D., et al., *HITS-CLIP yields genome-wide insights into brain alternative RNA processing.* Nature, 2008. **456**(7221): p. 464-U22.
64. Ule, J., et al., *An RNA map predicting Nova-dependent splicing regulation.* Nature, 2006. **444**(7119): p. 580-586.
65. Llorian, M., et al., *Position-dependent alternative splicing activity revealed by global profiling of alternative splicing events regulated by PTB.* Nature Structural & Molecular Biology, 2010. **17**(9): p. 1114-U12.
66. Xue, Y.C., et al., *Genome-wide Analysis of PTB-RNA Interactions Reveals a Strategy Used by the General Splicing Repressor to Modulate Exon Inclusion or Skipping.* Molecular Cell, 2009. **36**(6): p. 996-1006.
67. Erkelenz, S., et al., *Position-dependent splicing activation and repression by SR and hnRNP proteins rely on common mechanisms (vol 19, pg 96, 2013).* Rna, 2013. **19**(7): p. 1015-1015.
68. Chen, M. and J.L. Manley, *Mechanisms of alternative splicing regulation: insights from molecular and genomics approaches.* Nat Rev Mol Cell Biol, 2009. **10**(11): p. 741-54.
69. Warf, M.B., et al., *The protein factors MBNL1 and U2AF65 bind alternative RNA structures to regulate splicing.* Proceedings of the National Academy of Sciences of the United States of America, 2009. **106**(23): p. 9203-9208.
70. Dvinge, H., *Regulation of alternative mRNA splicing: old players and new perspectives.* Febs Letters, 2018. **592**(17): p. 2987-3006.
71. Gates, D.P., L.A. Coonrod, and J.A. Berglund, *Autoregulated splicing of muscleblind-like 1 (MBNL1) Pre-mRNA.* J Biol Chem, 2011. **286**(39): p. 34224-33.
72. Kanadia, R.N., et al., *A muscleblind knockout model for myotonic dystrophy.* Science (New York, N.Y.), 2003. **302**(5652): p. 1978-1980.

73. Choi, J., et al., *Muscleblind-like 3 deficit results in a spectrum of age-associated pathologies observed in myotonic dystrophy.* Scientific Reports, 2016. **6**: p. 30999.
74. Jog, S.P., et al., *RNA Splicing Is Responsive to MBNL1 Dose.* Plos One, 2012. **7**(11).
75. Wagner, S.D., et al., *Dose-Dependent Regulation of Alternative Splicing by MBNL Proteins Reveals Biomarkers for Myotonic Dystrophy.* PLoS Genet, 2016. **12**(9): p. e1006316.
76. Ellis, J.A., et al., *Alternative splicing outcomes across an RNA-binding protein concentration gradient.* J Mol Biol, 2023: p. 168156.
77. Nakamori, M., et al., *Splicing Biomarkers of Disease Severity in Myotonic Dystrophy.* Annals of Neurology, 2013. **74**(6): p. 862-872.
78. Wang, E.T., et al., *Antagonistic regulation of mRNA expression and splicing by CELF and MBNL proteins.* Genome Res, 2015. **25**(6): p. 858-71.
79. Paul, S., et al., *Interaction of muscleblind, CUG-BP1 and hnRNP H proteins in DM1-associated aberrant IR splicing.* EMBO J, 2006. **25**(18): p. 4271-83.
80. Kuyumcu-Martinez, N.M., G.S. Wang, and T.A. Cooper, *Increased steady-state levels of CUGBP1 in myotonic dystrophy 1 are due to PKC-mediated hyperphosphorylation.* Mol Cell, 2007. **28**(1): p. 68-78.
81. Lee, K.-Y., et al., *Compound loss of muscleblind-like function in myotonic dystrophy.* EMBO Molecular Medicine, 2013. **5**(12): p. 1887-1900.
82. Suenaga, K., et al., *Muscleblind-Like 1 Knockout Mice Reveal Novel Splicing Defects in the Myotonic Dystrophy Brain.* PLoS ONE, 2012. **7**(3): p. e33218.
83. Sznajder, L.J., et al., *Loss of MBNL1 induces RNA misprocessing in the thymus and peripheral blood.* Nature Communications, 2020. **11**(1).
84. Hao, M., et al., *Muscleblind-like 2 (Mbnl2) -deficient mice as a model for myotonic dystrophy.* Dev Dyn, 2008. **237**(2): p. 403-10.
85. Kanadia, R.N., et al., *Developmental expression of mouse muscleblind genes Mbnl1, Mbnl2 and Mbnl3.* Gene Expr Patterns, 2003. **3**(4): p. 459-62.
86. Thomas, J.D., et al., *Disrupted prenatal RNA processing and myogenesis in congenital myotonic dystrophy.* Genes & Development, 2017. **31**(11): p. 1122-1133.
87. Huang, C.W., et al., *Muscleblind-like 2 knockout shifts adducin 1 isoform expression and alters dendritic spine dynamics of cortical neurons during brain development.* Neuropathol Appl Neurobiol, 2023. **49**(2): p. e12890.
88. Frison-Roche, C., et al., *MBNL deficiency in motor neurons disrupts neuromuscular junction maintenance and gait coordination.* Brain, 2024.
89. Lee, K.Y., et al., *Mice lacking MBNL1 and MBNL2 exhibit sudden cardiac death and molecular signatures recapitulating myotonic dystrophy.* Human Molecular Genetics, 2022. **31**(18): p. 3144-3160.
90. Dixon, D.M., et al., *Loss of muscleblind-like 1 results in cardiac pathology and persistence of embryonic splice isoforms.* Sci Rep, 2015. **5**: p. 9042.
91. Yadava, R.S., M. Mandal, and M.S. Mahadevan, *Studying the Effect of MBNL1 and MBNL2 Loss in Skeletal Muscle Regeneration.* Int J Mol Sci, 2024. **25**(5).
92. Nitschke, L., et al., *Alternative splicing mediates the compensatory upregulation of MBNL2 upon MBNL1 loss-of-function.* Nucleic Acids Research, 2023. **51**(3): p. 1245-1259.
93. Mérien, A., et al., *CRISPR gene editing in pluripotent stem cells reveals the function of MBNL proteins during human in vitro myogenesis.* Human Molecular Genetics, 2021: p. ddab218.
94. Kino, Y., et al., *Muscleblind protein, MBNL1/EXP, binds specifically to CHHG repeats.* Human Molecular Genetics, 2004. **13**(5): p. 495-507.

95. Sasagawa, N., et al., *Identification of Caenorhabditis elegans K02H8.1 (CeMBL), a functional ortholog of mammalian MBNL proteins.* Journal of Neuroscience Research, 2009. **87**(5): p. 1090-1097.
96. Sönnichsen, B., et al., *Full-genome RNAi profiling of early embryogenesis in Caenorhabditis elegans.* Nature, 2005. **434**(7032): p. 462-469.
97. Spilker, K.A., et al., *Caenorhabditis elegans Muscleblind homolog mbl-1 functions in neurons to regulate synapse formation.* Neural Development, 2012. **7**: p. 7.
98. Antonacci, S., et al., *Conserved RNA-Binding Proteins Required for Dendrite Morphogenesis in Caenorhabditis elegans Sensory Neurons.* G3-Genes Genomes Genetics, 2015. **5**(4): p. 639-653.
99. Fujita, M., et al., *The role of the ELAV homologue EXC-7 in the development of the Caenorhabditis elegans excretory canals.* Developmental Biology, 2003. **256**(2): p. 290-301.
100. Norris, A.D., X. Gracida, and J.A. Calarco, *CRISPR-mediated genetic interaction profiling identifies RNA binding proteins controlling metazoan fitness.* eLife. **6**: p. e28129.
101. Matilainen, O., et al., *Loss of muscleblind splicing factor shortens Caenorhabditis elegans lifespan by reducing the activity of p38 MAPK/PMK-1 and transcription factors ATF-7 and Nrf/SKN-1.* Genetics, 2021. **219**(2).
102. Pascual, M., et al., *A GFP-tagged muscleblind C protein isoform reporter construct.* Fly, 2010. **4**(4): p. 333-337.
103. Vicente, M., et al., *Muscleblind isoforms are functionally distinct and regulate alpha-actinin splicing.* Differentiation; Research in Biological Diversity, 2007. **75**(5): p. 427-440.
104. Juni, N. and D. Yamamoto, *Genetic analysis of chaste, a new mutation of Drosophila melanogaster characterized by extremely low female sexual receptivity.* Journal of Neurogenetics, 2009. **23**(3): p. 329-340.
105. Machuca-Tzili, L., et al., *Flies deficient in Muscleblind protein model features of myotonic dystrophy with altered splice forms of Z-band associated transcripts.* Hum Genet, 2006. **120**(4): p. 487-99.
106. Picchio, L., et al., *Novel Drosophila model of myotonic dystrophy type 1: phenotypic characterization and genome-wide view of altered gene expression.* Human Molecular Genetics, 2013. **22**(14): p. 2795-2810.
107. de Haro, M., et al., *MBNL1 and CUGBP1 modify expanded CUG-induced toxicity in a Drosophila model of myotonic dystrophy type 1.* Human Molecular Genetics, 2006. **15**(13): p. 2138-2145.
108. Llamusi, B., et al., *Muscleblind, BSF and TBPH are mislocalized in the muscle sarcomere of a Drosophila myotonic dystrophy model.* Disease Models & Mechanisms, 2013. **6**(1): p. 184-196.
109. Monferrer, L. and R. Artero, *An interspecific functional complementation test in Drosophila for introductory genetics laboratory courses.* J Hered, 2006. **97**(1): p. 67-73.
110. Gabut, M., et al., *An alternative splicing switch regulates embryonic stem cell pluripotency and reprogramming.* Cell, 2011. **147**(1): p. 132-46.
111. Venables, J.P., et al., *MBNL1 and RBFOX2 cooperate to establish a splicing programme involved in pluripotent stem cell differentiation.* Nature Communications, 2013. **4**: p. 2480.
112. Solana, J., et al., *Conserved functional antagonism of CELF and MBNL proteins controls stem cell-specific alternative splicing in planarians.* Elife, 2016. **5**.

113. Batra, R., et al., *Loss of MBNL Leads to Disruption of Developmentally Regulated Alternative Polyadenylation in RNA-Mediated Disease.* Molecular cell, 2014. **56**(2): p. 311-322.
114. Holt, I., et al., *Muscleblind-Like Proteins.* The American Journal of Pathology, 2009. **174**(1): p. 216-227.
115. Bland, C.S., et al., *Global regulation of alternative splicing during myogenic differentiation.* Nucleic Acids Research, 2010. **38**(21): p. 7651-7664.
116. Mankodi, A., et al., *Ribonuclear inclusions in skeletal muscle in myotonic dystrophy types 1 and 2.* Annals of Neurology, 2003. **54**(6): p. 760-768.
117. Lee, K.S., et al., *RNA-binding Protein Muscleblind-like 3 (MBNL3) Disrupts Myocyte Enhancer Factor 2 (Mef2) beta-Exon Splicing.* Journal of Biological Chemistry, 2010. **285**(44): p. 33779-33787.
118. Lee, K.S., R.M. Squillace, and E.H. Wang, *Expression Pattern of Muscleblind-like Proteins Differs in Differentiating Myoblasts.* Biochemical and biophysical research communications, 2007. **361**(1): p. 151-155.
119. Holt, I., et al., *Muscleblind-like proteins: Similarities and differences in normal and myotonic dystrophy muscle.* Neuromuscular Disorders, 2008. **18**(9-10): p. 799-799.
120. Piasecka, A., et al., *MBNL splicing factors regulate the microtranscriptome of skeletal muscles.* Nucleic Acids Res, 2024. **52**(19): p. 12055-12073.
121. Kalsotra, A., et al., *A postnatal switch of CELF and MBNL proteins reprograms alternative splicing in the developing heart.* Proceedings of the National Academy of Sciences of the United States of America, 2008. **105**(51): p. 20333-20338.
122. Terenzi, F. and A.N. Ladd, *Conserved developmental alternative splicing of muscleblind-like (MBNL) transcripts regulates MBNL localization and activity.* RNA biology, 2010. **7**(1): p. 43-55.
123. Mahadevan, M.S., et al., *Reversible model of RNA toxicity and cardiac conduction defects in myotonic dystrophy.* Nat Genet, 2006. **38**(9): p. 1066-70.
124. Mankodi, A., et al., *Myotonic dystrophy in transgenic mice expressing an expanded CUG repeat.* Science, 2000. **289**(5485): p. 1769-1772.
125. Tanner, M.K., Z. Tang, and C.A. Thornton, *Targeted splice sequencing reveals RNA toxicity and therapeutic response in myotonic dystrophy.* Nucleic Acids Res, 2021. **49**(4): p. 2240-2254.
126. Freyermuth, F., et al., *Splicing misregulation of SCN5A contributes to cardiac-conduction delay and heart arrhythmia in myotonic dystrophy.* Nat Commun, 2016. **7**: p. 11067.
127. Wang, E.T., et al., *Transcriptome alterations in myotonic dystrophy skeletal muscle and heart.* Human Molecular Genetics, 2019. **28**(8): p. 1312-1321.
128. Philips, A.V., L.T. Timchenko, and T.A. Cooper, *Disruption of splicing regulated by a CUG-binding protein in myotonic dystrophy.* Science, 1998. **280**(5364): p. 737-41.
129. Lee, K.Y., et al., *Deprivation of Muscleblind-Like Proteins Causes Deficits in Cortical Neuron Distribution and Morphological Changes in Dendritic Spines and Postsynaptic Densities.* Frontiers in Neuroanatomy, 2019. **13**.
130. Ramon-Duaso, C., et al., *Methylphenidate Attenuates the Cognitive and Mood Alterations Observed in Mbnl2 Knockout Mice and Reduces Microglia Overexpression.* Cerebral Cortex, 2019. **29**(7): p. 2978-2997.
131. Nutter, C.A., et al., *Choroid plexus mis-splicing and altered cerebrospinal fluid composition in myotonic dystrophy type 1.* Brain, 2023. **146**(10): p. 4217-4232.
132. Sta Maria, N.S., et al., *Mbnl1 and Mbnl2 regulate brain structural integrity in mice.* Commun Biol, 2021. **4**(1): p. 1342.

133. Wang, P.Y., et al., *Ubiquitination of MBNL1 Is Required for Its Cytoplasmic Localization and Function in Promoting Neurite Outgrowth.* Cell Reports, 2018. **22**(9): p. 2294-2306.
134. Carpentier, C., et al., *Tau exon 2 responsive elements deregulated in myotonic dystrophy type I are proximal to exon 2 and synergistically regulated by MBNL1 and MBNL2.* Biochim Biophys Acta, 2014. **1842**(4): p. 654-64.
135. Sznajder, L.J., et al., *Autism-related traits in myotonic dystrophy type 1 model mice are due to MBNL sequestration and RNA mis-splicing of autism-risk genes.* Nat Neurosci, 2025.
136. Cheng, A.W., et al., *Muscleblind-like 1 (Mbnl1) regulates pre-mRNA alternative splicing during terminal erythropoiesis.* Blood, 2014. **124**(4): p. 598-610.
137. Kingsley, P.D., et al., *Ontogeny of erythroid gene expression.* Blood, 2013. **121**(6): p. E5-E13.
138. Liu, H., et al., *Alternative splicing analysis in human monocytes and macrophages reveals MBNL1 as major regulator.* Nucleic Acids Research, 2018. **46**(12): p. 6069-6086.
139. Itoh, H., et al., *Cardiac Conduction Disorders as Markers of Cardiac Events in Myotonic Dystrophy Type 1.* J Am Heart Assoc, 2020. **9**(17): p. e015709.
140. Nguyen, H.H., et al., *Pathology of the cardiac conduction system in myotonic dystrophy: a study of 12 cases.* J Am Coll Cardiol, 1988. **11**(3): p. 662-71.
141. Thornton, C.A., R.C. Griggs, and R.T. Moxley, *Myotonic-Dystrophy with No Trinucleotide Repeat Expansion.* Annals of Neurology, 1994. **35**(3): p. 269-272.
142. Ricker, K., et al., *Proximal Myotonic Myopathy - a New Dominant Disorder with Myotonia, Muscle Weakness, and Cataracts.* Neurology, 1994. **44**(8): p. 1448-1452.
143. Meola, G., et al., *A family with an unusual myotonic and myopathic phenotype and no CTG expansion (proximal myotonic myopathy syndrome): A challenge for future molecular studies.* Neuromuscular Disorders, 1996. **6**(3): p. 143-150.
144. Udd, B., et al., *Proximal myotonic dystrophy - A family with autosomal dominant muscular dystrophy, cataracts, hearing loss and hypogonadism: Heterogeneity of proximal myotonic syndromes?* Neuromuscular Disorders, 1997. **7**(4): p. 217-228.
145. Ranum, L.P.W., et al., *Genetic mapping of a second myotonic dystrophy locus.* Nature Genetics, 1998. **19**(2): p. 196-198.
146. Liquori, C.L., et al., *Myotonic dystrophy type 2 caused by a CCTG expansion in intron 1 of ZNF9.* Science (New York, N.Y.), 2001. **293**(5531): p. 864-867.
147. Day, J.W., et al., *Myotonic dystrophy type 2: molecular, diagnostic and clinical spectrum.* Neurology, 2003. **60**(4): p. 657-664.
148. Wong, L.J.C., et al., *Somatic Heterogeneity of the Ctg Repeat in Myotonic-Dystrophy Is Age and Size-Dependent.* American Journal of Human Genetics, 1995. **56**(1): p. 114-122.
149. Monckton, D.G., et al., *Somatic Mosaicism, Germline Expansions, Germline Reversions and Intergenerational Reductions in Myotonic-Dystrophy Males - Small Pool Pcr Analyses.* Human Molecular Genetics, 1995. **4**(1): p. 1-8.
150. Harper, P.S., *New genes for old diseases: The molecular basis of myotonic dystrophy and Huntington's disease - The Lumleian Lecture 1995.* Journal of the Royal College of Physicians of London, 1996. **30**(3): p. 221-231.
151. Martorell, L., et al., *Progression of somatic CTG repeat length heterogeneity in the blood cells of myotonic dystrophy patients.* Human Molecular Genetics, 1998. **7**(2): p. 307-312.
152. Thornton, C.A., K. Johnson, and R.T. Moxley, *Myotonic-Dystrophy Patients Have Larger Ctg Expansions in Skeletal-Muscle Than in Leukocytes.* Annals of Neurology, 1994. **35**(1): p. 104-107.

153. Napierala, M. and W.J. Krzyzosiak, *CUG repeats present in myotonin kinase RNA form metastable "slippery" hairpins.* Journal of Biological Chemistry, 1997. **272**(49): p. 31079-31085.
154. Taneja, K.L., et al., *Foci of Trinucleotide Repeat Transcripts in Nuclei of Myotonic-Dystrophy Cells and Tissues.* Journal of Cell Biology, 1995. **128**(6): p. 995-1002.
155. Davis, B.M., et al., *Expansion of a CUG trinucleotide repeat in the 3' untranslated region of myotonic dystrophy protein kinase transcripts results in nuclear retention of transcripts.* Proceedings of the National Academy of Sciences of the United States of America, 1997. **94**(14): p. 7388-7393.
156. Mankodi, A., et al., *Muscleblind localizes to nuclear foci of aberrant RNA in myotonic dystrophy types 1 and 2.* Human Molecular Genetics, 2001. **10**(19): p. 2165-2170.
157. Sobczak, K., et al., *RNA structure of trinucleotide repeats associated with human neurological diseases.* Nucleic Acids Res, 2003. **31**(19): p. 5469-82.
158. Yuan, Y., et al., *Muscleblind-like 1 interacts with RNA hairpins in splicing target and pathogenic RNAs.* Nucleic Acids Res, 2007. **35**(16): p. 5474-86.
159. Querido, E., et al., *Stochastic and reversible aggregation of mRNA with expanded CUG-triplet repeats.* J Cell Sci, 2011. **124**(Pt 10): p. 1703-14.
160. Ozimski, L.L., et al., *The hallmarks of myotonic dystrophy type 1 muscle dysfunction.* Biological Reviews, 2021. **96**(2): p. 716-730.
161. López-Martínez, A., et al., *An Overview of Alternative Splicing Defects Implicated in Myotonic Dystrophy Type I.* Genes, 2020. **11**(9): p. 1109.
162. Charlet-B, N., et al., *Loss of the muscle-specific chloride channel in type 1 myotonic dystrophy due to misregulated alternative splicing.* Molecular Cell, 2002. **10**(1): p. 45-53.
163. Mankodi, A., et al., *Expanded CUG repeats trigger aberrant splicing of ClC-1 chloride channel pre-mRNA and hyperexcitability of skeletal muscle in myotonic dystrophy.* Molecular Cell, 2002. **10**(1): p. 35-44.
164. Lueck, J.D., et al., *Chloride channelopathy in myotonic dystrophy resulting from loss of posttranscriptional regulation for CLCN1.* Am J Physiol Cell Physiol, 2007. **292**(4): p. C1291-7.
165. Lueck, J.D., et al., *Muscle chloride channel dysfunction in two mouse models of myotonic dystrophy.* J Gen Physiol, 2007. **129**(1): p. 79-94.
166. Wheeler, T.M., et al., *Correction of ClC-1 splicing eliminates chloride channelopathy and myotonia in mouse models of myotonic dystrophy.* J Clin Invest, 2007. **117**(12): p. 3952-7.
167. Tang, Z.Z., et al., *Muscle weakness in myotonic dystrophy associated with misregulated splicing and altered gating of Ca(V)1.1 calcium channel.* Hum Mol Genet, 2012. **21**(6): p. 1312-24.
168. Kimura, T., et al., *Altered mRNA splicing of the skeletal muscle ryanodine receptor and sarcoplasmic/endoplasmic reticulum Ca2+-ATPase in myotonic dystrophy type 1.* Human Molecular Genetics, 2005. **14**(15): p. 2189-2200.
169. Fugier, C., et al., *Misregulated alternative splicing of BIN1 is associated with T tubule alterations and muscle weakness in myotonic dystrophy.* Nature Medicine, 2011. **17**(6): p. 720-725.
170. Yamashita, Y., et al., *Four parameters increase the sensitivity and specificity of the exon array analysis and disclose 25 novel aberrantly spliced exons in myotonic dystrophy.* Journal of Human Genetics, 2012. **57**(6): p. 368-374.
171. Rau, F., et al., *Abnormal splicing switch of DMD's penultimate exon compromises muscle fibre maintenance in myotonic dystrophy.* Nat Commun, 2015. **6**: p. 7205.

172. Margolis, R.L. and D.D. Rudnicki, *Pathogenic insights from Huntington's disease-like 2 and other Huntington's disease genocopies.* Current Opinion in Neurology, 2016. **29**(6): p. 743-748.
173. Gu, X., et al., *Uninterrupted CAG repeat drives striatum-selective transcriptionopathy and nuclear pathogenesis in human Huntingtin BAC mice.* Neuron, 2022. **110**(7): p. 1173-1192 e7.
174. Li, L.B., et al., *RNA toxicity is a component of ataxin-3 degeneration in Drosophila.* Nature, 2008. **453**(7198): p. 1107-11.
175. Zu, T., A. Pattamatta, and L.P.W. Ranum, *Repeat-Associated Non-ATG Translation in Neurological Diseases.* Cold Spring Harbor Perspectives in Biology, 2018. **10**(12).
176. Hagerman, R.J. and P. Hagerman, *Fragile X-associated tremor/ataxia syndrome - features, mechanisms and management.* Nature Reviews Neurology, 2016. **12**(7): p. 403-412.
177. Mead, R.J., et al., *Amyotrophic lateral sclerosis: a neurodegenerative disorder poised for successful therapeutic translation.* Nature Reviews Drug Discovery, 2022.
178. Rudnicki, D.D., et al., *Huntington's disease-like 2 is associated with CUG repeat-containing RNA foci.* Annals of Neurology, 2007. **61**(3): p. 272-282.
179. Wilburn, B., et al., *An Antisense CAG Repeat Transcript at JPH3 Locus Mediates Expanded Polyglutamine Protein Toxicity in Huntington's Disease-like 2 Mice.* Neuron, 2011. **70**(3): p. 427-440.
180. Mykowska, A., et al., *CAG repeats mimic CUG repeats in the misregulation of alternative splicing.* Nucleic Acids Research, 2011. **39**(20): p. 8938-8951.
181. McLoughlin, H.S., L.R. Moore, and H.L. Paulson, *Pathogenesis of SCA3 and implications for other polyglutamine diseases.* Neurobiol Dis, 2020. **134**: p. 104635.
182. Cleary, J.D., S.H. Subramony, and L.P.W. Ranum, *Spinocerebellar Ataxia Type 8*, in *GeneReviews((R))*, M.P. Adam, et al., Editors. 1993: Seattle (WA).
183. Zu, T., et al., *Non-ATG-initiated translation directed by microsatellite expansions.* Proc Natl Acad Sci U S A, 2011. **108**(1): p. 260-5.
184. Moseley, M.L., et al., *Bidirectional expression of CUG and CAG expansion transcripts and intranuclear polyglutamine inclusions in spinocerebellar ataxia type 8.* Nat Genet, 2006. **38**(7): p. 758-69.
185. Merienne, K. and Y. Trottier, *SCA8 CAG/CTG expansions, a tale of two TOXICities: a unique or common case?* PLoS Genet, 2009. **5**(8): p. e1000593.
186. Daughters, R.S., et al., *RNA Gain-of-Function in Spinocerebellar Ataxia Type 8.* Plos Genetics, 2009. **5**(8).
187. Mutsuddi, M., et al., *The spinocerebellar ataxia 8 noncoding RNA causes neurodegeneration and associates with staufen in Drosophila.* Curr Biol, 2004. **14**(4): p. 302-8.
188. Brunberg, J.A., et al., *Fragile X premutation carriers: characteristic MR imaging findings of adult male patients with progressive cerebellar and cognitive dysfunction.* AJNR Am J Neuroradiol, 2002. **23**(10): p. 1757-66.
189. Jacquemont, S., et al., *Fragile X premutation tremor/ataxia syndrome: molecular, clinical, and neuroimaging correlates.* Am J Hum Genet, 2003. **72**(4): p. 869-78.
190. Tassone, F., et al., *Intranuclear inclusions in neural cells with premutation alleles in fragile X associated tremor/ataxia syndrome.* J Med Genet, 2004. **41**(4): p. e43.
191. Primerano, B., et al., *Reduced FMR1 mRNA translation efficiency in fragile X patients with premutations.* RNA, 2002. **8**(12): p. 1482-8.
192. Tassone, F., et al., *Elevated levels of FMR1 mRNA in carrier males: a new mechanism of involvement in the fragile-X syndrome.* Am J Hum Genet, 2000. **66**(1): p. 6-15.

193. Tassone, F., et al., *Fragile X males with unmethylated, full mutation trinucleotide repeat expansions have elevated levels of FMR1 messenger RNA.* Am J Med Genet, 2000. **94**(3): p. 232-6.
194. Kenneson, A., et al., *Reduced FMRP and increased FMR1 transcription is proportionally associated with CGG repeat number in intermediate-length and premutation carriers.* Hum Mol Genet, 2001. **10**(14): p. 1449-54.
195. Hagerman, R.J., et al., *Fragile X syndrome.* Nat Rev Dis Primers, 2017. **3**: p. 17065.
196. Sellier, C., et al., *Sam68 sequestration and partial loss of function are associated with splicing alterations in FXTAS patients.* Embo Journal, 2010. **29**(7): p. 1248-1261.
197. Sellier, C., et al., *Sequestration of DROSHA and DGCR8 by expanded CGG RNA repeats alters microRNA processing in fragile X-associated tremor/ataxia syndrome.* Cell Rep, 2013. **3**(3): p. 869-80.
198. Iwahashi, C.K., et al., *Protein composition of the intranuclear inclusions of FXTAS.* Brain, 2006. **129**(Pt 1): p. 256-71.
199. Sofola, O.A., et al., *RNA-binding proteins hnRNP A2/B1 and CUGBP1 suppress fragile X CGG premutation repeat-induced neurodegeneration in a Drosophila model of FXTAS.* Neuron, 2007. **55**(4): p. 565-71.
200. Jin, P., et al., *Pur alpha binds to rCGG repeats and modulates repeat-mediated neurodegeneration in a Drosophila model of fragile X tremor/ataxia syndrome.* Neuron, 2007. **55**(4): p. 556-64.
201. Derbis, M., et al., *Quantitative Evaluation of Toxic Polyglycine Biosynthesis and Aggregation in Cell Models Expressing Expanded CGG Repeats.* Front Genet, 2018. **9**: p. 216.
202. Konieczny, P., et al., *Cyclic mismatch binding ligands interact with disease-associated CGG trinucleotide repeats in RNA and suppress their translation.* Nucleic Acids Res, 2021. **49**(16): p. 9479-9495.
203. Todd, P.K., et al., *CGG repeat-associated translation mediates neurodegeneration in fragile X tremor ataxia syndrome.* Neuron, 2013. **78**(3): p. 440-55.
204. Krans, A., M.G. Kearse, and P.K. Todd, *Repeat-associated non-AUG translation from antisense CCG repeats in fragile X tremor/ataxia syndrome.* Ann Neurol, 2016. **80**(6): p. 871-881.
205. Sellier, C., et al., *Translation of Expanded CGG Repeats into FMRpolyG Is Pathogenic and May Contribute to Fragile X Tremor Ataxia Syndrome.* Neuron, 2017. **93**(2): p. 331-347.
206. Jung, S., et al., *FMRP deficiency leads to multifactorial dysregulation of splicing and mislocalization of MBNL1 to the cytoplasm.* PLoS Biol, 2023. **21**(12): p. e3002417.
207. Renton, A.E., A. Chio, and B.J. Traynor, *State of play in amyotrophic lateral sclerosis genetics.* Nat Neurosci, 2014. **17**(1): p. 17-23.
208. Wang, X., J.C. Schwartz, and T.R. Cech, *Nucleic acid-binding specificity of human FUS protein.* Nucleic Acids Res, 2015. **43**(15): p. 7535-43.
209. Assoni, A.F., F. Foijer, and M. Zatz, *Amyotrophic Lateral Sclerosis, FUS and Protein Synthesis Defects.* Stem Cell Rev Rep, 2023. **19**(3): p. 625-638.
210. Casci, I., et al., *Muscleblind acts as a modifier of FUS toxicity by modulating stress granule dynamics and SMN localization.* Nature Communications, 2019. **10**.
211. Campos-Melo, D., et al., *The Integral Role of RNA in Stress Granule Formation and Function.* Front Cell Dev Biol, 2021. **9**: p. 621779.
212. Streit, L., et al., *Stress induced TDP-43 mobility loss independent of stress granules.* Nat Commun, 2022. **13**(1): p. 5480.
213. Tang, L., P. Zhao, and D. Kong, *Muscleblind-like 1 destabilizes Snail mRNA and suppresses the metastasis of colorectal cancer cells via the Snail/E-cadherin axis.* International Journal of Oncology, 2019. **54**(3): p. 955-965.

214. Fish, L., et al., *Muscleblind-like 1 suppresses breast cancer metastatic colonization and stabilizes metastasis suppressor transcripts.* Genes & Development, 2016. **30**(4): p. 386-398.
215. Zhao, Y., et al., *The MBNL1/circNTRK2/PAX5 pathway regulates aerobic glycolysis in glioblastoma cells by encoding a novel protein NTRK2-243aa.* Cell Death Dis, 2022. **13**(9): p. 767.
216. Perron, G., et al., *A General Framework for Interrogation of mRNA Stability Programs Identifies RNA-Binding Proteins that Govern Cancer Transcriptomes.* Cell Rep, 2018. **23**(6): p. 1639-1650.
217. Tang, R., et al., *The polymorphic terminal-loop of pre-miR-1307 binding with MBNL1 contributes to colorectal carcinogenesis via interference with Dicer1 recruitment.* Carcinogenesis, 2015. **36**(8): p. 867-75.
218. Chen, Y.-S., et al., *The SRSF3-MBNL1-Acin1 circuit constitutes an emerging axis to lessen DNA fragmentation in colorectal cancer via an alternative splicing mechanism.* Neoplasia (New York, N.Y.), 2020. **22**(12): p. 702-713.
219. Voss, D.M., et al., *The Alternative Splicing Factor MBNL1 Inhibits Glioblastoma Tumor Initiation and Progression by Reducing Hypoxia-induced Stemness.* Cancer research, 2020. **80**(21): p. 4681-4692.
220. Wang, H.F., et al., *Involvement of circRNA Regulators MBNL1 and QKI in the Progression of Esophageal Squamous Cell Carcinoma.* Cancer Control, 2024. **31**: p. 10732748241257142.
221. Zhang, J., et al., *The natural compound neobractatin inhibits tumor metastasis by upregulating the RNA-binding-protein MBNL2.* Cell Death & Disease, 2019. **10**(8): p. 554.
222. Gao, L., et al., *Development and validation of a six-RNA binding proteins prognostic signature and candidate drugs for prostate cancer.* Genomics, 2020. **112**(6): p. 4980-4992.
223. Shapiro, I.M., et al., *An EMT-driven alternative splicing program occurs in human breast cancer and modulates cellular phenotype.* PLoS Genet, 2011. **7**(8): p. e1002218.
224. Lee, Y.-H., et al., *Paradoxical overexpression of MBNL2 in hepatocellular carcinoma inhibits tumor growth and invasion.* Oncotarget, 2016. **7**(40): p. 65589-65601.
225. Lin, G., et al., *RNA-binding Protein MBNL2 regulates Cancer Cell Metastasis through MiR-182-MBNL2-AKT Pathway.* Journal of Cancer, 2021. **12**(22): p. 6715-6726.
226. Fischer, S., et al., *Muscleblind-like 2 controls the hypoxia response of cancer cells.* RNA, 2020. **26**(5): p. 648-663.
227. Yuan, J.-H., et al., *The MBNL3 splicing factor promotes hepatocellular carcinoma by increasing PXN expression through the alternative splicing of lncRNA-PXN-AS1.* Nature Cell Biology, 2017. **19**(7): p. 820-832.
228. Cao, J., et al., *TATA-box-binding protein promotes hepatocellular carcinoma metastasis through epithelial-mesenchymal transition.* Hepatol Commun, 2023. **7**(7).
229. Tang, W., et al., *MBNL3 Acts as a Target of miR-302e to Facilitate Cell Proliferation, Invasion and Angiogenesis of Gastric Adenocarcinoma via AKT/VEGFA Pathway.* J Microbiol Biotechnol, 2024. **34**(7): p. 1433-1442.
230. Oladimeji, P.O., et al., *KANSL2 and MBNL3 are regulators of pancreatic ductal adenocarcinoma invasion.* Sci Rep, 2020. **10**(1): p. 1485.
231. Sun, X., et al., *Nanog-mediated stem cell properties are critical for MBNL3-associated paclitaxel resistance of ovarian cancer.* J Biochem, 2021. **169**(6): p. 747-756.
232. Yu, Z., et al., *LncRNA SBF2-AS1 affects the radiosensitivity of non-small cell lung cancer via modulating microRNA-302a/MBNL3 axis.* Cell Cycle, 2020. **19**(3): p. 300-316.

233. Raaijmakers, R.H.L., et al., *CRISPR/Cas Applications in Myotonic Dystrophy: Expanding Opportunities.* International Journal of Molecular Sciences, 2019. **20**(15).
234. Izzo, M., et al., *Molecular Therapies for Myotonic Dystrophy Type 1: From Small Drugs to Gene Editing.* International Journal of Molecular Sciences, 2022. **23**(9).
235. Lopez-Morato, M., J.D. Brook, and M. Wojciechowska, *Small Molecules which improve Pathogenesis of Myotonic Dystrophy Type 1.* Frontiers in Neurology, 2018. **9**.
236. Kanadia, R.N., et al., *Reversal of RNA missplicing and myotonia after muscleblind overexpression in a mouse poly(CUG) model for myotonic dystrophy.* Proceedings of the National Academy of Sciences of the United States of America, 2006. **103**(31): p. 11748-11753.
237. Chamberlain, C.M. and L.P.W. Ranum, *Mouse model of muscleblind-like 1 overexpression: skeletal muscle effects and therapeutic promise.* Human Molecular Genetics, 2012. **21**(21): p. 4645-4654.
238. Li, M.Y., et al., *HNRNPA1-induced spliceopathy in a transgenic mouse model of myotonic dystrophy.* Proceedings of the National Academy of Sciences of the United States of America, 2020. **117**(10): p. 5472-5477.
239. Chou, C.C., et al., *Optical Mapping Approaches on Muscleblind-Like Compound Knockout Mice for Understanding Mechanistic Insights Into Ventricular Arrhythmias in Myotonic Dystrophy.* Journal of the American Heart Association, 2017. **6**(4).
240. Davis, J., et al., *MBNL1-mediated regulation of differentiation RNAs promotes myofibroblast transformation and the fibrotic response.* Nature Communications, 2015. **6**.
241. Yadava, R.S., et al., *MBNL1 overexpression is not sufficient to rescue the phenotypes in a mouse model of RNA toxicity.* Human Molecular Genetics, 2019. **28**(14): p. 2330-2338.
242. Arandel, L., et al., *Reversal of RNA toxicity in myotonic dystrophy via a decoy RNA-binding protein with high affinity for expanded CUG repeats.* Nature Biomedical Engineering, 2022. **6**(2): p. 207-+.
243. Rogalska, Z. and K. Sobczak, *Sustainable recovery of MBNL activity in autoregulatory feedback loop in myotonic dystrophy.* Mol Ther Nucleic Acids, 2022. **30**: p. 438-448.
244. Hu, R.C., et al., *MBNL overexpression rescues cardiac phenotypes in a myotonic dystrophy type 1 heart mouse model.* J Clin Invest, 2025. **135**(7).
245. Bargiela, A., et al., *Increased Muscleblind levels by chloroquine treatment improve myotonic dystrophy type 1 phenotypes in in vitro and in vivo models.* Proceedings of the National Academy of Sciences of the United States of America, 2019. **116**(50): p. 25203-25213.
246. Overby, S.J., et al., *Proof of concept of peptide-linked blockmiR-induced MBNL functional rescue in myotonic dystrophy type 1 mouse model.* Molecular Therapy-Nucleic Acids, 2022. **27**: p. 1146-1155.
247. Zhang, F., et al., *A flow cytometry-based screen identifies MBNL1 modulators that rescue splicing defects in myotonic dystrophy type I.* Human Molecular Genetics, 2017. **26**(16): p. 3056-3068.
248. Neault, N., et al., *Vorinostat Improves Myotonic Dystrophy Type 1 Splicing Abnormalities in DM1 Muscle Cell Lines and Skeletal Muscle from a DM1 Mouse Model.* International Journal of Molecular Sciences, 2023. **24**(4).
249. Musiala-Kierklo, N., et al., *Promoter-targeted small RNA duplexes increase MBNL1 transcription and mitigate myotonic dystrophy-associated spliceopathy.* Nucleic Acids Res, 2025. **53**(15).
250. Jenquin, J.R., et al., *Furamidine Rescues Myotonic Dystrophy Type I Associated Mis-Splicing through Multiple Mechanisms.* ACS Chem Biol, 2018. **13**(9): p. 2708-2718.

251. Huang, K., et al., *Calcitriol increases MBNL1 expression and alleviates myotonic dystrophy phenotypes in HSA(LR) mouse models.* Journal of Translational Medicine, 2022. **20**(1).
252. Cerro-Herreros, E., et al., *AntimiR treatment corrects myotonic dystrophy primary cell defects across several CTG repeat expansions with a dual mechanism of action.* Sci Adv, 2024. **10**(41): p. eadn6525.
253. Huang, K., et al., *Inhibition of cyclooxygenase-1 by nonsteroidal anti-inflammatory drugs demethylates MeR2 enhancer and promotes Mbnl1 transcription in myogenic cells.* Scientific Reports, 2020. **10**(1).
254. Garcia-Lopez, A., et al., *Genetic and Chemical Modifiers of a CUG Toxicity Model in Drosophila.* Plos One, 2008. **3**(2).
255. Terracciano, C., et al., *Vitamin D deficiency in myotonic dystrophy type 1.* Journal of Neurology, 2013. **260**(9): p. 2330-2334.
256. Li, L.C., et al., *Small dsRNAs induce transcriptional activation in human cells.* Proc Natl Acad Sci U S A, 2006. **103**(46): p. 17337-42.
257. Janowski, B.A., et al., *Activating gene expression in mammalian cells with promoter-targeted duplex RNAs.* Nat Chem Biol, 2007. **3**(3): p. 166-73.
258. Chu, Y., et al., *Involvement of argonaute proteins in gene silencing and activation by RNAs complementary to a non-coding transcript at the progesterone receptor promoter.* Nucleic Acids Res, 2010. **38**(21): p. 7736-48.
259. Portnoy, V., et al., *saRNA-guided Ago2 targets the RITA complex to promoters to stimulate transcription.* Cell Res, 2016. **26**(3): p. 320-35.

3.1.1 Co-author's contribution statements

Mgr Nikola Musiała-Kierklo

Doktorantka Szkoły Doktorskiej Nauk Przyrodniczych

Wydział Biologii

Uniwersytet im. Adama Mickiewicza w Poznaniu

Zespół Biologii RNA

Katedra Biochemii i Biotechnologii

Wydział Rolnictwa, Ogrodnictwa i Biotechnologii

Uniwersytet Przyrodniczy w Poznaniu

22.09.2025 Poznań

OŚWIADCZENIE WSPÓŁAUTORA ARTYKUŁU

Oświadczam, że mój udział w przygotowaniu manuskryptu artykułu stanowiącego część mojej rozprawy doktorskiej, pt. ***„MBNL proteins in health, disease and terapeutic applications"***, autorstwa: Nikola Musiała-Kierklo#, Patryk Konieczny, Patrycja Plewka, Adam Jasiok, Ewa Stępniak-Konieczna#*, złożonego / wysłanego do czasopisma naukowego we wrześniu 2025, polegał na: współudziale w konceptualizacji pracy; wiodącej wspólnie z ostatnim autorem roli w napisaniu manuskryptu; współudziale w przygotowaniu tabel 1-2 oraz ryciny 6; współudziale w korekcie edytorskiej całości manuskryptu.

* Autor korespondencyjny

Wymienieni autorzy w równym stopniu przyczynili się do napisania manuskryptu

Podpis współautora

Podpis promotora

prof. UAM dr hab. Patryk Konieczny

Kierownik Laboratorium Chorób Nerwowo-Mięśniowych

Instytut Biologii i Ewolucji Człowieka

Wydział Biologii

Uniwersytet im. Adama Mickiewicza w Poznaniu

22.09.2025 Poznań

OŚWIADCZENIE WSPÓŁAUTORA ARTYKUŁU

Oświadczam, że mój udział w przygotowaniu manuskryptu artykułu stanowiącego część rozprawy doktorskiej Nikoli Musiała-Kierklo, pt. ***„MBNL proteins in health, disease and therapeutic applications”***, autorstwa: Nikola Musiała-Kierklo#, Patryk Konieczny Patrycja Plewka, Adam Jasiok, Ewa Stępniak-Konieczna#*, złożonego / wysłanego do czasopisma naukowego we wrześniu 2025, polegał na: napisaniu rozdziału *Roles of MBNLs in other nucleotide repeat-expansion disorders*; współudziale w napisaniu rozdziałów *Skeletal muscle biology, Cardiac muscle biology* oraz *Nervous system development and function*; współudziale w redagowaniu i korekcie edytorskiej całości manuskryptu.

* Autor korespondencyjny

Wymienieni autorzy w równym stopniu przyczynili się do napisania manuskryptu

.....

Podpis współautora

Dr Patrycja Plewka

Zespół Biologii RNA

Katedra Biochemii i Biotechnologii

Wydział Rolnictwa, Ogrodnictwa i Biotechnologii

Uniwersytet Przyrodniczy w Poznaniu

22.09.2025 Poznań

OŚWIADCZENIE WSPÓŁAUTORA ARTYKUŁU

Oświadczam, że mój udział w przygotowaniu manuskryptu artykułu przeglądowego, stanowiącego część rozprawy doktorskiej Nikoli Musiała-Kierklo, pt. ***„MBNL proteins in health, disease and therapeutic applications”***, autorstwa: Nikola Musiała-Kierklo#, Patryk Konieczny, Patrycja Plewka, Adam Jasiok, Ewa Stępniak-Konieczna#*, złożonego / wysłanego do czasopisma naukowego we wrześniu 2025, polegał na napisaniu części rozdziału *Direct transcriptional stimulation of MBNL promoter by small RNAs*, a także współudziale w korekcie edytorskiej całości manuskryptu.

* Autor korespondencyjny

Wymienieni autorzy w równym stopniu przyczynili się do napisania manuskryptu

Patrycja Plewka

Podpis współautora

Mgr Adam Jasiok

Doktorant Szkoły Doktorskiej UPP

Uniwersytet Przyrodniczy w Poznaniu

Zespół Biologii RNA

Katedra Biochemii i Biotechnologii

Wydział Rolnictwa, Ogrodnictwa i Biotechnologii

Uniwersytet Przyrodniczy w Poznaniu

22.09.2025 Poznań

OŚWIADCZENIE WSPÓŁAUTORA ARTYKUŁU

Oświadczam, że mój udział w przygotowaniu manuskryptu artykułu przeglądowego, stanowiącego część rozprawy doktorskiej Nikoli Musiała-Kierklo, pt. ***„MBNL proteins in health, disease and therapeutic applications”***, autorstwa: Nikola Musiała-Kierklo#, Patryk Konieczny, Patrycja Plewka, Adam Jasiok, Ewa Stępniak-Konieczna#*, złożonego / wysłanego do czasopisma naukowego we wrześniu 2025, polegał na napisaniu części rozdziału *Direct transcriptional stimulation of MBNL promoter by small RNAs*.

* Autor korespondencyjny

równy udział w napisaniu manuskryptu

Jasiok

.....

Podpis współautora

Prof. UPP dr hab. inż. Ewa Stępniak-Konieczna

Kierownik Laboratorium Biologii RNA

Katedra Biochemii i Biotechnologii

Wydział Rolnictwa, Ogrodnictwa i Biotechnologii

Uniwersytet Przyrodniczy w Poznaniu

22.09.2025 Poznań

OŚWIADCZENIE WSPÓŁAUTORA ARTYKUŁU

Oświadczam, że mój udział w przygotowaniu manuskryptu artykułu przeglądowego stanowiącego część rozprawy doktorskiej Nikoli-Musiała Kierklo, pt. ***„MBNL proteins in health, disease and therapeutic applications”,*** autorstwa: Nikola Musiała-Kierklo#, Patryk Konieczny, Patrycja Plewka, Adam Jasiok, Ewa Stępniak-Konieczna#*, złożonego / wysłanego do czasopisma naukowego we wrześniu 2025, polegał na: konceptualizacji pracy oraz pozyskaniu finansowania; wiodącej roli wspólnie z pierwszym autorem w napisaniu manuskryptu; przygotowaniu tabel 1-2 oraz rycin 1-7; redagowaniu i korekcie edytorskiej całości manuskryptu.

* Autor korespondencyjny

Wymienieni autorzy w równym stopniu przyczynili się do napisania manuskryptu

.....

Podpis współautora

3.2 THE ORIGINAL MANUSCRIPT

Major findings of article ***"Promoter-targeted small RNA duplexes increase MBNL1 transcription and mitigate myotonic dystrophy-associated spliceopathy"*** are presented below. In this work we aimed to explore RNA activation mechanisms as therapeutic intervention for DM1. Currently, major DM1 therapeutic strategies are limited to alleviating the symptoms, rather than addressing the cause of the disease. Interestingly, augmenting MBNL protein levels represents a particularly promising strategy. However, forced overexpression of MBNL isoforms, while beneficial in certain animal models, has been associated with potential toxicity, including fibrotic responses, altered differentiation, and reduced survival. These findings underscore the necessity of therapeutic strategies capable of inducing controlled and physiological restoration of endogenous *MBNL* activity. RNA activation provides a promising strategy for such interventions, yet, its potential in rare genetic disorders remains underexplored. MBNL1 is the most abundantly expressed paralog across various tissues, hence is an attractive target for RNAa-based therapy in DM1. Therefore, targeted activation of the most active promoter 2 provides an opportunity to increase endogenous *MBNL*1 expression while preserving uncontrolled boost of MBNL1 protein.

In this study, rationally designed saRNAs were screened against *MBNL1* promoters P2 and P3, leading to the identification of two lead duplexes that targeted P2 and effectively enhanced *MBNL1* transcription in patient-derived fibroblasts and myoblasts. Mechanistic analyses demonstrated AGO2-mediated promoter targeting, RNAPII recruitment, and exclusion of any requirement for the lncRNA *MBNL1-AS1* or promoter-associated cryptic RNAs. Furthermore, the data suggest a role for specific transcription factors recruited to saRNA target sites, supporting *MBNL1* transcriptional activation. Crucially, saRNA-mediated *MBNL1* upregulation corrected alternative splicing defects of multiple biomarker exons in DM1 cellular models, thereby mitigating the disease-associated spliceopathy.

This work provides the first evidence that endogenous *MBNL1* expression can be specifically augmented through promoter-targeted saRNAs to restore proper splicing in DM1. These findings underscore the translational potential of saRNA-based approaches for DM1 and, more broadly, for disorders characterized by functional insufficiency of RNA-binding proteins.

Nucleic Acids Research, 2025, **53**, gkaf756
https://doi.org/10.1093/nar/gkaf756
NAR Breakthrough Article

NAR Breakthrough Article

Promoter-targeted small RNA duplexes increase *MBNL1* transcription and mitigate myotonic dystrophy-associated spliceopathy

Nikola Musiała-Kierklo [1,2], Patrycja Plewka [1], Adam Jasiok [1,3], Ewa Stępniak-Konieczna [1,*]

[1]Laboratory of RNA Biology, Department of Biochemistry and Biotechnology, Poznan University of Life Sciences, Dojazd 11, 60-632 Poznan, Poland
[2]Doctoral School of Natural Sciences, Adam Mickiewicz University, Uniwersytetu Poznanskiego 2, 61-614 Poznan, Poland
[3]Poznan University of Life Sciences Doctoral School, Collegium Maximum, Wojska Polskiego 28, 60-637 Poznan, Poland
[*]To whom correspondence should be addressed. Email: ewa.stepniak-konieczna@up.poznan.pl

Abstract

Functional depletion of Muscleblind-like (MBNL) proteins is a key trigger of myotonic dystrophy (DM)-associated alternative splicing (AltS) defects. To overcome MBNL insufficiency in DM cell models, we harnessed a conserved endogenous mechanism of RNA activation (RNAa) via rationally designed small activating RNA (saRNA) targeted to the most active promoter of *MBNL1* gene. We report on two lead saRNA duplexes that stimulated *MBNL1* transcription via an on-site mechanism that involves AGO2-mediated loading of the antisense strand onto target sequence, followed by recruitment of RNAPII and auxiliary RNAa pathway components. We demonstrate that neither the antisense lncRNA *MBNL1-AS1* overlapping *MBNL1* promoter nor promoter-associated cryptic RNAs are mechanistically involved in saRNA-induced *MBNL1* gene activation. Our data highlight putative transcription factors whose binding recruitment via identified saRNAs may affect *MBNL1* expression. Most importantly, we show that RNAa-based approach upregulates MBNL1 protein content in distinct DM cell models and corrects the AltS of multiple MBNL1-regulated biomarker exons, underscoring the feasibility of adapting saRNA into novel therapeutic designs. This is the first report that site-specific augmentation of the endogenous *MBNL1* transcription mitigates disease-associated AltS defects and as such, it offers new perspectives into therapeutic options against DM.

Graphical abstract

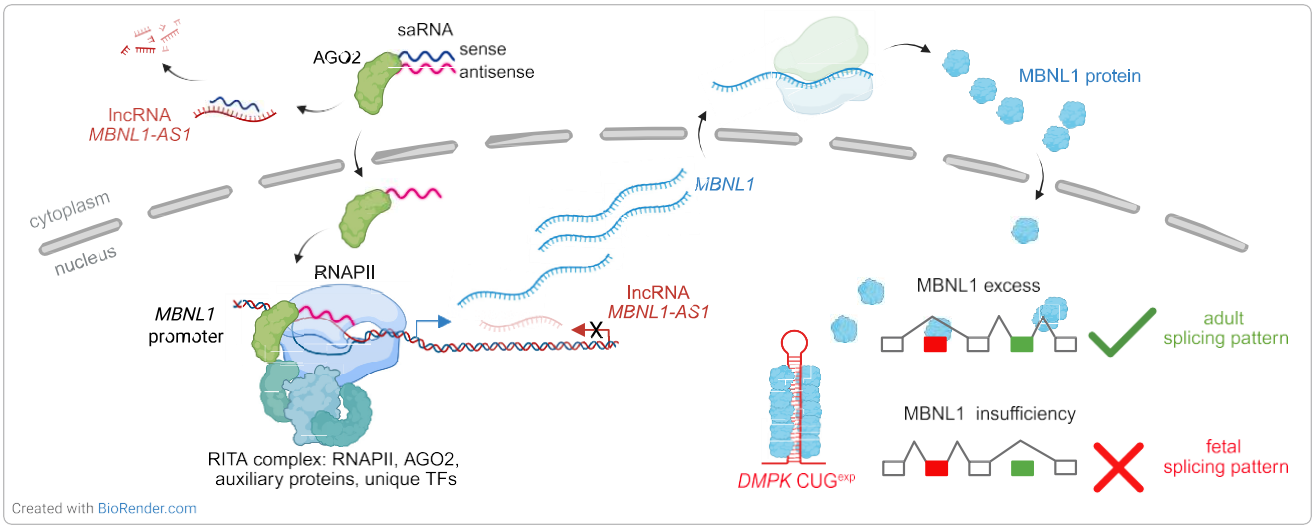

Introduction

RNA-binding proteins of the Muscleblind-like (MBNL) family are master regulators of cellular RNA metabolism and homeostasis, including the control of alternative splicing (AltS), alternative polyadenylation, microRNA biogenesis as well as stability and localization of distinct mRNA species [1–4]. All three MBNL paralogs (MBNL1, 2 and 3) bind RNA via four zinc finger (ZnF) domains arranged in two tandems coupled by a long linker. MBNLs modulate AltS events via sequence- and position-dependent binding to cognate sequence motifs within target pre-mRNAs, relative to the regulated exon [5–7]. This positional mode of action predicts

Received: September 11, 2024. **Revised:** June 13, 2025. **Editorial Decision:** June 30, 2025. **Accepted:** July 21, 2025

that MBNL binding within the alternative exon or upstream intronic sequences promotes exon skipping, while binding to downstream intronic regions facilitates alternative exon inclusion [2, 7, 8]. In essence, MBNL proteins repress a program of alternative exons specific of embryonic stem cells (ESCs) and fetal tissues in favor of alternative exons characteristic of differentiated tissues, which is consistent with their prominent role in promotion of differentiation and development [9–11]. The significance of MBNLs in AltS regulation is best illustrated in myotonic dystrophy (DM) type 1 (DM1), a multisystem disorder in which functional depletion of MBNL proteins from the nucleoplasm via sequestration on CUG-expanded (CUG^{exp}) *DMPK* transcripts underlies massive dysregulation in the AltS of hundreds of target pre-mRNAs [9, 12, 13]. The DM1 spliceopathy, manifested as a shift in the AltS pattern from splice isoforms characteristic of adult and differentiated tissues toward those typical of ESCs and fetal tissues, results in translation of proteins inapt to perform their functions in the adult organism. Because distinct AltS events respond with different strength to the concentration of free MBNL [14], even small fluctuations in the amount of functional protein may affect the severity of the ensuing splice defects in DM1 [15]. Ultimately, functional deficiency of MBNL proteins and subsequent spliceopathy lead to pathological hallmarks of DM1 including skeletal muscle myotonia, atrophy and wasting as well as plethora of other multiorgan dysfunctions.

Current DM1 therapeutics is limited to alleviating disease symptoms and providing supportive care for the patients. Multiple experimental strategies are being extensively tested to halt the disease at distinct pathogenetic levels. These include the removal of the expanded CTG-repeated region (CTG^{exp}) within the mutated *DMPK* gene (e.g. via repeat contraction [16–18], transcription inhibition [19] or CRISPR-Cas9-mediated CTG^{exp} excision [20]) as well as degradation of toxic *DMPK* transcripts (e.g. by antisense oligonucleotides directed at the repeats [21] and sequences outside the repeat region [22–26], by RNA interference [27, 28] or by engineered hU7-snRNAs [29]). Another category involves prevention of MBNL:RNA CUG^{exp} interaction or release of MBNL proteins from CUG-imposed sequestration (e.g. by RNA-directed small-molecule compounds [30–32], antisense reagents [33, 34] or engineered MBNL1-based decoy protein [35]) as well as upregulation of MBNL expression to restore the cellular pool of functional protein. The latter approach has proven successful in multiple studies grounded either on forced overexpression of various exogenous MBNL isoforms in mice, e.g. via AAV-mediated overexpression of a single *Mbnl1* [36] or *Mbnl2* [37] isoform or via constitutive multisystemic overexpression of a transgene carrying humanized version of the major *MBNL1* isoform found in adult skeletal muscles [38]. However, overexpression-based gene therapy tools may prompt excessive activity of MBNL and trigger damaging consequences. For example, adenoviral MBNL1 delivery to rat cardiac fibroblasts induced transformation and acquisition of a contractile myofibroblast phenotype [39]. Similarly, transgenic overexpression of MBNL1 *in vivo* in quiescent fibroblasts led to fibrotic response in multiple tissues, including heart, kidney, and lung, that progressed with age [39]. Further, local intramuscular overexpression of MBNL1 in mice demonstrated decreased body weight and increased muscle histopathology [40] or even reduced survival [38]. Controlled autoregulatory expression of the protein may be one way to overcome limitations associated with excessive MBNL activity, as shown by hybrid *MBNL1* overexpression construct capable of self-limiting of its own expression [41]. On the downside, overexpression of only one isoform rules out the potential effect of a balanced splice isoform diversity that could otherwise be achieved by endogenous modulation. The therapeutic utility of endogenous *MBNL1* enhancement was demonstrated with antisense reagents including, e.g. miRNA sponges [42], antagomiRs [43], or peptide-conjugated antimiRs [44], directly targeting microRNA translational inhibitors of *MBNL1.* More recent refinement of this strategy used blockmiR-based site-specific inhibition of microRNA binding within 3[1]UTR of *MBNL1* mRNA [45]. Upregulation of endogenous *MBNL1* was also achieved with chemical compounds including non-steroidal anti-inflammatory drugs and unspecific epigenetic modulators (e.g. phenylbutazone [46] or HDAC inhibitors [47]).

Encouraged by these data, we hypothesized that a more directed approach utilizing a site-specific, targeted transcriptional modulation of the endogenous *MBNL1* promoter within its natural context may trigger therapeutic effect at a much lower level of the target gene upregulation compared to, e.g. exogenous overexpression, thus minimizing potential side-effects. To achieve this, we leveraged a conserved endogenous mechanism of gene activation termed RNA activation (RNAa). RNAa is a nuclear process mediated via short, naturally occurring or synthetic promoter-targeted double-stranded RNAs (dsRNA) termed small activating RNAs (saRNA) [48, 49]. RNAa activity is strictly dependent on the nuclear presence of Argonaute 2 (AGO2) protein [48, 50, 51] which, upon loading of the saRNA duplex in the cytoplasm, cleaves off and discards the passenger strand (sense, S) and forms an active complex with the guide strand (antisense, AS) complementary to cognate promoter target sequence. Following translocation to the nucleus, AGO2 docks to the saRNA-guided promoter target site and serves as a recruitment platform for the assembly of RNA-induced transcriptional activation (RITA) complex comprising auxiliary proteins, including RNA helicase A (RHA), RNA polymerase-associated protein CTR9 homolog (CTR9; part of the PAF1 complex), and DEAD-box helicase 5 (DDX5), among many other protein components. RITA interacts with RNA polymerase II (RNAPII) to initiate transcription and productive elongation of the mRNA [51]. A role of natural antisense transcripts complementary to sense genes, their promoters or regulatory regions, has been also implicated in the RNAa pathway [52]. RNAa has been effectively used for upregulation of numerous targets including, e.g. $p21^{WAF1/CIP1}$, *CDH1*, *VEGF* [48], *PR*, *MVP* [49], and *CEBPA* [53]. Notably, therapeutic utility of saRNA effectors was evidenced in several cell cancer models and even clinical trials in patients with advanced liver cancer (lipid nanoparticle encapsulated saRNA drug MTL-CEBPA [53, 54]).

MBNL1 is the most prominently expressed mammalian *MBNL* paralog and plays a major role in the AltS regulation, particularly in the context of DM1 [4, 13]. *MBNL1* expression is driven by three annotated promoters, with promoter 2 (P2) being the most prominent driver in the majority of tissues [55]. Intriguingly, P2-derived *MBNL1* pre-mRNAs undergo autoregulation through a feedback loop mechanism based on MBNL binding and exclusion of the first coding exon (e1), whose absence negatively affects the protein activity and stability due to the loss of two ZnFs encoded by e1 [55, 56]. This protective mechanism allows for self-buffering of the protein

amount according to cellular demands [55, 56] and is active in DM1, though often exhausted with increasing CUG expansion size and as the disease progresses [55]. This opens up novel possibilities for therapeutic designs based on endogenous modulation of *MBNL1* expression through manipulation of P2 activity. Hypothetically, increasing the activity of P2 could augment transcription of a balanced *MBNL1* splice isoform diversity capable of undergoing autoregulation via AltS of e1 to prevent excessive protein accumulation. As such, P2 provides an attractive target to develop novel therapeutic strategies against DM1, aimed not only at increasing the cellular MBNL1 pool, but ensuring self-limiting of the protein [55, 56].

In the current work, we present a comprehensive investigation of RNAa feasibility in molecular therapy of DM1, including screening of saRNAs targeted to distinct *MBNL1* promoters and identification of the lead duplexes effectively enhancing P2-derived *MBNL1* expression in cellular models of DM1. Using chemical modifications of identified saRNAs, CUT&RUN scanning across their target sites as well as gene reporter assays, we provide molecular insights into the underlying on-site mechanism, which involves AGO2-mediated loading of the antisense strand of saRNA duplex onto target DNA and stimulation of transcription. Our data rules out the involvement of antisense lncRNA *MBNL1-AS1* overlapping *MBNL1* P2 and demonstrates that cryptic promoter-associated RNAs are unlikely to be involved in *MBNL1* RNAa. We also address the possible off-target effect of identified saRNAs and show that correct chemical modification of the sense strand can readily eliminate it without compromising RNAa. Furthermore, our study highlights putative transcription factors (TFs) whose binding recruitment via identified saRNAs may affect *MBNL1* transcription, thus underscoring the use of RNAa as a molecular toolbox to uncover novel factors in *MBNL1* expression regulation. Most importantly, we show that the two identified lead saRNAs enhance cellular MBNL1 protein content and significantly mitigate DM1-spliceopathy. In all, the ability of RNAa to selectively upregulate *MBNL1*, the key player in DM1 pathophysiology, expands possible points of therapeutic interventions for future drug developments against this rare disease.

Materials and methods

Design of short double-stranded saRNA duplexes

saRNA duplexes containing 19-nt sequence complementary to selected regions of the targeted promoter (+ DNA strand) were designed following a published set of guidelines [48, 57]. Target sequences within *MBNL1* promoter P2 (Eukaryotic Promoter Database (EPD) *MBNL1_1*) and P3 (EPD *MBNL1_2*) were selected between −200 and −3000 bp upstream of the EPD annotated transcription start site (TSS). A BLAT search against the UCSC Genome Browser database (GRCh38/hg38) excluded potential off-target sequences and targets falling within SNPs. Control RNA duplexes, validated and used interchangeably in all experiments, included: (i) non-targeting control saRNA (saCtrl) lacking homology to any annotated human genomic sequence (extensively validated and published by others, e.g. [48]), (ii) scrambled versions of the two lead saRNAs (saMB1_1-scrA, B or C and saMB1_2-scrA, B or C) and (iii) seed-region mutant versions of the two lead saRNAs (saMB1_1-MM4, 6 or 8 and saMB1_2-MM4, 6 or 8; with point mutations at positions 4, 6, or 8 from the 5′end of the AS strand, designed based on [58]). 5′-end biotinylation (5′BIO) of either the sense (5′BIO-S) or the antisense (5′BIO-AS) strand of the selected saRNA duplexes was used to interfere with AGO2 function and block RNAa activity [59]. Mismatched saRNAs were designed to carry a mismatched base opposite the 5′-most nucleotide of either the sense (MM-S) or the antisense (MM-AS) strand of the duplex, in order to lower the 5′-terminus thermodynamic stability and force the selection of a given strand as the guide/leading strand [59]. saP21 was described previously [48, 51]. All saRNA duplexes were synthesized by Sigma–Aldrich/Merck and sequences are listed in Supplementary Tables S1 and S2.

Design of siRNA and GapmeRs

Previously validated and published siRNAs targeting *MBNL1* [32], *AGO2* [59, 60], *CTR9* [51], *RHA* [51], *MEIS1* [61], and *MEIS2* [62] were purchased from Sigma–Aldrich/Merck. The *MBNL1-AS1* Lincode SMARTPool siRNA (pool of 4 siRNAs) was purchased from Dharmacon/Horizon Discovery (LOC401093), and non-targeting siCtrl duplex was purchased from Thermo Fisher Scientific (Ambion™ *Silencer*™ Select Negative Control #2 siRNA). Antisense LNA GapmeRs targeting *MBNL1-AS1* were designed using GeneGlobe Design&Analysis Hub (Qiagen) and synthesized by Qiagen. GapmerR targeting *DMPK* intron 14 was described previously [63] and purchased from Qiagen. All siRNA and GapmeR sequences are listed in Supplementary Table S3.

Cell lines, culture conditions, and transfection of antisense reagents

Primary fibroblasts derived from DM1 patients' skin biopsies (cell lines GM03987, GM04033, GM03132 and GM03989 expressing *DMPK* gene carrying ∼500, ∼1000, ∼1700, and ∼2000 CTG repeats, respectively) and control fibroblasts derived from a non-DM1 patient skin biopsy (cell line GM07492) were obtained from the Coriell Cell Repository at the Coriell Institute for Medical Research. Fibroblasts were grown in Eagle's minimal essential medium (EMEM) with stable glutamine (Biowest), supplemented with 10% fetal bovine serum (FBS) (Biowest), 1% antibiotic/antimycotic solution (Sigma–Aldrich/Merck) and 1% non-essential amino acids solution (Sigma–Aldrich/Merck) in 5% CO_2 at 37◦C. Normal Human Skeletal Myoblasts (HSkM) were purchased from Thermo Fisher Scientific. Non-DM1 myoblasts (9936) and DM1 patient-derived myoblasts (10009) were obtained from Telethon Biobank Network. Myoblasts were grown in Ham's F10 medium with L-glutamine (Biowest) supplemented with 20% FBS, 0.4 μg/ml dexamethasone (Sigma–Aldrich/Merck), 10 ng/ml epidermal growth factor (Sigma–Aldrich/Merck), 1% antibiotic/antimycotic solution, in 5% CO_2 at 37◦C. HeLa and HEK293T cell lines were purchased from ATCC and Thermo Fisher Scientific, respectively, and grown in a high-glucose Dulbecco's Modified Eagle Medium (DMEM) (Biowest) with L-glutamine, supplemented with 10% FBS and 1% antibiotic/antimycotic solution in 5% CO_2 at 37◦C. For delivery of saRNAs, siRNAs or GapmeRs to fibroblasts, cells were seeded at ∼50–60% confluency and transfected 24 h post-plating using Lipofectamine RNAiMAX (Invitrogen) per manufacturer's instructions. Unless otherwise indicated, 75 nM saRNA was transfected for 120 h in all experiments. In all transfection experiments, mock refers to

lipofectamine-treated cells. Experimental design for saRNA co-transfection or sequential transfection of siRNA/saRNA and GapmeRs/saRNA is detailed in the main text and figure legends. For analyses of saRNAs efficiency to upregulate *MBNL1* in cell lines other than fibroblasts (Supplementary Fig. S4), the following conditions were used. HSkM cells were seeded at ∼30–40% confluency and transfected 6 h later. After 72 h, 50% of the cells were collected and the remaining 50% cells were seeded, transfected again 6 h post-plating and harvested 72 h post-second transfection for analyses. Myoblasts lines 9936 and 10009 were seeded at ∼30% confluency and transfected 6 h later with saRNAs for 96 h. HeLa and HEK293T cells were seeded at ∼30–40% confluency and transfected ∼18 h later with saRNAs for 72 h. After 72 h, 50% of the transfected cells were collected and the remaining 50% cells were re-plated and allowed to grow for additional 24 h before harvesting for analyses.

RNA isolation and cDNA synthesis

Cells were harvested in 500 μl TRIzol Reagent (Thermo Fisher Scientific) or Fenozol reagent (A&A Biotechnology), and total RNA was isolated with either Total RNA Zol-Out D (A&A Biotechnology) or MagnifiQ™ 16 Total RNA Plus instant kit (A&A Biotechnology) using Auto-Pure Mini (A&A Biotechnology), per manufacturer's protocol. To obtain cDNA from fibroblasts and myoblasts, 200 ng total RNA was reverse transcribed using either High-Capacity cDNA Reverse Transcription Kit with RNase Inhibitor (Thermo Fisher Scientific) or PrimeScript™ RT Reagent Kit with gDNA Eraser (Takara). To obtain cDNA from HeLa and HEK293T cells, 500 ng total RNA was reverse transcribed using TranScriba kit (A&A Biotechnology) per manufacturer's instructions.

Gene expression analyses

Real-time quantitative reverse transcriptase polymerase chain reactions (RT-qPCRs) were performed with QuantStudio 6 and 7 Flex System (Applied Biosystems) or CFX Opus 96 Real-Time PCR System (BioRad) using PowerTrack™ SYBR Green Master Mix or PowerUp SYBR Green Master Mix (Applied Biosystems) per manufacturers' instructions. All RT-qPCR data were analyzed in Microsoft Excel using the 2−ΔΔCt method [64]. Ct values of the analyzed target gene were normalized against the reference housekeeping gene GAPDH. Primer sequences used for gene expression analyses are listed in Supplementary Table S4.

Alternative splicing assays

For alternative splicing analyses, RT-PCRs were performed using GoTaq DNA Polymerase (Promega) and specific primer pairs listed in Supplementary Table S5. Reaction products were separated in 1.8–2% agarose gels with 10 mg/ml ethidium bromide or 1:20 SimplySafe (EURx). PCR images were captured and analyzed using G:Box EF2 (Syngene) and GeneTools software (Syngene), or GelDoc Go Gel Imaging System (BioRad) and Image Lab software (BioRad), respectively. Percent Spliced In (PSI) represents percentage of alternative exon inclusion calculated according to the formula: PSI = (band intensity of a PCR product with included exon × 100)/(sum of band intensities for PCR products with included as well as excluded exon).

Actinomycin D treatment

GM04033 cells were seeded in a 6-well plate and transfected 24 h later with 75 nM indicated saRNAs or mock-treated. Actinomycin D (Sigma–Aldrich/Merck) was added directly to the medium 120 h post-transfection, at a concentration of 5 μg/ml (diluted in DMSO). Next, cells were harvested at timepoints 0, 2, 4, 6, and 8 h after actinomycin D treatment for RNA isolation and RT-qPCR-based expression analyses of *MBNL1*, lncRNA *MBNL1-AS1* and reference *GAPDH*. Results were plotted to show percentage of the remaining transcript, normalized to reference, relative to timepoint 0 (100%). Upregulation of *MBNL1* at timepoint 0 (before actinomycin D treatment) corresponding to 120 h of saRNA transfection was verified by RT-qPCR.

Nascent RNA capture

The amount of newly synthesized RNA was determined using Click-iT™ Nascent RNA Capture Kit (Invitrogen) per manufacturer's protocol. Briefly, cells were seeded in 6-well plates and transfected 6 h later (HEK293T) or next day (GM04033) with 75 nM saRNA for 48 h (HEK293T) or 72 h (GM04033), followed by 24 h 5-Ethynyl Uridine (EU) pulse at a concentration of 0.2 mM. Next, labeled RNA was biotinylated, captured and extracted per manufacturer's instructions using either 1 μg EU-RNA and 0.5 mM biotin azide (HEK293T) or 400 ng EU-RNA and 0.25 mM biotin azide (GM04033). RNA bound to the beads was used as a template for cDNA synthesis using the SuperScript VILO™ cDNA synthesis kit (Invitrogen), per manufacturer's instructions. Nascent RNA expression was quantified by RT-qPCR using *MBNL1*, lncRNA *MBNL1-AS1*, *DMPK*, and *GAPDH* (reference) specific primers listed in Supplementary Table S4.

Directional RT-PCR

Directional RT-PCR analysis [65] in HeLa cells was employed to detect the presence and define the directionality of *MBNL1* P2 promoter associated RNAs. Briefly, direction-specific primer (either forward, F: GCAGATAGAAAGTTCCCATCCCT or reverse, R: GGTGCCTCTTCCCAGCGTTA) was used for reverse transcription (RT) reaction using TranScriba kit (A&A Biotechnology) and 350 ng total RNA, followed by amplification of cDNA (DreamTaq PCR MasterMix; Thermo Fisher Scientific) using both F and R primers for 35 cycles. PCR product amplified from cDNA derived from RT with F primer but not with R primer indicates antisense transcription in the analyzed region. Conversely, product amplification from cDNA derived from RT with R primer but not with F primer indicates sense transcription in the analyzed region. Amplicons obtained in both reactions indicate bidirectional transcription. PCR reactions on control "-RT" samples (containing all of the RT reaction components except for the reverse transcriptase enzyme and RT primers) were performed to exclude contamination by amplification of residual genomic DNA. Non-template control was set up to control for extraneous nucleic acid contamination.

Generation of luciferase reporter vectors and luciferase assay

To generate the *MBNL1* promoter 2 constructs (*MBNL1* P2-Luc and P2-Luc_short), the region of *MBNL1* P2 (positions -1516/+60 and -1082/+60 relative to TSS2, respec-

tively) was PCR amplified from HeLa genomic DNA with oligos: 5′ TTTGGTACCGGCGTTATCCTTGAGTGTAGG 3′ and 5′ TTTGCTAGCGTCAGCTCCTTGTCATGGGA 3′ (*MBNL1* P2-Luc); 5′ TTTGGTACCCTGCAGGAAGAATGTTGTACCA 3′ and 5′ TTTGCTAGCGTCAGCTCCTTGTCATGGGA 3′ (*MBNL1* P2-Luc_short) and cloned into pGL4.10[luc2] vector (Promega) using the KpnI and NheI restriction sites. The *MBNL1* P2-LucΔsaMB1_2 construct, with a deletion of the saMB1_2 target site, was prepared using Q5® Site-Directed Mutagenesis Kit (NEB) according to the manufacturer's instructions, using the following oligos: 5′ TTAAACGATTAACGCTGG 3′ and 5′ CAGTTTAAGCAAACTAAAAGAAC 3′. To generate pmirGlo_saMB1_2-S vector, oligos containing the target sequence of saMB1_2 sense (S) strand as well as an additional diagnostic KpnI restriction site were annealed and cloned 3[1] off of firefly luciferase gene (*luc2*) in a pmirGLO Dual-Luciferase miRNA Target Expression Vector (Promega) in between NheI and XhoI sites. Oligo sequences were as follows: 5′ CTAGCGGTACCAAGGACTCAAGTACCCACAC 3′ (the underlined sequence marks the target sequence of the S strand of saMB1_2) and 5′ TCGAGTGTGGGTACTTGAGTCCTTGGTACCG 3′. The pmirGlo vector carries internal Renilla luciferase gene reporter for normalization of the primary reporter – the firefly luciferase. All constructs were verified by Sanger sequencing. For luciferase assay, 1.2×10^4 HeLa cells/well were seeded in a 96-well plate one day before transfection. 50 ng *MBNL1* P2-Luc, *MBNL1* P2-Luc_short or *MBNL1* P2-LucΔsaMB1_2 construct was co-transfected with 2 ng pGL4.75 [hRluc CMV] (Promega) and 50 nM indicated saRNA, while 50 ng pmirGlo_saMB1_2-S vector was co-transfected with 50 nM saRNA (Lipofectamine 2000; Invitrogen). Firefly luciferase and Renilla luciferase activities were measured 48 h post co-transfection using Dual-Glo-Luciferase Assay System (Promega), per manufacturer's instructions. Firefly activity was normalized to that of Renilla for each sample.

Protein isolation and western blot analyses

Cells were washed in phosphate-buffered saline (PBS), harvested in 1 ml ice-cold PBS, pelleted at 5000 x g for 5 min at 4◦C and lysed with 75 μl radioimmunoprecipitation assay (RIPA) buffer (Thermo Fisher Scientific) supplemented with 1X Halt Protease Inhibitor Cocktail (Thermo Fisher Scientific). Lysates were cleared by centrifugation at 15 000 x g for 15 min at 4◦C. Protein concentration was determined using Pierce BCA Protein Assay Kit (Thermo Fisher Scientific) per manufacturer's protocol. Samples were mixed with Laemmli Sample Buffer (Bio-Rad) containing β−mercaptoethanol and denatured at 95◦C for 5 min. Protein extracts (7–10 μg) were separated in a 10% precast polyacrylamide gel (10% Mini-PROTEAN® TGX™ Precast Protein Gels, Bio-Rad) and transferred to a polyvinylidene difluoride (PVDF) membrane (Invitrogen) for 1 h at 100 V at 4◦C, using Mini-PROTEAN Tetra System (Bio-Rad). Transfer efficiency was evaluated using Ponceau S Staining Solution (Thermo Fisher Scientific) per manufacturer's instructions. Membranes were blocked for 1 h at room temperature (RT) in 1X TBS-T buffer (tris-buffered saline [TBS], 0.1% Tween 20 [T]) containing 5% skim milk powder (Sigma–Aldrich/Merck) [1X TBS-T-MLK], then incubated O/N at 4◦C with either mouse anti-human MBNL1 primary antibody (MBNL1 clone 4A8; Wolfson Centre for Inherited Neuromuscular Disease; 1:1000) or mouse anti-human HRP-conjugated Vinculin (sc-73614; Santa Cruz; 1:2500), diluted in 1X TBS-T-MLK. Membranes were washed 3×5 min in 1X TBS-T and incubated 1 h at RT with a secondary rabbit HRP-conjugated anti-mouse antibody (12–349, Millipore), diluted 1:10 000 in 1X TBS-T-MLK. After membrane washing, signal was detected using SuperSignal West Femto Maximum Sensitivity Substrate (Thermo Fisher Scientific). Images were captured using G:Box Chemi-XR5 (Syngene) and signal intensity was quantified using GeneTools image analysis software (Syngene).

Cleavage under target and release using nuclease (CUT&RUN)

CUT&RUN assay (Cell Signaling) was used per manufacturer's protocol to analyze binding enrichment of specific proteins around predicted saRNA target sites during RNAa induction by selected saRNA duplexes. Briefly, GM04033 cells were seeded in 6-well plates and transfected with 75 nM saRNAs for 120 h. 1×10^5 cells were harvested for each antibody reaction and additional same number of cells for input sample control. The following amounts of antibodies were used: 4 μg anti-AGO2 (PA5-117725; Invitrogen), 5 μg anti-RNAPII (clone CTD4H8; Sigma–Aldrich/Merck), 10 μg anti-RNAPII Ser2P (clone 3E10; Active Motif), 10 μg anti-RNAPII Ser5P (clone E8; Active Motif), 2 μg anti-MEIS2 (sc-515470 X; Santa Cruz) and 2 μg negative control Normal Rabbit IgG (#2729; Cell Signaling). Following manufacturer's protocol, the resulting DNA products were quantified by qPCR using 8 primer pairs (Supplementary Table S6) designed to amplify short products (60 – 80 bp) spanning genomic region from −3.5 kb to +4.2 kb relative to *MBNL1* TSS2 or −3.9 kb to +5.6 kb relative to $p21^{WAF1/CIP1}$ TSS [51]. IP efficiency was calculated using the Percent Input Method with the following formula: % Input = 100% x 2(C[T] 100% Input Sample - C[T] IP Sample) and obtained data were plotted as % of input. Results were normalized by adding 5 ng of the Sample Normalization Spike-In DNA into each CUT&RUN reaction after DNA digestion step. For sample normalization, signal from the Sample Normalization Spike-In yeast DNA was quantified using the Sample Normalization Primer Set. The sample with the lowest C[T] value was selected to calculate the Normalization Factor (2(C[T] Selected Sample - C[T] the Other Sample)) per manufacturer's protocol. Finally, CUT&RUN reactions signals were normalized by each Normalization Factor.

RNA fluorescent in situ hybridization (RNA-FISH)

For RNA-FISH, GM03989 cells were seeded into 4-well chamber slides (Nunc™ Lab-Tek™ II Chamber Slide™ System; Thermo Fisher Scientific) and transfected with 75 nM saRNAs or mock-treated for 120 h. Cells were fixed in 4% PFA/PBS for 15 min at 4◦C and washed three times in 1X PBS. Pre-hybridization was performed with 30% formamide in 2X SSC for 10 min, followed by hybridization in buffer containing 30% formamide, 2X SSC, 0.02% BSA, 66 μg/ml yeast tRNA, 120 U/ml RNasin (Promega) and 2 ng/μl DNA/LNA probe (CAG)6-CA labelled at the 5[1]-end with Cy-3 and modified at positions 2, 5, 8, 13, 16, and 19 with LNA (FutureSynthesis). Post-hybridization washing was performed with 30% formamide in 2X SSC at 37◦C for 30 min followed by 1X SSC washing at 37◦C for 30 min. Slides were mounted in DAPI-containing VECTASHIELD Mounting Media with anti-fade

reagent (Vector Laboratories). Images were taken on a Zeiss Axio Observer Z1 microscope with Zeiss EC Plan-Neofluar 63x/1.25 oil objective and analyzed using Zeiss ZEN blue 3.2 – Lite software. Foci were counted in $n = 100$ nuclei per experimental sample and each sample was duplicated to verify reproducibility. Negative controls included samples hybridized in the absence of (CAG)6-CA probe.

Immunofluorescence

GM04033 cells were seeded in 2-well chamber slides (Nunc™ Lab-Tek™ II Chamber Slide™ System; Thermo Fisher Scientific) and transfected with 75 nM saRNA or mock-treated for 96 h. Cells were fixed with 4% PFA for 15 min in 1X PBS at room temperature followed by three washes in 1X PBS. Next, cells were permeabilized with 0.5% Triton X-100 in 1X PBS for 15 min followed by three washes in 1X PBS and blocked in 2.5% Normal Horse Serum (Vector Laboratories) for 30 min at RT. After blocking, cells were incubated with primary mouse antibody anti-MBNL1 (MBNL1 clone 4A8; Wolfson Centre for Inherited Neuromuscular Disease; 1:100) at 4◦C O/N. Slides were washed three times in 1X PBS containing 0.1% Tween 20 (1X PBS-T) for 5 min each and then incubated for 1 h in dark with VectaFluor Duet Reagent containing anti-mouse IgG (DyLight594 - red signal) (Vector Laboratories). After two washes in 1X PBS-T, slides were mounted using DAPI-containing VECTASHIELD Mounting Media with anti-fade reagent (Vector Laboratories). Images were taken on a Nikon A1Rsi confocal microscope with Plan Apo VC 100X/1.4 Oil DIC N2 objective and analyzed using ImageJ software. Corrected total cell fluorescence (CTCF) was calculated using the formula: CTCF = Integrated density – (Area of selected cell x Mean fluorescence of background readings). CTCF was calculated from 20 different fields (confocal images taken from $n = 2$ biological replicates using the same settings in one session) containing the following total number of nuclei (n): mock, $n = 156$; saCtrl, $n = 199$; saMB1_1, $n = 126$; saMB1_2, $n = 110$.

RNA-FISH coupled with IF (RNA-FISH-IF)

GM03989 cells were seeded into 4-well chamber slides and transfected with 75 nM saRNA or mock-treated for 120 h. RNA-FISH protocol was performed, omitting DAPI staining and mounting in the last step. Subsequently, slides were processed as described in the immunofluorescence (IF) protocol. Images of DM1 fibroblasts were taken on LEICA Stellaris 8 confocal microscope with HC PL APO 63x/1.40 OIL CS2 objective and analyzed using LAS X Office 1.4.7 software.

Cell viability, cytotoxicity, and apoptosis analyses

ApoTox-Glo Triplex Assay (Promega) was used per manufacturer's instructions to determine cell viability, cytotoxicity and apoptosis. The assay was performed in GM04033 cells seeded in black 96-well plates with clear bottom and transfected with 25, 50, 75, or 100 nM saRNA or mock-treated for 120 h. No-cell control served as a control for background fluorescence and luminescence. Fluorescence (measured at the following wavelength sets: $400_{Ex}/505_{Em}$ (viability) and $480_{Ex}/525_{Em}$ (cytotoxicity)) and luminescence were determined using Tecan Infinite M200 Pro plate reader. Viability and cytotoxicity (cell fluorescence) as well as apoptosis (luminescence) were calculated as a fold change in signal intensities compared to the lipofectamine-treated cells (mock).

Statistical analyses and data visualization

Unless otherwise indicated, experiments were repeated at least three times using a minimum of $n = 3$ independent biological replicates. Group data are presented as mean ± standard error of mean (SEM) and results obtained for each individual sample are marked on bar graphs as black dots. Two-tailed Student's *t*-test was used for statistical analyses using GraphPad Prism 8.3.0 software with the following criteria for statistical significance: $^{*}P < 0.05$; $^{**}P < 0.01$; $^{***}P < 0.001$; $^{****}P < 0.0001$. Unless otherwise indicated, statistical significance is shown relative to control RNA duplex (saCtrl). All graphs were generated using GraphPad Prism 8.3.0 software.

Results

Small RNA duplexes targeted to *MBNL1* gene promoter increase *MBNL1* transcript levels

To test the feasibility of RNAa for targeted upregulation of *MBNL1*, we used human fibroblasts derived from DM1-affected patients. These primary cells constitute a natural and physiologically relevant model in which MBNL proteins, nuclear CUG^{exp} foci, and spliceopathy have been extensively studied and can be readily measured [32, 33, 41, 66], providing us with a reliable tool for assessing the therapeutic potential of saRNA duplexes in the context of DM1. We designed a set of saRNA duplexes with antisense strands complementary to genomic sequences (+ DNA strand) within *MBNL1* gene promoter (P) regions (Fig. 1A). Initial analyses included two *MBNL1* promoters annotated within the EPD as *MBNL1_1* and *MBNL1_2* (hereafter referred to as P2 and P3 [55], respectively) (Fig. 1A, Supplementary Fig. S1A–C). Promoter 1 (P1) of *MBNL1* was omitted from analyses, as mRNAs derived from TSS1 by default lack e1, and the activity of P1 is significantly lower compared to P2 and P3 [55]. RT-qPCR analyses of TSS2- and TSS3-derived *MBNL1* transcript levels in human primary fibroblasts affected by DM1 (GM04033 cell line carrying 1000 CTG repeats; Supplementary Fig. S1D) as well as meta-analyses of EPD-deposited data on promoter-specific *MBNL1* expression in skin fibroblasts from DM1 donors (Supplementary Fig. S1E) and overall promoter-specific *MBNL1* expression profile in all samples in which P2 and P3 promoters are active (Supplementary Fig. S1F), confirmed superior activity of P2 over P3. These results are concordant with our previous data [55, 56].

Initial screening of rationally designed 21-nt long (19-nt target sequence and 2-nt dT overhangs) dsRNAs targeting *MBNL1* P2 (21 saRNAs) and P3 (18 saRNAs), within the region spanning ~3 kb upstream of the respective transcription start site (TSS2 and TSS3), revealed that the significantly more active P2 was amenable to RNAa in patient-derived primary DM1 fibroblasts, while P3 did not respond to the tested saRNAs (Supplementary Fig. S2A and B). The two top scoring P2-directed duplexes identified in initial screening, saMB1_1 and saMB1_2, targeted *MBNL1* at positions −882 and −1319 bp upstream of the EPD annotated TSS2, respectively, and enhanced *MBNL1* pre-mRNA and mRNA levels by 1.5 up to 2-fold (Fig. 1B, Supplementary Fig. S2B). None of the tested control RNA duplexes were able to induce *MBNL1* upregulation (Fig. 1B). These controls included scrambled versions of the two top-scoring saRNAs saMB1_1 and saMB1_2 (saMB1_1-scrA, B and C and saMB1_2-scrA, B and C) as well as their derivatives with point mutations introduced at distinct po-

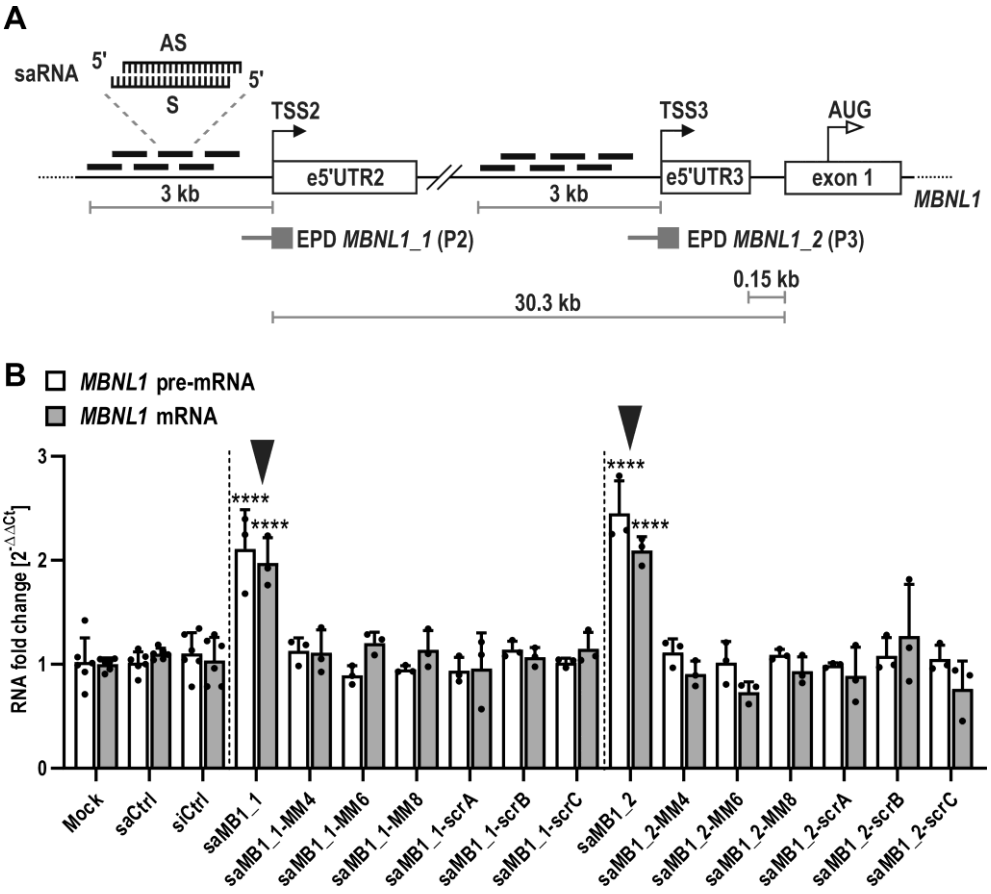

Figure 1. saRNA duplexes targeted to *MBNL1* gene promoter 2 upregulate *MBNL1* transcript levels in a DM1 cell model. (**A**) Schematic representation of a genomic region covering *MBNL1* promoter 2 (P2) and 3 (P3) with indicated transcription start sites (TSS2 and 3, respectively), corresponding 5′ UTR exons (e5′UTR2 and 3, respectively) as well as the first coding exon (exon 1) and translation start site (AUG). The schematic of saRNA duplex is shown with antisense (AS) and sense (S) strands marked. Genomic regions targeted by saRNAs (up to ~3kb upstream of TSS2 and 3) are indicated. EPD annotated *MBNL1* promoters *MBNL1_1* (P2) and *MBNL1_2* (P3) are depicted, with the thick part representing annotated TSS and sequences downstream, and the thin part indicating sequences upstream of the TSS and defining the orientation of the promoter. (**B**) Representative results of RT-qPCR analyses of *MBNL1* pre-mRNA and mRNA levels in GM04033 DM1 fibroblasts transfected for 120 h with: lipofectamine alone (mock), 75 nM control dsRNA (saCtrl and siCtrl), saRNA against *MBNL1* P2 (saMB1_1 and saMB1_2), and mutant versions of saMB1_1 and saMB1_2 carrying a single nucleotide mismatch introduced at positions 4–8 within the seed region (MM4-8) or sequence-scrambled versions of saMB1_1 and saMB1_2 (scrA-C). Inverted arrowheads mark samples in which saRNA triggered significant *MBNL1* upregulation.

sitions within the seed region (saMB1_1-MM4, 6 or 8 and saMB1_2-MM4, 6 or 8). Moreover, previously validated non-targeting saCtrl [51] and commercial RNA duplex (siCtrl) were used as additional controls.

The lead saRNA duplexes, saMB1_1 and saMB1_2, specifically increased the level of P2-, but not P3-derived *MBNL1* transcripts (Supplementary Fig. S2C). saRNA dose-response and RNAa kinetics analyses in primary DM1 fibroblasts indicated optimal amount of saRNA (75 nM) and timepoint (120 h) required for the most significant *MBNL1* boost (Supplementary Fig. S3A (left panel) and S3B). A comparative dose-response analysis examining the effects of saRNAs and a well-characterized siRNA against AGO2 [59, 60] at a defined dose range starting at 75 nM (saRNA response peak) up to 150 nM revealed that siRNA duplex worked similarly effective at the whole concentration range while saRNA response gradually declined above 75 nM dose (Supplementary Fig. S3A, middle and right panels). Since both analyses were performed using the same amount of transfection reagent, the limitation in saRNAs transfection efficiency arising from insufficient dsRNA to lipofectamine ratio is unlikely the cause for the observed phenomenon. In general, cytoplasmic RNAi works effectively within low concentration ranges of siRNA, depending on the targeted transcript abundance, while nuclear RNAa requires higher saRNA amounts [67]. In our study, increasing the saRNA dose above the 75 nM threshold did not enhance its response, likely because the target site, which, by default, is a sequence within the genomic DNA, may be already fully occupied or because of the chromatin context and accessibility of the *MBNL1* promoter. Our results suggest that the observed decline in saRNA response may be intrinsic to RNAa mechanism involving the two identified molecules, in which saRNA processing as well as the delayed kinetics of RNAa due to, e.g. nuclear import of saRNA and chromatin remodeling at the target promoter, may be the rate limiting steps. Broader studies involving more examples of siRNA and saRNA duplexes should examine the ubiquitousness of the observed phenomenon in the RNAa mechanism. Finally, no induction of *MBNL2* paralog was detected upon saMB1_1 and saMB1_2, supporting the specificity of the identified duplexes toward *MBNL1* (Supplementary Fig. S3C). Notably, transfection of both lead saRNAs simultaneously (data not

shown) or sequentially (Supplementary Fig. S3D) failed to trigger *MBNL1* upregulation.

saRNAs upregulate *MBNL1* RNA in distinct cell models

Both lead saRNA duplexes directed at P2 upregulated *MBNL1* RNA in distinct DM1 cell models, including patient-derived primary fibroblasts carrying *DMPK* with ~500, ~1700, or ~2000 CTG triplet repeats and control non-DM1 fibroblasts derived from unaffected individuals (Supplementary Fig. S4A). Importantly, myoblasts (both unaffected and DM1) which represent the proliferating precursors of skeletal muscle tissue most affected by DM1, were also amenable to RNAa, albeit only via saMB1_2 (Supplementary Fig. S4B-C). In general, saMB1_2 induced stronger effect compared to saMB1_1 in majority of the tested cell lines, regardless of the experimental conditions (i.e. repeated transfection, as shown in Supplementary Fig. S4B). Other cell models, including HeLa (Supplementary Fig. S4D) and HEK293T cells (Supplementary Fig. S4E, left panel), were also responsive to RNAa upon either of the two lead saRNA duplexes. Long-term and persistent effect of saMB1_2 was evident in HeLa and HEK293T cells, where *MBNL1* levels remained elevated even after splitting the cells by half 72 h post-saRNA transfection and allowing the remaining cells to grow for additional 24 h (Supplementary Fig. S4D and S4E, left panel). Moreover, strong induction of nascent *MBNL1* RNA was observed upon saMB1_1 in HEK293T cells, even though other cell models were less responsive to this saRNA (Supplementary Fig. S4E, right panel).

saRNAs increase *MBNL1* transcription at both the initiation and elongation step

The RNAa mechanism involves the activation of gene expression at the transcriptional level. Having observed that saRNA-mediated increase in *MBNL1* mRNA is accompanied by increased pre-mRNA levels (Fig. 1B), likely indicative of enhanced transcription, we corroborated these data by examining the level of nascent, newly transcribed RNAs in DM1 fibroblasts treated with saRNAs using nascent RNA capture protocol. We observed a significant increase in nascent *MBNL1* RNA, but not unrelated control *DMPK* transcripts (Fig. 2A). Similar results were obtained in HEK293T (Supplementary Fig. S4E, right panel). Altogether, these data strongly support the notion that *MBNL1* promoter-targeted saRNAs enhance *MBNL1* gene transcription. Further, to exclude the possible effect of saRNA on *MBNL1* transcript stability, we inhibited mRNA synthesis using actinomycin D (Act-D) starting at 120 h post-saMB1_1 delivery. *MBNL1* transcript decay kinetics followed a similar pattern to the one in controls at distinct timepoints after Act-D addition, thus ruling out unspecific effect of saRNA on *MBNL1* mRNA turnover (Fig. 2B).

To support these findings, we next assessed the binding of factors associated with active transcription and RNAa pathway by scanning the region around *MBNL1* TSS2 via CUT&RUN assay. Upon saRNA delivery, chromatin was immunoprecipitated with antibodies recognizing RNA polymerase II (RNAPII; corresponding to total RNA polymerase II) as well as Ser5 and Ser2 phosphorylation status of the C-terminal domain of RNAPII (RNAPII Ser5P and RNAPII Ser2P; corresponding to initiating and elongating polymerase, respectively) as well as AGO2. Subsequently, qPCR with eight sets of primers specific for *MBNL1* gene, ranging from −3.5 kb to +4.2 kb relative to *MBNL1* TSS2 (Fig. 2C schematic), was used to scan the indicated genomic region for binding of these proteins. We detected a massive binding enrichment of RNAPII and RNAPII Ser2P to *MBNL1* P2 in primary DM1 fibroblasts transfected with either of the two top scoring saRNAs (Fig. 2D). While the enrichment of RNAPII Ser2P in saCtrl-treated cells was minimal, both saMB1_1 and saMB1_2 triggered a significant increase in RNAPII Ser2P occupancy near TSS2 that extended across the transcribed region of the gene. Conversely, strong signal for RNAPII Ser5P was detected specifically around TSS2 only in saCtrl-treated cells, indicating that this region is likely poised for transcription but not actively transcribed in the absence of saMB1_1 or saMB1_2 (Fig. 2D). However, RNAPII Ser5P enriched signals were detected in saRNA-transfected cells between −1 and −2 kb from TSS2, a region covering their respective binding sites (Fig. 2D). Next, we analyzed the binding of AGO2, a crucial component of the RNAa pathway [50, 51]. In response to saMB1_1 and saMB1_2 delivery, a significant enrichment in AGO2 binding was detected in regions encompassing saRNA target sites (Fig. 2D). This enrichment corresponded to RNAPII as well as RNAPII Ser5P / Ser2P binding at the same locations and was not detected upon saCtrl. Importantly, control CUT&RUN experiments confirmed that scrambled version of saMB1_2 (saMB1_2-scrA) and seed-region mutant version of saMB1_2 (saMB1_2-MM4) recruited neither RNAPII nor AGO2, as opposed to unmodified saMB1_2 duplex (Fig. 2E). Overall, these data demonstrate strong sequence specificity of RNAa complex guidance to *MBNL1* promoter by identified saRNAs. We conclude that saRNA-AGO2 complex targets *MBNL1* P2 and associates with RNAPII to promote formation of the transcription initiation complex that stimulates both transcription initiation and productive elongation, which is concordant with the current understanding of RNAa mechanism [51].

The lack of RNAa response upon combined sequential or simultaneous treatment with saMB1_1 and saMB1_2 (Supplementary Fig. S3D and data not shown) was unexpected and could suggest that saRNAs might interfere with each other through direct interaction. However, this is unlikely considering the lack of sequence complementarity between both saRNAs. Alternatively, reduced target site accessibility due to steric hindrance while loading the saRNAs onto closely located target sequences by AGO2 may be the cause. This scenario is supported by the lack of RNAPII and AGO2 binding to the *MBNL1* promoter region upon combined saMB1_1 and saMB1_2 transfection as opposed to transfection of either of these saRNAs separately, where clear enrichment of both proteins was detected using CUT&RUN assay (Fig. 2F, upper panel). To further dissect this phenomenon, we performed CUT&RUN upon sequential transfection of saMB1_2 and a well characterized saP21 [51], targeting the $p21^{WAF1/CIP1}$ gene promoter. As expected, a massive enrichment of RNAPII and AGO2 was detected at both target sites when saP21 and saMB1_2 were used in combination (Fig. 2F). We conclude that steric hindrance and an interference in RNAa complexes assembly at the promoter target site are most likely responsible for the lack of *MBNL1* induction when prompted by two saRNAs, saMB1_1, and saMB1_2, targeting nearby sequences.

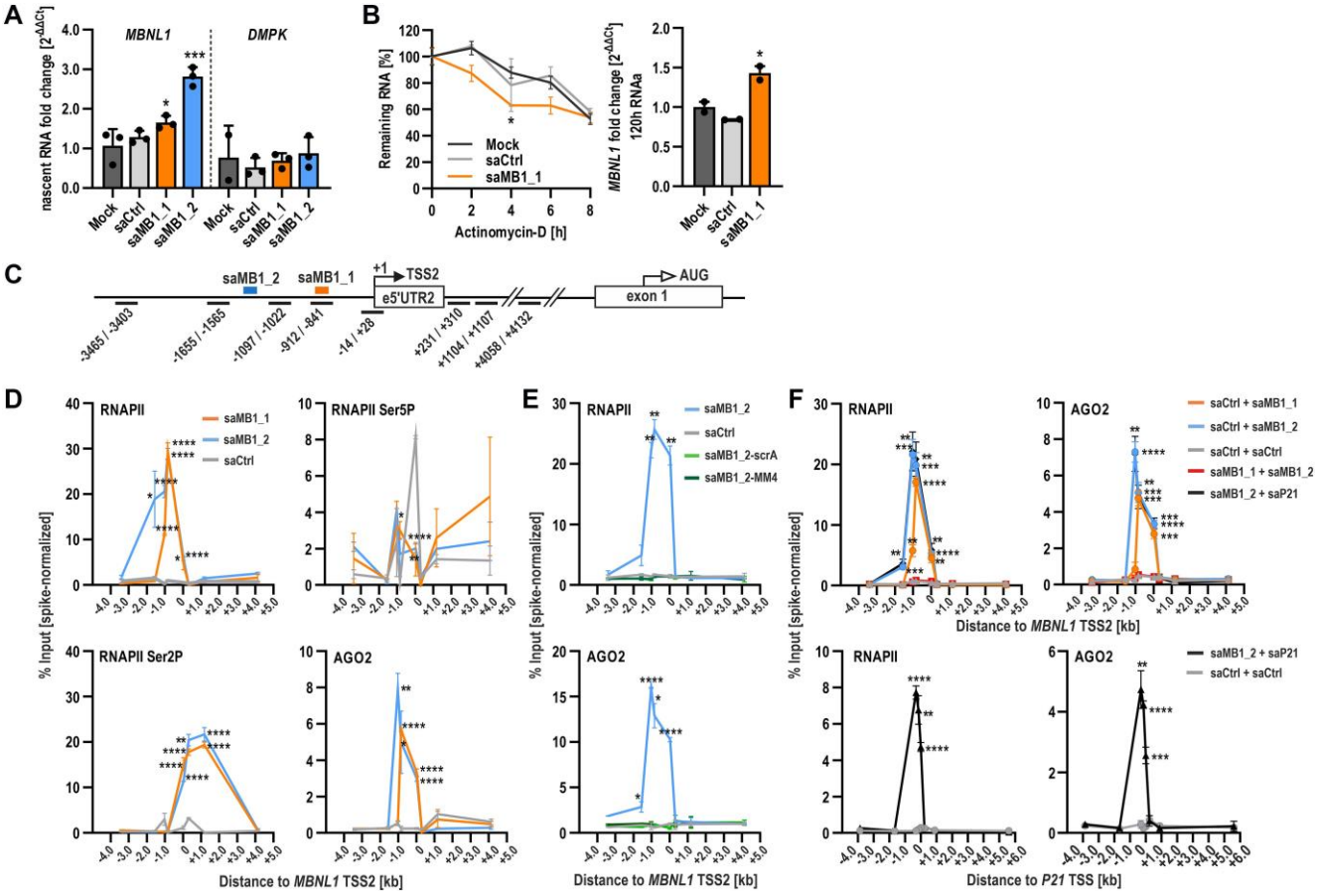

Figure 2. saRNA-mediated *MBNL1* upregulation occurs at the level of transcription initiation and elongation. (**A**) Nascent mRNA capture in GM04033 DM1 fibroblasts transfected with 75 nM indicated saRNA for 72 h, followed by 24 h EU pulse. Expression of nascent mRNA of *MBNL1* and *DMPK* (control) was assayed by RT-qPCR. (**B**) Line chart to the left shows representative RT-qPCR-based time course analysis (0–8 h) of the remaining *MBNL1* mRNA upon actinomycin D (Act-D) treatment of GM04033 cells transfected with 75 nM saMB1_1 (orange) or control duplex saCtrl (grey) for 120 h. Results obtained in lipofectamine-treated cells (mock, black) are shown for reference. Act-D was added 120 h post-saRNA transfection (timepoint 0 of the time course analysis). The bar graph to the right shows RT-qPCR verification of *MBNL1* upregulation 120 h post-saRNA treatment in GM04033 cells used for Act-D experiment. (**C**) Schematic representation of *MBNL1* genomic region scanned for specific protein-binding enrichment using CUT&RUN assay. TSS2 (+1) is indicated. The thick short lines indicate saRNA binding sites (blue and orange). The thin black lines below the schematic represent analyzed qPCR products and indicate their positions relative to TSS2. (**D**) Summary of the qPCR results of CUT&RUN analyses in GM04033 cells transfected with 75 nM indicated saRNA for 120 h, demonstrating binding enrichment of RNAPII, RNAPII Ser5P, RNAPII Ser2P, and AGO2 following saMB1_1 (orange) or saMB1_2 (blue) delivery. Non-targeting dsRNA (saCtrl; grey) was used as a control. (**E**) Results of the control CUT&RUN experiment in which scrambled sequence (light green) as well seed-region mutant version of saMB1_2 (dark green) failed to recruit RNAPII and AGO2, signifying sequence specificity of saMB1_2. (**F**) Summary of the qPCR results of CUT&RUN analyses in GM04033 cells transfected for a total of 120 h with indicated saRNA delivered sequentially such that 24 h treatment with 75 nM of one saRNA was followed by transfection with an equal amount of the second saRNA for additional 96 h. The order of transfection is as labelled. Binding enrichment of RNAPII and AGO2 was detected at saRNA target sites following transfection of saCtrl + saMB1_1 (orange), saCtrl + saMB1_2 (blue), saMB1_2 + saP21 (black) but not saMB1_1 + saMB1_2 (red) or saCtrl + saCtrl (grey). saP21 [48, 51] targets the promoter of $p21^{WAF1/CIP1}$ gene at 322 bases upstream TSS. Results were normalized using Spike-In DNA and are represented as % of input. Primer sequences used for CUT&RUN analyses of the respective genes are listed in Supplementary Table S6.

saRNAs stimulate transcription by recruiting specific TFs to *MBNL1* promoter

To reinforce the conclusions on the effect of saRNA on *MBNL1* transcription, we next scanned experimentally validated genome-wide TF-binding profiles in the JASPAR CORE 2024 collection and UCSC Genome Browser to search for unique TFs whose binding sites may overlap saRNA target sites. Annotated PBX2, MEIS1 and MEIS2 binding sites were found to overlap the cognate target genomic sequence of saMB1_1 (Supplementary Fig. S5A). All these TFs may act as transcriptional activators [68, 69]. To verify their possible involvement in *MBNL1* RNAa, we silenced the expression of *MEIS1* and *MEIS2* via RNAi in DM1 fibroblasts and assessed the effect on saRNA-mediated *MBNL1* enhancement. While efficient silencing of *MEIS1* and *MEIS2* prevented *MBNL1* upregulation via saMB1_1 (Supplementary Fig. S5B and C), it did not affect saMB1_2-mediated RNAa (Supplementary Fig. S5D and E), strongly suggesting specific cooperation of these TFs in transcription driven by the saRNA whose target site overlaps their respective binding sites. In support, enriched binding of MEIS2 to *MBNL1* P2 was detected by CUT&RUN scanning only upon saMB1_1 transfection, but not saMB1_2 (Supplementary Fig. S5F). In all, these data suggest that saRNA may operate via recruitment of specific transcriptional activators whose binding sites overlap its cognate sequence. This highlights a unique opportunity to identify novel *MBNL1* expression regulators using RNAa as a molecular toolbox and necessitates

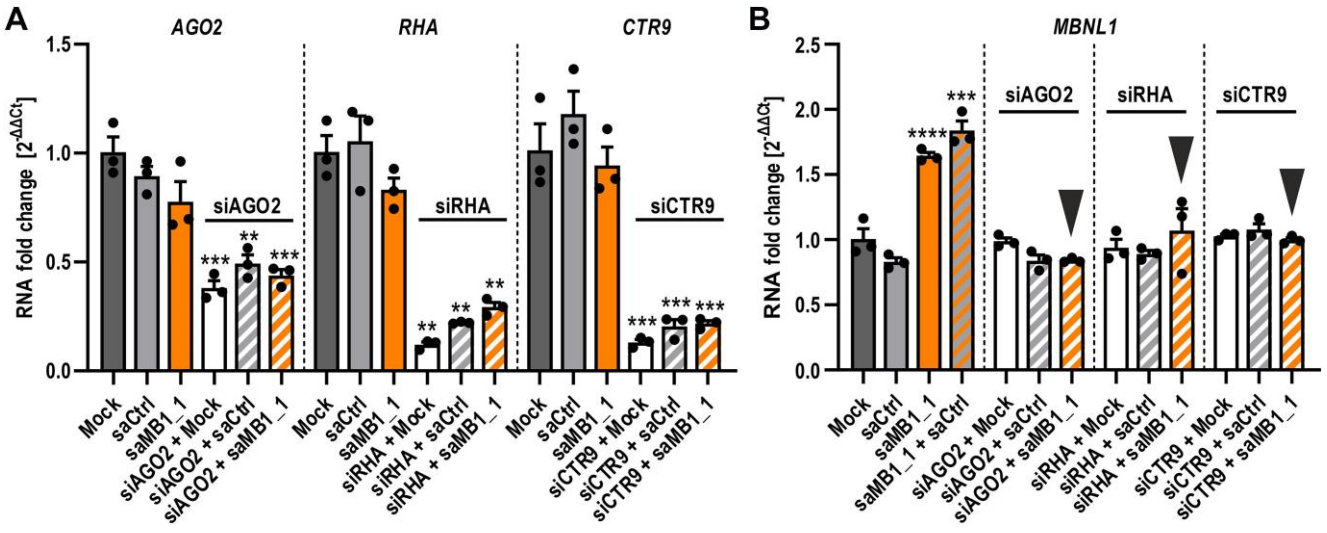

Figure 3. saRNA duplex upregulates *MBNL1* via RNAa pathway. (**A** and **B**) Knock-down of *AGO2*, *RHA*, and *CTR9* expression (**A**) and fold change of *MBNL1* induction (**B**) verified by RT-qPCR in GM04033 DM1 fibroblasts transfected for a total of 120 h with lipofectamine alone (mock) or 75 nM indicated dsRNA delivered solo, or sequentially such that 24 h treatment with 75 nM siRNA against indicated RNAa complex component (siAGO2, siRHA, and siCTR9) was followed by mock-transfection or transfection with an equal amount of saCtrl or saMB1_1 for additional 96 h. Inverted arrowheads in (B) indicate samples in which knock-down of the indicated RNAa complex component inhibited *MBNL1* induction.

further studies on the role of these saRNAs in *MBNL1* regulation.

Silencing of RNAa complex components prevents saRNA-mediated increase in *MBNL1* expression

Finally, to provide direct evidence that saMB1_1 and saMB1_2 enhance *MBNL1* transcription specifically via RNAa mechanism, we used RNA interference (RNAi) to knock-down the expression of major established RNAa pathway components required for the assembly of the RITA complex, including AGO2, RHA and CTR9 [51, 67]. siRNAs against specific RNAa pathway components were delivered into GM04033 cells either alone or sequentially, i.e. followed by transfection of saMB1_1 or saCtrl duplex. We observed that efficient knock-down of RITA components (~50–80%) by their corresponding siRNAs (siAGO2, siRHA, siCTR9; Fig. 3A) completely blocked *MBNL1* upregulation via saMB1_1 (Fig. 3B). In contrast, combined transfection of saMB1_1 and saCtrl permitted *MBNL1* enhancement to the same extent as in saMB1_1-treated samples. These analyses were extended to saMB1_2 duplex, in which case downregulation of *AGO2* likewise prevented *MBNL1* transcriptional upregulation (Supplementary Fig. S6A and B). Cumulatively, these data support RNAa pathway involvement in saRNA-mediated transcriptional upregulation of *MBNL1*.

Distinct mechanisms may be involved in RNAa of *MBNL1*

Having verified that the two identified saRNAs stimulate *MBNL1* transcription specifically via RNAa-dependent pathway, we next investigated possible scenarios explaining how these saRNAs might operate at *MBNL1* promoter. Based on the available published data, we hypothesized two main models (Fig. 4A and B; based on [67]). The RNA:DNA hybrid model predicts that RNAa is an on-site process mediated by AGO2-dependent loading of the antisense (AS) or the sense (S) strand of saRNA duplex onto complementary target sequence within the coding (+) or template (−) DNA strand, respectively (Fig. 4A). AGO2 may recruit DNA/RNA helicases such as RHA to unwind DNA duplex and allow for RNA:DNA hybrid pairing, and other auxiliary proteins like CTR9 to stimulate active *MBNL1* transcription via assembly of the RITA complex [58, 67]. Another scenario, based on the RNA:RNA model, predicts that the sense strand (S) of saRNA duplex plays the leading role in RNAa by binding to the natural antisense long non-coding RNA (lncRNA) *MBNL1-AS1* originating from the complementary strand of *MBNL1* gene and partially overlapping the genomic P2 region (Fig. 4B). In this on-site process, association of the S strand of saRNA with the lncRNA *MBNL1-AS1* could act as a molecular scaffold for the assembly of the RITA complex and the recruitment of additional proteins, including histone modifiers, to alter local chromatin structure and ultimately drive transcription [52, 67]. Alternatively, promoter-associated short nascent cryptic transcripts in either sense or antisense orientation could also serve as docking sites for respective saRNA strands complexed with AGO2 (Fig. 4B). To investigate which of the proposed models operates at *MBNL1* P2, we first utilized chemical modifications of saRNA duplexes to verify specific strand involvement in *MBNL1* RNAa, followed by examining of the putative physical association of the individual saRNA strands with their target sites using *MBNL1* promoter-luciferase reporter assays. These studies were complemented by comprehensive analyses of lncRNA *MBNL1-AS1* requirement for RNAa-mediated upregulation of *MBNL1*. We also examined the presence of nascent cryptic transcripts at *MBNL1* promoter.

AGO2-guided antisense strand of saRNA duplex is required for MBNL1 RNAa

To gain insights into the saRNA strand involvement in RNAa at *MBNL1* promoter, we first leveraged chemical modifications of the lead saRNA duplexes to specifically inhibit or promote selection of either the S or the AS strand by AGO2. While modifications to the 5′-end of either strand are known

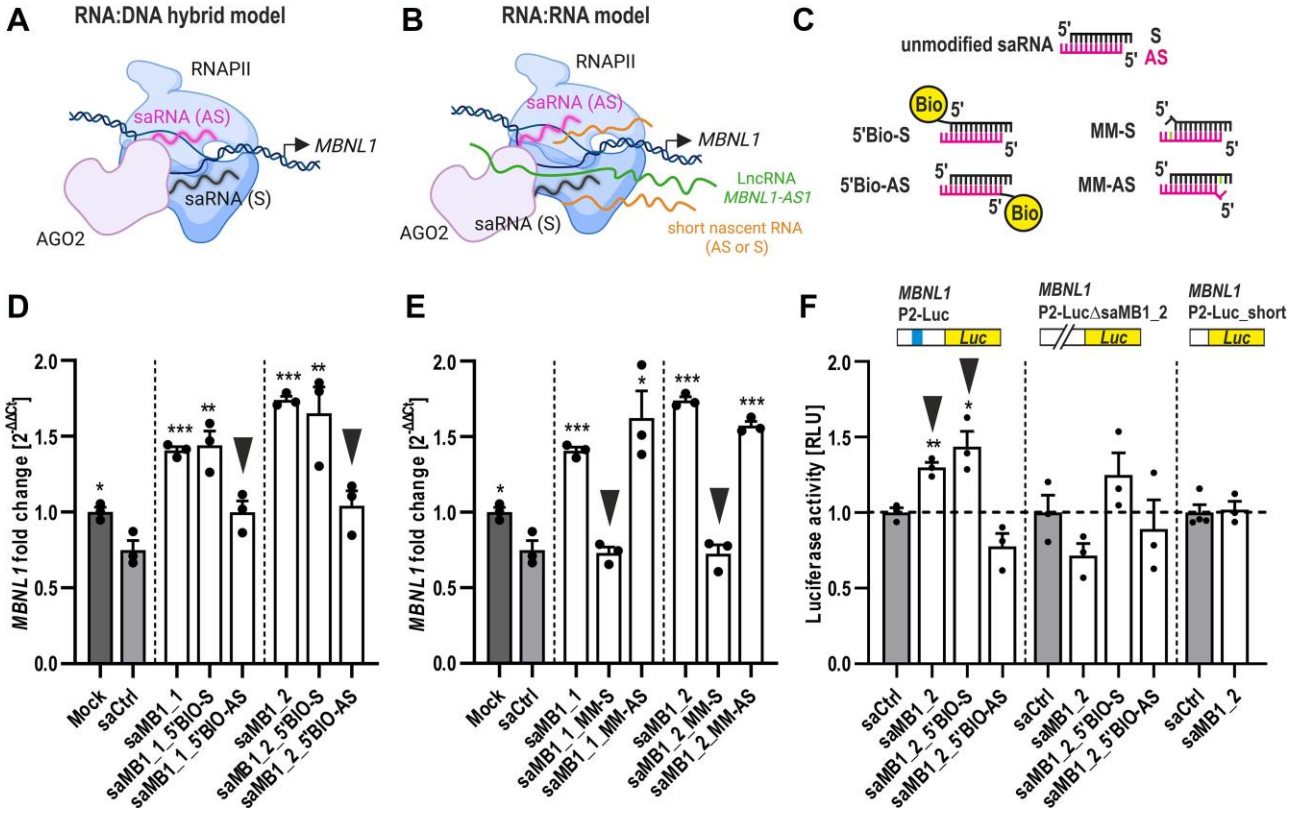

Figure 4. AGO2-guided antisense strand of saRNA duplex is required for *MBNL1* RNAa. (**A** and **B**) Schematic of putative RNA activation mechanism models at *MBNL1* P2 predicting the major role of either the antisense (AS) or the sense (S) strand of saRNA duplex and considering the involvement of lncRNA *MBNL1-AS1* as well as nascent cryptic promoter-associated transcripts. Created in BioRender. Stepniak-Konieczna, E. (2025) https://BioRender.com/sz1613a. The RNA:DNA hybrid model (**A**) presumes an on-site mechanism in which respective saRNA strands target their complementary DNA sequences to facilitate transcriptional complex assembly. The RNA:RNA model (**B**) predicts that lncRNA *MBNL1-AS1* and/or nascent promoter-associated transcripts in either orientation are targeted by respective saRNA strands to promote the assembly of transcriptional machinery. Detailed description in main text. (**C**) Schematic representation of saRNA modifications used to either inhibit (5^{1}BIO) or promote (MM) the selection of indicated strands by AGO2. (**D** and **E**) RT-qPCR analyses of *MBNL1* levels assayed in GM04033 DM1 fibroblasts transfected for 120 h with 75 nM indicated unmodified saRNAs or their modified versions covalently linked to biotin at the 5^1-end of either the antisense (5^{1}BIO-AS) or the sense (5^{1}BIO-S) strand (**D**), or modified saRNAs containing mismatched bases at the 3^{1}end opposite to the 5^1-most nucleotide of either the antisense (MM-AS) or the sense (MM-S) strand (**E**). Inverted arrowheads indicate chemical modifications of the AS (D) or S strand (E) that either blocked (D) or were incompatible with (E) *MBNL1* RNAa, respectively. (**F**) Dual-luciferase assay of *MBNL1* promoter activity in HeLa cells co-transfected with an indicated reporter vector (schematic), saRNA and Renilla reporter for normalization. saMB1_2 binding site is represented as a blue rectangle. Luciferase activities were measured 48 h post-co-transfection and are represented as RLU (relative light unites) normalized to that of Renilla for each sample.

to interfere with AGO2 function and block RNAa, lowering of the thermodynamic stability at the 5′-end of either strand promotes its preferential loading onto AGO2 as the guide (active) strand [59]. Accordingly, we designed chemically modified saRNAs derived from saMB1_1 and saMB1_2 that were covalently linked to biotin at the 5′-end of either the AS (5′BIO-AS) or the S (5′BIO-S) strand to inhibit their selection by AGO2 (Fig. 4C). Conversely, promotion of strand selection was achieved by introducing a mismatched base at the 3′-end of the opposite strand. This mismatched base would directly face the 5′-most nucleotide of either the AS (MM-AS) or S (MM-S) strand (Fig. 4C), thus lowering its 5′-end thermodynamic stability and marking it for preferential selection. We observed that inhibition of the AS strand in either of the two lead saRNA duplexes (5′BIO-AS) completely blocked *MBNL1* upregulation in DM1 primary fibroblasts, while inhibition of the S strand (5^{1}BIO-S) had no effect on saRNA activity (Fig. 4D). In line with this observation, MM-S modified saRNA duplexes were not able to induce *MBNL1* upregulation (Fig. 4E), indicating that promotion of the S strand selection by AGO2 is incompatible with *MBNL1* RNAa. Conversely, promotion of the AS strand selection (AS-MM) permitted *MBNL1* RNAa to a similar level as in the case of unmodified duplexes (Fig. 4E). Altogether, these data strongly indicate that in the case of both identified saRNA duplexes, the AS strand is the leading (guide) strand selected by AGO2 during RNAa, while the S strand has no impact on RNAa activity.

saMB1_2 binds to the target region of the *MBNL1* gene promoter

To verify whether the AS strand of saMB1_2 may bind the intended target within the *MBNL1* gene promoter, we assessed the enrichment in *MBNL1* promoter activity upon saRNA transfection. The *MBNL1* promoter containing saMB1_2 binding site was cloned upstream of the luciferase gene to generate the *MBNL1* P2-Luc construct (Fig. 4F, schematic). This reporter was co-transfected into HeLa cells with either saCtrl, unmodified saMB1_2 or modified saMB1_2 linked to biotin at the 5^1-end of either the sense (5^{1}BIO-S) or the antisense (5^{1}BIO-AS) strand. A dual-luciferase reporter assay

showed that both the unmodified as well as the 5′BIO-S version of the saMB1_2 can significantly activate the *MBNL1* P2-Luc reporter compared to the saCtrl and 5′BIO-AS, thus reinforcing the lead role of the antisense strand of saMB1_2 in *MBNL1* RNAa (Fig. 4F). To confirm that *MBNL1* acti- vation by saMB1_2 is mediated by the physical interaction with complementary site within *MBNL1* promoter, we generated *MBNL1* P2-LucΔsaMB1_2 construct with a deletion of saMB1_2 binding site (Fig. 4F, schematic). Notably, saMB1_2 and its 5[1]BIO-S version were unable to trigger an increase in the luciferase activity when co-transfected with *MBNL1* P2-LucΔsaMB1_2 (Fig. 4F). These results indicate that saMB1_2 can directly interact with *MBNL1* promoter. Consistently, saMB1_2 failed to stimulate the luciferase activity when co-transfected with a reporter containing a shorter fragment of the *MBNL1* promoter, deprived of the larger region encompassing saMB1_2 target site (*MBNL1* P2-Luc_short) (Fig. 4F). These data reinforce the sequence-specificity of saMB1_2 for the predicted binding site and suggest that during the RNAa process saMB1_2 binds to the genomic DNA of the target site within the *MBNL1* promoter to facilitate its transcriptional stimulation. Altogether, these findings point to the RNA:DNA hybrid model of *MBNL1* RNAa, but do not exclude other players potentially serving as additional docking sites for identified saRNAs.

LncRNA *MBNL1-AS1* is dispensable for RNA activation of *MBNL1*

Because antisense transcripts overlapping sense genes have been implicated in RNAa of their sense counterparts, we set out to investigate whether the lncRNA *MBNL1-AS1* overlapping *MBNL1* P2 participates in saMB1_2-mediated RNAa at *MBNL1* promoter, as predicted in the RNA:RNA model (Fig. 4B). For this purpose, we silenced *MBNL1-AS1* via classical RNAi as well as via GapmeR-mediated RNaseH-dependent degradation. Two distinct approaches were undertaken to eliminate lncRNA *MBNL1-AS1* isoforms from both cytoplasmic (RNA interference, Fig. 5A) as well as nuclear compartment (GapmeR-mediated degradation, Fig. 5B). Remarkably, knock-down of *MBNL1-AS1* had no inhibitory effect on *MBNL1* upregulation upon subsequent transfection of saMB1_2, regardless of the silencing approach (Fig. 5A and B). Further, silencing of *MBNL1-AS1* by itself did not alter *MBNL1* expression level, demonstrating that this lncRNA unlikely serves as a negative regulator of its sense counterpart. Overall, these findings rule out the requirement for *MBNL1-AS1* in *MBNL1* RNAa and reinforce the conclusion that *MBNL1* upregulation is the sole result of saRNA-dependent transcriptional enhancement.

Importantly, the RNA:RNA model predicts that promoter-associated cryptic transcripts (in both orientations) may also serve as binding sites for saRNAs and thus may be involved in RNAa (Fig. 4B). We tested this hypothesis via directional RT-PCR analyses [65] which allowed us to determine the presence and orientation of potential short transcripts deriving from the saMB1_2 target region of the *MBNL1* P2 promoter. Obtained data clearly indicate that only antisense (most likely corresponding to *MBNL1-AS1*) but not sense RNAs are produced at the analyzed region of the *MBNL1* promoter (Supplementary Fig. S7A and B). Lack of sense amplicons likely mirrors enhanced transcription of the full length *MBNL1* RNA and interference with the transcription of nascent promoter-associated RNAs. Although these data are not quantitative, the intensity of bands representing antisense amplicons was clearly reduced upon saRNA transfection (Supplementary Fig. S7B). Collectively, these findings provide evidence that neither the lncRNA *MBNL1-AS1* nor the promoter-associated cryptic transcripts are mechanistically involved in *MBNL1* RNAa via the identified saRNAs. Furthermore, they support the conclusion that saRNAs target the *MBNL1* promoter via an on-site mechanism, in which the AS strand of the saRNA duplex binds complementary *MBNL1* DNA coding strand to facilitate transcriptional stimulation of *MBNL1* promoter.

LncRNA *MBNL1-AS1* is downregulated upon RNA activation of *MBNL1*

The comprehensive study on *MBNL1-AS1* involvement in RNAa of the *MBNL1* gene revealed an intriguing and consistent downregulation of lncRNA *MBNL1-AS1* at distinct timepoints following delivery of saMB1_1 and saMB1_2 to DM1 fibroblasts (Supplementary Fig. S8A), which is consistent with the results of directional RT-PCR. Sequence-scrambled versions of saRNAs were unable to reduce lncRNA *MBNL1-AS1*; however, varying degrees of reduction were observed with control saRNA duplexes carrying mutations at distinct positions within the seed region (Supplementary Fig. S8B). This implies that the mechanism underlying *MBNL1-AS1* reduction does not require perfect sequence complementarity. Downregulation was evident even upon transfection of saRNAs that failed to enhance *MBNL1* but were targeted to genomic sites overlapping *MBNL1-AS1* (Supplementary Fig. S8C). We hypothesized that this effect could be driven by the S strand of saRNA duplex via classical RNAi. Alternatively, saRNA-mediated assembly of the transcriptional complex at *MBNL1* promoter could interfere with the antisense transcription. Intriguingly, knock-down of AGO2, a crucial component in both RNAi as well as RNAa, did not prevent *MBNL1-AS1* reduction upon saRNA, thus ruling out the former scenario (Supplementary Fig. S9A). In contrast, the level of nascent, newly synthesized *MBNL1-AS1* was significantly downregulated upon saMB1_1 or saMB1_2, thus pointing to the latter possibility (Supplementary Fig. S9B). Moreover, when transcription was blocked with actinomycin D following saRNA delivery, we detected a significant reduction in the remaining lncRNA *MBNL1-AS1* compared to controls, pointing to its decreased stability (Supplementary Fig. S9C). In all, these data allow us to conclude that at least two distinct mechanisms participate in lncRNA *MBNL1-AS1* reduction upon effective RNAa of its sense counterpart. On the one hand, reduced transcription of *MBNL1-AS1,* which stems likely from transcriptional collision with the complex transcribing *MBNL1.* On the other hand, reduction in lncRNA stability, which likely mirrors the secondary miRNA-like effect of the S strand of saRNA. Prompted by these results, we used chemically modified saRNA duplexes to verify the hypothesis that the S strand drives downregulation of *MBNL1-AS1.* Strikingly, AS strand inhibition by 5[1]-end biotinylation (5[1]BIO-AS) had no impact on *MBNL1-AS1* reduction, while 5[1]BIO-S modification completely inhibited it in the case of saMB1_1, but not saMB1_2 (Supplementary Fig. S10A). Similarly, the saRNA harboring a single 3[1]-most nucleotide mismatch within the S strand (MM-AS) prevented *MBNL1-AS1* decrease, but only in the case of saMB1_1 and not saMB1_2

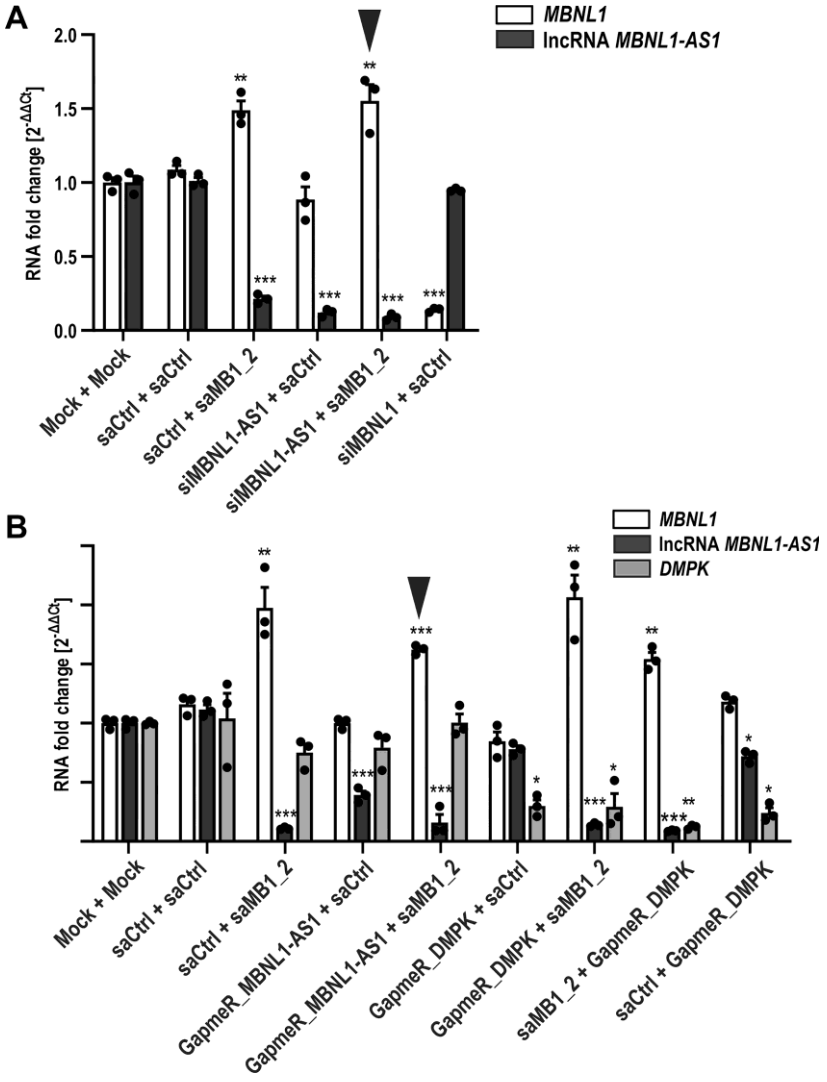

Figure 5. LncRNA *MBNL1-AS1* is dispensable for RNAa of *MBNL1.* (**A** and **B**) RT-qPCR analyses of indicated transcript levels in GM04033 DM1 fibroblasts subjected to silencing of lncRNA *MBNL1-AS1* using RNA interference (**A**) or GapmeR-mediated knock-down (**B**). In (A), cells underwent two successive transfections including mock or 75 nM indicated dsRNA (saCtrl, saMB1_2, siMBNL1-AS1, or siMBNL1) for 24 h, followed by second transfection, including mock or 75 nM indicated dsRNA (saCtrl, saMB1_2) for additional 96 h. In (B) cells were mock-transfected or transfected with 75 nM indicated reagent (saCtrl, saMB1_2, GapmeR against *MBNL1-AS1* or *DMPK*) for 24 h, followed by additional 96 h mock-transfection or transfection with 75 nM indicated dsRNA (saCtrl and saMB1_2) or GapmeR against *DMPK*. Samples were harvested for analyses after a total of 120 h. Order of transfected reagents is as labeled. Inverted arrowheads indicate samples in which silencing of *MBNL1-AS1* using RNAi (A) or GapmeRs (B) failed to interfere with RNAa of *MBNL1*.

(Supplementary Fig. S10B). In all, these data demonstrate that *MBNL1-AS1* downregulation is controlled by the S but not the AS strand of saMB1_1 duplex. Conversely, saMB1_2 du- plex is either more tolerant to modifications of the 5′ (in 5′BIO-S) as well as 3′ end (in MM-AS) of the S strand or alternatively, *MBNL1-AS1* downregulation in this case may be triggered by an additional factor which remains to be identified.

The off-target potential of the S strand of saMB1_2 can be eliminated by chemical modification

The S strands of the identified saRNA duplexes, when incorporated into AGO2 complex, may lead to off-target effects by interacting with complementary non-specific transcripts or gene promoters. To assess the off-target potential of the S strand of saMB1_2, we generated pmirGlo_saMB1_2-S reporter vector, in which the target sequence of the S strand was cloned into the 3′UTR of the firefly luciferase gene within a dual-luciferase reporter vector pmirGlo, which also carries Renilla luciferase gene for normalization (Supplementary Fig. S10C, schematic). We hypothesized that reduction in luciferase activity upon binding of the S strand to luciferase mRNA, due to destabilization of its mRNA and blocked translation, would be indicative of the miRNA-like off-target potential of the S strand. As predicted, a significant loss in reporter activity was observed in HeLa cells co-transfected with pmirGlo_saMB1_2-S and saMB1_2 or its modified version carrying 5[1]-biotin on the AS strand (5[1]BIO-AS), but not on the S strand (5[1]BIO-S) (Supplementary Fig. S10C, chart). The latter allowed robust luciferase luminescence, underscoring the miRNA-like off-target potential of the S strand. Notably, these data also indicate that correct chemical modification of the S strand can diminish this unanticipated off-target effect with-

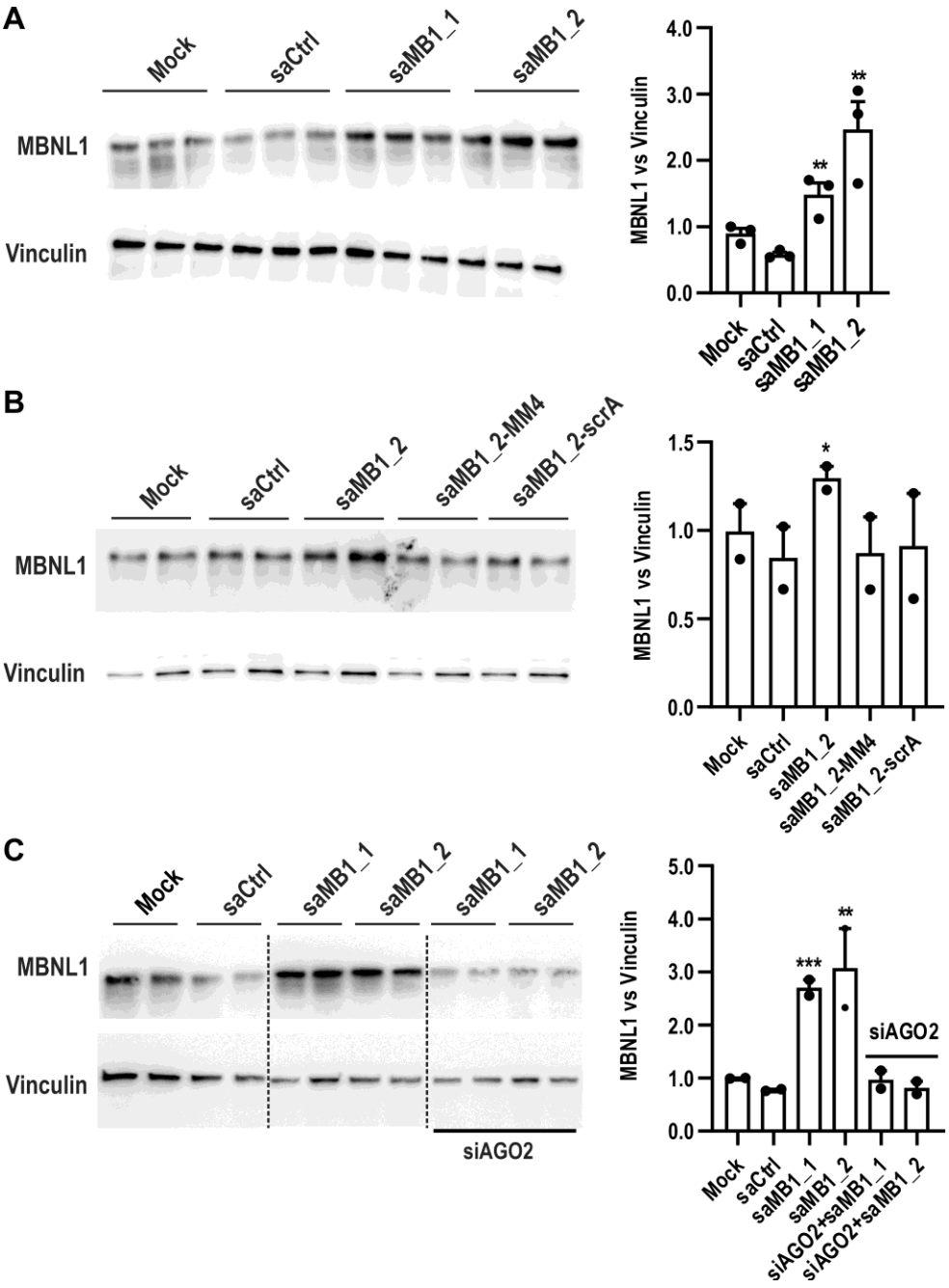

Figure 6. RNA activation enhances MBNL1 protein content in a cellular model of myotonic dystrophy. (**A**–**C**) Representative western blot analyses of MBNL1 protein levels in GM04033 DM1 fibroblasts transfected with 75 nM saMB1_1 and saMB1_2 for 120 h (**A**), scrambled and seed-region mutant versions of saMB1_2 (**B**) as well as saRNAs transfected on the background of *AGO2* knock-down (siRNA against *AGO2* transfected for 24 h, followed by second transfection with the indicated saRNA for additional 96 h) (**C**). Quantifications are shown to the right of gel images. MBNL1 and Vinculin (loading control) blots are derived from the same experiment and a single gel. Data are presented as mean ± SEM of triplicate (A) or duplicate (B and C) biological repeats. Lanes in (C) were rearranged and the boundary between non-adjacent rearranged lanes is indicated by vertical dashed lines. Original uncropped scans are shown in Supplementary Fig. S11.

out compromising saRNA activity to upregulate the target gene.

saRNA duplexes increase MBNL1 protein content in myotonic dystrophy cell models

To evaluate the therapeutic impact of *MBNL1* RNAa, we assessed the level of cellular pool of MBNL1 protein upon saMB1_1 and saMB1_2 delivery to DM1 fibroblasts. Both lead duplexes triggered a significant increase in MBNL1 protein level ranging from 1.3- up to 3-fold at 120 h post-transfection (Fig. 6A–C and Supplementary Fig. S11A–C). Overall, these results mirror increased levels of *MBNL1* RNA detected by RT-qPCR analyses. Importantly, neither scrambled (saMB1_2-scrA) nor seed-region mutant versions (saMB1_2-MM4) of saMB1_2, which are incompatible with RNAa (Fig. 1B), were able to trigger MBNL1 protein increase (Fig. 6B and Supplementary Fig. S11B). Consistently with data demonstrating AGO2 requirement for RNAa, RNAi-mediated silencing of AGO2 prevented MBNL1 protein boost

(Fig. 6C and Supplementary Fig. S11C). Moreover, time course RNAa revealed the induction of MBNL1 protein across 72 h up to 120 h post-saMB1_2 transfection, and the gradual decline to basal levels at 144 h (Supplementary Fig. S12A). Because P2-derived *MBNL1* pre-mRNAs undergo autoregulation through a feedback loop mechanism based on MBNL binding and exclusion of the first coding exon (e1), whose presence governs protein activity and stability, we also looked at the correlation of MBNL1 elevation with e1 exclusion from *MBNL1* transcripts. Indeed, a drop in e1 content corresponded with the elevated MBNL1 protein at 72–120 h, after which its inclusion returned to the basal level observed in control samples (Supplementary Fig. S12B).

In agreement with the protein data, IF analyses of MBNL1 in DM1 cells 120 h post-saRNA delivery revealed significantly higher intensity of MBNL1 signal in nuclei of saMB1_1- and saMB1_2-transfected cells compared to controls (Fig. 7A and B). Because excessive MBNL1 levels could possibly enhance RNA foci formation, we quantified CUG^{exp} foci in saRNA-treated DM1 fibroblasts. RNA fluorescent *in situ* hybridization analyses (RNA-FISH) clearly indicated similar numbers of nuclear RNA inclusions across all samples, regardless of the treatment type (mock and control duplexes vs. saMB1_1 and saMB1_2) (Fig. 7C–E). Moreover, co-localization of MBNL1 with RNA inclusions was unaltered in saMB1_1 and saMB1_2-transfected cells, as visualized by RNA-FISH coupled with immunofluorescent (IF) detection of MBNL1 protein (RNA-FISH-IF), and did not seem to lead to increase in foci number or size (Supplementary Fig. S13).

MBNL1 RNAa corrects alternative splicing defects in DM1 fibroblasts and myoblasts

Because even small fluctuations in the cellular pool of MBNL1 may affect the outcome of the overall alternative splicing pattern in diseased cells, we investigated whether the increase in MBNL1 content following RNAa was sufficient to correct the AltS defects in DM1 cell models including patient-derived fibroblasts (Fig. 8A, Supplementary Fig. S14) and myoblasts (Fig. 8B, Supplementary Fig. S15). We assessed the splicing of alternative exons negatively as well as positively regulated by MBNL1, i.e. exons whose inclusion is repressed by MBNL1 (*MBNL1* e1, e5, e7; *MBNL2* e7; *NFIX* e7; *NCOR2* e45a; *SYNE1* e65) or promoted by MBNL1 (*INSR* e11; *FLNB* e31; *MYO5A* e32; *TEAD1* e4), respectively. These selected splicing events are altered in diseased cells in the absence of functional MBNL proteins and were extensively validated as biomarkers of DM1 spliceopathy [32, 66, 70]. Strikingly, delivery of either of the two lead saRNA duplexes triggered a consistent shift in the splicing pattern of the analyzed exons from the one observed in DM1 (marked by red dashed lines) toward the pattern typical of healthy, non-affected cells (marked by green dashed lines) (Fig. 8A and B). In both tested cell models saRNAs consistently decreased the inclusion of alternative exons normally repressed by MBNL1 (Fig. 8A and B). Analogous observation was made for the group of biomarker exons positively regulated by MBNL1, i.e. saRNAs enhanced their inclusion. The effects of saMB1_1 on AltS correction were generally weaker compared to saMB1_2, which is consistent with more efficient upregulation of *MBNL1* mRNA and protein via saMB1_2 (Figs 1B, 2A, and 6; Supplementary Fig. S4). In DM1 fibroblasts, the rescue effect of saMB1_2 ranged from almost a ~100% (e.g. *MBNL1* e1 and e5, *NFIX* e7, *INSR* e11) to between 30% and 50% splicing correction (e.g. *MBNL2* e7 and *NCOR2* e45a, respectively), depending on the analyzed exon. In contrast, splicing correction in DM1 myoblasts, although evident, was much less pronounced compared to DM1 fibroblasts due to the weaker induction of MBNL1 which most likely mirrors poorer efficiency of saRNA uptake by muscle cells. Importantly, sequence-scrambled or seed region mutant saRNA duplexes had no effect on AltS of MBNL1 target exons (Supplementary Fig. S16A and B). Moreover, no adverse cellular effects were noted upon delivery of saRNA duplexes to DM1 cells, as judged by unaltered cell viability, cytotoxicity and apoptosis for up to 5 days post-transfection (Supplementary Fig. S17A–C). Overall, these data clearly demonstrate a significant therapeutic utility of RNA activation in the treatment of AltS defects in DM1 via targeted upregulation of *MBNL1* gene transcription and at the same time, necessitate further studies on efficient delivery of these therapeutics to muscle cells.

Discussion

The fact that molecular hallmarks of DM1 stem from the depletion of MBNL proteins, but not *MBNL* genes mutations, offers a unique therapeutic possibility to compensate for protein deficiency with extra endogenous expression. This approach has been pioneered using miRNA translational repressors of transcript isoforms originating from *MBNL1* and *MBNL2* genes, which were targeted with *miR-23b* and *miR-218* antagonists to elevate MBNL1 and 2 proteins in skeletal muscles and correct DM1-like alterations ([71] and reviewed in [72]). In this work, we took an alternative approach based on a direct transcriptional stimulation of the endogenous *MBNL1* gene promoter via natural, conserved cellular mechanism of gene activation – RNAa. Our screening of rationally designed RNAa effectors, saRNA duplexes, targeted to the most active promoter of *MBNL1*, resulted in identification of the two lead molecules, saMB1_1 and saMB1_2, that enhanced *MBNL1* pre-mRNA, mRNA and protein levels *in cellulo* up to ~2-fold. Importantly, studies utilizing distinct approaches to boost endogenous content of MBNL1 protein, including aforementioned miRNA repressors as well as e.g. generic HDAC inhibitors [47, 73] or globally acting DNA methylation inhibitors [46], demonstrated that even a relatively small increase of MBNL1 level (between 1 and 2-fold) can be beneficial in mitigating DM1 disease phenotypes. Additionally, benefits of moderate *MBNL1* increase include: (i) prevention from unwanted side-effects associated with uncontrolled MBNL1 overexpression (as shown by others, e.g. [38, 39]) and (ii) in the case of saRNA – a specific, site-directed action on *MBNL1* transcription. Mechanistically, we show that direct transcriptional stimulation of *MBNL1* promoter by saRNA is sufficient to boost the cellular pool of MBNL1 protein and counteract the AltS defects associated with MBNL1 depletion via CUG^{exp} RNA – a cellular hallmark of DM1. The level of MBNL1 protein upregulation was sufficient to significantly ameliorate spliceopathy, yet it did not trigger increased RNA foci number and size nor did it lead to cellular toxicity. This study therefore constitutes the first report that site-specific augmentation of *MBNL1* transcription may mitigate disease-associated AltS alterations in DM1 cells and hence, may foster studies on novel therapeutic designs.

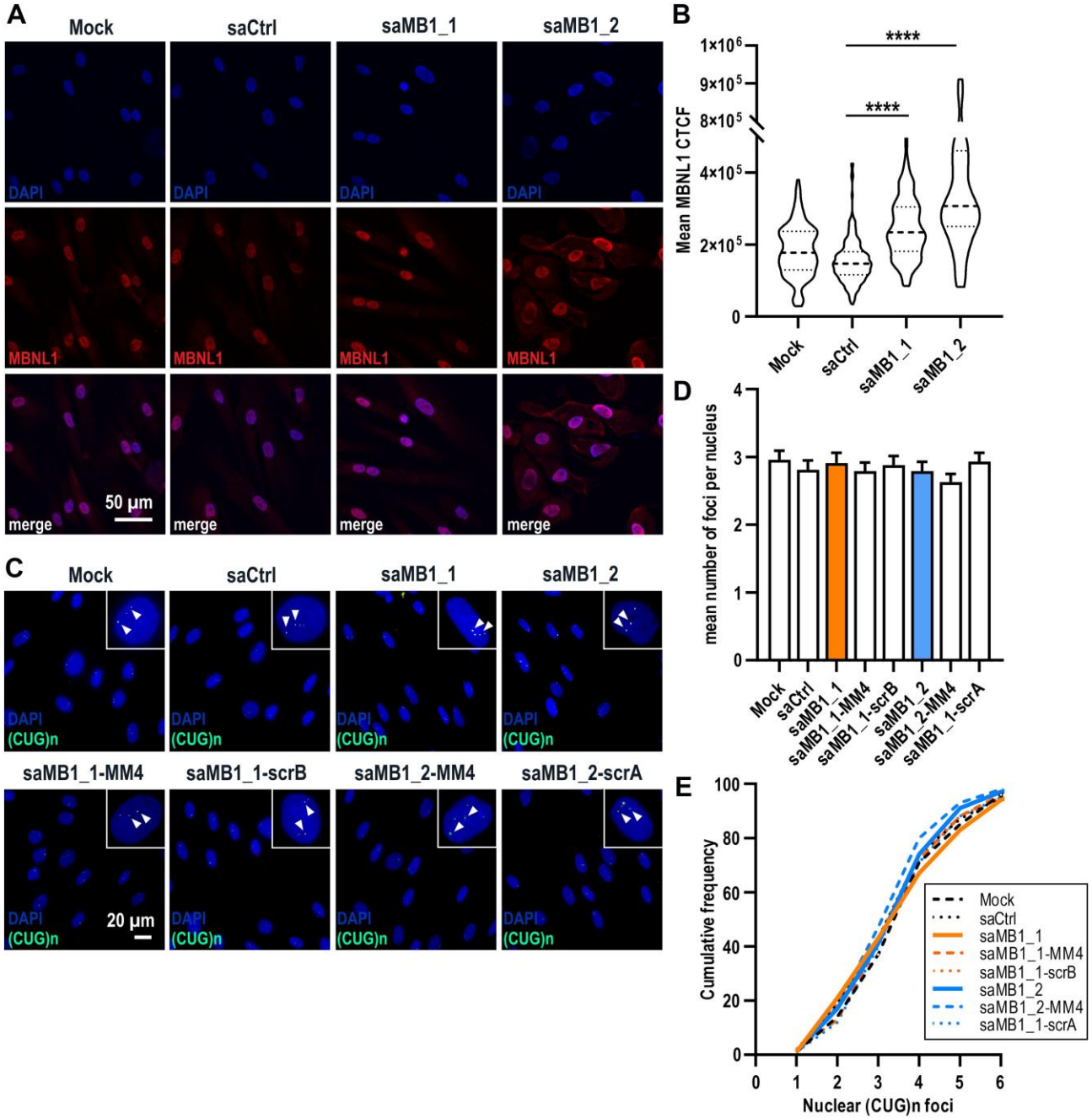

Figure 7. saRNA duplexes increase MBNL1 protein content in DM1 cells without enhancing nuclear RNA foci accumulation. (**A**) Representative confocal images of MBNL1 IF (red; DyLight594) in GM04033 DM1 primary fibroblasts transfected with 75 nM indicated saRNAs or mock-treated for 120 h. Nuclei were counterstained with DAPI (blue). Scale bar (50 μm) is indicated. (**B**) Quantification of total MBNL1 signal intensity and its distribution across sample types shown in (A). CTCF was calculated from 20 different fields (confocal images taken from $n = 2$ biological replicates using the same settings in one session) of the following total nuclei number (n): mock $n = 156$; saCtrl $n = 199$; saMB1_1 $n = 126$; saMB1_2 $n = 110$. Thick dashed lines indicate median and thin dotted lines indicate quartiles. (**C**) Representative RNA-FISH analyses of (CUG)n foci (green; Cy3) in GM03989 DM1 primary fibroblasts transfected with 75 nM indicated saRNAs or mock-treated for 120 h. Nuclei were counterstained with DAPI (blue). Arrowheads in blow-up panels indicate examples of nuclear RNA foci. Scale bar (20 μm) is indicated. (**D** and **E**) Quantification of the mean number of RNA foci per nucleus (D) and cumulative frequency of nuclear CUG^{exp} RNA aggregates (E) in sample types shown in (C). Data in (D and E) are presented as mean ± SEM of $n = 100$ nuclei/sample type.

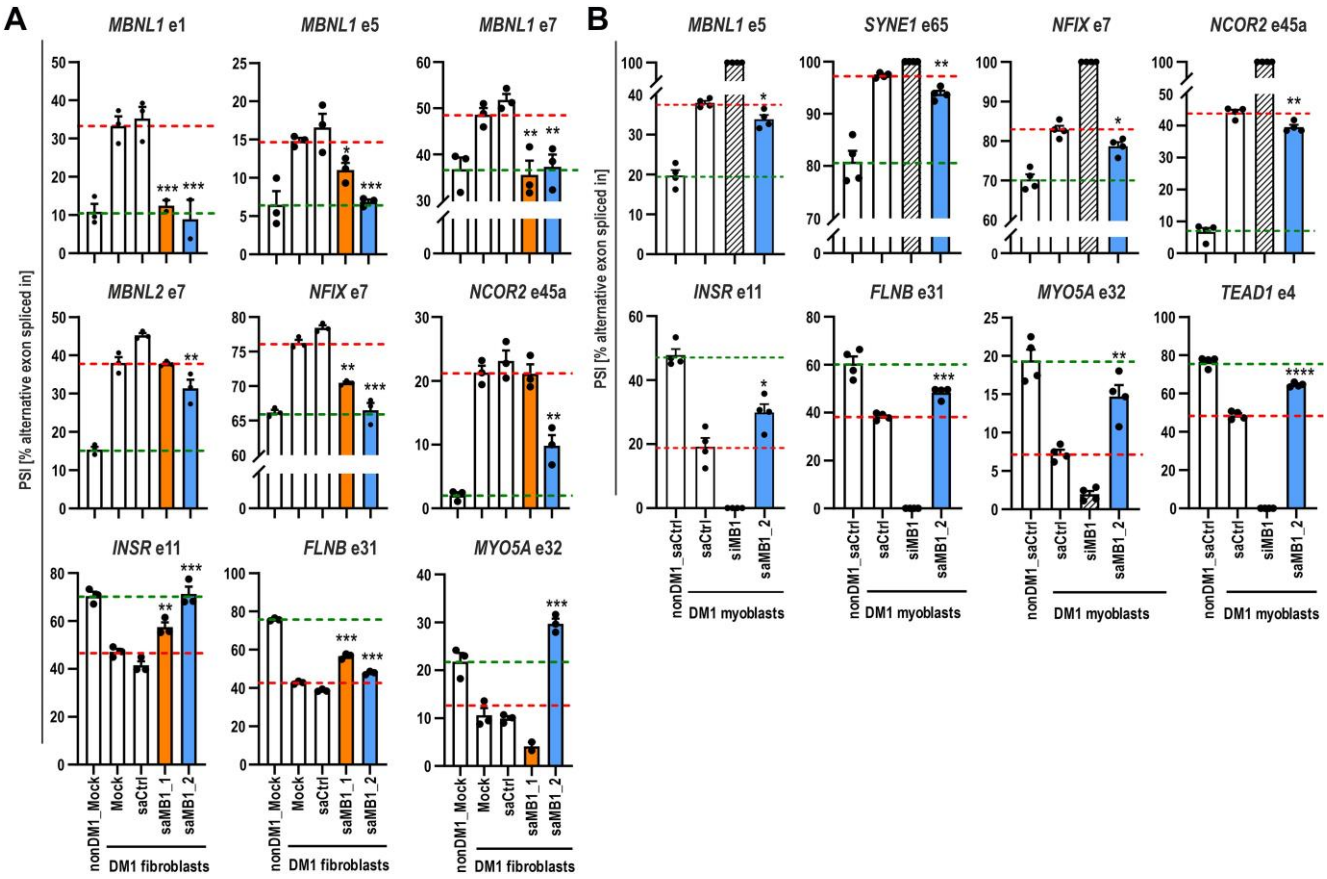

Figure 8. RNA activation of *MBNL1* mitigates DM1-spliceopathy. (**A**-**B**) RT-PCR-based quantification of indicated alternative splicing events in GM04033 DM1 fibroblasts (**A**) and DM1 10009 myoblasts (**B**) transfected with 75 nM indicated saRNA for 120 and 96 h, respectively. NonDM1_Mock (A) and nonDM1_saCtrl (B) represent unaffected fibroblasts transfected with lipofectamine or saCtrl, respectively. Red and green dashed lines mark the level of alternative exon inclusion in DM1 and unaffected cells, respectively. Data are presented as mean ± SEM of triplicate (A) and quadruple (B) samples and refer to % alternative exon inclusion (PSI; % exon spliced in). For each splicing event, quantification refers to a single representative experiment, which was repeated three times for consistency. Representative RT-PCR gel images used for quantification are shown in Supplementary Figs S14 and S15.

Our data indicate that P2 promoter was susceptible to RNAa, while all tested P3-directed saRNAs failed to upregulate *MBNL1* expression. Because effective saRNA design is largely a "hit-or-miss" process [74], it is possible that the number of tested saRNAs and the coverage of genomic sites within P3 were not sufficient. However, it also specifically highlights the importance of promoter selection in RNAa strategies. Particularly, considering the higher occupancy of permissive histone marks around P2/TSS2 than TSS3/P3, based on UCSC Genome Browser-deposited data, as well as superior activity of P2 over P3 observed in the current and in our previous studies [55, 56]. Basal level of gene expression from a particular promoter is crucial for effective RNAa, as both the susceptibility and the magnitude of gene induction by RNAa require the target gene to be poised for transcription and manifest low to intermediate levels of mRNA expression. It is plausible that P3 was refractory to RNAa in our studies because of epigenetic chromatin modifications and lesser accessibility of this promoter region. Nonetheless, identifying effective saRNAs directed at *MBNL1* P3 would allow to directly compare the effects of *MBNL1* transcriptional stimulation from a promoter by default giving rise to transcripts containing the first coding exon (e1) and thus highly functional and stable protein, versus P2-derived RNAs that undergo autoregulation via alternative splicing of e1.

saRNA duplexes identified in our study increased nascent *MBNL1* mRNA without altering mRNA decay kinetics, strongly indicating that RNAa at *MBNL1* P2 occurs at the transcriptional level. This is consistent with published works [51, 54] and moreover, concordant with previous ChIP-based analyses [50, 51] showing saRNA-triggered enrichment of RNAPII occupancy at targeted promoter regions. Massive accumulation of initiating and elongating RNAPII at saMB1_1 and saMB1_2 target sites, extending across the gene body, strongly supported saRNA-mediated formation of the transcription initiation complex as well as effective elongation. Together with the requirement for the key RITA complex components including AGO2, RHA, and CTR9, these data clearly indicate that saMB1_1 and saMB1_2 mediate *MBNL1* transcriptional enhancement specifically via canonical RNAa pathway. An interesting observation is that two saRNAs targeting one gene and directed at cognate sequences located within a relatively small distance (which in the case of saMB1_1 and saMB1_2 is ~450 bp) failed to induce RNAa, likely due to spatial interference of a transcribing complex initiating at one site and arrival or assembly of another complex at another site within close proximity. Our hypothesis on steric hindrance is supported by the lack of AGO2 and RNAPII recruitment when both duplexes targeting nearby sites are used in combination. Consistently, saRNAs targeting

genes located on distinct chromosomes recruited key RNAa components and were able to induce RNAa when used concurrently. This may have important implications for simultaneous RNAa-based enhancement of *MBNL* paralogs for potentially additive and/or synergistic therapeutic effect.

RNAa can be harnessed to identify gene expression regulators. We demonstrated the contribution of specific transcription activators, MEIS1 and MEIS2, to saMB1_1-mediated *MBNL1* upregulation. MEIS proteins belong to the TALE (Three-Amino-acid Loop Extension) family of homeobox genes and can directly or cooperatively bind DNA with various TFs (e.g. HOX, PBX, and PARP1), hence their role in effective transcriptional activation, regulation of chromatin dynamics and gene expression in multiple processes [68]. It is plausible that MEIS proteins associate with RITA complex in *MBNL1* transcriptional upregulation via saMB1_1. To uncover novel *MBNL1* expression regulators, further studies should investigate protein components participating in *MBNL1* RNAa via identified saRNAs, e.g. via pull-down of their chemically modified derivatives complexed with interacting partners, followed by proteomic analyses.

Our comprehensive study involving experiments with chemical modifications of saRNA strands as well as *MBNL1* promoter luciferase assays indicated that the identified saMB1_1 and saMB1_2 saRNAs target DNA via an on-site mechanism involving the AS strand. While inhibition of the AS strand completely blocked *MBNL1* induction, promotion of the S strand selection by AGO2 failed to induce RNAa. Accordingly, luciferase assays suggested a direct physical interaction of the AS strand of saMB1_2 with the cognate target site within the *MBNL1* promoter. Although several lines of evidence suggest that saRNA may also bind natural antisense transcripts overlapping promoters to increase target gene expression [50, 52], we ruled out lncRNA *MBNL1-AS1* requirement for *MBNL1* RNAa. Consistently with published works [59], our data allow to conclude that the AS strand serves as the guide/leading strand and targets complementary DNA sequence within the *MBNL1* promoter, whereas the S strand has minimal impact on RNAa. Intriguingly, our study revealed that the lead saRNAs triggered consistent downregulation of *MBNL1-AS1* overlapping *MBNL1* P2, but only when their S strands were active. One likely scenario is that the S strand of saRNA directly interacts with antisense transcript through RNA-RNA base pairing, potentially leading to its destabilization, higher transcript turnover or degradation via mechanism other than RNAi, as we ruled out the role of AGO2 in this process. Alternatively, saRNA could recruit chromatin-modifying complexes to the promoter region of the target gene, indirectly affecting transcription of neighboring antisense transcripts by altering the accessibility of their promoters or enhancer regions. The former scenario is supported by higher *MBNL1-AS1* turnover observed in our experiments with actinomycin D-mediated transcription inhibition. The latter possibility, however, is also reinforced by reduced levels of nascent lncRNA *MBNL1-AS1*. It is plausible that both mechanisms participate independently to bring about *MBNL1-AS1* reduction upon *MBNL1* RNAa. Notably, saRNAs' effects on antisense transcripts can vary depending on the specific genomic context and regulatory mechanisms involved. In support, Schwartz *et al.* [52] proposed that progesterone receptor (PR) activation is attributable to an association between saRNA and the antisense transcript AT-2 overlapping the PR promoter. This view was challenged by another study showing AT-2 dispensability for PR RNAa [58] and our own results also excluded the requirement for *MBNL1-AS1* in *MBNL1* RNAa. Further, silencing of *MBNL1-AS1* affected neither the basal expression level of *MBNL1* nor saRNA-mediated *MBNL1* upregulation. This demonstrates that first, this lncRNA is not a negative regulator whose removal can relieve negative pressure on its sense counterpart and second, it is mechanistically dispensable for *MBNL1* RNAa. Moreover, we demonstrated that saRNA treatment does not induce the production of promoter-associated nascent sense transcripts originating from the saMB1_2 target region that could serve as docking sites for the AS strand of saRNA at *MBNL1* promoter. Altogether, our results negate the contribution of the RNA:RNA model in RNA activation of *MBNL1* gene by the two identified saRNAs.

An important caveat to be considered with all RNA-based antisense approaches is potential off-targeting, mediated via binding to unintended RNA targets even in the case of partial sequence complementarity. In our work, an unexpected effect involved downregulation of lncRNA *MBNL1-AS1* overlapping *MBNL1* P2, mediated clearly via S strand of saRNA duplex. Even though saRNAs did not adversely affect cell viability, cytotoxicity or apoptosis for up to 5 days post-transfection, we cannot exclude the long-term effect of persistent *MBNL1-AS1* downregulation upon *MBNL1* RNAa. Importantly, this unanticipated effect could be eliminated completely in the case of saMB1_1, and partially in the case of saMB1_2, via simple chemical modification that inhibited the S strand activity: 5^{1}-end biotin conjugation. Moreover, introducing only one 3^{1}-most nucleotide mismatch within the S strand was sufficient to fully abolish *MBNL1-AS1* downregulation without affecting the overall RNAa efficiency, but only in the case of saMB1_1 and not saMB1_2. Together with data showing that saRNA seed region mutations were unable to prevent *MBNL1-AS1* downregulation, all these results support two conclusions (i) that the off-target effect mediated via the S strand does not rely on a perfect sequence complementarity, and (ii) that careful manipulation of the S strand activity can completely or partially abrogate unwanted side effects without compromising RNAa efficiency.

All cell models used in this work were susceptible to *MBNL1* induction via RNAa, albeit with varying efficiency. These differences may stem from local epigenetic status (e.g. DNA methylation) and chromatin accessibility across diverse human cell lines as well as efficiency of saRNA uptake by e.g. fibroblasts vs. muscle cells and inherent differences in metabolic properties of distinct cell lines. Indeed, delivery of dsRNA to patients' diseased cells and tissues has been a major challenge in RNA-based therapy [75]. Intriguingly, siRNA delivery *in vivo* can be significantly improved through lipid conjugation e.g. cholesterol [76], while lipid- and polymer-based nanoparticles are well known to prolong their circulation time, stability, and bioavailability *in vivo* [77]. Likewise, recent work within the RNAa field has shown an effective intravenous delivery into mice of *HNF4A*-targeted saRNA linked with dendrimer nanoparticles [78] or conjugated aptamers [79]. Moreover, advanced saRNA-based therapy in clinical trials in patients with advanced hepatocellular carcinoma consists of *CEBPA*-targeted saRNA linked to liposomal nanoparticles (SMARTICLES™) delivered via intravenous infusion [80]. Further, recently launched phase I clinical trial will examine lipid-conjugated (LiCO™) *p21*-targeted saRNA in patients with non-muscle-invasive bladder cancer, delivered

through intravesical instillation (clinicaltrials.gov identifier NCT06351904) [81]. In this novel saRNA-based drug, RAG-01, *p21*-targeted saRNA is conjugated with a lipid-based delivery system via a benzimidazole linker. It would be interesting to test whether lipid-based modifications could positively affect saMB1_1 and saMB1_2 uptake and response in cellular DM1 models.

RNAa strategy presented in this work targets solely *MBNL1* with potential implications for normalized skeletal muscle function, which warrants further studies in DM1 myoblasts. However, the disease affects multiple other tissues and cell types that express varying levels and intracellular locations of distinct *MBNL* paralogs. Brain and heart, apart for muscle, are major organs affected by DM1. Considering the feasibility of combined RNAa of distinct genes, simultaneous targeting of *MBNL* paralogs expressed in distinct organs (e.g. *MBNL1* and the major paralog in the brain, *MBNL2*) poses an attractive option to significantly increase therapeutic benefits through e.g. synergistic or additive effect. However, poor delivery and uptake to differentiated cells constitute serious limitations. For example, none of the currently available disease modifying treatments have the potential to cross the blood brain barrier, so remediating compromised CNS functions remains a challenge. Caveats aside, RNA-based therapeutics, unlike gene editing approaches, are not permanent and temporarily but often long-lastingly mitigate disease severity. Although this necessitates repeated rounds of treatment, it offers the benefit of dose adjustment and withdrawal whenever more advanced therapeutic options become available. Currently, however, evaluation of the pharmacokinetics, biodistribution, and the mechanism of tissue penetration by saRNAs in DM1 is limited by lack of suitable mouse models due to poor promoter conservation between human and mouse.

In conclusion, this is the first report of a directed, site-specific manipulation of the endogenous *MBNL1* promoter to enhance *MBNL1* transcription. Our data distinctly revealed therapeutic potential of RNAa in DM1, reflected by increased MBNL1 protein content and correction of AltS of MBNL1 target pre-mRNAs. This directed approach, when adapted into RNAa-based therapy, may offer several advantages including high specificity, reversibility, dose-control, and potential for tissue-specific delivery when coupled with distinct carriers. Future studies should address chemical modifications for improved delivery, minimized off-target effect, as well as putative synergistic and/or additive effect of saRNAs targeted simultaneously to other *MBNL* paralogs for enhanced splicing correction. Finally, saRNA-based approach not only expands possible points of therapeutic interventions for future drug developments in DM but may also serve as a novel molecular toolbox to interrogate protein factors involved in *MBNL1* transcription. As such, our findings offer brand new perspectives on *MBNL1* gene expression regulation and may likely foster future research on RNAa in the context of targeted DM1 therapy.

Acknowledgements

The graphical abstract was created in BioRender. Stepniak-Konieczna, E. (2025) https://BioRender.com/r2pnjel.

Author contributions: Conceptualization, funding acquisition, and project supervision: E.S-K.; Experimental design: E.S-K., N.M-K., and P.P.; Investigation and data collection: N.M-K., P.P., and A.J.; Data analysis and interpretation: E.S-K., N.M-K., and P.P.; Original draft of the manuscript: E.S-K. and N.M-K.; Manuscript revision, editing, and proofreading: E.S-K. and P.P.; Figure preparation: E.S-K. and N.M-K.; Final approval of the manuscript: all authors.

Supplementary data

Supplementary data is available at NAR online.

Conflict of interest

The authors declare no competing interests.

Funding

This study was supported by the National Science Centre grants 2020/37/B/NZ5/01263 (to E.S-K.) and 2022/46/E/NZ5/00088 (to E.S-K.). Funding to pay the Open Access publication charges for this article was provided by National Science Centre grants: 2020/37/B/NZ5/01263 and 2022/46/E/NZ5/00088.

Data availability

All data generated or analyzed during this study are included in this published article and its supplementary information files.

References

1. Batra R, Charizanis K, Manchanda M *et al.* Loss of MBNL leads to disruption of developmentally regulated alternative polyadenylation in RNA-mediated disease. *Mol Cell* 2014;**56**:311–22. https://doi.org/10.1016/j.molcel.2014.08.027
2. Wang ET, Cody NAL, Jog S *et al.* Transcriptome-wide regulation of pre-mRNA splicing and mRNA localization by muscleblind proteins. *Cell* 2012;**150**:710–24. https://doi.org/10.1016/j.cell.2012.06.041
3. Masuda A, Andersen HS, Doktor TK *et al.* CUGBP1 and MBNL1 preferentially bind to 3[1] UTRs and facilitate mRNA decay. *Sci Rep* 2012;**2**:209. https://doi.org/10.1038/srep00209
4. Konieczny P, Stepniak-Konieczna E, Sobczak K. MBNL proteins and their target RNAs, interaction and splicing regulation. *Nucleic Acids Res* 2014;**42**:10873–87. https://doi.org/10.1093/nar/gku767
5. Ho TH, Charlet-B N, Poulos MG *et al.* Muscleblind proteins regulate alternative splicing. *EMBO J* 2004;**23**:3103–12. https://doi.org/10.1038/sj.emboj.7600300
6. Teplova M, Patel DJ. Structural insights into RNA recognition by the alternative-splicing regulator muscleblind-like MBNL1. *Nat Struct Mol Biol* 2008;**15**:1343–51. https://doi.org/10.1038/nsmb.1519
7. Goers ES, Purcell J, Voelker RB *et al.* MBNL1 binds GC motifs embedded in pyrimidines to regulate alternative splicing. *Nucleic Acids Res* 2010;**38**:2467–84. https://doi.org/10.1093/nar/gkp1209
8. Fernandez-Costa JM, Llamusi MB, Garcia-Lopez A *et al.* Alternative splicing regulation by muscleblind proteins: from development to disease. *Biol Rev Camb Philos Soc* 2011;**86**:947–58. https://doi.org/10.1111/j.1469-185X.2011.00180.x
9. Lin X, Miller JW, Mankodi A *et al.* Failure of MBNL1-dependent post-natal splicing transitions in myotonic dystrophy. *Hum Mol Genet* 2006;**15**:2087–97. https://doi.org/10.1093/hmg/ddl132
10. Kalsotra A, Xiao X, Ward AJ *et al.* A postnatal switch of CELF and MBNL proteins reprograms alternative splicing in the

developing heart. *Proc Natl Acad Sci USA* 2008;**105**:20333–8. https://doi.org/10.1073/pnas.0809045105
11. Han H, Irimia M, Ross PJ *et al.* MBNL proteins repress embryonic stem cell-specific alternative splicing and reprogramming. *Nature* 2013;**498**:241–5. https://doi.org/10.1038/nature12270
12. Fardaei M, Larkin K, Brook JD *et al.* In vivo co-localisation of MBNL protein with DMPK expanded-repeat transcripts. *Nucleic Acids Res* 2001;**29**:2766–71. https://doi.org/10.1093/nar/29.13.2766
13. Fardaei M, Rogers MT, Thorpe HM *et al.* Three proteins, MBNL, MBLL and MBXL, co-localize *in vivo* with nuclear foci of expanded-repeat transcripts in DM1 and DM2 cells. *Hum Mol Genet* 2002;**11**:805–14. https://doi.org/10.1093/hmg/11.7.805
14. Wagner SD, Struck AJ, Gupta R *et al.* Dose-dependent regulation of alternative splicing by MBNL proteins reveals biomarkers for myotonic dystrophy. *PLoS Genet* 2016;**12**:e1006316. https://doi.org/10.1371/journal.pgen.1006316
15. Jog SP, Paul S, Dansithong W *et al.* RNA splicing is responsive to MBNL1 dose. *PLoS One* 2012;**7**:e48825. https://doi.org/10.1371/journal.pone.0048825
16. Gomes-Pereira M, Monckton DG. Chemically induced increases and decreases in the rate of expansion of a CAG*CTG triplet repeat. *Nucleic Acids Res* 2004;**32**:2865–72. https://doi.org/10.1093/nar/gkh612
17. Hashem VI, Sinden RR. Chemotherapeutically induced deletion of expanded triplet repeats. *Mutat Res* 2002;**508**:107–19. https://doi.org/10.1016/S0027-5107(02)00190-2
18. Cinesi C, Aeschbach L, Yang B *et al.* Contracting CAG/CTG repeats using the CRISPR-Cas9 nickase. *Nat Commun* 2016;**7**:13272. https://doi.org/10.1038/ncomms13272
19. Pinto BS, Saxena T, Oliveira R *et al.* Impeding transcription of expanded microsatellite repeats by deactivated Cas9. *Mol Cell* 2017;**68**:479–90. https://doi.org/10.1016/j.molcel.2017.09.033
20. van Agtmaal EL, Andre LM, Willemse M *et al.* CRISPR/Cas9-induced (CTG · CAG)(n) repeat instability in the myotonic dystrophy type 1 locus: implications for therapeutic genome editing. *Mol Ther* 2017;**25**:24–43. https://doi.org/10.1016/j.ymthe.2016.10.014
21. Lee JE, Bennett CF, Cooper TA. RNase H-mediated degradation of toxic RNA in myotonic dystrophy type 1. *Proc Natl Acad Sci USA* 2012;**109**:4221–6. https://doi.org/10.1073/pnas.1117019109
22. Pandey SK, Wheeler TM, Justice SL *et al.* Identification and characterization of modified antisense oligonucleotides targeting DMPK in mice and nonhuman primates for the treatment of myotonic dystrophy type 1. *J Pharmacol Exp Ther* 2015;**355**:329–40. https://doi.org/10.1124/jpet.115.226969
23. Yadava RS, Yu Q, Mandal M *et al.* Systemic therapy in an RNA toxicity mouse model with an antisense oligonucleotide therapy targeting a non-CUG sequence within the DMPK 3'UTR RNA. *Hum Mol Genet* 2020;**29**:1440–53. https://doi.org/10.1093/hmg/ddaa060
24. Jauvin D, Chretien J, Pandey SK *et al.* Targeting DMPK with antisense oligonucleotide improves muscle strength in myotonic dystrophy type 1 mice. *Mol Ther Nucleic Acids* 2017;**7**:465–74. https://doi.org/10.1016/j.omtn.2017.05.007
25. Wheeler TM, Leger AJ, Pandey SK *et al.* Targeting nuclear RNA for in vivo correction of myotonic dystrophy. *Nature* 2012;**488**:111–5. https://doi.org/10.1038/nature11362
26. Hu N, Kim E, Antoury L *et al.* Antisense oligonucleotide and adjuvant exercise therapy reverse fatigue in old mice with myotonic dystrophy. *Mol Ther Nucleic Acids* 2021;**23**:393–405. https://doi.org/10.1016/j.omtn.2020.11.014
27. Sobczak K, Wheeler TM, Wang W *et al.* RNA interference targeting CUG repeats in a mouse model of myotonic dystrophy. *Mol Ther* 2013;**21**:380–7. https://doi.org/10.1038/mt.2012.222
28. Bisset DR, Stepniak-Konieczna EA, Zavaljevski M *et al.* Therapeutic impact of systemic AAV-mediated RNA interference in a mouse model of myotonic dystrophy. *Hum Mol Genet* 2015;**24**:4971–83. https://doi.org/10.1093/hmg/ddv219
29. Francois V, Klein AF, Beley C *et al.* Selective silencing of mutated mRNAs in DM1 by using modified hU7-snRNAs. *Nat Struct Mol Biol* 2011;**18**:85–7. https://doi.org/10.1038/nsmb.1958
30. Angelbello AJ, Gonzalez AL, Rzuczek SG *et al.* Development of pharmacophore models for small molecules targeting RNA: application to the RNA repeat expansion in myotonic dystrophy type 1. *Bioorg Med Chem Lett* 2016;**26**:5792–6. https://doi.org/10.1016/j.bmcl.2016.10.037
31. Childs-Disney JL, Hoskins J, Rzuczek SG *et al.* Rationally designed small molecules targeting the RNA that causes myotonic dystrophy type 1 are potently bioactive. *ACS Chem Biol* 2012;**7**:856–62. https://doi.org/10.1021/cb200408a
32. Childs-Disney JL, Stepniak-Konieczna E, Tran T *et al.* Induction and reversal of myotonic dystrophy type 1 pre-mRNA splicing defects by small molecules. *Nat Commun* 2013;**4**:2044. https://doi.org/10.1038/ncomms3044
33. Wojtkowiak-Szlachcic A, Taylor K, Stepniak-Konieczna E *et al.* Short antisense-locked nucleic acids (all-LNAs) correct alternative splicing abnormalities in myotonic dystrophy. *Nucleic Acids Res* 2015;**43**:3318–31. https://doi.org/10.1093/nar/gkv163
34. Hsieh WC, Bahal R, Thadke SA *et al.* Design of a "mini" nucleic acid probe for Cooperative binding of an RNA-repeated transcript associated with myotonic dystrophy type 1. *Biochemistry* 2018;**57**:907–11. https://doi.org/10.1021/acs.biochem.7b01239
35. Arandel L, Matloka M, Klein AF *et al.* Reversal of RNA toxicity in myotonic dystrophy via a decoy RNA-binding protein with high affinity for expanded CUG repeats. *Nat Biomed Eng* 2022;**6**:207–20. https://doi.org/10.1038/s41551-021-00838-2
36. Kanadia RN, Shin J, Yuan Y *et al.* Reversal of RNA missplicing and myotonia after muscleblind overexpression in a mouse poly(CUG) model for myotonic dystrophy. *Proc Natl Acad Sci USA* 2006;**103**:11748–53. https://doi.org/10.1073/pnas.0604970103
37. Li MY, Zhuang Y, Batra R *et al.* HNRNPA1-induced spliceopathy in a transgenic mouse model of myotonic dystrophy. *Proc Natl Acad Sci USA* 2020;**117**:5472–7. https://doi.org/10.1073/pnas.1907297117
38. Chamberlain CM, Ranum LPW. Mouse model of muscleblind-like 1 overexpression: skeletal muscle effects and therapeutic promise. *Hum Mol Genet* 2012;**21**:4645–54. https://doi.org/10.1093/hmg/dds306
39. Davis J, Salomonis N, Ghearing N *et al.* MBNL1-mediated regulation of differentiation RNAs promotes myofibroblast transformation and the fibrotic response. *Nat Commun* 2015;**6**:10084. https://doi.org/10.1038/ncomms10084
40. Yadava RS, Kim YK, Mandal M *et al.* MBNL1 overexpression is not sufficient to rescue the phenotypes in a mouse model of RNA toxicity. *Hum Mol Genet* 2019;**28**:2330–8. https://doi.org/10.1093/hmg/ddz065
41. Rogalska Z, Sobczak K. Sustainable recovery of MBNL activity in autoregulatory feedback loop in myotonic dystrophy. *Mol Ther Nucleic Acids* 2022;**30**:438–48. https://doi.org/10.1016/j.omtn.2022.10.023
42. Cerro-Herreros E, Fernandez-Costa JM, Sabater-Arcis M *et al.* Derepressing muscleblind expression by miRNA sponges ameliorates myotonic dystrophy-like phenotypes in Drosophila. *Sci Rep* 2016;**6**:36230. https://doi.org/10.1038/srep36230
43. Cerro-Herreros E, González-Martínez I, Moreno N *et al.* Preclinical characterization of antagomiR-218 as a potential treatment for myotonic dystrophy. *Mol Ther Nucleic Acids* 2021;**26**:174–91. https://doi.org/10.1016/j.omtn.2021.07.017
44. Gonzalez-Martinez I, Cerro-Herreros E, Moreno N *et al.* Peptide-conjugated antimiRs improve myotonic dystrophy type 1 phenotypes by promoting endogenous MBNL1 expression. *Mol Ther Nucleic Acids* 2023;**34**:102024. https://doi.org/10.1016/j.omtn.2023.09.001
45. Overby SJ, Cerro-Herreros E, Gonzalez-Martinez I *et al.* Proof of concept of peptide-linked blockmiR-induced MBNL functional rescue in myotonic dystrophy type 1 mouse model. *Mol Ther*

Nucleic Acids 2022;**27**:1146–55. https://doi.org/10.1016/j.omtn.2022.02.003
46. Chen GY, Masuda A, Konishi H *et al.* Phenylbutazone induces expression of MBNL1 and suppresses formation of MBNL1-CUG RNA foci in a mouse model of myotonic dystrophy. *Sci Rep* 2016;**6**:25317. https://doi.org/10.1038/srep25317
47. Zhang F, Bodycombe NE, Haskell KM *et al.* A flow cytometry-based screen identifies MBNL1 modulators that rescue splicing defects in myotonic dystrophy type I. *Hum Mol Genet* 2017;**26**:3056–68. https://doi.org/10.1093/hmg/ddx190
48. Li LC, Okino ST, Zhao H *et al.* Small dsRNAs induce transcriptional activation in human cells. *Proc Natl Acad Sci USA* 2006;**103**:17337–42. https://doi.org/10.1073/pnas.0607015103
49. Janowski BA, Younger ST, Hardy DB *et al.* Activating gene expression in mammalian cells with promoter-targeted duplex RNAs. *Nat Chem Biol* 2007;**3**:166–73. https://doi.org/10.1038/nchembio860
50. Chu Y, Yue X, Younger ST *et al.* Involvement of argonaute proteins in gene silencing and activation by RNAs complementary to a non-coding transcript at the progesterone receptor promoter. *Nucleic Acids Res* 2010;**38**:7736–48. https://doi.org/10.1093/nar/gkq648
51. Portnoy V, Lin SH, Li KH *et al.* saRNA-guided Ago2 targets the RITA complex to promoters to stimulate transcription. *Cell Res* 2016;**26**:320–35. https://doi.org/10.1038/cr.2016.22
52. Schwartz JC, Younger ST, Nguyen NB *et al.* Antisense transcripts are targets for activating small RNAs. *Nat Struct Mol Biol* 2008;**15**:842–8. https://doi.org/10.1038/nsmb.1444
53. Reebye V, Huang KW, Lin V *et al.* Gene activation of CEBPA using saRNA: preclinical studies of the first in human saRNA drug candidate for liver cancer. *Oncogene* 2018;**37**:3216–28. https://doi.org/10.1038/s41388-018-0126-2
54. Voutila J, Reebye V, Roberts TC *et al.* Development and mechanism of small activating RNA targeting CEBPA, a novel therapeutic in clinical trials for liver cancer. *Mol Ther* 2017;**25**:2705–14. https://doi.org/10.1016/j.ymthe.2017.07.018
55. Konieczny P, Stepniak-Konieczna E, Taylor K *et al.* Autoregulation of MBNL1 function by exon 1 exclusion from MBNL1 transcript. *Nucleic Acids Res* 2017;**45**:1760–75. https://doi.org/10.1093/nar/gkw1158
56. Konieczny P, Stepniak-Konieczna E, Sobczak K. MBNL expression in autoregulatory feedback loops. *RNA Biol* 2018;**15**:1–8. https://doi.org/10.1080/15476286.2017.1384119
57. Wang J, Place RF, Portnoy V *et al.* Inducing gene expression by targeting promoter sequences using small activating RNAs. *J Biol Methods* 2015;**2**:e14. https://doi.org/10.14440/jbm.2015.39
58. Meng X, Jiang Q, Chang N *et al.* Small activating RNA binds to the genomic target site in a seed-region-dependent manner. *Nucleic Acids Res* 2016;**44**:2274–82. https://doi.org/10.1093/nar/gkw076
59. Place RF, Noonan EJ, Foldes-Papp Z *et al.* Defining features and exploring chemical modifications to manipulate RNAa activity. *Curr Pharm Biotechnol* 2010;**11**:518–26. https://doi.org/10.2174/138920110791591463
60. Meister G, Landthaler M, Patkaniowska A *et al.* Human Argonaute2 mediates RNA cleavage targeted by miRNAs and siRNAs. *Mol Cell* 2004;**15**:185–97. https://doi.org/10.1016/j.molcel.2004.07.007
61. Choi JH, Jang TY, Jeon SE *et al.* The small-molecule wnt inhibitor ICG-001 efficiently inhibits colorectal cancer stemness and metastasis by suppressing MEIS1 expression. *Int J Mol Sci* 2021;**22**:13413. https://doi.org/10.3390/ijms222413413
62. Wu YH, Zhao H, Zhou LP *et al.* miR-134 modulates the proliferation of Human cardiomyocyte progenitor cells by targeting Meis2. *Int J Mol Sci* 2015;**16**:25199–213. https://doi.org/10.3390/ijms161025199
63. Stepniak-Konieczna E, Konieczny P, Cywoniuk P *et al.* AON-induced splice-switching and DMPK pre-mRNA degradation as potential therapeutic approaches for Myotonic Dystrophy type 1. *Nucleic Acids Res* 2020;**48**:2531–43. https://doi.org/10.1093/nar/gkaa007
64. Livak KJ, Schmittgen TD. Analysis of relative gene expression data using real-time quantitative PCR and the 2(-Delta Delta C(T)) method. *Methods* 2001;**25**:402–8. https://doi.org/10.1006/meth.2001.1262
65. Napoli S. Detailed analysis of promoter-associated RNA. *Methods Mol Biol* 2013;**1049**:199–213. https://doi.org/10.1007/978-1-62703-547-7_15
66. Jenquin JR, O'Brien AP, Poukalov K *et al.* Molecular characterization of myotonic dystrophy fibroblast cell lines for use in small molecule screening. *iScience* 2022;**25**:104198. https://doi.org/10.1016/j.isci.2022.104198
67. Li LC. Small RNA-guided transcriptional gene activation (RNAa) in mammalian cells. *Adv Exp Med Biol* 2017;**983**:1–20. https://doi.org/10.1007/978-981-10-4310-9_1
68. Schulte D, Geerts D. MEIS transcription factors in development and disease. *Development* 2019;**146**:dev174706. https://doi.org/10.1242/dev.174706
69. Okada Y, Nagai R, Sato T *et al.* Homeodomain proteins MEIS1 and PBXs regulate the lineage-specific transcription of the platelet factor 4 gene. *Blood* 2003;**101**:4748–56. https://doi.org/10.1182/blood-2002-02-0380
70. Sznajder ŁJ, Michalak M, Taylor K *et al.* Mechanistic determinants of MBNL activity. *Nucleic Acids Res* 2016;**44**:10326–42. https://doi.org/10.1093/nar/gkw915
71. Cerro-Herreros E, Sabater-Arcis M, Fernandez-Costa JM *et al.* miR-23b and miR-218 silencing increase muscleblind-like expression and alleviate myotonic dystrophy phenotypes in mammalian models. *Nat Commun* 2018;**9**:2482. https://doi.org/10.1038/s41467-018-04892-4
72. Castel LO A., Artero R. MicroRNA-based therapeutic perspectives in myotonic dystrophy. *Int J Mol Sci* 2019;**20**:5600. https://doi.org/10.3390/ijms20225600
73. Neault N, Ravel-Chapuis A, Baird SD *et al.* Vorinostat improves myotonic dystrophy type 1 splicing abnormalities in DM1 muscle cell lines and skeletal muscle from a DM1 mouse model. *Int J Mol Sci* 2023;**24**:3794. https://doi.org/10.3390/ijms24043794
74. Huang V, Qin Y, Wang J *et al.* RNAa is conserved in mammalian cells. *PLoS One* 2010;**5**:e8848. https://doi.org/10.1371/journal.pone.0008848
75. Roberts TC, Langer R, Wood MJA. Advances in oligonucleotide drug delivery. *Nat Rev Drug Discov* 2020;**19**:673–94. https://doi.org/10.1038/s41573-020-0075-7
76. Osborn MF, Khvorova A. Improving siRNA delivery *in vivo* through lipid conjugation. *Nucleic Acid Ther* 2018;**28**:128–36. https://doi.org/10.1089/nat.2018.0725
77. Schroeder A, Levins CG, Cortez C *et al.* Lipid-based nanotherapeutics for siRNA delivery. *J Intern Med* 2010;**267**:9–21. https://doi.org/10.1111/j.1365-2796.2009.02189.x
78. Huang KW, Reebye V, Czysz K *et al.* Liver activation of hepatocellular nuclear factor-4alpha by small activating RNA rescues dyslipidemia and improves metabolic profile. *Mol Ther Nucleic Acids* 2020;**19**:361–70. https://doi.org/10.1016/j.omtn.2019.10.044
79. Yoon S, Huang KW, Andrikakou P *et al.* Targeted delivery of C/EBPalpha-saRNA by RNA aptamers shows anti-tumor effects in a mouse model of advanced PDAC. *Mol Ther Nucleic Acids* 2019;**18**:142–54. https://doi.org/10.1016/j.omtn.2019.08.017
80. Sarker D, Plummer R, Meyer T *et al.* MTL-CEBPA, a small activating RNA therapeutic upregulating C/EBP-alpha, in patients with advanced liver cancer: a first-in-Human, multicenter, open-label, phase I trial. *Clin Cancer Res* 2020;**26**:3936–46. https://doi.org/10.1158/1078-0432.CCR-20-0414
81. Qu F, Darji S, Thompson DH. Recent advances in drug delivery strategies for high-risk BCG-unresponsive non-muscle invasive bladder cancer: a brief review from 2018 to 2024. *Pharmaceutics* 2024;**16**:1154. https://doi.org/10.3390/pharmaceutics16091154

Received: September 11, 2024. **Revised:** June 13, 2025. **Editorial Decision:** June 30, 2025. **Accepted:** July 21, 2025

Supplementary Material For:

Promoter-targeted small RNA duplexes increase *MBNL1* transcription and mitigate myotonic dystrophy-associated spliceopathy.

Nikola Musiała-Kierklo[1,2], Patrycja Plewka[1], Adam Jasiok[1,3] and Ewa Stępniak-Konieczna[1,*]

[1]Laboratory of RNA Biology, Department of Biochemistry and Biotechnology, Poznan University of Life Sciences, Dojazd 11, 60-632 Poznan, Poland

[2]Doctoral School of Natural Sciences, Adam Mickiewicz University, Uniwersytetu Poznanskiego 2, 61-614 Poznan, Poland

[3]Poznan University of Life Sciences Doctoral School, Collegium Maximum, Wojska Polskiego 28, 60-637 Poznan, Poland

* To whom correspondence should be addressed: ewa.stepniak-konieczna@up.poznan.pl

CONTENT:

1. LIST OF SUPPLEMENTARY FIGURES S1-S17 AND TABLES S1-S6

Supplementary Figure S1. The activity of *MBNL1* promoters differs in DM1 cells.

Supplementary Figure S2. Screening of saRNAs directed at *MBNL1* promoters identifies two top scoring duplexes, saMB1_1 and saMB1_2, specifically enhancing P2-derived *MBNL1* mRNA levels in DM1 fibroblasts.

Supplementary Figure S3. Dose-response, kinetics, specificity and combined effect of saRNA duplexes in DM1 fibroblasts.

Supplementary Figure S4. saRNA duplexes upregulate *MBNL1* RNA in distinct cell models.

Supplementary Figure S5. saRNA duplexes stimulate the recruitment of specific transcription factors to induce *MBNL1* RNAa.

Supplementary Figure S6. RNA interference-mediated knock-down of AGO2 prevents RNA activation of *MBNL1*.

Supplementary Figure S7. Directional RT-PCR reveals absence of cryptic short sense RNA and downregulation of antisense RNA at the saMB1_2 target site within *MBNL1* promoter P2.

Supplementary Figure S8. saRNA duplexes targeted to *MBNL1* promoter P2 induce downregulation of lncRNA *MBNL1-AS1*.

Supplementary Figure S9. Reduced antisense transcription and higher transcript turnover contribute to the reduction of lncRNA *MBNL1-AS1* upon *MBNL1*-directed saRNAs.

Supplementary Figure S10. The sense strand of *MBNL1*-directed saRNA mediates lncRNA *MBNL1-AS1* downregulation.

Supplementary Figure S11. Unadjusted and uncropped western blot images corresponding to Figure 6.

Supplementary Figure S12. Timecourse analyses show correlation of MBNL1 protein induction upon saRNA treatment with MBNL1-dependent e1 exclusion from *MBNL1* pre- mRNA.

Supplementary Figure S13. Colocalization of MBNL1 and CUG^{exp} RNA foci in DM1 fibroblasts is not affected by saRNA-mediated *MBNL1* upregulation.

Supplementary Figure S14. Unadjusted and uncropped RT-PCR gel images of alternative splicing events in DM1 fibroblasts shown in Figure 8A.

Supplementary Figure S15. Unadjusted and uncropped RT-PCR gel images of alternative splicing events in DM1 myoblasts shown in Figure 8B.

Supplementary Figure S16. Sequence-scrambled or seed region mutant versions of saMB1_1 and saMB1_2 do not affect *MBNL1*-regulated alternative splicing.

Supplementary Figure S17. saRNA duplexes do not affect cell viability, toxicity and apoptosis.

Supplementary Table S1. Sequences of saRNAs and control RNA duplexes used in this study.

Supplementary Table S2. Sequences of chemically modified and mismatch-containing saRNA duplexes for strand inhibition or promotion.

Supplementary Table S3. siRNA and GapmeR sequences.

Supplementary Table S4. Expression primers for RT-qPCR.

Supplementary Table S5. Alternative splicing primers.

Supplementary Table S6. CUT&RUN primers for qPCR.

2. SUPPLEMENTARY FIGURES S1-S17 AND CORRESPONDING FIGURE LEGENDS

Supplementary Figure S1.

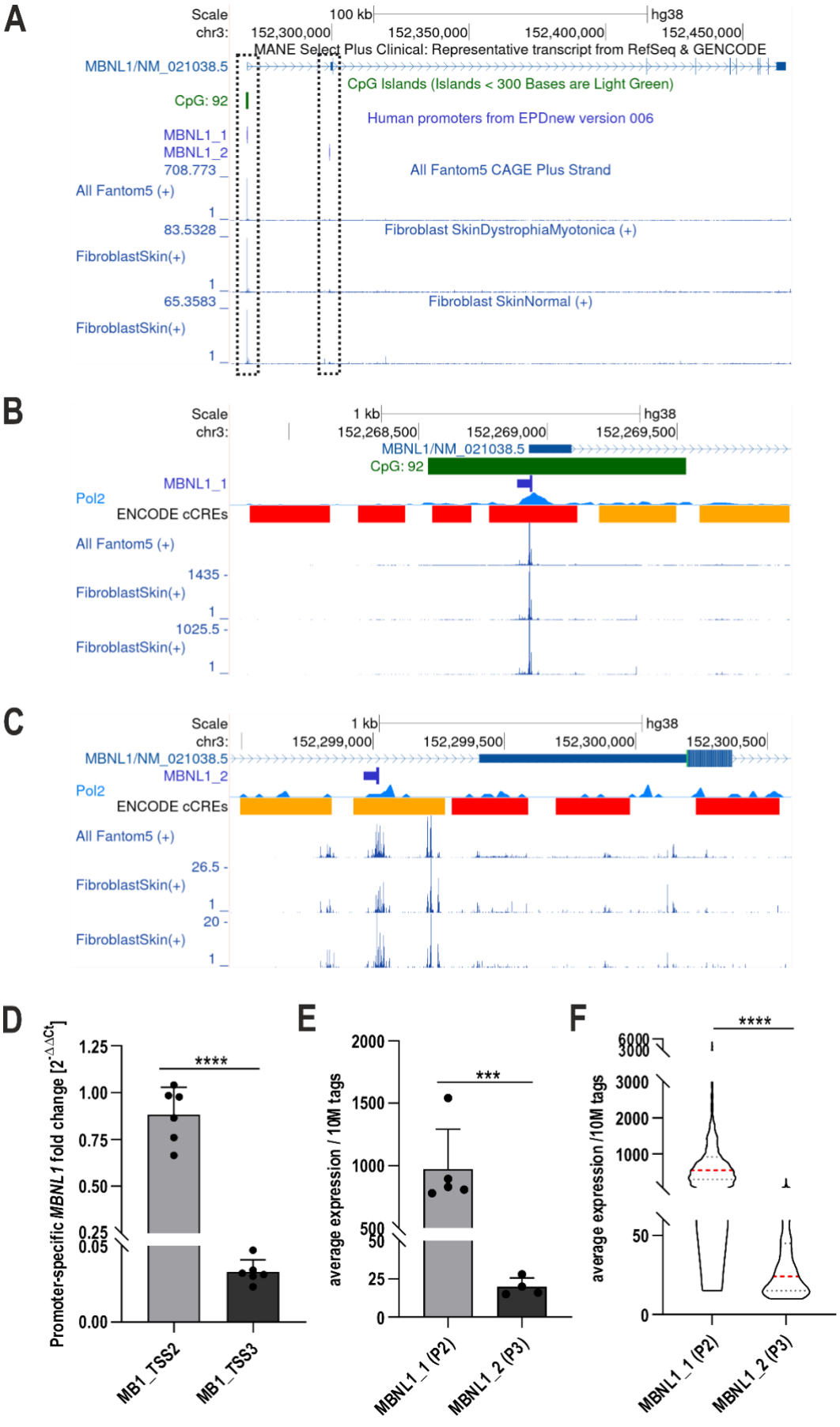

Supplementary Figure S1. The activity of *MBNL1* promoters differs in DM1 cells. (A-C) UCSC Genome Browser view of *MBNL1* gene with track display including EPD v006 promoters *MBNL1_1* (P2) and *MBNL1_2* (P3), CpG islands, ENCODE candidate Cis-Regulatory Elements (cCREs), ChIP-seq for RNA polymerase II in CD4 cells (1) and FANTOM5 mapped transcription start sites (TSS) in normal as well as myotonic dystrophy skin fibroblasts. cCREs color code in (B-C) marks promoter-like signatures (red) and proximal enhancer-like signature (orange). Blow-up panels of *MBNL1* P2 and P3-associated TSS2 and TSS3 regions in **(B)** and **(C)**, respectively, correspond to regions marked in (A) by dotted line rectangles. **(D)** Relative *MBNL1* transcript levels derived from TSS2 and TSS3 assessed via RT-qPCR-based analyses in GM04033 DM1 fibroblasts. Data are presented as mean ± SEM of n=6 samples. **(E)** Meta-analysis of promoter-specific *MBNL1* expression in DM1 patients' skin-derived fibroblasts based on data deposited in Eukaryotic Promoter Database (EPD). Analyzed data represent either whole-cell lysates or nuclear fractions from 3 distinct DM1 donors (n=5 samples available for P2 and n=4 samples available for P3). **(F)** Meta-analysis of the average expression level of P2- and P3- derived *MBNL1,* in all samples in which these promoters are active (n=1051 for P2; n=371 for P3), based on data deposited in Eukaryotic Promoter Database (EPD). Average expression in (E) and (F) represents the number of tags in a 100-bp region centered on the EPD-annotated respective TSS and normalized to 10M total tags. Red horizontal lines in (F) represent average expression: 695.655 tags per 10M for P2 and 35.5714 tags per 10M for P3, grey dashed lines in
(F) indicate quartiles.

Supplementary Figure S2.

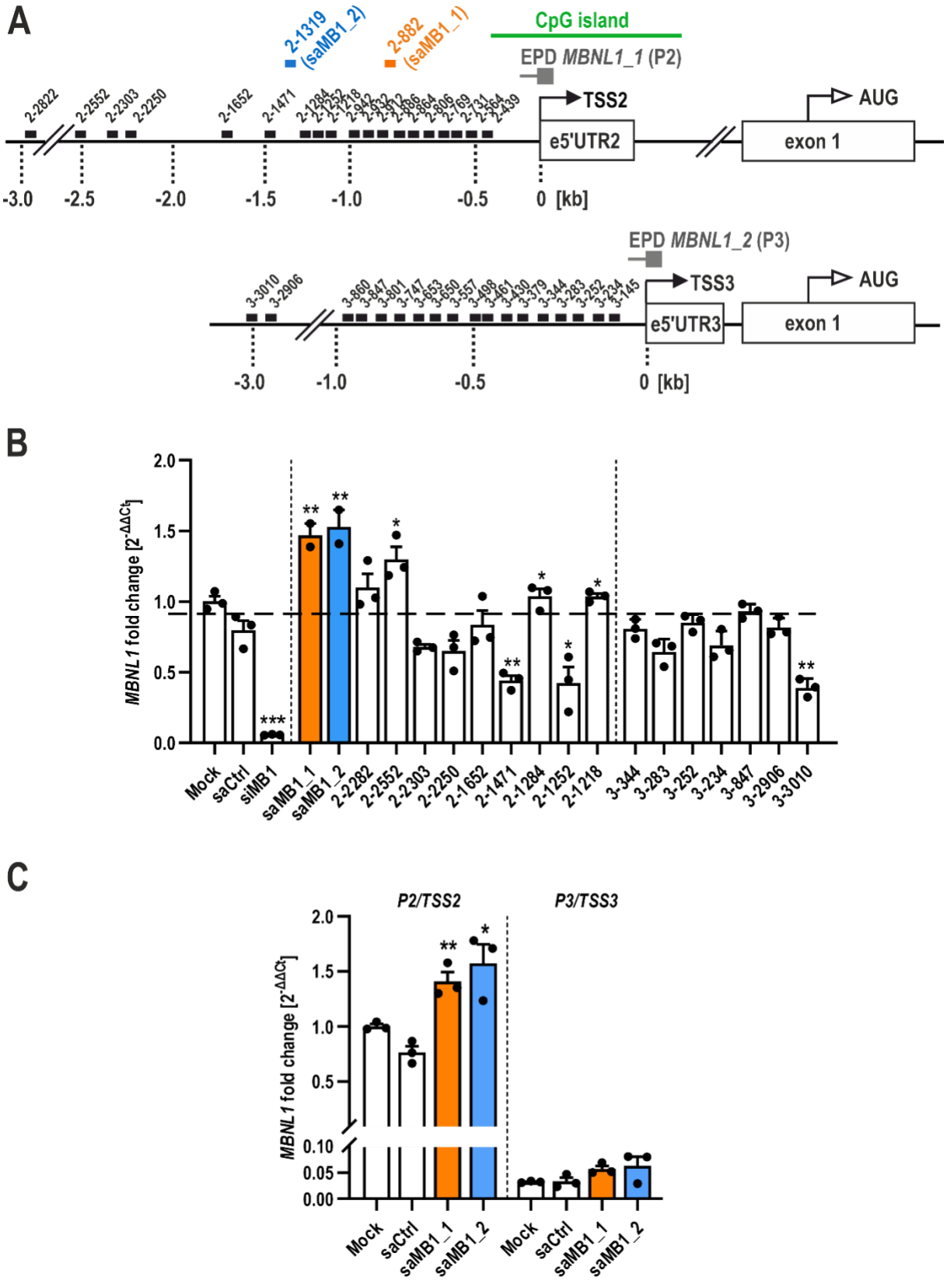

Supplementary Figure S2. Screening of saRNAs directed at *MBNL1* promoters identifies two top scoring duplexes, saMB1_1 and saMB1_2, specifically enhancing P2-derived *MBNL1* mRNA levels in DM1 fibroblasts. (A) Schematic representation, not to scale, of *MBNL1* genomic regions (according to NCBI RefSeq Select and MANE subset: a single representative transcript) spanning P2 (upper panel) and P3 (lower panel). Indicated features

include: EPD-annotated promoters (*MBNL1_1* (P2) and *MBNL1_2* (P3), respectively), transcription start sites (TSS2 and 3, respectively), 5′ UTR exons (e5′UTR2 and 3, respectively) and the first coding exon (exon 1) with translation start site (AUG). Target sites of saRNAs are indicated. **(B)** Representative results of saRNAs screening (selected duplexes), based on RT-qPCR analyses of *MBNL1* mRNA levels in GM04033 cells transfected with 75 nM indicated saRNAs targeting P2 and P3, for 120 h. siMB1 refers to samples with RNAi-mediated knock-down of *MBNL1*. **(C)** RT-qPCR expression analysis of P2- and P3-derived *MBNL1* transcripts in GM04033 cells transfected with 75 nM indicated saRNA for 120 h.

Supplementary Figure S3.

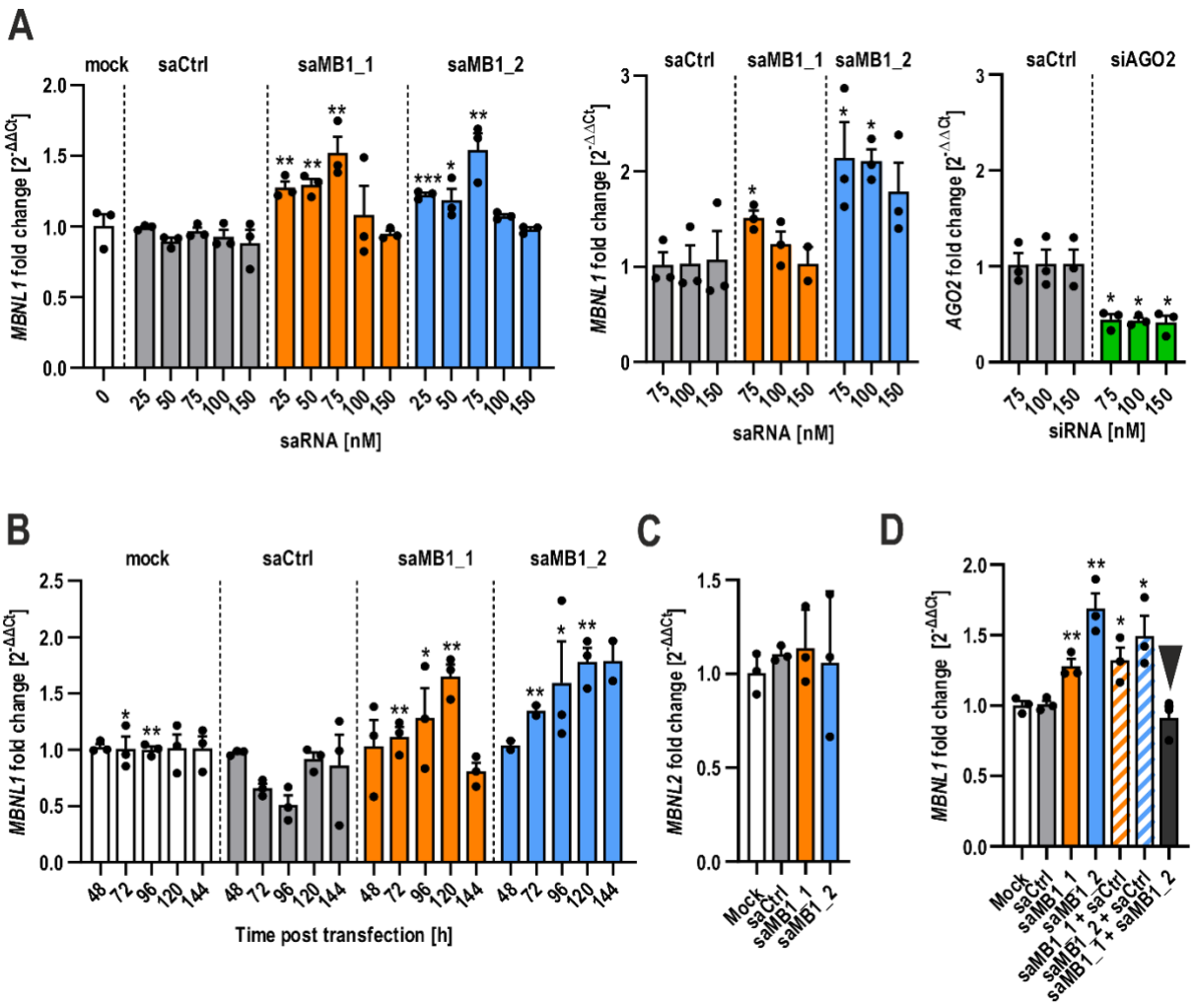

Supplementary Figure S3. Dose-response, kinetics, specificity and combined effect of saRNA duplexes in DM1 fibroblasts. (A) RT-qPCR analyses of indicated transcripts in GM04033 cells transfected for 120 h with indicated amounts of dsRNA. The saRNA dose-response study at a broad range of concentrations (25-150 nM; left panel) as well as a comparative dose-response study of saRNAs (middle panel) and a well characterized siRNA against *AGO2* transcripts (right panel) at a defined range of high doses (75-150 nM) were performed. **(B)** Timecourse RT-qPCR analysis of *MBNL1*, showing RNAa kinetics at 75 nM saRNA across indicated timepoints post-transfection. **(C-D)** RT-qPCR analysis of *MBNL2* (C) or *MBNL1* (D) expression in GM04033 cells transfected with 75 nM indicated saRNA for 120 h. In (D) 75 nM saMB1_1 and 75 nM saMB1_2 were transfected sequentially such that 24 h treatment with one saRNA was followed by transfection of the second saRNA for additional 96 h (black inverted arrowhead). The order of transfection is as labelled. Sequential transfection of either saMB1_1 or saMB1-2 followed by saCtrl (striped bars) was used as a control.

Supplementary Figure S4.

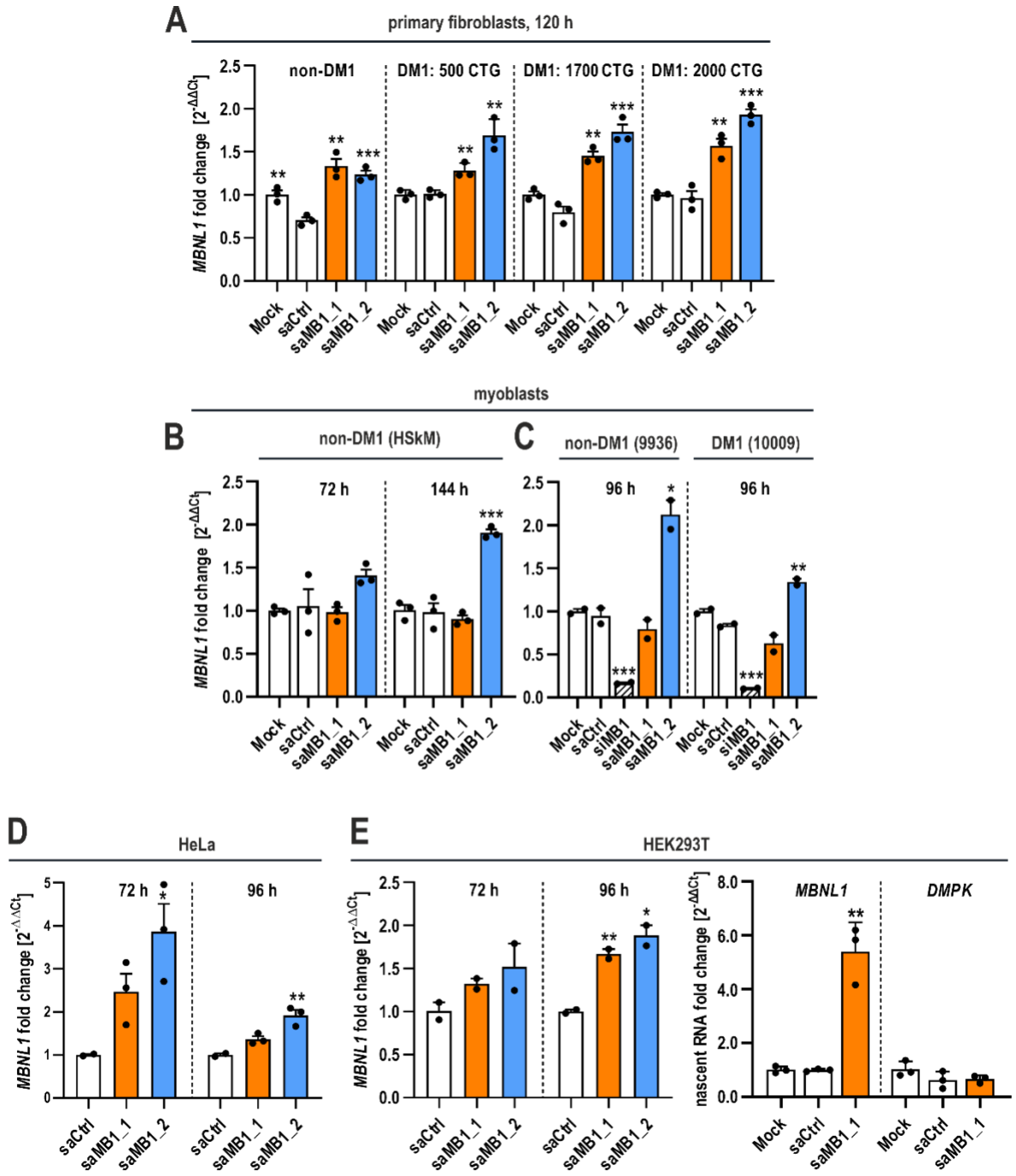

Supplementary Figure S4. saRNA duplexes upregulate *MBNL1* RNA in distinct cell models. (A-D) Representative results of RT-qPCR analyses of *MBNL1* expression upon transfection with indicated top scoring saMB1_1 and saMB1_2 in distinct cell models: **(A)** primary fibroblasts GM07492 (non-DM1) or GM03987, GM03132 and GM03989 expressing *DMPK* gene with ~500, ~1700 and ~2000 CTG repeats, respectively, **(B)** Primary Normal Human Skeletal Myoblasts (HSkM), **(C)** myoblasts 9936 (non-DM1; left) and 10009 (DM1; right), **(D)** HeLa and **(E, left panel)** HEK293T. The following experimental conditions were used: 75 nM saRNA for 120 h (A), 75 nM saRNA for 72 h and 144 h (B), 75 nM saRNA for 96 h (C), 75 nM saRNA for 72 h and 96 h (D and E, left panel). In (B), HSkM cells were first transfected with 75 nM saRNA for 72 h upon which 50% cells were collected (first analysis – 72 h, left) and the remaining 50% cells were seeded, transfected again with 75 nM saRNA and harvested 72 h post second transfection (second analysis – 144 h, right). In (D) and (E, left panel), Hela and

HEK293T cells, respectively, were transfected and 50% were collected 72 h later for the first analysis (72 h) and the remaining 50% cells were seeded and allowed to grow for additional 24 h, upon which second analysis was performed (96 h). **(E, right panel)** RT-qPCR results of nascent RNA capture of *MBNL1* and *DMPK* (control) in HEK293T cells transfected with 75 nM saMB1_1 for 48 h, followed by 24 h 5-EU pulse. Results were normalized to *GAPDH* and presented as mean ± SEM of triplicate (A, B, D and right panel in E) or duplicate samples (C and left panel in E).

Supplementary Figure S5.

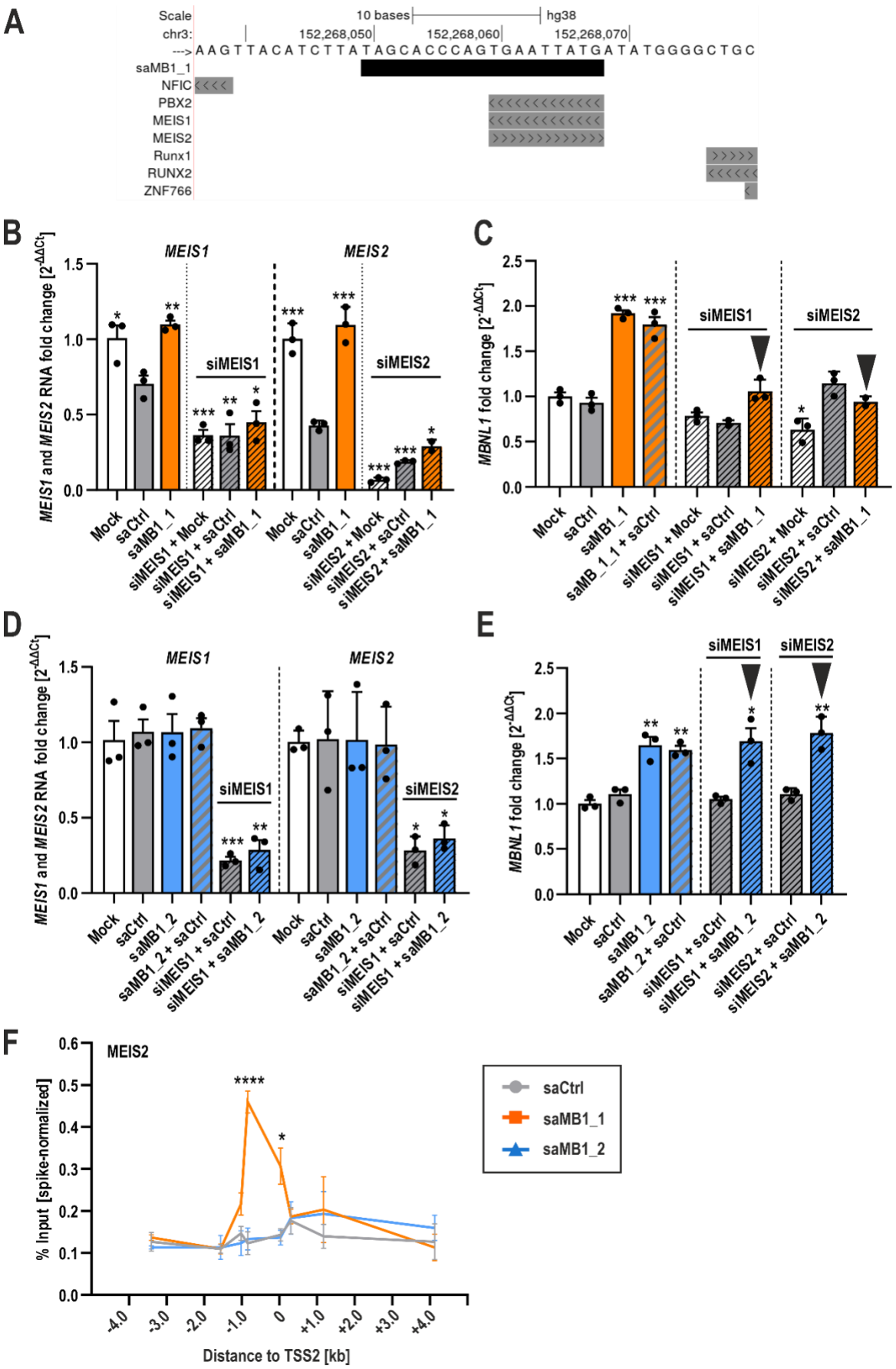

Supplementary Figure S5. saRNA duplexes stimulate the recruitment of specific transcription factors to induce *MBNL1* RNAa. (A) UCSC Genome Browser track image

showing saMB1_1 target genomic sequence within *MBNL1* promoter 2 region. Predicted transcription factors binding sites overlapping saMB1_1 target site are indicated (PBX2, MEIS1, MEIS2). **(B-C)** RT-qPCR assay of *MEIS1* and *MEIS2* (B) or *MBNL1* (C) in GM04033 DM1 fibroblasts upon knock-down of *MEIS1* (siMEIS1) or *MEIS2* (siMEIS2) and subsequent RNAa of *MBNL1* via saMB1_1. Cells were transfected with lipofectamine (mock) or 75 nM indicated dsRNA (saCtrl, saMB1_1, siMEIS1 or siMEIS2). After 24 h, siMEIS1 and siMEIS2-treated samples were subjected to a second transfection round with lipofectamine alone (mock) or 75 nM indicated dsRNA (saCtrl or saMB1_1) for additional 96 h. In (C), additional control included cells transfected sequentially with 75 nM saMB1_1 and an equal amount of saCtrl added 24 h later, for a total of 120 h (orange / grey striped bar). Black inverted arrowheads in (C) indicate samples in which knock-down of MEIS1 or MEIS2 inhibited *MBNL1* induction via saMB1_1. **(D-E)** RT-qPCR assay of *MEIS1* and *MEIS2* (D) or *MBNL1* (E) in GM04033 cells upon knock-down of *MEIS1* (siMEIS1) or *MEIS2* (siMEIS2) and subsequent RNAa of *MBNL1* via saMB1_2. Experimental settings in (D) and (E) are analogous to those shown in (B) and (C), respectively, with the exception that saMB1_2 was used instead of saMB1_1. Black inverted arrowheads in (E) indicate samples in which knock-down of MEIS1 or MEIS2 failed to inhibit *MBNL1* induction via saMB1_2. **(F)** qPCR results of CUT&RUN analyses in GM04033 cells transfected with 75 nM indicated saRNA for 120 h, demonstrating binding enrichment of MEIS2 to indicated genomic regions(ranging from −3.5 kb to +4.2 kb relative to *MBNL1* TSS2), following transfection of saMB1_1 (orange line), but not saMB1_2 (blue line) or saCtrl (grey line). Results were normalized using Spike-In DNA and are represented as % of input.

Supplementary Figure S6.

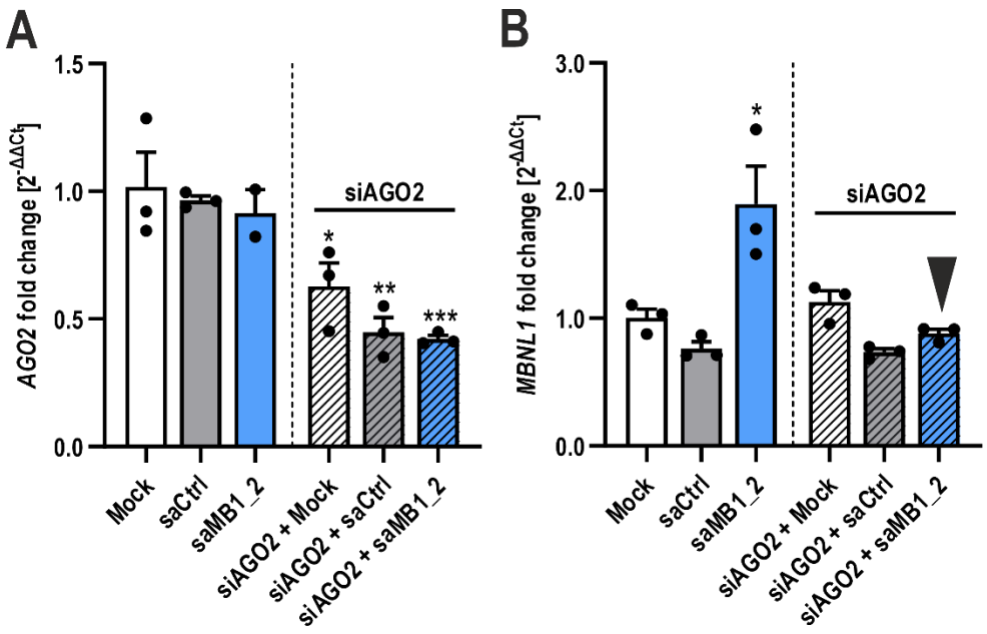

Supplementary Figure S6. RNA interference-mediated knock-down of AGO2 prevents RNA activation of *MBNL1*. RT-qPCR analyses of *AGO2* **(A)** and *MBNL1* **(B)** expression in GM04033 DM1 fibroblasts transfected for 24 h with lipofectamine alone (mock) or 75 nM indicated dsRNA (saCtrl, saMB1_2 or siAGO2). After 24 h, only siAGO2-transfected samples (right parts of the graphs) were subjected to a second round of transfection with lipofectamine alone (mock) or 75 nM saCtrl or saMB1_2, for additional 96 h. After a total of 120 h, all samples were harvested for analyses. Black inverted arrowhead in **(B)** indicates the samples in which knock-down of AGO2 inhibited *MBNL1* induction by saMB1_2.

Supplementary Figure S7.

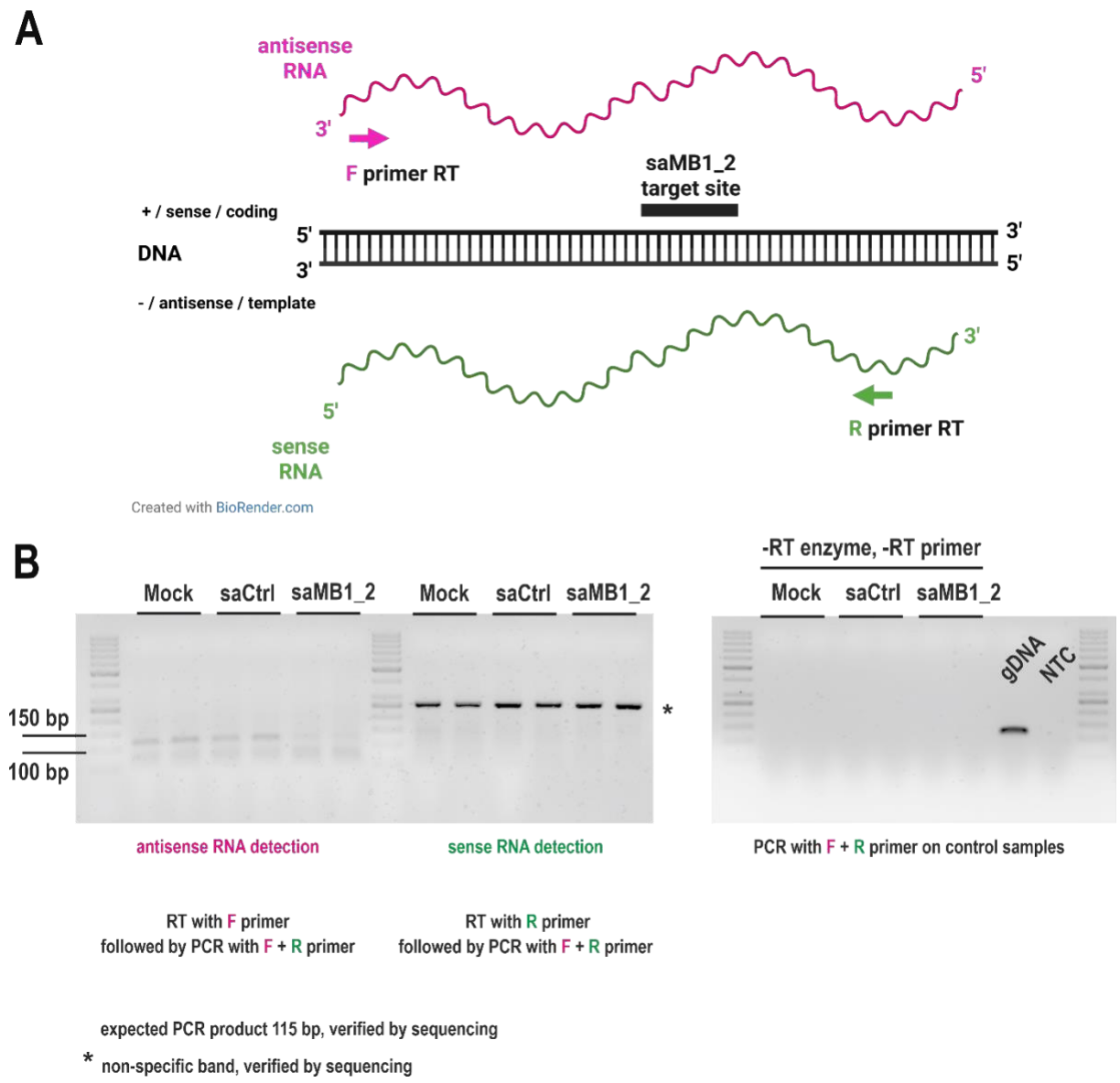

Supplementary Figure S7. Directional RT-PCR reveals absence of cryptic short sense RNA and downregulation of antisense RNA at the saMB1_2 target site within *MBNL1* promoter P2. (A) Schematic illustration of the directional RT-PCR assay used to detect and verify the directionality of the transcripts originating from the saMB1_2 target genomic region. Note that F (forward primer) and R (reverse primer) flank the saMB1_2 binding site. created in BioRender. Stepniak-Konieczna, E. (2025) https://BioRender.com/noo48m8. **(B)** Directional RT-PCR analysis of antisense and sense transcripts derived from the genomic region encompassing saMB1_2 binding site in HeLa cells treated for 72 h with lipofectamine alone (mock) or 75 nM indicated saRNAs (left panel). To exclude contamination by amplification of residual genomic DNA, control samples containing all reaction components except for the reverse transcriptase (RT enzyme) and RT primers were included in PCR reactions (right panel). gDNA- genomic DNA control; NTC- no-template control.

Supplementary Figure S8.

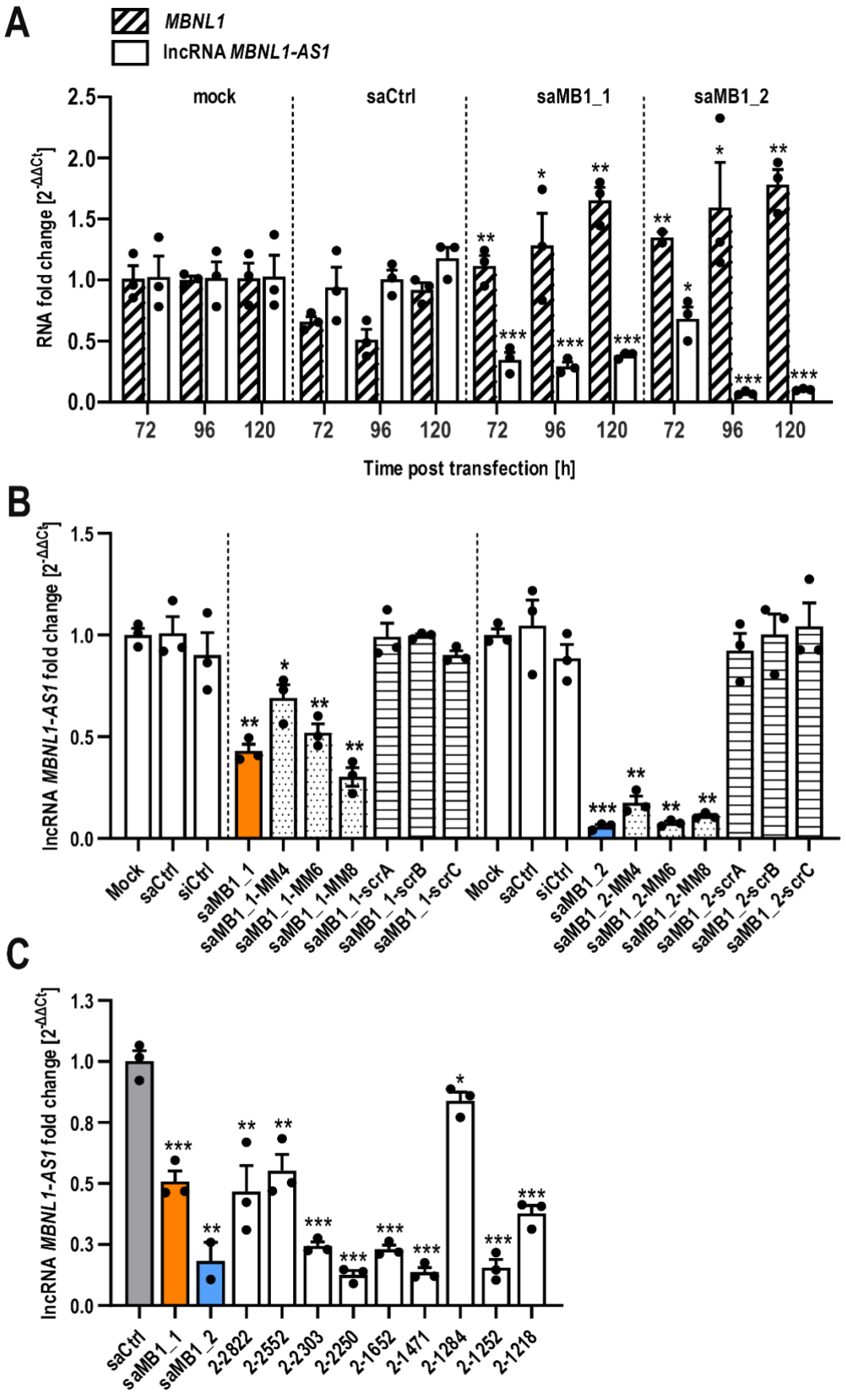

Supplementary Figure S8. saRNA duplexes targeted to *MBNL1* promoter P2 induce downregulation of lncRNA *MBNL1-AS1*. (A) RT-qPCR-based timecourse analyses (72 – 120

h) of *MBNL1* and *MBNL1-AS1* levels in GM04033 DM1 fibroblasts transfected with 75 nM indicated saRNA duplexes targeted to *MBNL1* gene promoter 2. **(B)** RT-qPCR analysis of lncRNA *MBNL1-AS1* level in GM04033 cells transfected for 120 h with 75 nM of control RNA duplexes (saCtrl or siCtrl), lead saRNAs (saMB1_1 and saMB1_2) or their modified versions carrying a single nucleotide mismatch within the seed region at position 4, 6 or 8 (MM4, 6, 8), or their scrambled sequence versions (scrA-C). **(C)** RT-qPCR analysis of lncRNA *MBNL1-AS1* level in GM04033 cells transfected with 75 nM indicated saRNA for 120 h.

Supplementary Figure S9.

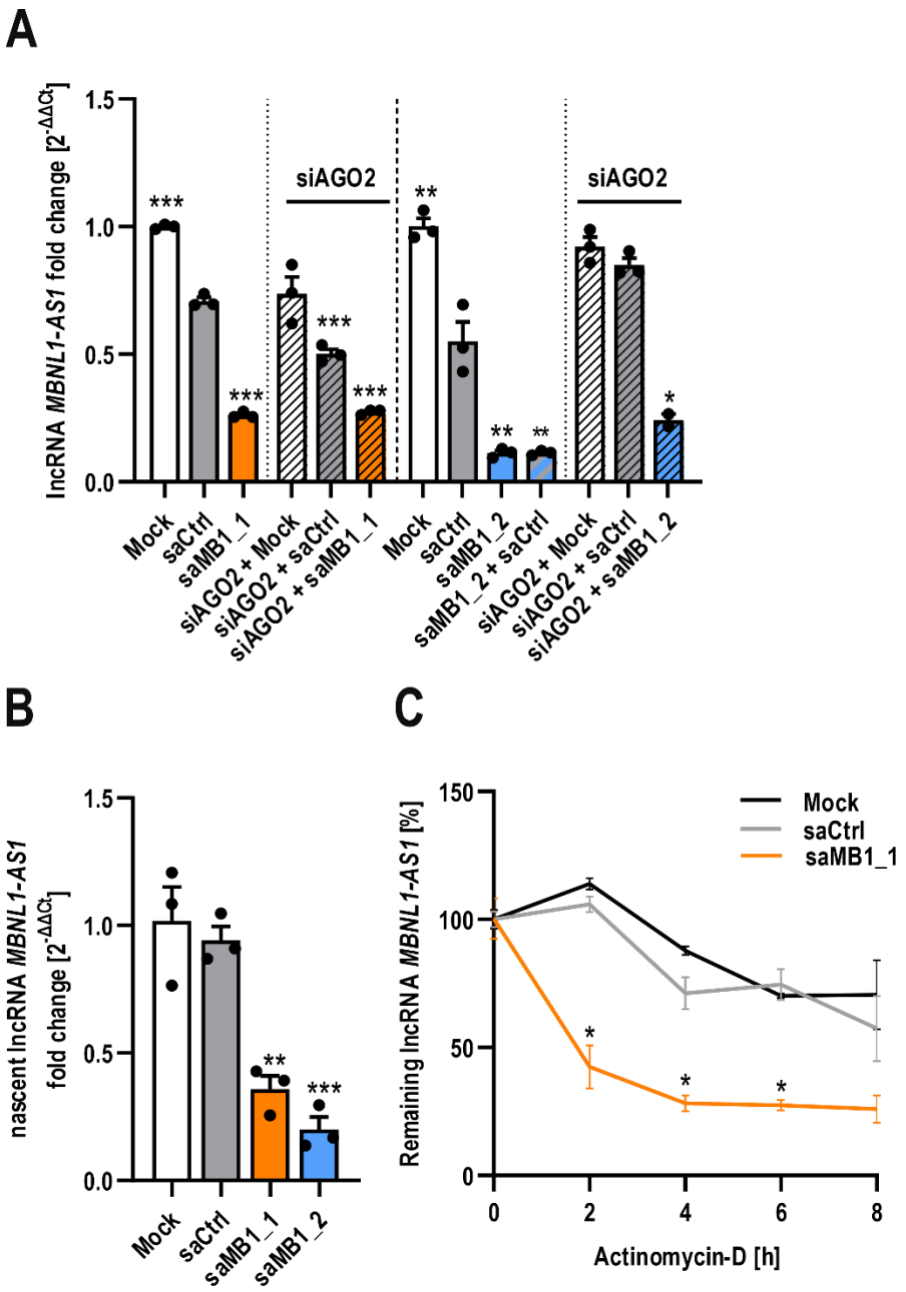

Supplementary Figure S9. Reduced antisense transcription and higher transcript turnover contribute to the reduction of lncRNA *MBNL1-AS1* upon *MBNL1*-directed saRNAs. (A) RT-qPCR of *MBNL1-AS1* in GM04033 DM1 fibroblasts transfected with lipofectamine (mock) or 75 nM indicated saRNA delivered solo (saCtrl, saMB1_1 or saMB1_2), or sequentially such that the 24 h transfection of 75 nM siAGO2 was followed by a second transfection of either lipofectamine alone (mock), 75 nM saCtrl or one of the two lead saRNA duplexes (saMB1_1 or saMB1_2) for additional 96 h. In the case of saMB1_2-transfected samples, additional control also included a second transfection with 75 nM saCtrl (blue / grey striped bar). All analyses were performed after a total of 120 h. **(B)** RT-qPCR-based analysis of nascent RNA capture of *MBNL1-AS1* assayed in GM04033 cells transfected with lipofectamine alone (mock) or 75 nM indicated saRNA for 72 h, followed by 24 h EU pulse and capture using Click-iT chemistry. **(C)** RT-qPCR-based timecourse analysis (0-8 h) of the remaining lncRNA *MBNL1-AS1* upon actinomycin D (Act-D) treatment of GM04033 cells transfected with 75 nM saMB1_1 (orange) or saCtrl (grey) for 120 h. Results obtained in lipofectamine-treated cells

(mock, black) are shown for reference. Act-D was added 120 h post saRNA transfection (timepoint 0 of the timecourse analysis). Verification of *MBNL1* upregulation 120 h post saRNA treatment is shown in Figure 2B, right panel. Data in (C) are presented as mean ± SEM of duplicate samples normalized to *GAPDH*.

Supplementary Figure S10.

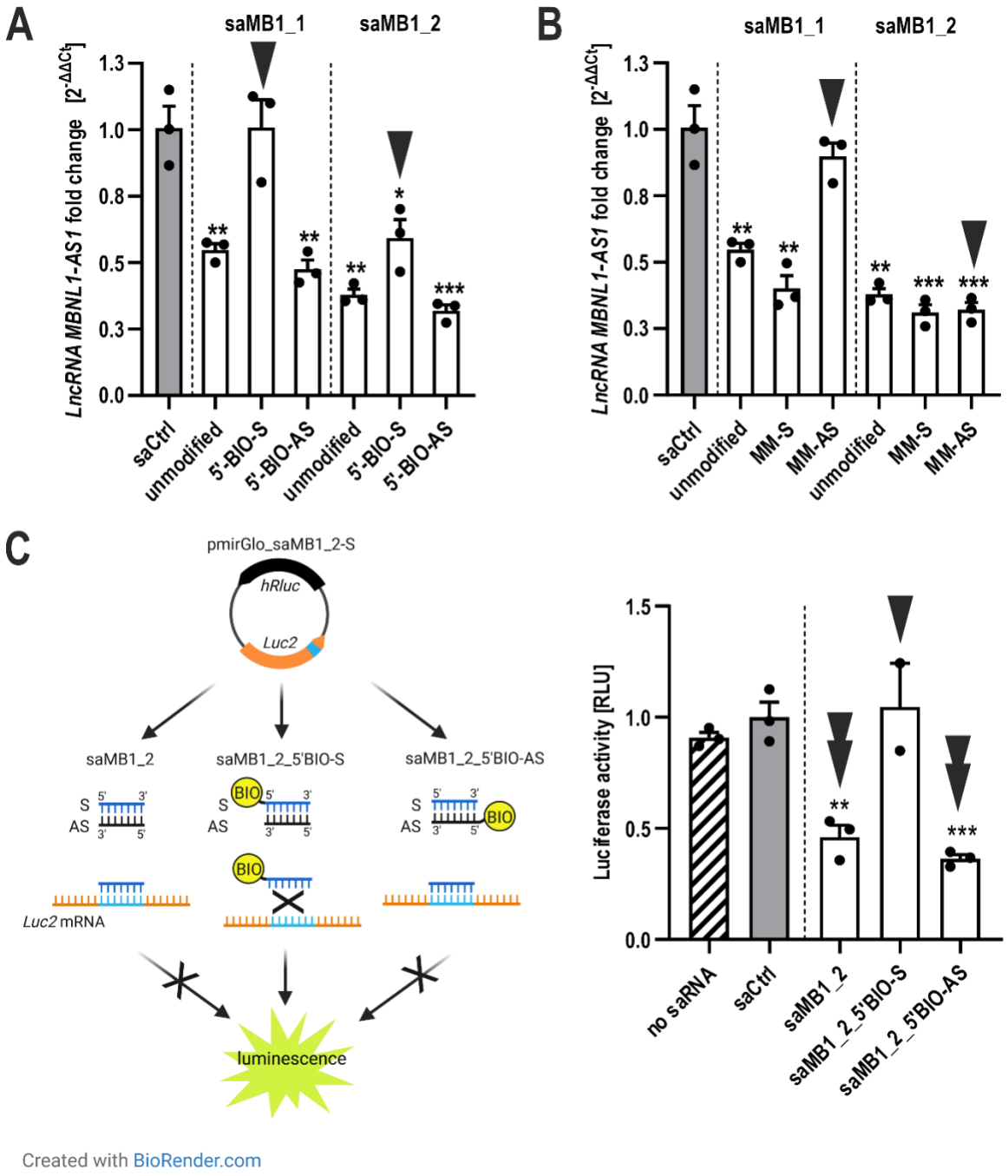

Supplementary Figure S10. The sense strand of *MBNL1*-directed saRNA mediates lncRNA *MBNL1-AS1* downregulation. (A-B) RT-qPCR analyses of lncRNA *MBNL1-AS1* in samples shown in Figure 4D-E, demonstrating correlation of *MBNL1-AS1* reduction with saMB1_1- and saMB1_2-mediated *MBNL1* mRNA upregulation. Black inverted arrowheads in (A) denote samples in which inhibition of the S strand blocked completely (saMB1_1) or partially (saMB1_2) the reduction of *MBNL1-AS1*. Black inverted arrowheads in (B) mark samples in which promotion of the AS strand selection (equivalent to a mismatch within the 3'-most nucleotide of the S strand) blocked completely (saMB1_1) or failed to block (saMB1_2) lncRNA *MBNL1-AS1* reduction. **(C)** The panel to the left shows schematic of dual luciferase assay designed to analyze the off-target potential of the S strand of saMB1_2 by cloning its target sequence into the 3'UTR of luciferase gene to generate the pmirGlo_saMB1_2-S vector. Created in BioRender. Stepniak-Konieczna, E. (2025) https://BioRender.com/j4v7vj1. The panel to the right shows

results of dual luciferase assay in HeLa cells co-transfected for 48 h with pmirGlo-saMB1_2-S and either unmodified or modified versions of saMB1_2. Double black inverted arrowheads mark samples in which active S strand of saMB1_2 inhibited luciferase activity (unmodified saMB1_2 and saMB1_2-5′BIO-AS). Single black inverted arrowhead marks the sample in which inhibition of the S strand by 5′-biotinylation (saMB1_2-5′BIO-S) allowed robust luciferase activity. Transfections of vector alone (no saRNA; striped bar) and saCtrl (grey bar) were used as controls. Results were normalized to Renilla luciferase luminescence and are represented as RLU (relative light unit).

Supplementary Figure S11.

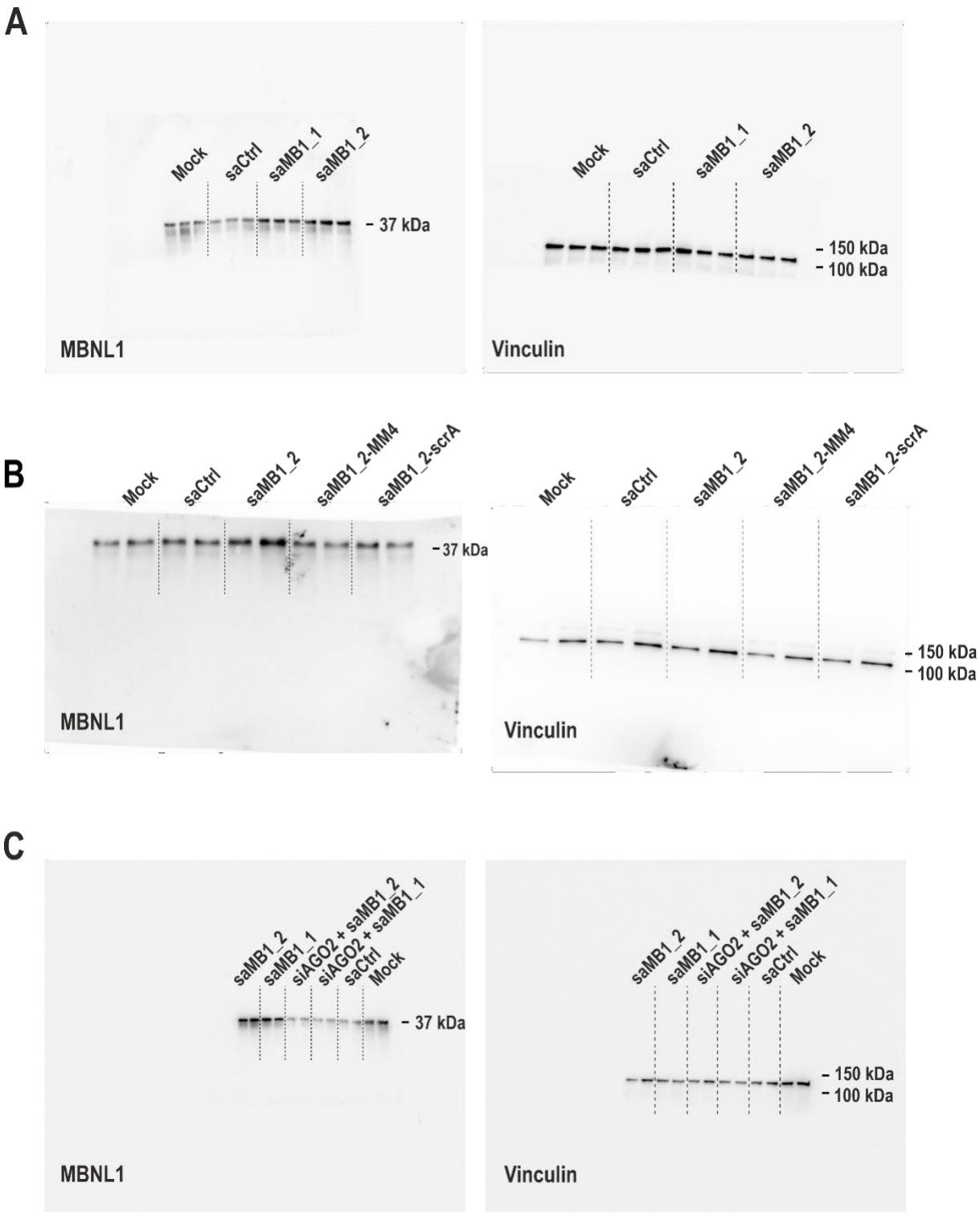

Supplementary Figure S11. Unadjusted and uncropped western blot images corresponding to Figure 6. (A-C) Blots corresponding to results shown in Figure 6A, 6B and 6C, respectively. Distinct sample types are described and separated by dotted lines. Each lane represents an individual biological sample.

Supplementary Figure S12.

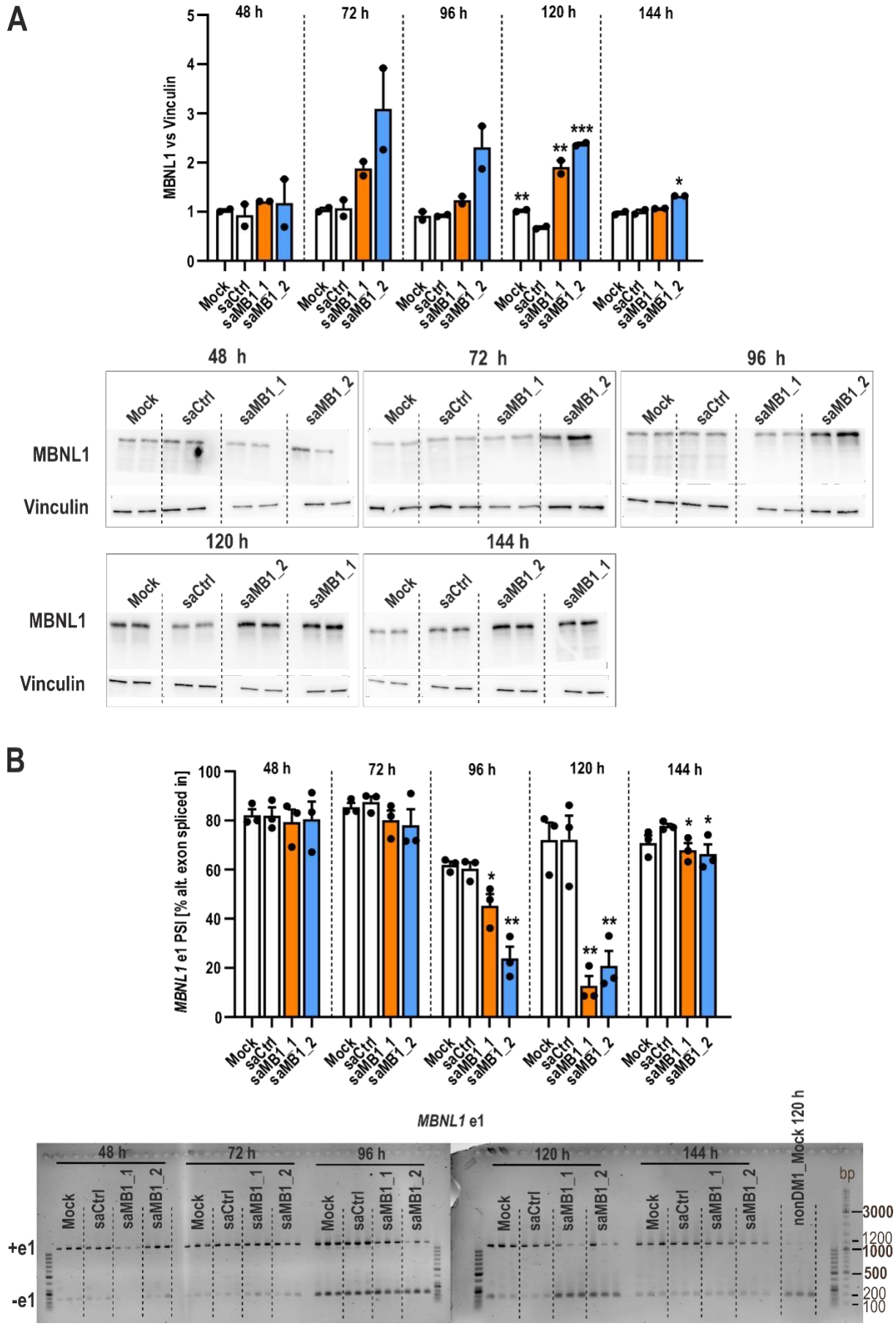

Supplementary Figure S12. Timecourse analyses show correlation of MBNL1 protein induction upon saRNA treatment with MBNL1-dependent e1 exclusion from *MBNL1* pre-mRNA. (A) Western blot quantification (top) and corresponding blot images (bottom) of MBNL1 protein levels in GM04033 DM1 fibroblasts transfected with lipofectamine alone (mock) or 75 nM indicated saRNA for indicated timepoints. MBNL1 and Vinculin blots are derived from the same experiment and the same gel. Data are presented as mean ± SEM of duplicate samples. **(B)** RT-PCR-based quantification (top) and corresponding RT-PCR gel images (bottom) of *MBNL1* e1 alternative splicing in GM04033 transfected with lipofectamine alone (mock) or 75 nM indicated saRNA for indicated timepoints.

Supplementary Figure S13.

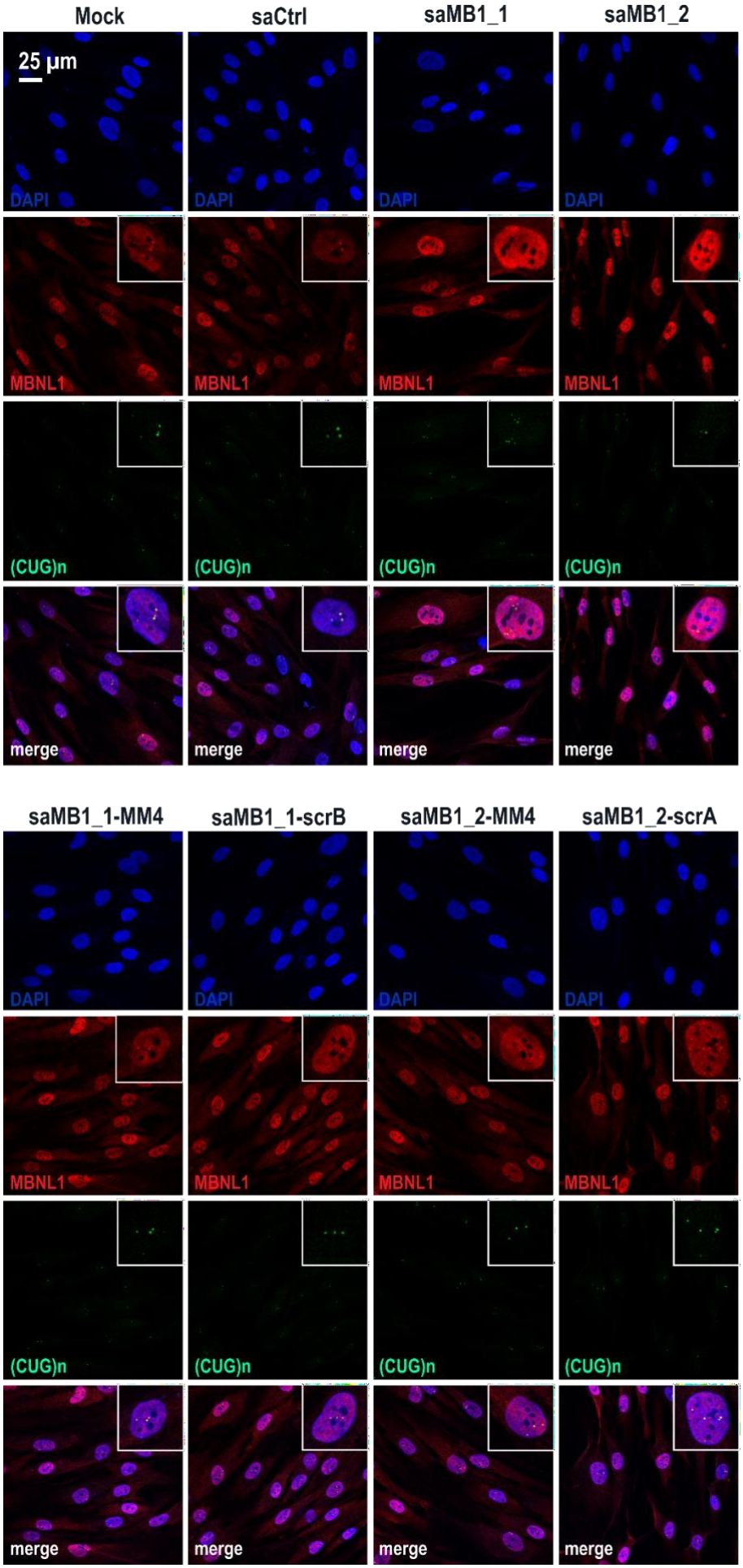

Supplementary Figure S13. Colocalization of MBNL1 and CUG^{exp} RNA foci in DM1 fibroblasts is not affected by saRNA-mediated *MBNL1* upregulation. Representative confocal images of RNA-FISH-IF showing MBNL1 (red; DyLight594) and (CUG)n RNA foci (green; Cy3) in GM03989 DM1 fibroblasts transfected with 75 nM indicated saRNA or mock-treated for 120 h. Nuclei were counterstained with DAPI (blue). Scale bar=25 μm.

Supplementary Figure S14.

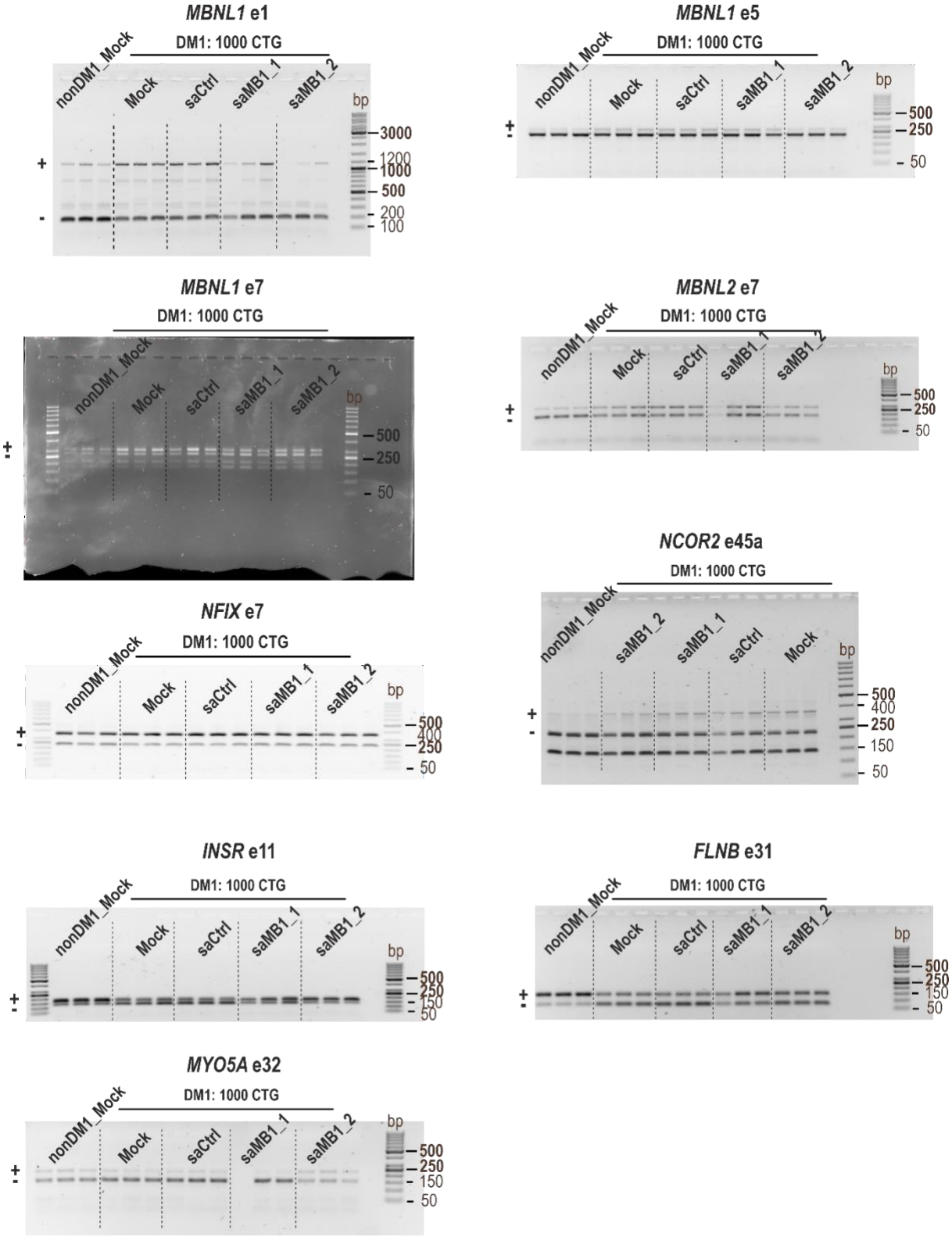

Supplementary Figure S14. Unadjusted and uncropped RT-PCR gel images of alternative splicing events in DM1 fibroblasts shown in Figure 8A. Distinct sample types are described and separated by dotted lines. Each lane represents an individual sample. + and – mark alternative exon inclusion and exclusion, respectively.

Supplementary Figure S15.

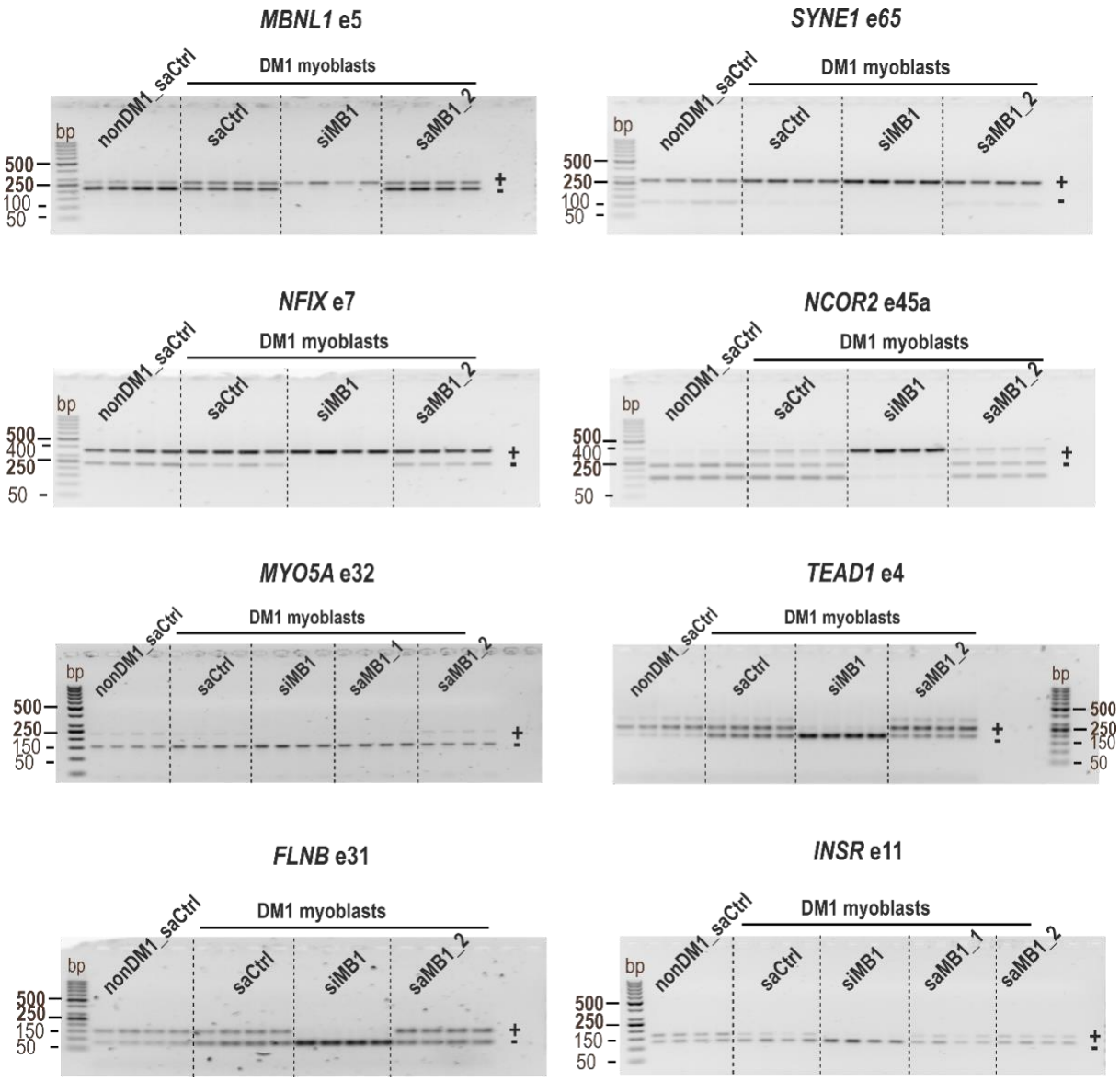

Supplementary Figure S15. Unadjusted and uncropped RT-PCR gel images of alternative splicing events in DM1 myoblasts shown in Figure 8B. Distinct sample types are described and separated by dotted lines. Each lane represents an individual sample. + and – mark alternative exon inclusion and exclusion, respectively.

Supplementary Figure S16.

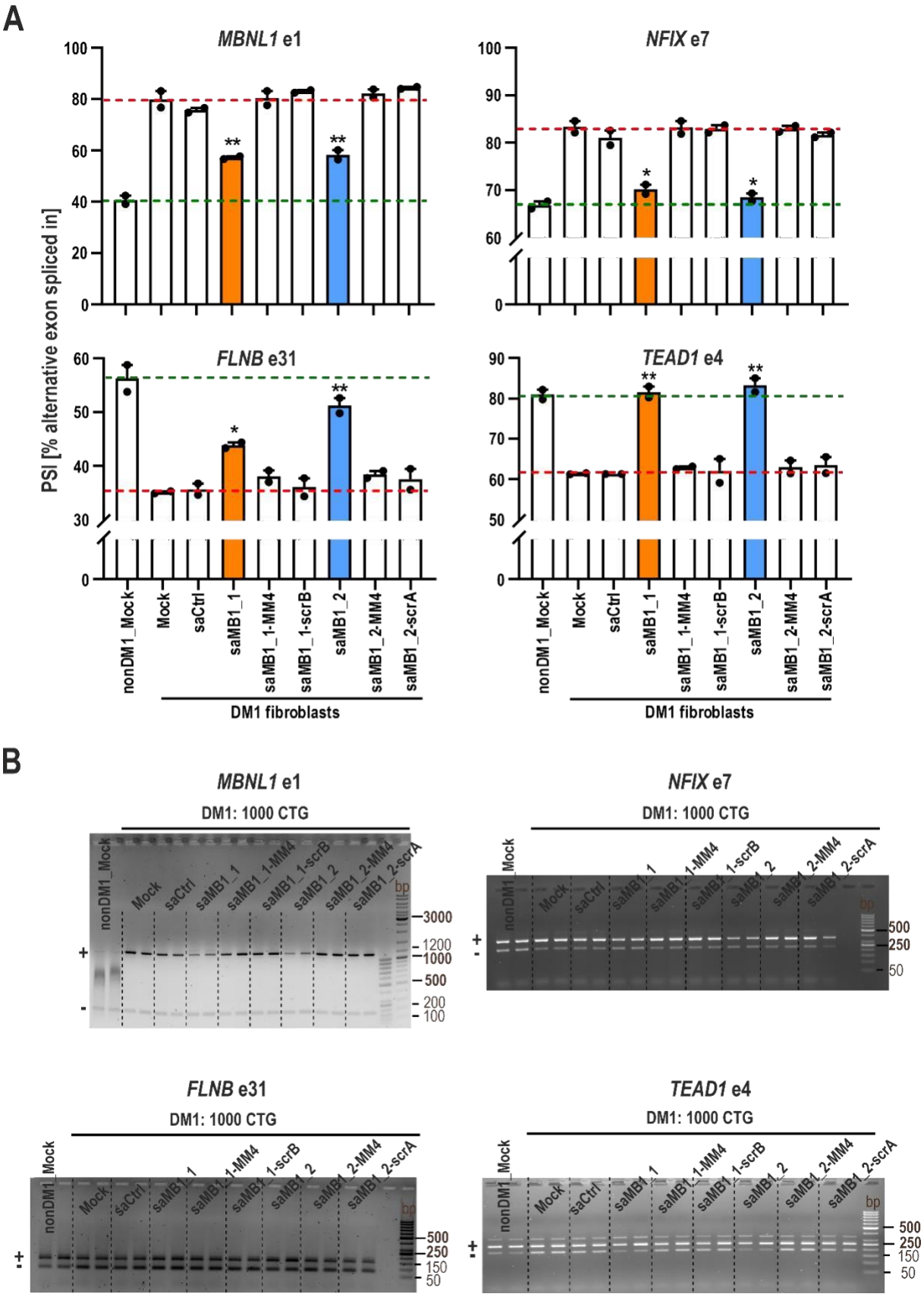

Supplementary Figure S16. Sequence-scrambled or seed region mutant versions of saMB1_1 and saMB1_2 do not affect *MBNL1*-regulated alternative splicing. (A) RT-PCR-based quantification of selected splicing events in GM04033 DM1 fibroblasts transfected with 75 nM indicated saRNA for 120 h. NonDM1_Mock represents unaffected and untreated control

fibroblasts. Red and green horizontal dashed lines mark the level of alternative exon inclusion (PSI) in DM1 and unaffected cells, respectively. Data are presented as mean ± SEM of duplicate samples and refer to PSI. **(B)** Representative RT-PCR gel images used for quantification. Lane description is shown, and each lane represents an individual sample. Sample groups are separated by dotted lines. + and – mark PCR products corresponding to the splice isoforms with alternative exon inclusion and exclusion, respectively.

Supplementary Figure S17.

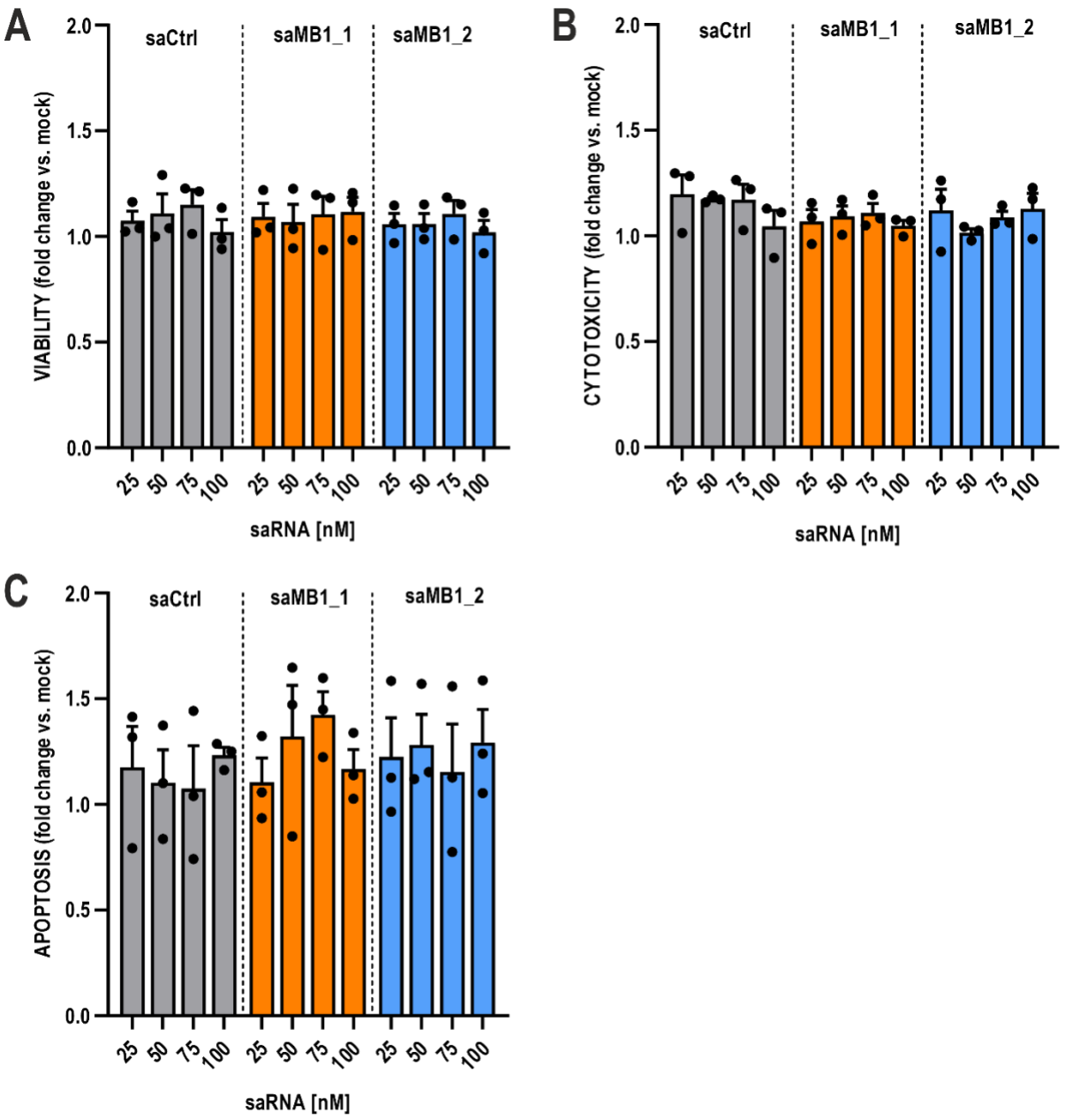

Supplementary Figure S17. saRNA duplexes do not affect cell viability, toxicity and apoptosis. Viability **(A),** cytotoxicity **(B)** and apoptosis **(C)** analyses of saRNA dose-response effect at 120 h timepoint in GM04033 DM1 fibroblasts. Results are demonstrated as mean ± SEM of fold change in viability, cytotoxicity, and apoptosis over mock control (untreated cells transfected with lipofectamine alone) of triplicate samples.

3. SUPPLEMENTARY TABLES S1-S6

Supplementary Table S1. Sequences of saRNAs and control RNA duplexes used in this study. Bases marked red point out single nucleotide mutations introduced within the seed region of saMB1_1 or saMB1_2 duplexes at indicated positions (4,6,8) counted from the 5′ end of the AS strand.

saRNA	Position of cognate target site relative to TSS2	Sequence (5' - 3') of sense (S) and antisense (AS) strand of saRNA duplex
2-2822	-2822	**S:** UAGGCCAAAUCAGUGGUAA [dT][dT] **AS:** UUACCACUGAUUUGGCCUA [dT][dT]
2-2552	-2552	**S:** CUCCUCCAGUGUUGAAGUA [dT][dT] **AS:** UACUUCAACACUGGAGGAG [dT][dT]
2-2303	-2303	**S:** ACCUGCUAGCAGAUGCAAA [dT][dT] **AS:** UUUGCAUCUGCUAGCAGGU [dT][dT]
2-2250	-2250	**S:** ACAGACAAUGGGAGGCAAA [dT][dT] **AS**: UUUGCCUCCCAUUGUCUGU [dT][dT]
2-1652	-1652	**S:** CUUUCAAGGCACCAGUUAA [dT][dT] **AS:** UUAACUGGUGCCUUGAAAG [dT][dT]
2-1471	-1471	**S:** ACUGGCAUAGUAGGCACUA [dT][dT] **AS:** UAGUGCCUACUAUGCCAGU [dT][dT]
2-1319 **(saMB1_2)**	-1319	**S:** UGUGGGUACUUGAGUCCUU [dT][dT] **AS:** AAGGACUCAAGUACCCACA [dT][dT]
2-1284	-1284	**S:** GGGAAGAGGCACCAUUUAA [dT][dT] **AS:** UUAAAUGGUGCCUCUUCCC [dT][dT]
2-1252	-1252	**S:** UCUGGAAGGGAUCAGUGUA [dT][dT] **AS**: UACACUGAUCCCUUCCAGA [dT][dT]
2-1218	-1218	**S**: GCUUUGUGGAUCUAGCUAA [dT][dT] **AS**: UUAGCUAGAUCCACAAAGC [dT][dT]
2-942	-942	**S:** UCAUCACAUCACAGACGUU [dT][dT] **AS:** AACGUCUGUGAUGUGAUGA [dT][dT]
2-932	-932	**S:** ACAGACGUUCAGGAUUCUU [dT][dT] **AS:** AAGAAUCCUGAACGUCUGU [dT][dT]
2-912	-912	**S:** CCAUUCAAAGCAAAGCCAA [dT][dT] **AS:** UUGGCUUUGCUUUGAAUGG [dT][dT]

2-886	-886	**S:** CUUAUAGCACCCAGUGAAU [dT][dT] **AS:** AUUCACUGGGUGCUAUAAG [dT][dT]
2-882 **(saMB1_1)**	-882	**S:** UAGCACCCAGUGAAUUAUG [dT][dT] **AS:** CAUAAUUCACUGGGUGCUA [dT][dT]
2-864	-864	**S:** GAUAUGGGGCUGCGGUUUA [dT][dT] **AS:** UAAACCGCAGCCCCAUAUC [dT][dT]
2-806	-806	**S:** UCCCGGUAUUUCAGAAGUA [dT][dT] **AS:** UACUUCUGAAAUACCGGGA [dT][dT]
2-769	-769	**S:** GGGAGCUUUGCUUUCUCUA [dT][dT] **AS:** UAGAGAAAGCAAAGCUCCC [dT][dT]
2-731	-731	**S:** GGGAAUACAGUGGCCUGUA [dT][dT] **AS:** UACAGGCCACUGUAUUCCC [dT][dT]
2-564	-564	**S:** UUAGCCCUCCAGGUUCAAA [dT][dT] **AS:** UUUGAACCUGGAGGGCUAA [dT][dT]
2-439	-439	**S:** GUGCAAGGGCCUCUUUCAA [dT][dT] **AS:** UUGAAAGAGGCCCUUGCAC [dT][dT]
saRNA	**Position of cognate target site relative to TSS3**	**Sequence (5' - 3') of sense (S) and antisense (AS) strand of saRNA duplex**
3-3010	-3010	**S:** UCCUGACAGCAUUGAUGAA [dT][dT] **AS:** UUCAUCAAUGCUGUCAGGA [dT][dT]
3-2906	-2906	**S:** CACGGUAGAUGACUCUUUA [dT][dT] **AS:** UAAAGAGUCAUCUACCGUG [dT][dT]
3-860	-860	**S:** CCAUAUGCCAAUAGAGCAA [dT][dT] **AS:** UUGCUCUAUUGGCAUAUGG [dT][dT]
3-847	-847	**S:** GAGCAAUUUUGGCUCAUGA [dT][dT] **AS:** UCAUGAGCCAAAAUUGCUC [dT][dT]
3-801	-801	**S:** CUGUGUCAUUGCCUCUUUA [dT][dT] **AS:** UAAAGAGGCAAUGACACAG [dT][dT]
3-747	-747	**S:** CCUCAUUGGCAACAUUCAA [dT][dT] **AS:** UUGAAUGUUGCCAAUGAGG [dT][dT]
3-653	-653	**S:** GUCUUGUGGUGCUGAGUUA [dT][dT] **AS:** UAACUCAGCACCACAAGAC [dT][dT]

3-650	-650	**S:** UCUUGUGGUGCUGAGUUAA [dT][dT] **AS:** UUAACUCAGCACCACAAGA [dT][dT]
3-557	-557	**S:** UCACGCUGCUCAAAUCAAA [dT][dT] **AS:** UUUGAUUUGAGCAGCGUGA [dT][dT]
3-498	-498	**S:** CUCCCUUGAGGUUGACUUC [dT][dT] **AS:** GAAGUCAACCUCAAGGGAG [dT][dT]
3-461	-461	**S:** GACAACACUGUACUCCUUA [dT][dT] **AS:** UAAGGAGUACAGUGUUGUC [dT][dT]
3-430	-430	**S:** GACCUCAGCUUCUGCUUUA [dT][dT] **AS:** UAAAGCAGAAGCUGAGGUC [dT][dT]
3-379	-379	**S:** AUCUUGCCUGCCUGUGAUA [dT][dT] **AS:** UAUCACAGGCAGGCAAGAU [dT][dT]
3-344	-344	**S:** CUGCGGGCUCAAUGGAAUA [dT][dT] **AS:** UAUUCCAUUGAGCCCGCAG [dT][dT]
3-283	-283	**S:** UGGGCUUUAGAAGGAAGUG [dT][dT] **AS:** CACUUCCUUCUAAAGCCCA [dT][dT]
3-252	-252	**S:** CAGGAGAAUGUACCAUUUG [dT][dT] **AS**: CAAAUGGUACAUUCUCCUG [dT][dT]
3-234	-234	**S:** GUAAACACCCCUUUCCUUU [dT][dT] **AS:** AAAGGAAAGGGGUGUUUAC [dT][dT]
3-145	-145	**S:** GCUUGGAAGUCAGCUGCAA [dT][dT] **AS:** UUGCAGCUGACUUCCAAGC [dT][dT]
control saRNA	**Additional information**	**Sequence (5' - 3') of sense (S) and antisense (AS) strand of saRNA duplex**
saCtrl	non-targeting control	**S**: ACUACUGAGUGACAGUAGA [dT][dT] **AS:** UCUACUGUCACUCAGUAGU [dT][dT]
saMB1_1_MM4	mutation within the seed region of saMB1_1 at position **4**	**S**: UAGCACCCAGUGAAU**C**AUG [dT][dT] **AS:** CAU**G**AUUCACUGGGUGCUA [dT][dT]
saMB1_1_MM6	mutation within the seed region of saMB1_1 at position **6**	**S**: UAGCACCCAGUGA**C**UUAUG [dT][dT] **AS:** CAUAA**G**UCACUGGGUGCUA [dT][dT]
saMB1_1_MM8	mutation within the seed region of saMB1_1 at position **8**	**S**: UAGCACCCAGU**U**AAUUAUG [dT][dT] **AS:** CAUAAUU**A**ACUGGGUGCUA [dT][dT]

saMB1_2_MM4	mutation within the seed region of saMB1_2 at position **4**	**S**: UGUGGGUACUUGAGU**U**CUU [dT][dT] **AS:** AAG**A**ACUCAAGUACCCACA [dT][dT]
saMB1_2_MM6	mutation within the seed region of saMB1_2 at position **6**	**S**: UGUGGGUACUUGA**U**UCCUU [dT][dT] **AS:** AAGGA**A**UCAAGUACCCACA [dT][dT]
saMB1_2_MM8	mutation within the seed region of saMB1_2 at position **8**	**S**: UGUGGGUACUU**U**AGUCCUU [dT][dT] **AS:** AAGGACU**A**AAGUACCCACA [dT][dT]
saMB1_1_scrA	scrambled sequence of saMB1_1	**S**: ACAAUUGAAGGCUCCUGUA [dT][dT] **AS:** UACAGGAGCCUUCAAUUGU [dT][dT]
saMB1_1_scrB	scrambled sequence of saMB1_1	**S**: AAGAGCUGGUCCUACAUAU [dT][dT] **AS:** AUAUGUAGGACCAGCUCUU [dT][dT]
saMB1_1_scrC	scrambled sequence of saMB1_1	**S**: CUAUAGACAUGUACGGUAC [dT][dT] **AS:** GUACCGUACAUGUCUAUAG [dT][dT]
saMB1_2_scrA	scrambled sequence of saMB1_2	**S**: GCGAUUUCCUGUAGUUGGU [dT][dT] **AS:** ACCAACUACAGGAAAUCGC [dT][dT]
saMB1_2_scrB	scrambled sequence of saMB1_2	**S**: GUGCAGUAUCGGUUCUGUU [dT][dT] **AS:** AACAGAACCGAUACUGCAC [dT][dT]
saMB1_2_scrC	scrambled sequence of saMB1_2	**S**: ACUCCGUUUUGGGGUAUUG [dT][dT] **AS:** CAAUACCCCAAAACGGAGU [dT][dT]
saRNA	**Position of cognate target site relative to TSS**	**Sequence (5' - 3') of sense (S) and antisense (AS) strand of saRNA duplex**
saP21	-322	**S:** CCAACUCAUUCUCCAAGUA[dT][dT] **AS:** UACUUGGAGAAUGAGUUGG[dT][dT]

Supplementary Table S2. Sequences of chemically modified and mismatch-containing saRNA duplexes for strand inhibition or promotion. Bases marked red point out a single mismatched base introduced in the 3′ end of the indicated strands. Abbreviations: BIO – Biotin; MM – mismatch; S – sense strand; AS – antisense strand.

saRNA	**Sequence (5' - 3') of sense (S) and antisense (AS) strand of saRNA duplex**
saMB1_1 5′BIO-S	**S: BIO**-UAGCACCCAGUGAAUUAUG [dT][dT] **AS:** CAUAAUUCACUGGGUGCUA [dT][dT]
saMB1_1 5′BIO-AS	**S:** UAGCACCCAGUGAAUUAUG [dT][dT] **AS: BIO**-CAUAAUUCACUGGGUGCUA [dT][dT]
saMB1_2_5′BIO-S	**S: BIO**-UGUGGGUACUUGAGUCCUU [dT][dT] **AS:** AAGGACUCAAGUACCCACA [dT][dT]
saMB1_2_5′BIO-AS	**S:** UGUGGGUACUUGAGUCCUU [dT][dT] **AS: BIO**-AAGGACUCAAGUACCCACA [dT][dT]
saMB1_1_MM-S	**S:** UAGCACCCAGUGAAUUAUG [dT][dT] **AS:** CAUAAUUCACUGGGUGCU**U** [dT][dT]
saMB1_1_MM-AS	**S:** UAGCACCCAGUGAAUUAU**C** [dT][dT] **AS:** CAUAAUUCACUGGGUGCUA [dT][dT]
saMB1_2_MM-S	**S:** UGUGGGUACUUGAGUCCUU [dT][dT] **AS:** AAGGACUCAAGUACCCAC**U** [dT][dT]
saMB1_2_MM-AS	**S:** UGUGGGUACUUGAGUCCU**A** [dT][dT] **AS:** AAGGACUCAAGUACCCACA [dT][dT]

Supplementary Table S3. siRNA and GapmeR sequences. Abbreviations: S-sense strand; AS-antisense strand; (*) phosphorothioate modifications; The Antisense LNA GapmeRs contain a central DNA part flanked by LNA; the position of the LNA modification is not shown (information proprietary to Qiagen).

siRNA or Antisense LNA GapmeR / target	**Sequence (5' - 3')**
siAGO2	**S:** GCACGGAAGUCCAUCUGAA [dT][dT] **AS:** UUCAGAUGGACUUCCGUGC [dT][dT]
siCTR9	**S:** GCACGUAUAGAUGGCAAUU [dT][dT] **AS:** AAUUGCCAUCUAUACGUGC [dT][dT]
siRHA	**S:** GCACGAGAACAUGGAUCAA [dT][dT] **AS:** UUGAUCCAUGUUCUCGUGC [dT][dT]
siMEIS1	**S:** CUGACAUUCAGGCCCAAGU [dT][dT] **AS:** ACUUGGGCCUGAAUGUCAG [dT][dT]
siMEIS2	**S:** CACCCUGGAAUGACUAUGU [dT][dT] **AS:** ACAUAGUCAUUCCAGGGUG [dT][dT]
siMBNL1	**S:** CACUGGAAGUAUGUAGAGA [dT][dT] **AS:** UCUCUACAUACUUCCAGUG [dT][dT]
siCtrl	Proprietary sequence (Ambion™ *Silencer*™ Select Negative Control #2)
siMBNL1-AS1 Lincode SMARTPool siRNA	**AS:** CUUCUGAAAUACCGGGAUA **AS:** GCUUAGAAUGCCUGCGAAC **AS:** CCAAACAUUUCUACGUAGU **AS:** AGACUAGAAUCCUGCGAUC
Antisense LNA GapmeR *MBNL1-AS1*	G*C*A*A*G*T*A*G*C*A*A*G*C*A*A*T
Antisense LNA GapmeR *DMPK*	A*A*A*T*G*C*G*C*A*G*C*T*A*A*G*C

Supplementary Table S4. Expression primers for RT-qPCR.

Transcript name	Primers Sequence (5' - 3')
MBNL1 (mRNA)	CTGCCGAACATCTGACTAGC TTGTGTGTGTTGCTTGACGA
MBNL1 (pre-mRNA)	GTGTGTGTGTGTAGGCCAAC GCTAGTCAGATGTTCGGCAG
MBNL1 (TSS2-derived transcripts)	CCACAATGCTCCCATGACAA CCCCACTGTCGACCAAGT
MBNL1 (TSS3-derived transcripts)	AGGCGCGACCTTTCATAAG CTGCTCTAGAAGCGGTTCCA
lncRNA MBNL1-AS1	TGGATAAGACAGTCCCTACA ATTGGATTGCTTCCCACATA
MBNL2	CCAAGGGCAGGTTCGATTCT AAGCTGGATGAAGTCTGGCA
DMPK	CACTGTCGGACATTCGGGAAGGTGC GCTTGCACGTGTGGCTCAAGCAGCTG
AGO2	CGCGTCCGAAGGCTGCTCTA TGGCTGTGCCTTGTAAAACGCT
CTR9	TTACCGGAGGGAGATGAAG AACTCTTCTGTTTTTCCTTGC
RHA	ACCTGCTATCATCAGCCAGTTGGA TCCATTGTCGTATCGGGCCATCTT
MEIS1	GTTGAAGTAGGAAGGGAGCCAG GCTGTGTGCGGGTACTGATG
MEIS2	GTGAGCCAAGGAGCAGCATA ACATGTAGTGCCATTGCCCA
GAPDH	TGAAGGTCGGAGTCAACGGA GATGACAAGCTTCCCGTTCTC
GAPDH (pre-mRNA, used for Click-IT assay*)*	AATCCCATCACCATCTTCCAG GAGCCACACCATCCTAGTTG

Supplementary Table S5. Alternative splicing primers.

Transcript name	Alternative exon	Primers Sequence (5' - 3')
MBNL1	e1	TCATGACTCCCACAATGCCT ATGGCCATGTTCTTCTGCTG
MBNL1	e5	GCTGCCCAATACCAGGTCAAC TGGTGGGAGAAATGCTGTATGC
MBNL1	e7	ACCAACAGGCTCTAGCCAACATGC CGTCCTTTACTCTAACCAAGC
MBNL2	e7	TCCTTTACCAAAGAGACAAGCAC CTCAATGCAGATTCTTGGCATTCC
NCOR2	e45a	ACACCCACAACCGGAATGAGCCTG GGACTTGGCTTTTCGGCTGCTG
NFIX	e7	GAGCCCTGTTGATGACGTGTTCTA CTGCACAAACTCCTTCAGTGAGTC
SYNE1	e65	GGTCCATGAAAGCAGCAATC ACTGATTGTGTTCTGCAACG
INSR	e11	CCAAAGACAGACTCTCAGAT AACATCGCCAAGGGACCTGC
FLNB	e31	GCTTCGGTGGTGTTGATATTC GTCACTCACTGGGACATAGG
MYO5A	e32	GAACAACCGACAGCAGCAG TTACGGACCGTCTTATCCTG
TEAD1	e4	GGAGGCCCTGGCTATCTATC GCTTGGAATGAAAATCACGAG

Supplementary Table S6. CUT&RUN primers for qPCR.

PCR product name (position of PCR product relative to TSS2 of *MBNL1*)	**Primers Sequence (5' - 3')**
MBNL1 (+4058;+4132)	CGTGGGGAGGTTAGCTAGTT ACAGACTCAAGATGGCACCA
MBNL1 (+1104;+1177)	CCTCGCACAGCACTTTACAA GCCCCAGAGAGCCTTAAGAA
MBNL1 (+231;+310)	GAAGGAGGAAGTGCGAGGAG CGAAACCAACTACCGCGAG
MBNL1 (-14;+28)	GCGATAAGAGGCTGCACAG CCACAACTCATTCAGCTGCA
MBNL1 (-912; -841)	CCATTCAAAGCAAAGCCAAGT CAAATAAACCGCAGCCCCAT
MBNL1 (-1097; -1022)	TCAACAAAACCGAACCTGCA CGTTTGTCCCATGTTTGTTGG
MBNL1 (-1655; -1565)	CACCTTTCAAGGCACCAGTT TGTATGTGGGAAGCAATCCA
MBNL1 (-3465; -3403)	GCTATGAATGTGGTATGCAGAAG GTAAGTGTGTGAGTGCCTGTG
PCR product name (position of PCR product relative to TSS of *p21*$^{WAF1/CIP1}$)	**Primers Sequence (5' - 3')**
P21 (+5469;+5606)	GACTGTGATGCGCTAATGG AGGTAGAGCTTGGGCAGG
P21 (+735;+888)	GAACGGACTGTATGAGGTCAG CAGTGCCCGGCTTCC
P21 (+107;+235)	CAGAGCCGAGCCAAGC CACCGACCCACGCCC
P21 (-1;+101)	TGCCGAAGTCAGTTCCTTG GGTCCCCTGTTGTCTGC
P21 (-141;+22)	AGCCAGGAGCCTGGGC CAAGGAACTGACTTCGGCA
P21 (-417; -262)	CAGCTGCATTGGGTAAATCC GACACATTTCCCCACGAAGT

P21 (-1668; -1222)	GAGAAGGTGCCTGTCCTCTG TCTGTGCCTGAAACATTTGC
P21 (-3861; -3777)	TCAATGCCACCACCTTAACA CAGAGCCAGGATGAATTGGT

4. SUPPLEMENTARY REFERENCES

REFERENCES

1. Barski, A., Cuddapah, S., Cui, K., Roh, T.Y., Schones, D.E., Wang, Z., Wei, G., Chepelev, I. and Zhao, K. (2007) High-resolution profiling of histone methylations in the human genome. *Cell*, **129**, 823-837.

3.2.1 Co-author's contribution statements

Mgr Nikola Musiała-Kierklo

Doktorantka Szkoły Doktorskiej Nauk Przyrodniczych

Wydział Biologii

Uniwersytet im. Adama Mickiewicza

Zespół Biologii RNA

Katedra Biochemii i Biotechnologii

Wydział Rolnictwa, Ogrodnictwa i Biotechnologii

Uniwersytet Przyrodniczy w Poznaniu

15 .09.2025 Poznań

OŚWIADCZENIE WSPÓŁAUTORA ARTYKUŁU

Oświadczam, że mój udział w przygotowaniu artykułu stanowiącego część mojej rozprawy doktorskiej, pt. ***„Promoter-targeted small RNA duplexes increase MBNL1 transcription and mitigate myotonic dystrophy-associated spliceopathy"***, autorstwa: Nikola Musiała-Kierklo, Patrycja Plewka, Adam Jasiok, Ewa Stępniak-Konieczna*, opublikowanego w czasopiśmie ***Nucleic Acids Research*** (2025), **doi: 10.1093/nar/gkaf756**, polegał na: udziale w zaplanowaniu eksperymentów; wiodącej roli w przeprowadzeniu eksperymentów (z wyłączeniem tych, które są wyszczególnione w oświadczeniach innych współautorów); wykonaniu analiz statystycznych; udziale w interpretacji wyników; przygotowaniu rycin (głównych i suplementarnych) oraz napisaniu manuskryptu we współudziale z ostatnim autorem; udziale w edycji i korekcie finalnej wersji manuskryptu i rycin.

*Autor korespondencyjny

Nikola Musiała-Kierklo

Podpis współautora

Ewa Stępniak-Konieczna

Podpis promotora

Dr Patrycja Plewka

Zespół Biologii RNA

Katedra Biochemii i Biotechnologii

Wydział Rolnictwa, Ogrodnictwa i Biotechnologii

Uniwersytet Przyrodniczy w Poznaniu

15 .09.2025 Poznań

OŚWIADCZENIE WSPÓŁAUTORA ARTYKUŁU

Oświadczam, że mój udział w przygotowaniu artykułu stanowiącego część rozprawy doktorskiej Nikoli Musiała-Kierklo, pt. ***„Promoter-targeted small RNA duplexes increase MBNL1 transcription and mitigate myotonic dystrophy-associated spliceopathy***", autorstwa: Nikola Musiała-Kierklo, Patrycja Plewka, Adam Jasiok, Ewa Stępniak-Konieczna*, opublikowanego w czasopiśmie ***Nucleic Acids Research*** (2025), ***doi: 10.1093/nar/gkaf756***, polegał na: przygotowaniu konstruktów lucyferazowych, przeprowadzeniu eksperymentów i analizie wyników ujętych na rycinie Figure 4F oraz rycinie suplementarnej S10C; zaprojektowaniu, przeprowadzeniu i interpretacji eksperymentów ujętych na rycinie suplementarnej S7; wykonaniu eksperymentów ujętych na rycinie suplementarnej S3A (środkowy i prawy wykres); napisaniu części materiałów i metod oraz rezultatów odpowiadających ww. eksperymentom; udziale w redagowaniu i korekcie całości manuskryptu.

*Autor korespondencyjny

Patrycja Plewka

Podpis współautora

Mgr Adam Jasiok

Doktorant Szkoły Doktorskiej

Uniwersytet Przyrodniczy w Poznaniu

15 .09.2025 Poznań

Zespół Biologii RNA

Katedra Biochemii i Biotechnologii

Wydział Rolnictwa, Ogrodnictwa i Biotechnologii

Uniwersytet Przyrodniczy w Poznaniu

OŚWIADCZENIE WSPÓŁAUTORA ARTYKUŁU

Oświadczam, że mój udział w przygotowaniu artykułu stanowiącego część rozprawy doktorskiej Nikoli Musiała-Kierklo, pt. ***„Promoter-targeted small RNA duplexes increase MBNL1 transcription and mitigate myotonic dystrophy-associated spliceopathy”***, autorstwa: Nikola Musiała-Kierklo, Patrycja Plewka, Adam Jasiok, Ewa Stępniak-Konieczna*, opublikowanego w czasopiśmie ***Nucleic Acids Research*** (2025), **doi: 10.1093/nar/gkaf756**, polegał na współudziale w przeprowadzeniu eksperymentów transfekcji saRNA do komórek HeLa i HEK293T oraz ocenie poziomu ekspresji *MBNL1* metodą RT-qPCR, przedstawionych na rycinach Supplementary Figure S4D oraz Supplementary Figure S4F (lewy wykres).

*Autor korespondencyjny

Jasiok

.....

Podpis współautora

Prof. UPP dr hab. inż. Ewa Stępniak-Konieczna

Kierownik Zespołu Biologii RNA

Katedra Biochemii i Biotechnologii

Wydział Rolnictwa, Ogrodnictwa i Biotechnologii

Uniwersytet Przyrodniczy w Poznaniu

15 .09.2025 Poznań

OŚWIADCZENIE WSPÓŁAUTORA ARTYKUŁU

Oświadczam, że mój udział w przygotowaniu artykułu stanowiącego część rozprawy doktorskiej Nikoli Musiała-Kierklo pt. ***„Promoter-targeted small RNA duplexes increase MBNL1 transcription and mitigate myotonic dystrophy-associated spliceopathy"***, autorstwa: Nikola Musiała-Kierklo, Patrycja Plewka, Adam Jasiok, Ewa Stępniak-Konieczna*, opublikowanego w czasopiśmie ***Nucleic Acids Research*** (2025), **doi: 10.1093/nar/gkaf756**, polegał na: konceptualizacji badań oraz pozyskaniu finansowania; zaplanowaniu i nadzorowaniu całości prac eksperymentalnych; interpretacji wyników; zaprojektowaniu saRNA oraz udziale we wstępnych analizach efektywności saRNA w fibroblastach DM1 (screening); analizie bioinformatycznej dla rycin suplementarnych S1A-C, S1E-F oraz S5A; przygotowaniu rycin głównych i suplementarnych oraz napisaniu manuskryptu we współudziale z pierwszym autorem; redagowaniu oraz korekcie finalnej wersji manuskryptu i rycin; zaprojektowaniu i przygotowaniu „graphical abstract"; przeprowadzeniu procesu składania manuskryptu do publikacji.

*Autor korespondencyjny

Ewa Stępniak-Konieczna

Podpis współautora

IV. RESULTS AND DISCUSSION - UNPUBLISHED DATA

4.1. Analyses of saRNA-mediated MBNL1 upregulation mechanism

4.1.1 *MBNL1* transcription start sites analyses

In human and in model organisms, the promoters of most genes have been identified through large-scale sequencing efforts. According to recent results, however, transcripts are quite often detected from the upstream regions of many genes that are outside of the previously defined transcribed regions. This indicates that additional TSSs and alternative promoters apart from those listed in databases may exist for many genes, including *MBNL1* (135,136). Identified saRNAs targeting *MBNL1* promoter 2 (P2) and 3 (P3) (137) were designed in the view of the TSS2 and 3 provided by previous studies (39), as well as by the Eukaryotic Promoter Database (EPD) new 006 (Figure 5A), annotated as *MBNL1_1* and *MBNL1_2* (referred to P2 and P3). However, UCSC (University of California, Santa Cruz) genome browser indicates several *MBNL1* transcripts initiated upstream of the TSS2. Therefore, rapid amplification of cDNA 5′ends was conducted (5′-RACE; a procedure for amplification of nucleic acid sequences from a messenger RNA template between a defined internal site and an unknown sequences at 5′-end of the mRNA) (136). Amplification of cDNA ends provides a powerful tool to quickly identify alternative transcripts of a gene when the partial or complete sequence of only one transcript is known. (136,138).

Analyses of *MBNL1* transcripts using 5′RACE were performed in RNA obtained from lipofectamine-treated GM04033 cells, using reverse primers (MBNL1_e1_GSP1, MBNL1_e1_GSP2) located within the coding sequence of the first coding exon (e1; 963 nt) of *MBNL1* (Figure 5B). This allowed investigation of the existence of RNA transcripts that could initiate upstream of the previously determined TSS2/TSS3. 5′RACE products sizes were predicted using UCSC genome browser by calculating length from each TSS to GSP2 primer end, and were as follows: 1053–1103 bp for TSS2 products; 983–1033 bp for TSS3 products. Agarose gel analysis of 5′RACE products detected amplification of only one product (~1.1kb) that corresponded size-wise to TSS2-derived *MBNL1* transcript. However, predicted P2-derived products could differ from those originating from P3 by only ~70–120 bp. Also, P2 and P3-derived products could comigrate as a single ~1.1 kb band (Figure 5C). Therefore, detected product was isolated from agarose gel and analyzed by Sanger sequencing (serviced by Genomed). However, sequencing analysis did not confirm that

5´RACE product is specific for *MBNL1* TSS2 (Supplementary Figure 1). Interestingly, nucleotide BLAST (Basic Local Alignment Search Tool) analysis found matches in several *MBNL1* transcripts that could be generated from all three promotores (P1-P2). Firstly, occurrence of *MBNL1* transcripts generated from promoter 1 is unexpected as it was previously shown that P1- derived *MBNL1* transcripts exhibit always skipped exon 1 in liver, spleen and thymus samples. Moreover, P1 is the least active *MBNL1* promoter (39). However, UCSC genome browser shows possible P1-derived *MBNL1* transcripts containing exon 1, so it is in line with the sequencing results. On the other hand, agarose gel analyses revealed only one product, so it is plausible that transcripts from all three promoters splice downstream into that same coding exon and are indistinguishable from each other by this experimental design. In other words, 5´RACE PCR may cover every isoform that joins into that exon, all at once, and they migrate as one ~1.1 kb band on agarose gel. However, analyses of sequencing results revealed that the detected band had a significant portion of its sequence matched to a total of 48 *MBNL1* transcripts, of which 7 were P1-derived, 32 were P2-derived, and 9 were P3-derived (Supplementary Figure 2). Therefore, I conclude that the majority of the analyzed *MBNL1* transcripts originated form TSS2, which is in line with the published data (39).

Therefore, second 5´RACE analysis was performed using different reverse primers (MBNL1_e2_GSP1, MBNL1_e2_GSP2) located within the second coding exon (e2; 171 nt) of *MBNL1* (Figure 5D). Selected exon 2 is constitutive, therefore transcripts without alternatively spliced exon 1 could be evaluated. Similarly as in 5´RACE analysis with primers located in exon 1, PCR products sizes were predicted for 5´RACE analysis with primers located in exon 2. Based on the UCSC genome browser, the calculated products lengths from each TSS to GSP2 primer end were as follows: 1282–1332 bp for TSS2 products; 1212–1262 bp for TSS3 products. In contrast to 5´RACE with primers located in exon 1, 5´RACE using reverse primers located in exon 2 detected a group of amplified products that did not directly correspond size-wise to transcript derived from UCSC-annotated TSS2 or TSS3, whereas the amount of those that could correspond to TSS2/TSS3 products were too low to perform sequencing analysis or further cloning (Figure 5E).

In summary, performed 5´RACE analyses did not allow for drawing of clear conclusions regarding *MBNL1* TSS2 and TSS3 activity. Given time constraints, the 5´RACE analyses could not be optimized or repeated. Because obtained data were ambiguous, additional meta-analyses of the activity of *MBNL1* promoters based on UCSC and EPD

available data, as well as RT-qPCR-based analyses of expression level of TSS2- and TSS3-derived *MBNL1* transcripts in DM1 patients' fibroblasts, were performed. These results confirmed superior activity of P2/TSS2 over P3/TSS3 (Supplementary Figure S1 and S2C in (137)) and enabled successful design of saRNAs based on the EDPnew-annotated TSS2 and TSS3 (36,39,137).

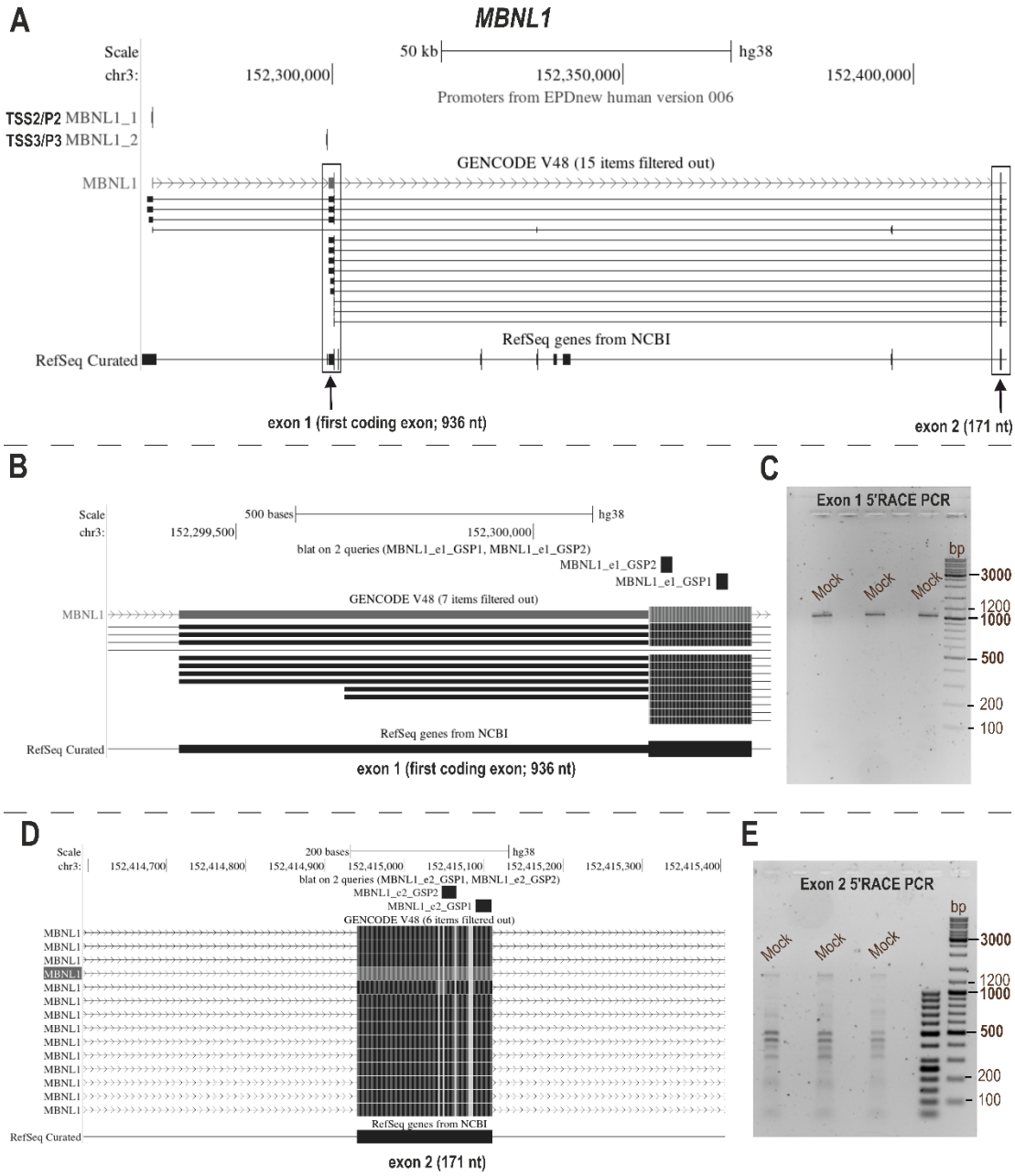

Figure 5. 5´RACE analyses of *MBNL1* transcripts. (A) UCSC genome browser image showing the location of TSS2/P2 (MBNL1_1) and TSS3/P3 (MBNL1_2) provided by the EPDnew human version 006. Black arrows indicated exon 1 (the first coding exon of *MBNL1*; 936 nt) and exon 2 (171 nt) that were marked with black frames **(B,D)** UCSC genome browser images showing the location of the primers used for 5´RACE analysis in exon 1 **(B)** or exon 2 **(D)**. **(C,E)** Representative gel images of exon 1 **(C)** and exon 2 **(E)** 5´RACE PCRs. Each lane represents the same biological sample (three technical replicates of one mock-treated DM1 sample). Abbreviations: TSS - transcription start site; P - promoter; nt - nucleotides.

4.1.2 Contribution of AGO1 in *MBNL1* RNA activation

Currently, AGO2 is the only AGO protein clearly demonstrated to play a direct role in RNA activation mechanism (115,116). The involvement of other human Argonaute proteins (AGO1, AGO3, and AGO4) in RNAa is less well-defined or not supported by strong experimental evidence (119,120). saRNA-mediated *MBNL1* upregulation requires AGO2 protein (137), consistently with previous studies (112,116,119). To verify possible involvement of other members of the AGO family in *MBNL1* RNAa, AGO1 was selected as previously published results suggested its supportive role in RNAa (112,119).

Therefore, *AGO1* was knocked-down via RNAi in GM04033 cells using 75 nM of siAGO1 alone or in combination with saCtrl or saMB1_1. Efficient knock-down of *AGO1* (~80-90%) (Figure 6A) completely blocked *MBNL1* upregulation via saMB1_1 (Figure 6B; left part of the graph). However, siAGO1 alone led to *MBNL1* downregulation (~60-70%) (Figure 6B; right part of the graph). Intriguingly, the expression level of unrelated genes was also significantly altered upon *AGO1* knock-down. These alterations included e.g., downregulation of *DMPK* (~60-80%) (Figure 6C) and *MBNL2* (~20-60%) (Figure 6D) mRNA and support the conclusion that knockdown of AGO1 worsens cell viability and led to cell toxicity. Importantly, siAGO1 transfection induced significant cell death as compared to mock- or saCtrl-treated cells, as judged by microscopic observation.

Although several works reported the involvement of AGO1 in RNAa using ChIP analysis (139) or siRNA-mediated knockdown (112,120), other works indicate that AGO1 is a less critical component than AGO2 in RNAa (112,116,120). Moreover, as RNAi regulates expression level of various genes, silencing of AGO proteins may lead to direct or indirect cell toxicity. Given that AGO1 is a core component of the RNA-induced silencing complex (RISC) that binds to small RNAs to regulate gene expression, its loss may have direct consequences and lead to severe defects in RNAi pathway and RNA processing within the cell (140). Thus, the downregulation of *MBNL1, MBNL2* and *DMPK* mRNAs expression may be an indirect effect of AGO1 silencing. Hence, the overall detrimental effect of AGO1 removal on the cells' viability precludes strong conclusions on its requirement for *MBNL1* RNAa with the two identified saRNAs.

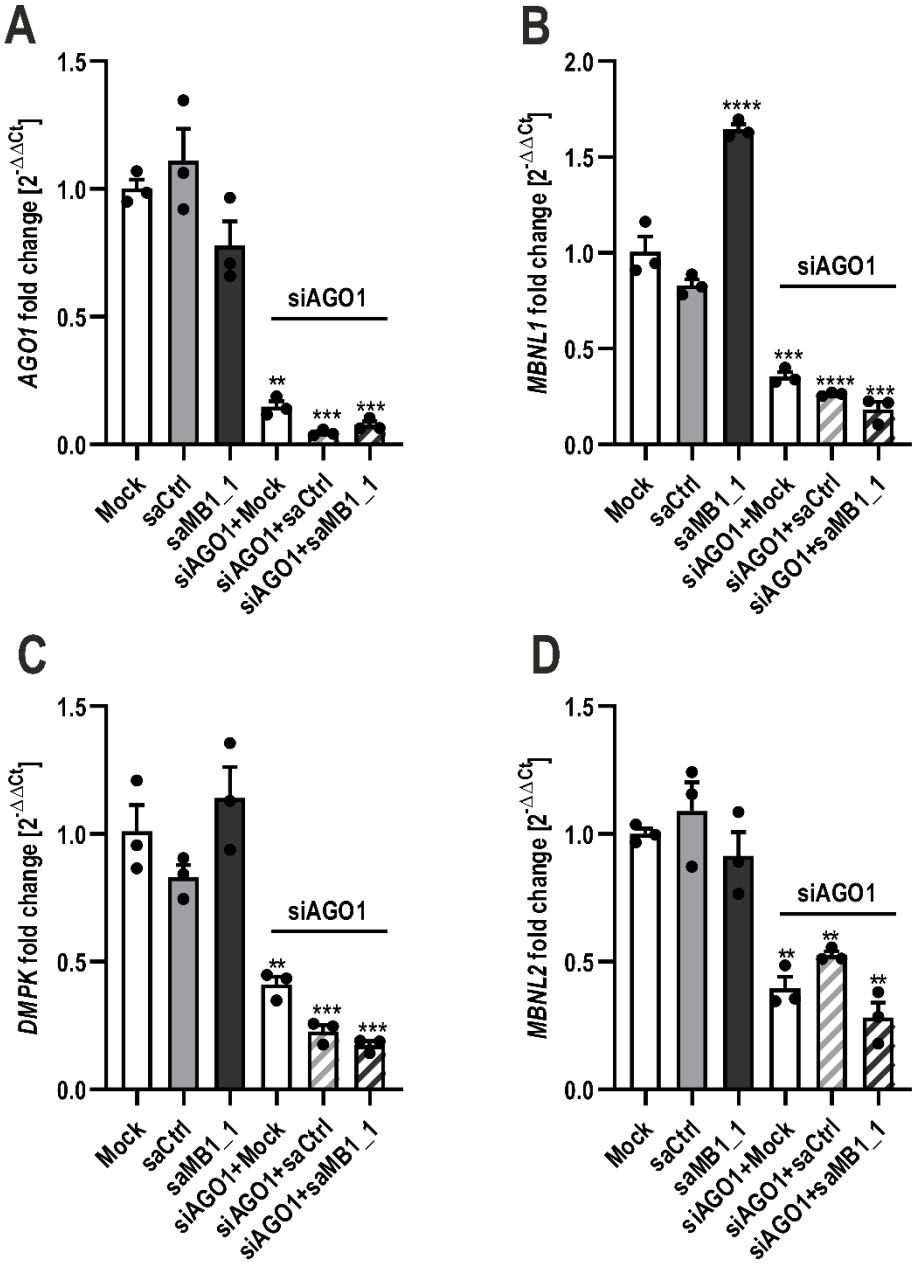

Figure 6. RNA interference-mediated knock-down of *AGO1* leads to global changes in cell viability, and correlates with downregulation of various transcripts. (A-D) RT-qPCR analyses of *AGO1* **(A)**, *MBNL1* **(B)**, *DMPK* **(C)** and *MBNL2* **(D)** expression in GM04033 DM1 fibroblasts transfected for 24 h with lipofectamine alone (mock) or 75 nM indicated dsRNA (saCtrl, saMB1_1 or siAGO1). After 24 h, siAGO1-transfected samples (right parts of the graphs) were subjected to a second round of transfection with lipofectamine alone (mock), or 75 nM saCtrl or saMB1_1, for additional 96 h. After a total of 120 h, all samples were harvested for analyses.

4.1.3 Analyzes of ZNF274 transcription factor involvement in *MBNL1* RNA activation

Transcription factors (TFs) are essential regulatory proteins that facilitate and control gene expression by binding to specific DNA sequences, typically in promoter or enhancer regions. Importantly, transcription factors play a crucial role in gene regulation in RNAa because during the facilitation of the RITA complex assembly, the promoter region becomes more accessible to TFs binding. Furthermore, the presence, concentration, and activation state of specific transcription factors determine the efficiency and specificity of RNAa. Thus, transcription factors not only enhance the activation initiated by saRNAs but also provide the necessary gene- and cell-type specificity that makes RNAa a precisely regulated process (115,116,141). In support, our laboratory reported that MEIS1 and MEIS2 transcription factors may contribute to saRNA-mediated *MBNL1* upregulation via cooperation with saMB1_1, as its target site overlaps their cognate binding sites (137). To evaluate the involvement of TFs whose binding sites overlap the target genomic sequence of saMB1_2, we examined the UCSC genome browser-deposited ChIP seq data. The binding site of one transcription factor in particular, ZNF274, was found to overlap the target site of saMB1_2, hence ZNF274 was chosen to verify its putative role in MBNL1 RNAa regulation (Figure 7A).

Zinc Finger Protein 274 (ZNF274) is in fact a transcriptional repressor that plays a key role in the regulation of epigenetic gene silencing, especially in heterochromatic regions of the human genome. It belongs to a large family of KRAB-containing zinc finger proteins (KRAB-ZFPs), which are known for their ability to bind DNA through zinc finger motifs and recruit silencing machinery via the KRAB domain. Once bound to DNA, ZNF274 recruits TRIM28 (KAP1), which in turn serves as a scaffold to recruit SET domain bifurcated histone lysine methyltransferase 1 (SETDB1), that deposits trimethyl marks on lysine 9 of histone H3 (H3K9me3). This histone modification is a classic marker of heterochromatin, leading to the compaction of DNA and the silencing of nearby genes or transposable elements (142).

Hypothetically, if the saMB1_2-AGO2 complex binds the same genomic site that is recognized by ZNF274 (usually via its zinc finger motifs), the physical occupancy of that DNA region by the saRNA-AGO2 complex may sterically hinder ZNF274 from binding or disrupt the recruitment of TRIM28 and SETDB1, which are necessary for forming a repressive complex. This would lead to a loss of H3K9me3 deposition and local chromatin

relaxation, allowing transcriptional machinery to access the promoter or enhancer, thereby enabling gene activation.

To verify possible involvement of ZNF274 in MBNL1 RNAa via saMB1_2, a series of attempts to silence the expression of *ZNF274* via RNAi in DM1 fibroblasts and analyses of that effect on saRNA-mediated *MBNL1* enhancement were performed. GM04033 cells were transfected using 75 nM of siZNF274 (siRNA ON-TARGET SMART POOL - siZNF274_SP) alone or in combination with the saCtrl or saMB1_2 for 120h. Firstly used siZNF274_SP failed to efficiently knock-down *ZNF274*, even upon repeated attempts (Figure 7B). Next, three new siRNAs were used to knock-down *ZNF274* (siZNF274_1-3) in GM04033 cells using 75 nM of each siZNF274 and saCtrl for 120 h. As shown in Figure 7C these siRNAs failed to silence *ZNF274* mRNA (siZNF274_1; siZNF274_si2), while (siZNF274_si3) resulted in *ZNF274* upregulation (~5 fold). To further evaluate transfection efficiency, additional control experiment was performed, using well studied siMBNL1 and aforementioned siRNAs targeting *ZNF274* (siZNF24_1-3). Transfection was carried out in GM04033 cells, using 75 nM of each siRNAs and saCtrl for 48 h. Similarly, no effects of tested siRNAs on *ZNF274* silencing were observed (Figure 7D), in contrast to the *MBNL1* which was successfully knocked down by its corresponding siRNA (~90%) (Figure 7E).

Next, ZNF274 protein level was evaluated, upon RNAi attempts, using western blot analyses. GM04033 cells were transfected with 75 nM of saCtrl or siZNF274 (siZNF274_1-3) for 120 h. However, there was no detectable signal corresponding to the ZNF274 protein even in control samples, whereas loading control (VINCULIN) was clearly detectable (Supplementary Figure 2).

Finally, to analyze changes in binding enrichment of the ZNF274 around saMB1_2 target site, CUT&RUN scanning was performed in GM04033 cells transfected with 75 nM of saCtrl, saMB1_1 or saMB1_2 for 120 h. Hypothetically, in cells transfected with saMB1_2, less enrichment compared to saCtrl or saMB1_1-treated cells would be expected if ZNF274 indeed acted as a transcriptional repressor of *MBNL1*. As a negative control, saMB1_1 was used, because its cognate target region has no binding site for ZNF274. However, no differences in ZNF274 enrichment between saCtrl, saMB1_1 and saMB1_2 were observed (Figure 7F). One should note that, at this time, there was only one commercially available antibody evaluated for ChIP analyses, which we used in this particular experiment. However, not all ChIP-validated antibodies work in CUT&RUN.

Although both ChIP and CUT&RUN assays are used to profile chromatin, there are significant differences between the methodologies that can impact antibody recognition e.g., sample preparation (crosslinking and cell lysis in ChIP vs biding cells to Concanavalin A-coated magnetic beads and permeabilizing the cell membrane with digitonin in CUT&RUN); or chromatin enrichment (*in vitro* immunoprecipitation in ChIP vs *in vivo* enrichment in CUT&RUN, where the antibody enters the nuclei after cell membrane permeabilization). Moreover, when performing the CUT&RUN analysis using ZNF274 antibody, MEIS2 binding - within saMB1_1 target sequence - was evaluated in the same samples in parallel, proving MEIS2 involvement in MBNL1 RNAa (137) and at the same time confirming that CUT&RUN experiment was performed properly.

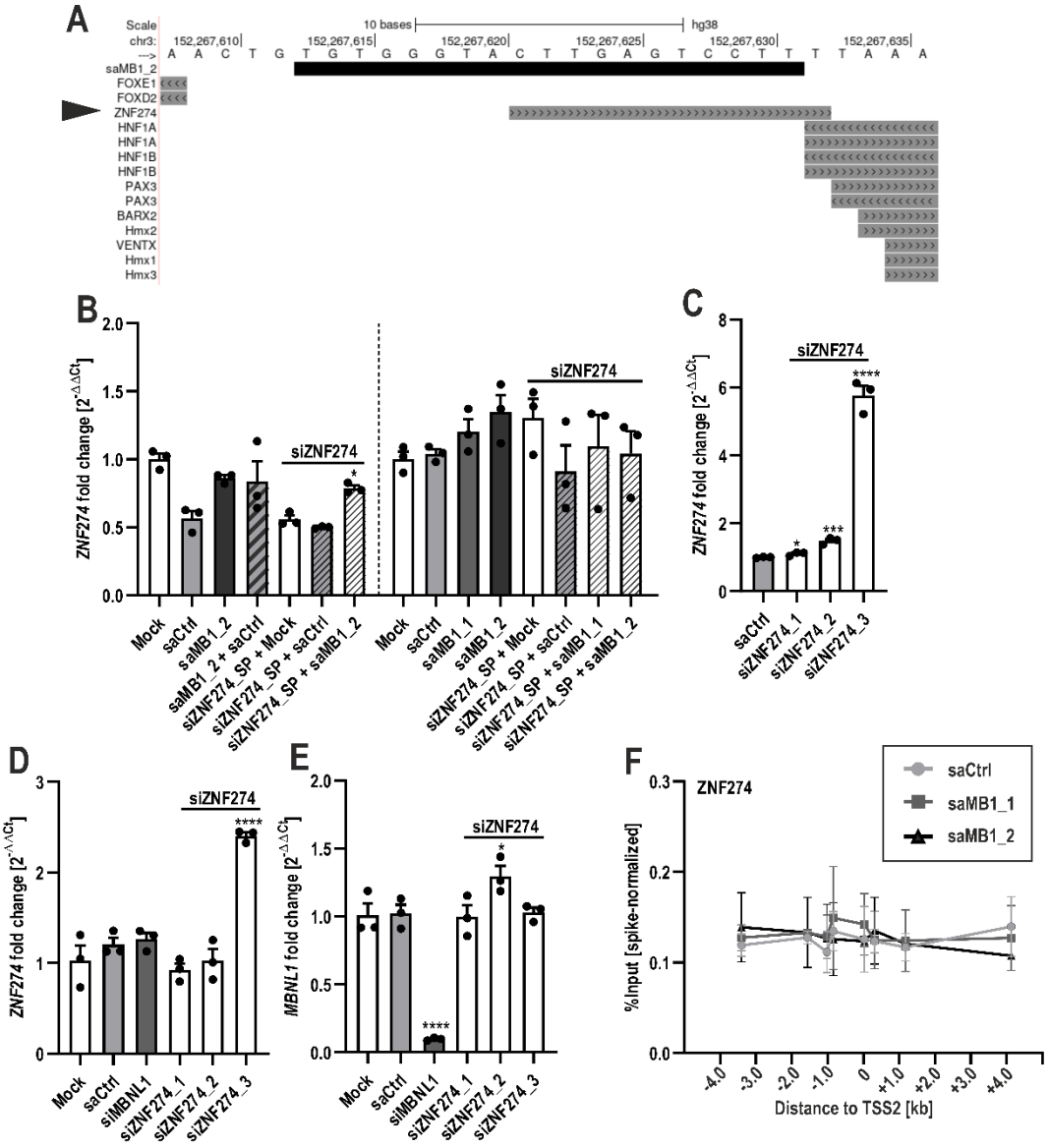

Figure 7.Analyses of potential ZNF274 involvement in MBNL1 RNA activation. (A) UCSC Genome Browser track image showing saMB1_2 target genomic sequence within *MBNL1* promoter 2 region. Predicted ZNF274 binding site overlapping saMB1_2 target site is indicated by black arrow**. (B-E)** RT-qPCR assays of *ZNF274* **(B-D)** or *MBNL1* **(E)** in GM04033 DM1 fibroblasts transfected with indicated siRNA. In **(B)** cells were transfected with lipofectamine (mock) or 75 nM indicated dsRNA (saCtrl, saMB1_1, saMB1_2, siZNF27_SP). After 24 h, indicated samples were subjected to a second transfection with lipofectamine alone (mock) or 75 nM indicated dsRNA (saCtrl, saMB1_1 or saMB1_2) for additional 96 h. **(C)** Cells were transfected with 75 nM saCtrl or indicated siZNF274 (siZNF274_1-3) for 120h. **(D-E)** Cells were transfected with lipofectamine (mock) or 75 nM indicated dsRNA (saCtrl, siMBNL1, siZNF274_1-3) for 48 h. siMBNL1 refers to samples with RNAi-mediated knock-down of *MBNL1*. **(F)** qPCR results of CUT&RUN analyses in GM04033 cells transfected with 75 nM indicated saRNA for 120 h, demonstrating no differences in binding enrichment of ZNF274 to indicated genomic regions (ranging from −3.5 kb to +4.2 kb relative to *MBNL1* TSS2), following transfection of saMB1_1 (orange line), saMB1_2 (blue line) or saCtrl (grey line). Results were normalized using Spike-In DNA and are represented as % of input. Abbreviations: TSS - transcription start site.

RITA complex components were identified and described using *CDKN1A* (p21) as a model gene for RNAa (116), and many of the proteins involved in RNAa, such as AGO2,

histone modifiers (e.g., histone acetyltransferases, methyltransferases), and transcriptional are common RNAa factors across different promoters (115,116,118).

In all, presented data did not allow to conclude whether or not ZNF274 plays important functions in saRNA-mediated *MBNL1* upregulation. Nevertheless, these results are preliminary. Because no silencing of *ZNF274* via RNAi was achieved and no validated CUT&RUN-suitable antibody against ZNF274 was available, these experiments will definitely have to be repeated in the future.. Additional attempts of *ZNF274* silencing should be made to using e.g. another set of siRNAs or GapmeRs. Additionally, ZNF274 mRNA and protein level should be determined, Finally, resented analyses used a candidate approach to find potential transcription factors involved in *MBNL1* expression regulation via RNAa. In future, precise characterization of transcriptional and epigenetic events occurring during *MBNL1* RNAa could be attempted e.g. via RNA-pull down techniques and mass spectrometry analyses.

4.2 Screening of small RNA duplexes targeted to murine *Mbnl1* gene promoter

RNAa is evolutionarily conserved in mammalian organisms, including human and mouse cells, indicating a fundamental role in endogenous gene regulation (128). Described *MBNL1* RNAa is the first therapeutic strategy in which site-specific augmentation of the human endogenous *MBNL1* transcription mitigates DM1-associated AltS defects (137). Therefore, to evaluate potential of RNAa-based therapy in DM1, there is a need to test this approach in a DM1 mouse model. However, it is technically challenging due to lack of promoter sequence conservation between human and mouse.

So far, design of effective saRNAs has largely been a "hit-or-miss process" due to inadequate understanding of the precise molecular mechanism of action (118). To test the feasibility of RNAa approach for site-specific modulation of the endogenous *Mbnl1* expression, analyses were restricted to the most active *Mbnl1* promoter, annotated within the EPDnew mouse version 003 as *Mbnl1_1* and corresponding to human P2 of *MBNL1* (Figure 8A-C). Promoters *Mbnl1_2* and *Mbnl1_3* of *Mbnl1* were excluded from saRNA design, as based on UCSC data sets (Figure 8A) and on meta-analyses performed on data deposited in EPDnew mouse version 003 (Figure 8B-C), the activity of those promoters is lower compared to *Mbnl1_1*, especially in skin. Adult and neonatal skin data was analyzed, because mouse fibroblasts were chosen as a cell model for saRNA screening. Therefore a total of 23 saRNA duplexes were designed, with antisense strands complementary to genomic sequences (+ DNA strand) within *Mbnl1* gene promoter *Mbnl1_1* (Figure 9A).

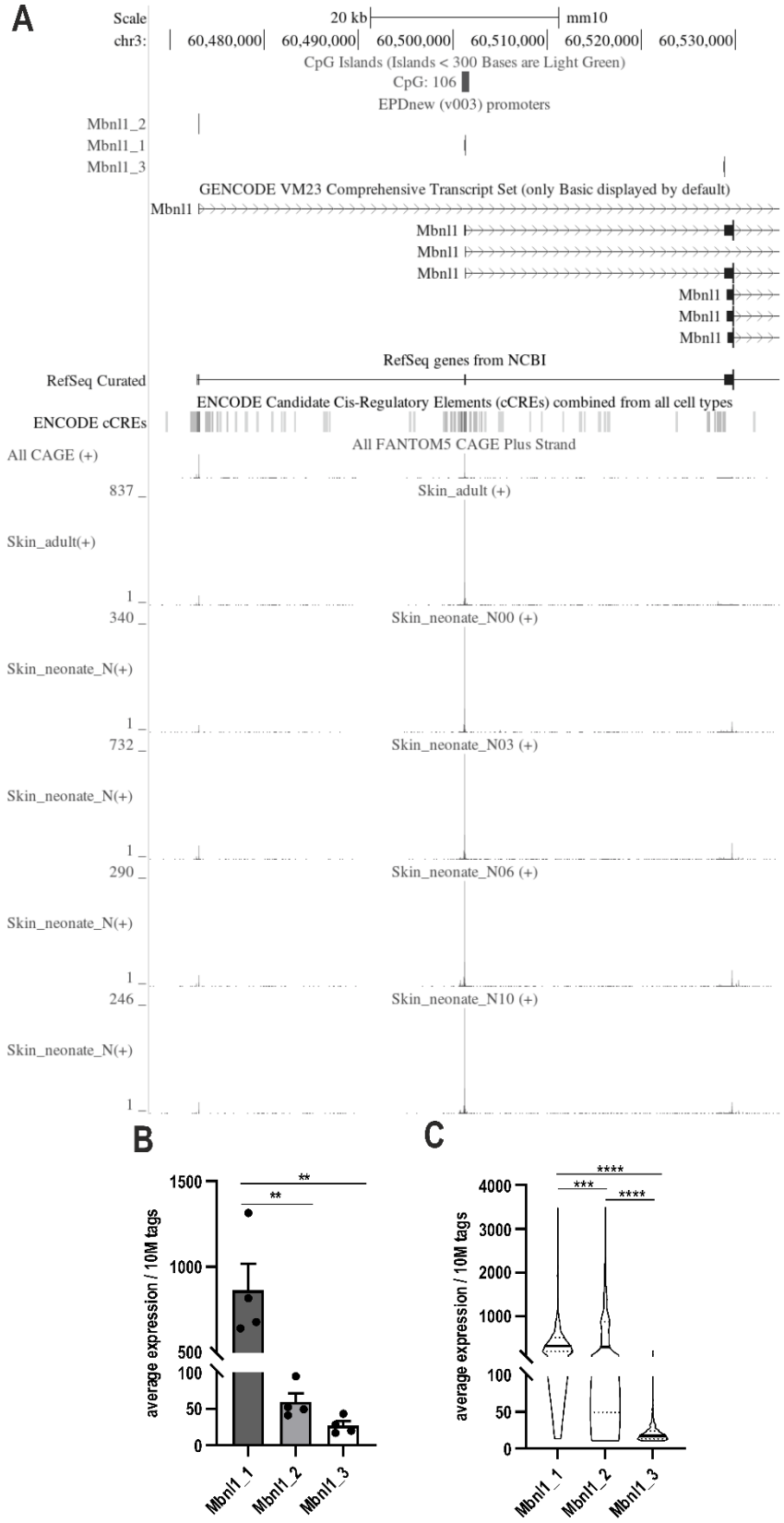

Figure 8. The activity of *Mbnl1* promoters differs in skin neonatal and adult cells. (A) UCSC Genome Browser image of *Mbnl1* gene with track display including Eukaryotic Promoter Database (EPD)new v003 promoters *Mbnl_1*, *Mbnl_2* and *Mbnl1_3*, CpG islands (green), ENCODE candidate Cis-Regulatory Elements (cCREs) and FANTOM 5' end of CAGE reads dataset of mapped transcription start sites (TSS) in adult and neonatal skin. cCREs colors indicate promoter-like signatures (red) and proximal enhancer-like signature

(orange). **(B)** Meta-analysis of promoter-specific *Mbnl1* expression in neonatal skin (n = 4; N0, N03, N06, N10) based on EPDnew v003 data. **(C)** Meta-analysis of the average expression profile of all samples in which indicated *Mbnl1* promoters are active, based on EPDnew v003 data *(Mbnl1_1* n = 696; *Mbnl1_2* n = 519; *Mbnl1_3* n = 238). Average expression represents the number of tags in a 100-bp region centered on the TSS and normalized to 10M total tags. Black lines indicate median: 318.0 tags per 10M for *Mbnl1_1*; 294.0 tags per 10M for *Mbnl1_2*; 17.0 tags per 10M for *Mbnl1_3*, grey dot lines indicate interquartile range (25th to 75th percentiles: 191.3 - 509.0 for *Mbnl1_1*; 49.0 - 868.0 for *Mbnl1_2*; 13.0 - 24.0 for *Mbnl1_3*).

A set of 12 saRNAs were transfected into NIH/3T3 cells for 72 h, at 75 nM, in a 12-well plate format (Figure 9B). Among these, one saRNA targeting2128 base pairs upstream of the EPD annotated TSS resulted in a slightly upregulated *Mbnl1* mRNA expression (~10%). Subsequently, to further evaluate saRNA m_2-2138 effect in two cell lines, NIH/3T3 and MEF WT, transfection was performed for 72 h and 96 h (NIH/3T3), and for 72 h (MEF WT) at 75 nM in 12-well plates. However, results clearly indicated that saRNA m_2-2138 failed to upregulate *Mbnl1* mRNA expression in NIH/3T3 (Figure 9C) and MEF WT (Figure 9D).

To determine whether effective *Mbnl1* upregulation could be obtained by saRNA targeting murine sequence that is similar to human sequence, targeting -1319 bp upstream of *MBNL1* TSS2 by saMB1_2 (137), saRNA targeting -1042 bp upstream of the EPDnew 003 annotated TSS was designed. As no sequence in mouse P2 corresponding to human P2 was identified, a partially homologous sequence was used (human saMB1_2: **AAG**GACT**CAAGT**A**CCC**ACA; mouse sa-1042: TAA**AAG**TTCC**CAAGTCCC**C; bold and underlined nucleotides correspond to similar sequences between both saRNAs). NIH/3T3 cells were transfected with 75 nM of saRNA for 72 h in 6-well and 12-well plates. Regardless of sequence similarity but no TSS distance similarity, between saMB1_2 and saRNA-1042, no *Mbnl1* mRNA upregulation was observed with saRNA-1042 (Figure 9E). Next, despite very poor sequence conservation in *MBNL1* promoter regions between mouse and human, previously identified saRNAs that upregulate human *MBNL1* expression level in DM1 patients' cells (saMB1_1 and saMB1_2) (137) were tested to upregulate murine *Mbnl1*. Both, NIH/3T3 and MEF WT cells were transfected with 75 nM of each saRNA for 72 h in 6-well plates. However, saRNAs upregulating human *MBNL1* expression failed to enhance murine *Mbnl1* mRNA in NIH/3T3 (Figure 9F) and MEF WT cells (Figure 9G).

Subsequently, *Mbnl1* RNAa was evaluated using set of 10 new saRNAs and previously published and validated saRNA targeting murine cyclin b1 (*Ccnb1*), dsCcnb1-597 (128), that served as positive control for RNAa mechanism. NIH/3T3 cells were transfected with aforementioned set of 10 new saRNAs and dsCcnb1-597 at 75 nM for 72 h in 12-well plates. Again, saRNAs did not upregulate *Mbnl1* expression (Figure 9H).

Importantly, dsCcnb1-597 failed to upregulate its target gene expression, *Ccnb1*. (Figure 9I). To exclude low transfection efficiency or technique issues, NIH/3T3 cells were once more transfected with dsCcnb1-597 at 50 nM and 75 nM for 120 h in 6-well plate (transfection conditions were the same as in (128)). However, dsCcnb1-597 failed to upregulate *Ccnb1* mRNA level (Figure 9J). To sum up, screening of 23 saRNAs designed to target *Mbnl1* promoter Mbnl1_1, within the region spanning ~3kb upstream of the transcription start site, failed to identify saRNA that could upregulate *Mbnl1* expression.

The concept of RNAa has emerged as an attractive strategy for therapeutic gene upregulation, with growing evidence demonstrating its evolutionary conservation across mammalian systems, including human and murine cells (128). In particular, the successful application of RNAa to augment *MBNL1* expression in human DM1 patients cells (137) represents a promising therapeutic strategy. Therefore, those results led to the need to explore whether a similar approach could be extended to murine *Mbnl1* for testing RNAa-based therapies in DM1 mouse models. However, presented results indicate significant challenges in adapting RNAa to murine systems, both at the level of *Mbnl1* gene regulation and in terms of validating positive RNAa controls. To maximize the likelihood of identifying effective saRNAs, analyses were restricted to the most active murine *Mbnl1* promoter, *Mbnl1_1*, based on EPDnew mouse 003 database and comparative transcriptomic datasets. This was a rational approach, as targeting weakly active promoters (*Mbnl1_2* and *Mbnl1_3*) would likely reduce the probability of saRNA-mediated *Mbnl1* upregulation. Although one saRNA (m_2-2138) initially showed a modest ~10% induction in *Mbnl1* expression level, this effect was not reproducible across time points, biological replicates, or cell types, suggesting either an artifactual observation or non-specific modulation. Moreover, given the potential of the therapeutic relevance of saRNAs targeting human *MBNL1* (saMB1_1 and saMB1_2) (137), their efficiency were tested against murine *Mbnl1*, but with no effect. These findings strongly indicate that poor promoter sequence conservation between human and mouse represents a critical barrier to use the same saRNAs across species. Notably, while RNAa has been shown to be mechanistically conserved (128,133), promoter and chromatin context are key determinants of RNAa efficiency, whereas they diverge significantly between species. Therefore, presented data highlight an intriguing limitations in implementing human-targeted RNAa strategies into murine systems. The inability to identify an effective murine *Mbnl1*-activating saRNA highlights a major barrier in the preclinical development of RNAa-based therapies for DM1. One possible solution would be the generation of a humanized

mouse model carrying the human *MBNL1* promoter region, which would provide a physiologically relevant context for testing saRNAs validated in patient-derived cells. Interestingly, this approach has been adapted by Ractigen Therapeutics, a pharmaceutical company that developed a Duchenne muscular dystrophy (DMD) program using saRNA to activate *UTRN* (134), a *DMD* paralog.

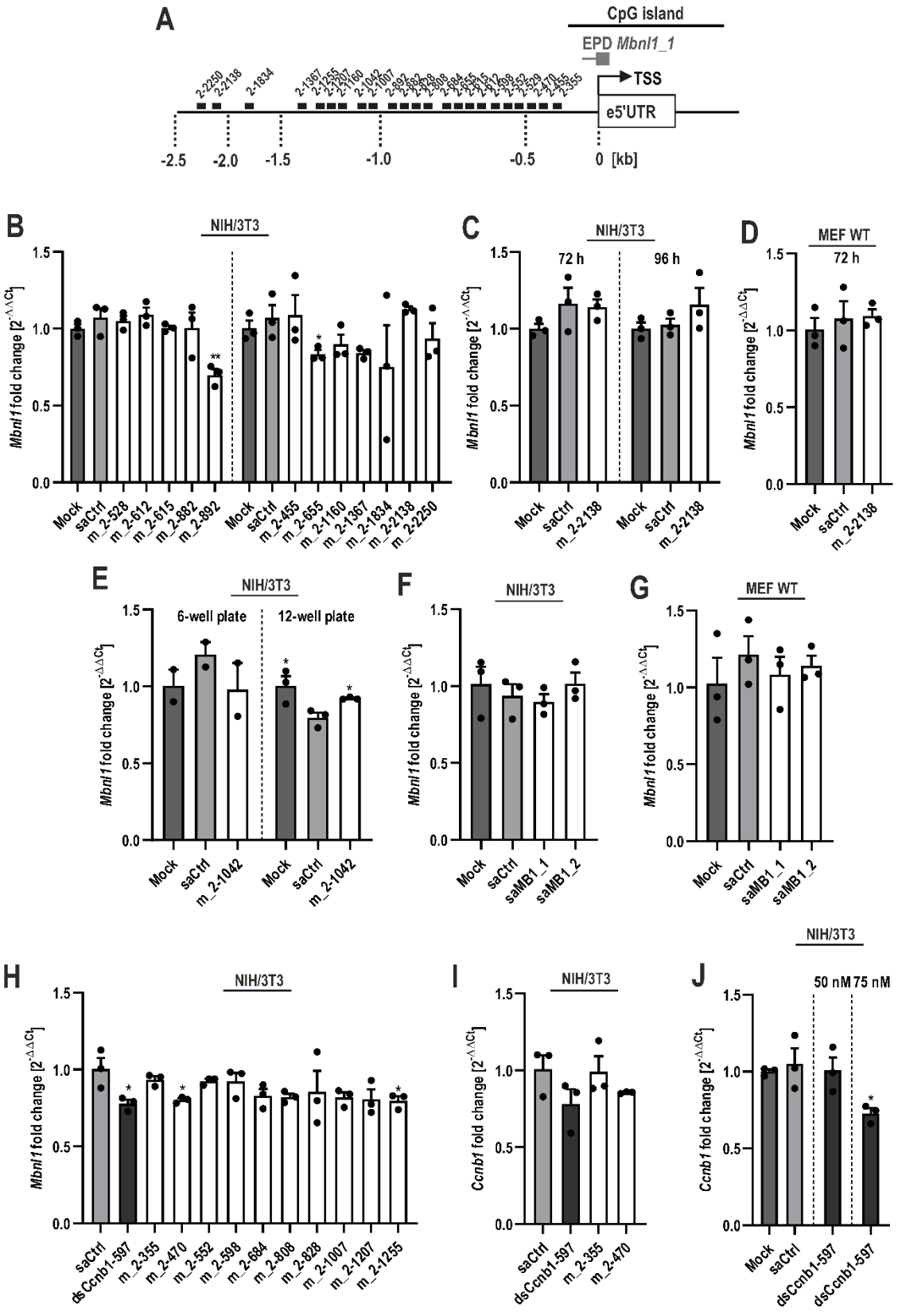

Figure 9. Screening of saRNAs directed at murine *Mbnl1* promoter. **(A)** Schematic representation, not to scale, of *Mbnl1* genomic regions (based on NCBI RefSeq Select and MANE subset: a single representative transcript) spanning *Mbnl1* promoter *Mbnl1_1* (EPD-annotated promoter). Transcription start site (TSS), 5' UTR exon and CpG islands (green line) are indicated. Target sites of saRNAs (black lines) are indicated. **(B-J)** Representative results of saRNAs screening based on RT-qPCR analyses of Mbnl1 **(B-H)** and Ccnb1 **(I-J)** mRNA levels in distinct cell models: NIH/3T3 **(B,C,E,F,H,I,J)** and MEF WT **(D,G)**. The following

experimental conditions were used: 75 nM dsRNA for 72 h **(B,D-I)**, 75 nM dsRNA for 72 h and 96 h **(C)**, 50 nM or 75 nM dsRNA for 120 h **(J)**.

4.3. Material and methods

4.3.1 5´RACE analysis

5´RACE System for Rapid Amplification of cDNA Ends, version 2.0 (Invitrogen) was performed per manufacturers' instructions on mock-treated RNA obtained from GM04033 cells seeded in a 12-well plate for 120 h. In general, rapid amplification of cDNA 5′ ends for *MBNL1* P2 and P3 region included: 1) first strand cDNA synthesis from total RNA using a gene-specific primers 1(GSP1); 2) removal of mRNA template via RNase Mix; 3) purification of cDNA by separation of unincorporated dNTPs, GSP1, and proteins on column; 4) addition of the homopolymeric tail to the 3'-end of the cDNA; 4) PCR amplification accomplished using Taq DNA polymerase, a nested, gene-specific primers 2 (GSP2) and deoxyinosine-containing anchor primer. Final products were analyzed in 2% agarose gel with 10 mg/ml ethidium bromide. The images were captured using G:Box EF2 (Syngene) and analyzed using GeneTools (Syngene). Next, DNA fragment were purified with the QIAquick system (QIAquick Gel Extraction Kit; Qiagen) and sequenced using GSP2 primer in Genomed. Primers sequences are listed in Supplementary Table T5.

4.3.2 Cell lines, culture conditions and transfection

Primary fibroblasts derived from DM1 patients' skin biopsies (cell line GM04033 expressing *DMPK* gene carrying ~1000 CTG repeats) were obtained from the Coriell Cell Repository at the Coriell Institute for Medical Research. GM04033 cells were grown in Eagle's minimal essential medium (EMEM) with stable glutamine (Biowest), supplemented with 10% fetal bovine serum (FBS) (Biowest), 1% antibiotic/antimycotic solution (Sigma-Aldrich/Merck) and 1% non-essential amino acids solution (Sigma-Aldrich/Merck) in 5% CO2 at 37°C. Immortalized fibroblasts derived from mouse embryo (cell line NIH/3T3) were purchased from the ATCC, wild type primary mouse embryonic fibroblast (cell line MEF WT) was a kind gift from / of Prof. Maurice Swanson, and grown in a high-glucose Dulbecco's Modified Eagle Medium (DMEM) (Biowest) with L-glutamine, supplemented with 10% FBS (Biowest) and 1% antibiotic/antimycotic solution (Sigma-Aldrich/Merck) in 5% CO2 at 37°C. For delivery of saRNAs to human and murine fibroblasts, cells were seeded at 6- or 12-well plates at ~50-60% confluency and transfected 24 h post-plating using Lipofectamine RNAiMAX (Invitrogen) per manufacturer's instructions. In all experiments, mock refers to lipofectamine treated cells. Experimental design for all transfections is detailed below..

For AGO1 knock-down analyses, GM04033 DM1 fibroblasts were transfected for 24 h using lipofectamine (mock) or 75 nM of indicated dsRNA (saCtrl, saMB1_1, siAGO1). Next, after 24 h samples transfected with siAGO1 were transfected again with lipofectamine (mock) or 75 nM of saCtrl or saMB1_1, for additional 96 h to obtain a total of 120 h after first transfection.

For ZNF274 knock-down analyses, GM04033 DM1 fibroblasts were transfected for: **(1)** 24 h with lipofectamine (mock) or 75 nM indicated dsRNA (saCtrl, saMB1_1, saMB1_2, siZNF27_SP). After 24 h, samples transfected with siZNF274_SP were transfected again with lipofectamine (mock) or 75 nM of indicated dsRNA (saCtrl, saMB1_1 or saMB1_2) for additional 96 h, to obtain a final time-point of 120 h; **(2)** 120 h with 75 nM indicated dsRNA (saCtrl or siZNF274 (siZNF274_1-3)); **(3)** 48 h with lipofectamine (mock) or 75 nM indicated dsRNA (saCtrl, siMBNL1, siZNF274_1-3).

Screenings of saRNAs targeted to *Mbnl1* were performed as follows: **(1)** NIH/3T3 were transfected for 72 h or 96 h with lipofectamine (mock) or 75 nM indicated dsRNA (saCtrl or saRNA); **(2)** MEF WT were transfected for 72 h with lipofectamine (mock) or 75 indicated dsRNA (saCtrl or saRNA); **(3)** NIH3/T3 were transfected for 120 h with lipofectamine (mock), or 75 nM of saCtrl, or 50 nM or 75 nM of dsCcnb1-597.

4.3.3 Design of saRNA duplexes targeting murine *Mbnl1*

saRNA duplexes used in this study were designed following a validated set of guidelines including: (i) 19-nt target sequence located on a (+) DNA strand, (ii) 40-60% GC content, (iii) lack of repeated or inverted sequences, (iv) lower thermodynamic stability at the 3' end of the saRNA duplex compared to 5' end, (v) avoiding CpG-rich regions within targeted sequence, (vi) avoiding sequences that have 5 or more consecutive nucleotide (117). All saRNAs were designed to target *Mbnl1* promoter *Mbnl1_1* sequences between -200 to -3000 bp upstream of the TSS (based on EPDnew mouse version 003). Potential off-target sequences and saRNAs targeting within single nucleotide polymorphism (SNPs) were excluded using a BLAT search against the UCSC Genome Browser database (GRCm38/mm10). In all experiments, saCtrl was used as control RNA duplex. This duplex lacks homology to any annotated genomic sequence and has been previously validated (112,116,137). Additional saRNA duplex, dsCcnb1 saRNA targeting *Ccnb1* at -597 bp relative to TSS (128), was used as positive control for RNAa studies. saRNA duplexes were synthesized by Sigma-Aldrich/Merck and sequences are listed in Supplementary Table T1.

siRNA targeting *AGO1* (143) and *MBNL1* (144) were previously described and purchased from Sigma-Aldrich/Merck. The ZNF274 Lincode SMARTPool siRNA (pool of 4 pre-designed siRNAs; siZNF274_SP) was purchased from Dharmacon/Horizon Discovery, and other three pre-designed siRNAs targeting *ZNF274* were purchased from Thermo Fisher Scientific (predesigned siRNA 6687, 116534 and 109980; siZNF274_1-3). All siRNA sequences are listed in Supplementary Table T2.

4.3.4 RNA isolation and cDNA synthesis

For RNA isolation, cells were harvested in 500 µl TRIzol Reagent (Thermo Fisher Scientific) or Fenozol reagent (A&A Biotechnology). Total RNA was isolated according to manufacturer's protocol with either Total RNA Zol-Out D (A&A Biotechnology) or MagnifiQ™ 16 Total RNA Plus instant kit (A&A Biotechnology) using Auto-Pure Mini (A&A Biotechnology). The cDNA was synthesized using 200 ng of total RNA and High-Capacity cDNA Reverse Transcription Kit with RNase Inhibitor (Thermo Fisher Scientific) per manufacturer's protocol.

4.3.5 Gene expression analyses

Real-time quantitative reverse transcriptase PCRs (RT-qPCRs) were performed in QuantStudio 6 and 7 Flex System (Applied Biosystems) or CFX Opus 96 Real-Time PCR System (BioRad) using PowerTrack™ SYBR Green Master Mix or PowerUp SYBR Green Master Mix (Applied Biosystems) according to the manufactures' instructions. Cycle threshold (Ct) values of the analyzed target gene were normalized against the reference housekeeping gene *GAPDH/Gapdh* (human/mouse). Targets were amplified with primers at 60°C annealing temperature. RT-qPCR data were analyzed in Microsoft Excel using the $2^{-\Delta\Delta Ct}$ method (145). Primer sequences used for gene expression analyses are listed in Supplementary Table T3.

4.3.6 Western blot

Cell pellets were lysed with 75 µl radioimmunoprecipitation assay (RIPA) buffer (Thermo Fisher Scientific) with 1X Halt Protease Inhibitor Cocktail (Thermo Fisher Scientific), and cleared by centrifugation at 15 000 x g for 15 min at 4◦C. Protein concentration was determined using Pierce BCA Protein Assay Kit (Thermo Fisher Scientific) per manufacturers' protocol. Samples were firstly heated with 4X Laemmli Sample Buffer (Bio-rad) with 2-βmercaptoethanol, then were loaded on an 10% precast polyacrylamide gel (10% Mini-PROTEAN® TGX™ Precast Protein Gels, 15-well, Bio-

Rad) and transferred to a polyvinylidene difluoride (PVDF) membrane (Invitrogen) for 1 h at 100 V at 4°C. Next, membrane was blocked in 5% Skim Milk Powder (Sigma-Aldrich) in 1xTBS-T buffer (Tris-buffered saline, 0.1% Tween 20) for 1h at room temperature. All antibodies were diluted in % Skim Milk Powder in 1xTBS-T. Mouse anti-human ZNF274 primary antibody (4C12; Novus Biologicals) was diluted 1:500, mouse anti-human HRP-conjugated Vinculin antibody (sc-73614; Santa Cruz) was diluted 1:2500 and both were incubated with the membrane O/N at 4°C. The blots were washed 3 × 5 min each in 1xTBS-T and incubated with a secondary rabbit HRP-conjugated anti-mouse antibody (12-349, Millipore), diluted 1:10 000 for 1h at room temperature. Signals were detected using SuperSignal West Femto Maximum Sensitivity Substrate (Thermo Scientific), captured on G:Box Chemi-XR5 (Syngene) and quantified using GeneTools image analysis software (Syngene).

4.3.7 Cleavage under target and release using nuclease (CUT&RUN)

GM04033 cells were seeded in a 6-well plate and transfected with 75 nM of indicated saRNA. After 120 h ~1×105 cells were harvested for each antibody reaction and for input samples. The amount of antibodies used were as follows: 5 µg anti-ZNF274 (4C12; Novus Biologicals) and 2 µg negative control Normal Rabbit IgG (#2729; Cell Signaling). The DNA products were quantified by qPCR using primers designed to amplify genomic regions spanning from -3.5kb downstream to +4.2kb upstream of the relative *MBNL1* TSS2 (Supplementary Table T4). Final results were calculated using the Percent Input Method with the following formula: % Input = 100% x $2^{(C[T]\ 100\%Input\ Sample\ -\ C[T]\ IP\ Sample)}$ and obtained data were plotted as % of input. Results were normalized using Sample Normalization Spike-In DNA.

4.3.8 Statistical analysis

All statistical analysis were based on minimum three independent biological replicates for each experimental group and all experiments were repeated twice. Group data are expressed as mean ± standard error of mean (SEM). For meta-analyses (Figure 8C) the frequency distribution of the data and descriptive statistics (mean, SEM and quartiles: median, 25^{th} and 75^{th} percentile) were performed using GraphPad Prism 8.3.0 software. Statistical analysis were performed relatively to control RNA duplex (saCtrl) (unless otherwise indicated in figure legend) by unpaired, two-tailed Student's t-test using GraphPad

Prism 8.3.0 software with the following criteria for statistical significance: *$p < 0.05$; **$p < 0.01$; ***$p < 0.001$.

4.4 Supplementary material

LIST OF SUPPLEMENTARY FIGURES

LIST OF SUPPLEMENTARY TABLES

4.4.1 Supplementary figures

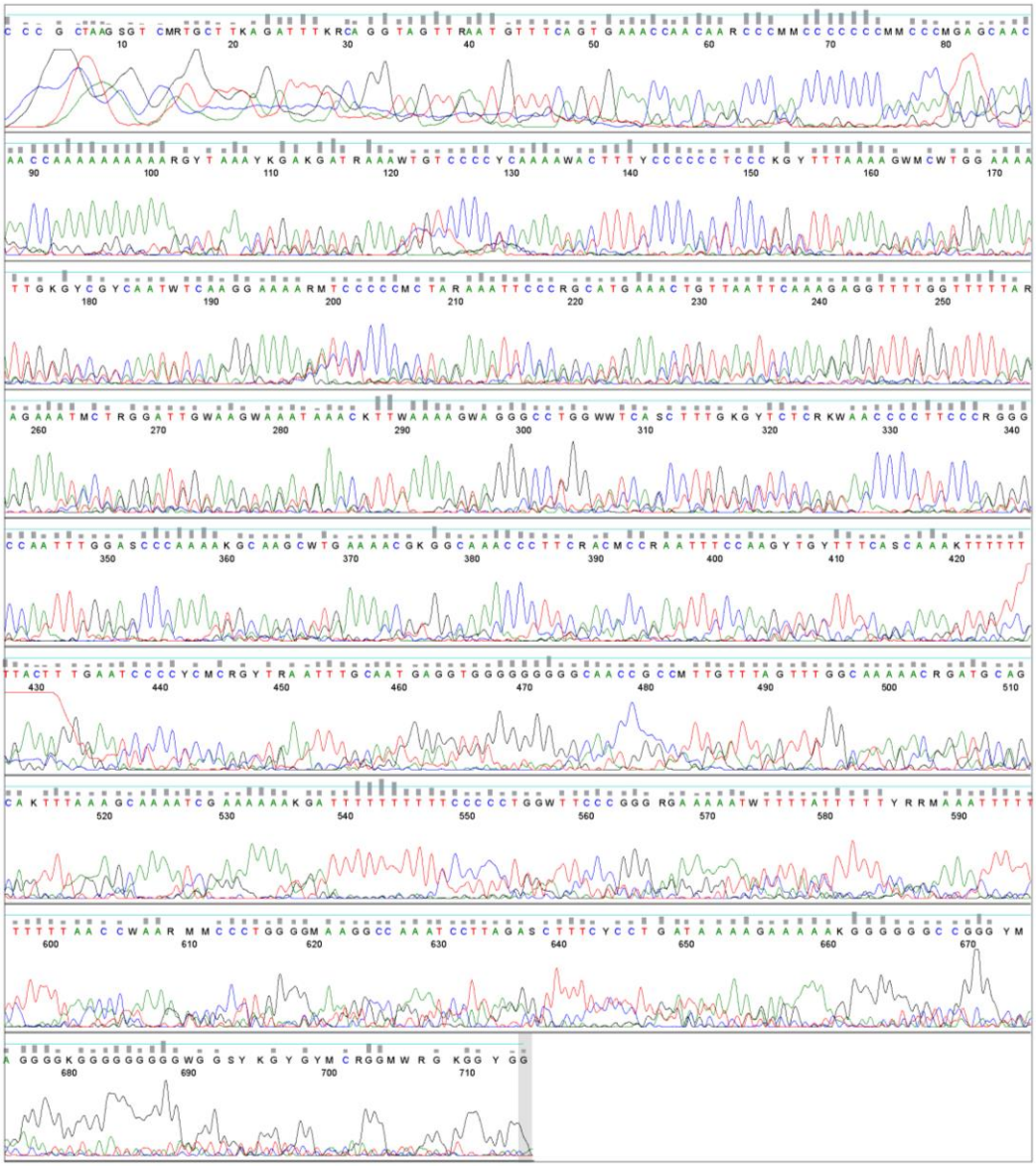

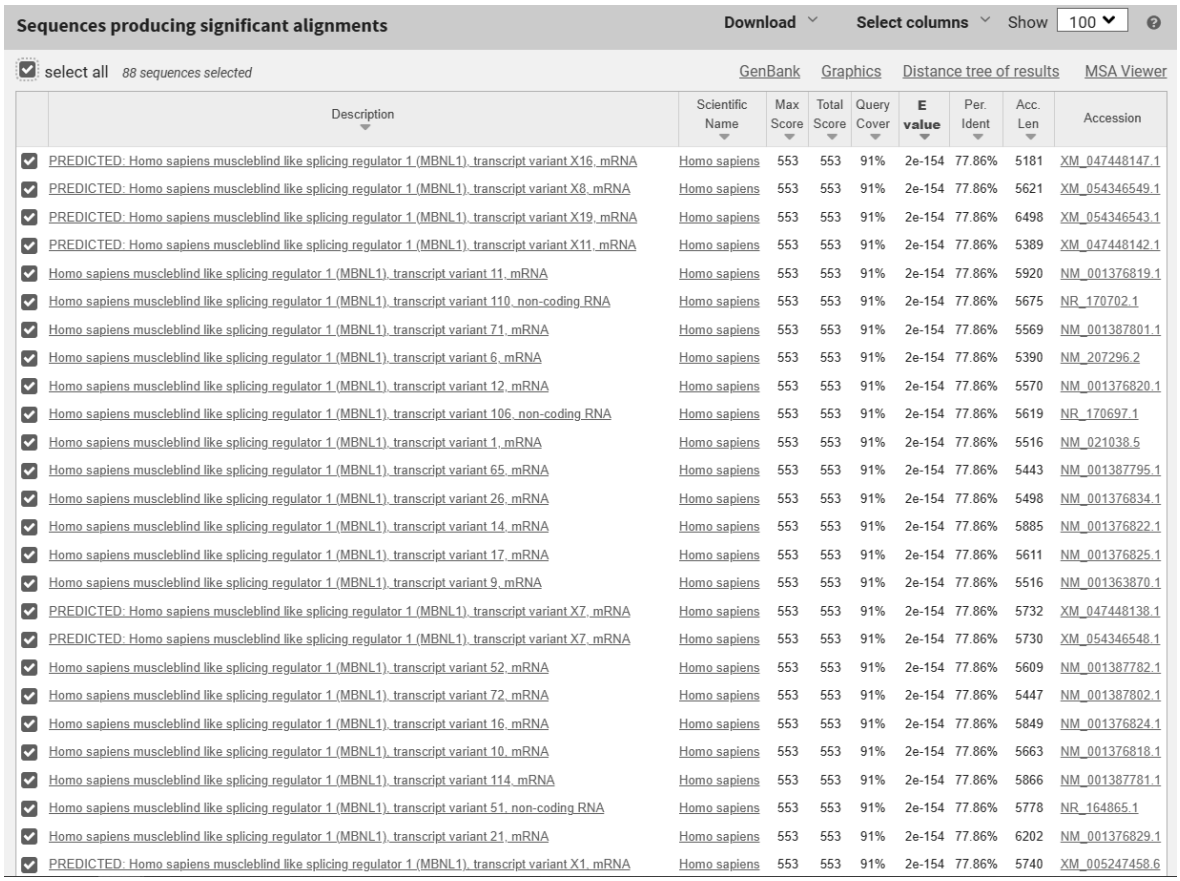

Sequences producing significant alignments Download Select columns Show 100

select all 88 sequences selected GenBank Graphics Distance tree of results MSA Viewer

Description	Scientific Name	Max Score	Total Score	Query Cover	E value	Per. Ident	Acc. Len	Accession
PREDICTED: Homo sapiens muscleblind like splicing regulator 1 (MBNL1), transcript variant X16, mRNA	Homo sapiens	553	553	91%	2e-154	77.86%	5181	XM_047448147.1
PREDICTED: Homo sapiens muscleblind like splicing regulator 1 (MBNL1), transcript variant X8, mRNA	Homo sapiens	553	553	91%	2e-154	77.86%	5621	XM_054346549.1
PREDICTED: Homo sapiens muscleblind like splicing regulator 1 (MBNL1), transcript variant X19, mRNA	Homo sapiens	553	553	91%	2e-154	77.86%	6498	XM_054346543.1
PREDICTED: Homo sapiens muscleblind like splicing regulator 1 (MBNL1), transcript variant X11, mRNA	Homo sapiens	553	553	91%	2e-154	77.86%	5389	XM_047448142.1
Homo sapiens muscleblind like splicing regulator 1 (MBNL1), transcript variant 11, mRNA	Homo sapiens	553	553	91%	2e-154	77.86%	5920	NM_001376819.1
Homo sapiens muscleblind like splicing regulator 1 (MBNL1), transcript variant 110, non-coding RNA	Homo sapiens	553	553	91%	2e-154	77.86%	5675	NR_170702.1
Homo sapiens muscleblind like splicing regulator 1 (MBNL1), transcript variant 71, mRNA	Homo sapiens	553	553	91%	2e-154	77.86%	5569	NM_001387801.1
Homo sapiens muscleblind like splicing regulator 1 (MBNL1), transcript variant 6, mRNA	Homo sapiens	553	553	91%	2e-154	77.86%	5390	NM_207296.2
Homo sapiens muscleblind like splicing regulator 1 (MBNL1), transcript variant 12, mRNA	Homo sapiens	553	553	91%	2e-154	77.86%	5570	NM_001376820.1
Homo sapiens muscleblind like splicing regulator 1 (MBNL1), transcript variant 106, non-coding RNA	Homo sapiens	553	553	91%	2e-154	77.86%	5619	NR_170697.1
Homo sapiens muscleblind like splicing regulator 1 (MBNL1), transcript variant 1, mRNA	Homo sapiens	553	553	91%	2e-154	77.86%	5516	NM_021038.5
Homo sapiens muscleblind like splicing regulator 1 (MBNL1), transcript variant 65, mRNA	Homo sapiens	553	553	91%	2e-154	77.86%	5443	NM_001387795.1
Homo sapiens muscleblind like splicing regulator 1 (MBNL1), transcript variant 26, mRNA	Homo sapiens	553	553	91%	2e-154	77.86%	5498	NM_001376834.1
Homo sapiens muscleblind like splicing regulator 1 (MBNL1), transcript variant 14, mRNA	Homo sapiens	553	553	91%	2e-154	77.86%	5885	NM_001376822.1
Homo sapiens muscleblind like splicing regulator 1 (MBNL1), transcript variant 17, mRNA	Homo sapiens	553	553	91%	2e-154	77.86%	5611	NM_001376825.1
Homo sapiens muscleblind like splicing regulator 1 (MBNL1), transcript variant 9, mRNA	Homo sapiens	553	553	91%	2e-154	77.86%	5516	NM_001363870.1
PREDICTED: Homo sapiens muscleblind like splicing regulator 1 (MBNL1), transcript variant X7, mRNA	Homo sapiens	553	553	91%	2e-154	77.86%	5732	XM_047448138.1
PREDICTED: Homo sapiens muscleblind like splicing regulator 1 (MBNL1), transcript variant X7, mRNA	Homo sapiens	553	553	91%	2e-154	77.86%	5730	XM_054346548.1
Homo sapiens muscleblind like splicing regulator 1 (MBNL1), transcript variant 52, mRNA	Homo sapiens	553	553	91%	2e-154	77.86%	5609	NM_001387782.1
Homo sapiens muscleblind like splicing regulator 1 (MBNL1), transcript variant 72, mRNA	Homo sapiens	553	553	91%	2e-154	77.86%	5447	NM_001387802.1
Homo sapiens muscleblind like splicing regulator 1 (MBNL1), transcript variant 16, mRNA	Homo sapiens	553	553	91%	2e-154	77.86%	5849	NM_001376824.1
Homo sapiens muscleblind like splicing regulator 1 (MBNL1), transcript variant 10, mRNA	Homo sapiens	553	553	91%	2e-154	77.86%	5663	NM_001376818.1
Homo sapiens muscleblind like splicing regulator 1 (MBNL1), transcript variant 114, mRNA	Homo sapiens	553	553	91%	2e-154	77.86%	5866	NM_001387781.1
Homo sapiens muscleblind like splicing regulator 1 (MBNL1), transcript variant 51, non-coding RNA	Homo sapiens	553	553	91%	2e-154	77.86%	5778	NR_164865.1
Homo sapiens muscleblind like splicing regulator 1 (MBNL1), transcript variant 21, mRNA	Homo sapiens	553	553	91%	2e-154	77.86%	6202	NM_001376829.1
PREDICTED: Homo sapiens muscleblind like splicing regulator 1 (MBNL1), transcript variant X1, mRNA	Homo sapiens	553	553	91%	2e-154	77.86%	5740	XM_005247458.6

TSS1 transcripts:

NM_001376819.1 Homo sapiens muscleblind like splicing regulator 1 (MBNL1), transcript variant 11, mRNA

NM_001387801.1 Homo sapiens muscleblind like splicing regulator 1 (MBNL1), transcript variant 71, mRNA

NM_001387781.1 Homo sapiens muscleblind like splicing regulator 1 (MBNL1), transcript variant 114, mRNA

TSS2 transcripts:

NM_207296.2 Homo sapiens muscleblind like splicing regulator 1 (MBNL1), transcript variant 6, mRNA

NM_001376820.1 Homo sapiens muscleblind like splicing regulator 1 (MBNL1), transcript variant 12, mRNA

NM_021038.5 Homo sapiens muscleblind like splicing regulator 1 (MBNL1), transcript variant 1, mRNA

NM_001376822.1 Homo sapiens muscleblind like splicing regulator 1 (MBNL1), transcript variant 14, mRNA

NM_001387782.1 Homo sapiens muscleblind like splicing regulator 1 (MBNL1), transcript variant 52, mRNA

NM_001376824.1 Homo sapiens muscleblind like splicing regulator 1 (MBNL1), transcript variant 16, mRNA

NM_001376818.1 Homo sapiens muscleblind like splicing regulator 1 (MBNL1), transcript variant 10, mRNA

NM_001376829.1 Homo sapiens muscleblind like splicing regulator 1 (MBNL1), transcript variant 21, mRNA

TTS3 transcripts:

NM_001387795.1 Homo sapiens muscleblind like splicing regulator 1 (MBNL1), transcript variant 65, mRNA

NM_001376834.1 Homo sapiens muscleblind like splicing regulator 1 (MBNL1), transcript variant 26, mRNA

NM_001376825.1 Homo sapiens muscleblind like splicing regulator 1 (MBNL1), transcript variant 17, mRNA

NM_001363870.1 Homo sapiens muscleblind like splicing regulator 1 (MBNL1), transcript variant 9, mRNA

Supplementary Figure 1. Upper panel: sequencing results of an Exon 1 5´RACE PCR product using mock-treated RNA obtained from DM1 patients' fibroblasts (GM04033), visualized in FinchTV. **Lower panel:** representative BLAST NCBI results of sequence showed in upper panel, with description of each identified *MBNL1* transcript variant. TSS- transcription start site.

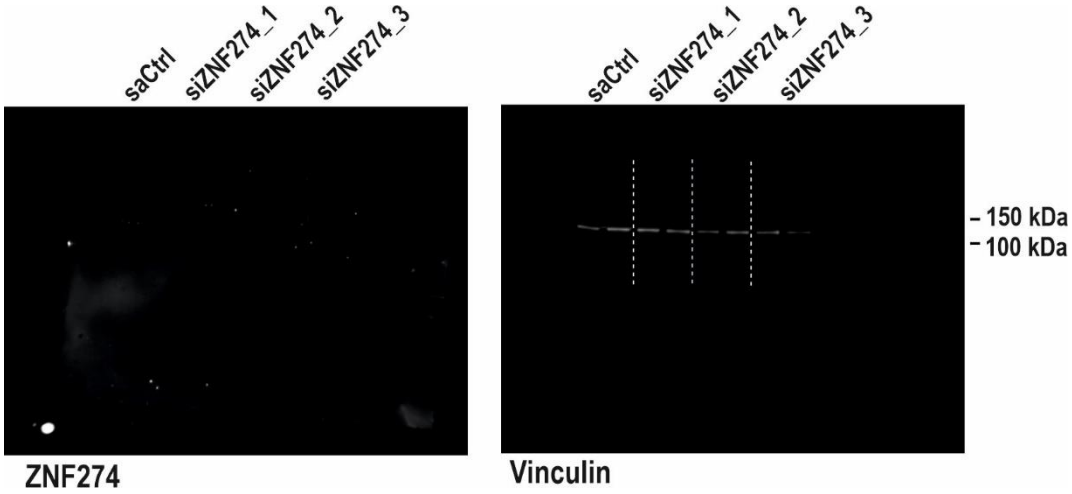

Supplementary Figure 2. Unadjusted and uncropped western blot images corresponding to results described in Chapter 4.1.3. Distinct sample types are described and separated by dotted lines. Each lane represents an individual biological sample.

4.4.2 Supplementary tables

Supplementary Table 1. Sequences of human and mouse saRNAs, and control saRNA duplexes.

saRNA	**Position of cognate target site relative to human TSS2**	**Sequence (5' - 3') of sense (S) and antisense (AS) strands of saRNA duplex**
2-882 (saMB1_1)	-882	**S:** UAGCACCCAGUGAAUUAUG [dT][dT] **AS:**CAUAAUUCACUGGGUGCUA [dT][dT]
2-1319 (saMB1_2)	-1319	**S:** UGUGGGUACUUGAGUCCUU [dT][dT] **AS:** AAGGACUCAAGUACCCACA [dT][dT]
saRNA	**Position of cognate target site relative to murine TSS**	**Sequence (5' - 3') of sense (S) and antisense (AS) strands of saRNA duplex**
m_2-355	-355	**S:** CCAAAACUGUGAGUGCUGA [dT][dT] **AS:** UCAGCACUCACAGUUUUGG[dT][dT]
m_2-455	-455	**S:** GGAAGUAAGGGAGCCUUUA[dT][dT] **AS:** UAAAGGCUCCCUUACUUCC[dT][dT]
m_2-470	-470	**S:** CCACACUGCAGAGUUGGAA [dT][dT] **AS:** UUCCAACUCUGCAGUGUGG[dT][dT]
m_2-529	-529	**S:**UGCAGCGCCUAAGAUGUUA[dT][dT] **AS:**UAACAUCUUAGGCGCUGCA[dT][dT]
m_2-552	-552	**S:** GCUUGUUUGCGUGGGAGUA [dT][dT] **AS:** UACUCCCACGCAAACAAGC [dT][dT]
m_2-598	-598	**S:** AACUAGGAGCUGGUGUUUC [dT][dT] **AS:** GAAACACCAGCUCCUAGUU[dT][dT]

m_2-612	-612	**S:** GACAGCAGCUAAUGAACUA[dT][dT] **AS:**UAGUUCAUUAGCUGCUGUC[dT][dT]
m_2-615	-615	**S:** CAGGACAGCAGCUAAUGAA [dT][dT] **AS:**UUCAUUAGCUGCUGUCCUG[dT][dT]
m_2-655	-655	**S:** UCUCAGAAGCCCAGAAUUC[dT][dT] **AS:**GAAUUCUGGGCUUCUGAGA[dT][dT]
m_2-684	-684	**S:** CCGUCCGCAGAUCUUCAAA [dT][dT] **AS:**UUUGAAGAUCUGCGGACGG[dT][dT]
m_2-808	-808	**S:** GAGGGAGAAAUCCAGUUUG [dT][dT] **AS:** CAAACUGGAUUUCUCCCUC[dT][dT]
m_2-828	-828	**S:** ACCCACUCAACAGAAACAG [dT][dT] **AS:**CUGUUUCUGUUGAGUGGGU[dT][dT]
m_2-882	-882	**S:** GGAGUACUUUAUUUAUUUA[dT][dT] **AS:**UAAAUAAAUAAAGUACUCC[dT][dT]
m_2-892	-892	**S:** GCAAACUAGUGGAGUACUU[dT][dT] **AS:**AAGUACUCCACUAGUUUGC[dT][dT]
m_2-1007	-1007	**S:** ACACUGAGAAGUGGUACUA [dT][dT] **AS:** UAGUACCACUUCUCAGUGU[dT][dT]
m_2-1042	-1042	**S:** GGGGACUUGGGAACUUUUA [dT][dT] **AS:** UAAAAGUUCCCAAGUCCCC[dT][dT]
m_2-1160	-1160	**S:** AUCCAGUUGCUGGAAUGAA [dT][dT] **AS:**UUCAUUCCAGCAACUGGAU[dT][dT]
m_2-1207	-1207	**S:** ACCUCCAUCCUACCUAUAC [dT][dT] **AS:**GUAUAGGUAGGAUGGAGGU[dT][dT]
m_2-1255	-1255	**S:** CAUGCUGCUCCAAAAAGUA [dT][dT]

		AS:UACUUUUUGGAGCAGCAUG[dT][dT]
m_2-1367	-1367	**S:** UCAAGGCGCUGCUUGCAUA [dT][dT] **AS:**UAUGCAAGCAGCGCCUUGA[dT][dT]
m_2-1834	-1834	**S:** CUUCCUUCUCUGCCGACAA [dT][dT] **AS:**UUGUCGGCAGAGAAGGAAG[dT][dT]
m_2-2138	-2138	**S:** CCAGAGCUCUUUGAUAGAA [dT][dT] **AS:**UUCUAUCAAAGAGCUCUGG[dT][dT]
m_2-2250	-2250	**S:** GGUCUGAGUGCAACUGUAA [dT][dT] **AS:** UUACAGUUGCACUCAGACC[dT][dT]
control saRNA	**Additional information**	**Sequence (5' - 3')**
saCtrl	non-targeting control	**S:** ACUACUGAGUGACAGUAGA [dT][dT] **AS:**UCUACUGUCACUCAGUAGU [dT][dT]
dsCcnb1-597	saRNA targeting *Ccnb1* at -597 bp rel. to TSS (128)	**S:** AGAGAAACCCUGUCCGA A [dT][dT] **AS:** UUCGAGACAGGGUUUCUCU[dT][dT]

Supplementary Table 2. siRNA sequences.

siRNA name	**Sequence (5' - 3')**
siAGO1	**S:** GAGAAGAGGUGCUCAAGAA [dT][dT] **AS:** UUCUUGAGCACCUCUUCUC [dT][dT]
siZNF274_SP (Lincode SMARTPool)	**AS:** GGACAUGGUGGAAUCGCA **AS:** CCACAAUAGGACAAAGCGA **AS:** GUACUAAACAGAUUACGUU

	AS: CGACACAGAGGACCGAGUA
siZNF274_1 (predesigned siRNA 6687; Thermo Fisher Scientific)	**S:** GGUUGUUGAGGUCCUCACA [dT][dT] **AS:** UGUGAGGACCUCAACAACC [dT][dT]
siZNF274_2 (predesigned siRNA 116534; Thermo Fisher Scientific)	**S:** GCCUGAAAGUACAAGAAUC [dT][dT] **AS:** GAUUCUUGUACUUUCAGGC [dT][dT]
siZNF274_3 (predesigned siRNA 109980; Thermo Fisher Scientific)	**S:** GGAAGGCAAUGGUUGUAGG [dT][dT] **AS:** CCUACAACCAUUGCCUUCC [dT][dT]
siMBNL1	**S:** CACUGGAAGUAUGUAGAGA [dT][dT] **AS:** UCUCUACAUACUUCCAGUG [dT][dT]

Supplementary Table 3. Expression primers for RT-qPCR.

Transcript name	**Primers Sequence (5' - 3')**
AGO1	GCGAATTGGGAAGAGTGGTA GCAGGTGCTGGGATAGAGAC
MBNL1	CTGCCGAACATCTGACTAGC TTGTGTGTGTTGCTTGACGA
MBNL2	CCAAGGGCAGGTTCGATTCT AAGCTGGATGAAGTCTGGCA
DMPK	CACTGTCGGACATTCGGGAAGGTGC GCTTGCACGTGTGGCTCAAGCAGCTG
ZNF274	CACAGAGGACCGAGTACCG

	TTTCCAGTGTAGTCTCCCACC
GAPDH	TGAAGGTCGGAGTCAACGGA GATGACAAGCTTCCCGTTCTC
Mbnl1	ACTGTCGGTTTGCTCATCCT CAGCCTGGTTGACCTGGTAT
Gapdh	CACGCACCATCCTATTCCTT CCCCTCTTCTCACTTCAACG
Ccnb1	CTCCCTGCTTCCTGTTATGC TTCGACAACTTCCGTTAGCC

Supplementary Table 4. CUT&RUN primers for qPCR.

PCR product name (position of PCR product relative to TSS2 of *MBNL1*)	**Primers Sequence (5' - 3')**
MBNL1 (+4058;+4132)	CGTGGGGAGGTTAGCTAGTT ACAGACTCAAGATGGCACCA
MBNL1 (+1104;+1177)	CCTCGCACAGCACTTTACAA GCCCCAGAGAGCCTTAAGAA
MBNL1 (+231;+310)	GAAGGAGGAAGTGCGAGGAG CGAAACCAACTACCGCGAG
MBNL1 (-14;+28)	GCGATAAGAGGCTGCACAG CCACAACTCATTCAGCTGCA

MBNL1 (-912; -841)	CCATTCAAAGCAAAGCCAAGT CAAATAAACCGCAGCCCCAT
MBNL1 (-1097; -1022)	TCAACAAAACCGAACCTGCA CGTTTGTCCCATGTTTGTTGG
MBNL1 (-1655; -1565)	CACCTTTCAAGGCACCAGTT TGTATGTGGGAAGCAATCCA
MBNL1 (-3465; -3403)	GCTATGAATGTGGTATGCAGAAG GTAAGTGTGTGAGTGCCTGTG

Supplementary Table 5. Primers for 5´RACE.

Transcript name (primer name)	**Primers Sequence (5' - 3')**
MBNL1 exon 1 GSP1 (MBNL1_e1_GSP1)	ACTTGGCAGCTTTTCGAAGG
MBNL1 exon 1 GSP2 (MBNL1_e1_GSP2)	AGCCATTTTGTGTCCCGAAT
MBNL1 exon 2 GSP1 (MBNL1_e2_GSP1)	ACGGGTTGTAATGGGGCACC
MBNL1 exon 2 GSP2 (MBNL1_e2_GSP2)	CATTTGCTGGGCCAACATG

V. CONCLUDING REMARKS

The main aim of this PhD thesis was to determine the feasibility of a RNAa, that is a conserved cellular mechanism of gene activation, in therapeutic site-specific upregulation of the endogenous *MBNL1* gene. Identified saRNA duplexes, saMB1_1 and saMB1_2, targeted to the most active promoter of *MBNL1,* P2, led to increase in MBNL1 pre-mRNA, mRNA and protein level *in cellulo*. Moreover, presented data demonstrated that saRNA-mediated *MBNL1* increase results from transcriptional stimulation of *MBNL1* promoter 2. Therefore, cellular pool of MBNL1 protein increased and mitigated the alternative splicing defects of multiple MBNL1 target pre-mRNAs. These results offer brand new perspectives in DM1 therapeutic options as well as in future studies on *MBNL* expression regulation.

Importantly, presented data highlighted the importance of promoter selection in RNAa, as only P2 promoter was susceptible to RNAa. Those results corroborate a superior activity of *MBNL1* P2 over P3, in agreement with previous studies (36,39). Additionally, chromatin/DNA accessibility and distance from the TSS, may determine susceptibility of each promoter region top RNAa. *MBNL1* P3 is less active than P2, and for this reason may be less accessible for RNAa machinery.

In particular, saRNA-mediated *MBNL1* upregulation has been shown to occur at the transcriptional level, as increase in nascent *MBNL1* mRNA and enrichment of RNAPII occupancy at saRNA-targeted promoter 2 regions were detected. What is more, presented data confirmed that both lead saRNA duplexes require key RITA complex components (AGO2, RHA and CTR9) to upregulate *MBNL1* expression. On the other hand, those results could not verify AGO1 contribution in RNAa, described in literature as a minor component in RNAa pathway (112,141). Another aim concerned transcription factors that may associate with RITA-complex in *MBNL1* RNAa. Two TFs harboring binding sites within were verified, MEIS1 and MEIS2, that stimulated only saMB1_1-mediated *MBNL1* upregulation. However, another tested transcription factor, ZNF274, whose binding site overlaps with saMB1_2 targeting sequence, had no effect on MBNL1 RNA. Therefore, future studies, e.g. pull-down with chemically modified saRNA and proteomic analyses, will need to identify and verify factors recruiting to RITA complex during saRNA-mediated *MBNL1* upregulation.

Chemical modifications of saRNA strands revealed that identified molecules target DNA via an on-site mechanism. Firstly, it was demonstrated that the AS strand serves as the

guide/leading strand and targets complementary DNA sequences within the *MBNL1* promoter 2, whereas the S strand has minimal impact on RNAa. Moreover, potential requirement of lncRNA *MBNL1-AS1* for RNAa at *MBNL1* promoter 2 was analyzed. Despite data from several studies suggesting that saRNAs may bind natural lncRNAs or antisense transcripts overlapping targeted promoter regions of indicated genes (121), presented data ruled out involvement of lncRNA *MNBL1-AS1* in saRNA-mediated *MBNL1* upregulation.

Interestingly, both identified saRNA duplexes downregulate lncRNA *MBNL1-AS1*, but only when the S strand was active. Moreover, lncRNA *MBNL1-AS1* downregulation occurred upon transfection of saRNAs that failed to upregulate *MBNL1* but target sequences overlapping *MBNL1-AS1*. Therefore, it is plausible that the S strand of saRNA duplex directly interacts with antisense transcript as it was describe in RNA:RNA model (118), hence leading to its degradation or sequestration via unknown mechanisms. Additionally, RNAi mechanism is also not involved in *MBNL1-AS1* downregulation, as it has not been prevented due to AGO2 knockdown. On the other hand, saRNA-mediated assembly of the transcriptional complex at *MBNL1* promoter 2 could interfere with the antisense transcription. Upon saRNA delivery nascent *MBNL1-AS1* analysis revealed downregulation of antisense transcript, and actinomycin-D treatment significantly reduced level of *MBNL1-AS1*, thus pointing out possible interference in antisense transcription by *MBNL1* RNAa complex. Perhaps, saRNA-mediated lncRNA *MBNL1-AS1* downregulation results from the overlapping action of both mechanisms, via RNA:RNA base pairing and affecting antisense transcription.

In view of the fact that RNAa is evolutionarily conserved mechanism in mammalian cells (128), I made an attempt to upregulate murine *Mbnl1* expression in mouse cell models. However, after screening of numerous saRNAs targeting *Mbnl1* promoter, I cannot identify saRNA duplexes capable of *Mbnl1* modulation. One should note that design and identification of saRNAs that could enhance *Mbnl1* expression is limited due to lack of adequate DM1 mouse models caused by lack of conservation in promoter sequences between human and mouse. Therefore, one possibility is to develop a humanized *Mbnl1* mouse DM1 model, with murine promoter swapped for a human one to test identified saRNA duplexes, saMB1_1 and saMB1_2, rather than design murine saRNAs. This approach will enable to test the feasibility of MBNL1 RNAa *in vitro* and *in vivo* using well described human saRNA duplexes.

In conclusion, saRNA-mediated *MBNL1* upregulation resulted in site-specific enhancing of its transcription that led to increase of MBNL1 protein content and correction of DM1-associated defects in alternative splicing of MBNL1 target pre-mRNAs. The two lead duplexes identified within the framework of this PhD project stimulated *MBNL1* transcription via AGO2-mediated loading of the antisense strand onto target sequence within *MBNL1* promoter 2. Importantly, obtained results highlight the mechanistic aspects of *MBNL1* RNAa, such as recruitment of RNAPII with canonical RNAa pathway proteins, and specific transcription factors. Furthermore, a variety of molecular and biochemical approaches used in these experiments provided detailed insights in to the role of the lncRNA *MBNL1-AS1* in *MBNL1* RNAa.

Summary of conclusions:

1. The feasibility of RNAa to upregulate the major paralog of the *MBNL* family, *MBNL1*, in DM1 cell models was precisely described using variety of molecular and biochemical approaches.

2. Presented data emphasized the importance of promoter selection in RNAa in the context of saRNA-mediated *MBNL1* upregulation.

3. Molecular mechanism underlying *MBNL1* RNAa was extensively investigated and the conclusions drawn from this are as follows:

a. saRNA-mediated *MBNL1* upregulation occurs at the transcriptional level.

b. MEIS1 and MEIS2 transcription factors positively regulate MBNL1 RNAa.

c. RITA complex facilitates *MBNL1* upregulation during saRNA-mediated RNAa.

d. Antisense strand of the saRNA duplex is loaded onto AGO2 as the guide strand

e. lncRNA *MBNL1-AS1* is dispensable for saRNA-mediated *MBNL1* expression upregulation.

f. Sense strand of the saRNA duplex controls downregulation of lncRNA *MBNL1-AS1*.

4. saRNA-mediated *MBNL1* upregulation led to correction of alternative splicing of multiple *MBNL1* target pre-mRNAs in DM1 cell models.

5. *MBNL1* RNAa did not lead to increase in CUG^{exp} foci number or size in DM1 patients' fibroblasts.

6. *Mbnl1* RNAa is not feasible with herein designed saRNAs, in currently tested murine cell models.

VI. REFERENCES

1. Sznajder ŁJ, Swanson MS. Short Tandem Repeat Expansions and RNA-Mediated Pathogenesis in Myotonic Dystrophy. Int J Mol Sci. 2019;20(13):3365.

2. Ellerby LM. Repeat Expansion Disorders: Mechanisms and Therapeutics. Neurotherapeutics. 2019;16(4):924–7.

3. Paulson H. Repeat expansion diseases. Handb Clin Neurol. 2018;147:105–23.

4. Depienne C, Mandel JL. 30 years of repeat expansion disorders: What have we learned and what are the remaining challenges? Am J Hum Genet. 2021;108(5):764–85.

5. Thornton CA. Myotonic Dystrophy. Neurol Clin. 2014;32(3):705–19.

6. Brook JD, McCurrach ME, Harley HG, Buckler AJ, Church D, Aburatani H, i in. Molecular basis of myotonic dystrophy: expansion of a trinucleotide (CTG) repeat at the 3' end of a transcript encoding a protein kinase family member. Cell. 1992;68(4):799–808.

7. Mahadevan M, Tsilfidis C, Sabourin L, Shutler G, Amemiya C, Jansen G, i in. Myotonic dystrophy mutation: an unstable CTG repeat in the 3' untranslated region of the gene. Science. 1992;255(5049):1253–5.

8. Miller JW, Urbinati CR, Teng-Umnuay P, Stenberg MG, Byrne BJ, Thornton CA, *et al*. Recruitment of human muscleblind proteins to (CUG)(n) expansions associated with myotonic dystrophy. EMBO J. 2000;19(17):4439–48.

9. Groh WJ, Groh MR, Saha C, Kincaid JC, Simmons Z, Ciafaloni E, *et al*. Electrocardiographic abnormalities and sudden death in myotonic dystrophy type 1. N Engl J Med. 2008;358(25):2688–97.

10. Redman JB, Fenwick RG, Fu YH, Pizzuti A, Caskey CT. Relationship between parental trinucleotide GCT repeat length and severity of myotonic dystrophy in offspring. JAMA. 1993;269(15):1960–5.

11. Liquori CL, Ricker K, Moseley ML, Jacobsen JF, Kress W, Naylor SL, *et al*. Myotonic dystrophy type 2 caused by a CCTG expansion in intron 1 of ZNF9. Science. 2001;293(5531):864–7.

12. Day JW, Ricker K, Jacobsen JF, Rasmussen LJ, Dick KA, Kress W, *et al*. Myotonic dystrophy type 2: molecular, diagnostic and clinical spectrum. Neurology. 2003;60(4):657–64.

13. Meola G. Myotonic dystrophy type 2: the 2020 update. Acta Myol. 2020;39(4):222–34.

14. Fardaei M, Rogers MT, Thorpe HM, Larkin K, Hamshere MG, Harper PS, *et al*. Three proteins, MBNL, MBLL and MBXL, co-localize in vivo with nuclear foci of expanded-repeat transcripts in DM1 and DM2 cells. Hum Mol Genet. 2002;11(7):805–14.

15. Pascual M, Vicente M, Monferrer L, Artero R. The Muscleblind family of proteins: an emerging class of regulators of developmentally programmed alternative splicing. Differ Res Biol Divers. 2006;74(2–3):65–80.

16. Wang ET, Cody NAL, Jog S, Biancolella M, Wang TT, Treacy DJ, *et al*. Transcriptome-wide Regulation of Pre-mRNA Splicing and mRNA Localization by Muscleblind Proteins. Cell. 2012;150(4):710–24.

17. Batra R, Charizanis K, Manchanda M, Mohan A, Li M, Finn DJ, *et al*. Loss of MBNL leads to disruption of developmentally regulated alternative polyadenylation in RNA-mediated disease. Mol Cell. 2014;56(2):311–22.

18. Masuda A, Andersen HS, Doktor TK, Okamoto T, Ito M, Andresen BS, *et al*. CUGBP1 and MBNL1 preferentially bind to 3' UTRs and facilitate mRNA decay. Sci Rep. 2012;2:209.

19. Rau F, Freyermuth F, Fugier C, Villemin JP, Fischer MC, Jost B, *et al* Misregulation of miR-1 processing is associated with heart defects in myotonic dystrophy. Nat Struct Mol Biol. 2011;18(7):840–5.

20. Begemann G, Paricio N, Artero R, Kiss I, Pérez-Alonso M, Mlodzik M. muscleblind, a gene required for photoreceptor differentiation in Drosophila, encodes novel nuclear Cys3His-type zinc-finger-containing proteins. Development. 1997;124(21):4321-31.

21. Sasagawa N, Ohno E, Kino Y, Watanabe Y, Ishiura S. Identification of Caenorhabditis elegans K02H8.1 (CeMBL), a functional ortholog of mammalian MBNL proteins. J Neurosci Res. 2009;87(5):1090–7.

22. Liu YF, Liu HY, Tu LC, Lin CW, Hsiao KM, Pan H. Zebrafish muscleblind-like genes: Identification, structural features and expression. Comp Biochem Physiol B Biochem Mol Biol. 2008;151(1):118–24.

23. Kanadia RN, Urbinati CR, Crusselle VJ, Luo D, Lee YJ, Harrison JK, *et al*. Developmental expression of mouse muscleblind genes *Mbnl1*, *Mbnl2* and *Mbnl3*. Gene Expr Patterns. 2003;3(4):459–62.

24. Squillace RM, Chenault DM, Wang EH. Inhibition of muscle differentiation by the novel muscleblind-related protein CHCR. Dev Biol. 2002;250(1):218–30.

25. Goers ES, Purcell J, Voelker RB, Gates DP, Berglund JA. MBNL1 binds GC motifs embedded in pyrimidines to regulate alternative splicing. Nucleic Acids Res. 2010;38(7):2467–84.

26. Kalsotra A, Xiao X, Ward AJ, Castle JC, Johnson JM, Burge CB, *et al*. A postnatal switch of CELF and MBNL proteins reprograms alternative splicing in the developing heart. Proc Natl Acad Sci U S A. 2008;105(51):20333–8.

27. Han H, Irimia M, Ross PJ, Sung HK, Alipanahi B, David L, *et al* MBNL proteins repress ES-cell-specific alternative splicing and reprogramming. Nature. 2013;498(7453):241–5.

28. Konieczny P, Stepniak-Konieczna E, Sobczak K. MBNL proteins and their target RNAs, interaction and splicing regulation. Nucleic Acids Res. 2014;42(17):10873–87.

29. Lin X, Miller JW, Mankodi A, Kanadia RN, Yuan Y, Moxley RT, *et al*. Failure of MBNL1-dependent post-natal splicing transitions in myotonic dystrophy. Hum Mol Genet. 2006;15(13):2087–97.

30. Charizanis K, Lee KY, Batra R, Goodwin M, Zhang C, Yuan Y, *et al*. Muscleblind-Like 2 Mediated Alternative Splicing in the Developing Brain and Dysregulation in Myotonic Dystrophy. Neuron. 2012;75(3):437.

31. Spruce T, Plass M, Gohr A, Ray D, Martínez de Lagrán M, Rot G, *et al*. The X-linked splicing regulator MBNL3 has been co-opted to restrict placental growth in eutherians. PLoS Biol. 2022;20(4):e3001615.

32. Poulos MG, Batra R, Li M, Yuan Y, Zhang C, Darnell RB, *et al*. Progressive impairment of muscle regeneration in muscleblind-like 3 isoform knockout mice. Hum Mol Genet. 2013;22(17):3547–58.

33. Lee KY, Li M, Manchanda M, Batra R, Charizanis K, Mohan A, *et al*. Compound loss of muscleblind-like function in myotonic dystrophy. EMBO Mol Med. 2013;5(12):1887–900.

34. Dixon DM, Choi J, El-Ghazali A, Park SY, Roos KP, Jordan MC, *et al*. Loss of muscleblind-like 1 results in cardiac pathology and persistence of embryonic splice isoforms. Sci Rep. 2015;5:9042.

35. Kanadia RN, Johnstone KA, Mankodi A, Lungu C, Thornton CA, Esson D, *et al*. A muscleblind knockout model for myotonic dystrophy. Science. 2003;302(5652):1978–80.

36. Konieczny P, Stepniak-Konieczna E, Sobczak K. MBNL expression in autoregulatory feedback loops. RNA Biol. 2017;15(1):1–8.

37. Nitschke L, Hu RC, Miller AN, Lucas L, Cooper TA. Alternative splicing mediates the compensatory upregulation of MBNL2 upon MBNL1 loss-of-function. Nucleic Acids Res. 2023;51(3):1245–59.

38. Sta Maria NS, Zhou C, Lee SJ, Valiulahi P, Li X, Choi J, *et al*. Mbnl1 and Mbnl2 regulate brain structural integrity in mice. Commun Biol. 2021;4(1):1342.

39. Konieczny P, Stepniak-Konieczna E, Taylor K, Sznajder ŁJ, Sobczak K. Autoregulation of MBNL1 function by exon 1 exclusion from MBNL1 transcript. Nucleic Acids Res. 2017;45(4):1760–75.

40. Napierala M, Krzyzosiak WJ. CUG Repeats Present in Myotonin Kinase RNA Form Metastable “Slippery” Hairpins*. J Biol Chem. 1997;272(49):31079–85.

41. Davis BM, McCurrach ME, Taneja KL, Singer RH, Housman DE. Expansion of a CUG trinucleotide repeat in the 3’ untranslated region of myotonic dystrophy protein kinase transcripts results in nuclear retention of transcripts. Proc Natl Acad Sci U S A. 1997;94(14):7388–93.

42. Mankodi A, Urbinati CR, Yuan QP, Moxley RT, Sansone V, Krym M, *et al*. Muscleblind localizes to nuclear foci of aberrant RNA in myotonic dystrophy types 1 and 2. Hum Mol Genet. 2001;10(19):2165–70.

43. Yuan Y, Compton SA, Sobczak K, Stenberg MG, Thornton CA, Griffith JD, *et al*. Muscleblind-like 1 interacts with RNA hairpins in splicing target and pathogenic RNAs. Nucleic Acids Res. 2007;35(16):5474–86.

44. Philips AV, Timchenko LT, Cooper TA. Disruption of splicing regulated by a CUG-binding protein in myotonic dystrophy. Science. 1998;280(5364):737–41.

45. Kuyumcu-Martinez NM, Wang GS, Cooper TA. Increased steady state levels of CUGBP1 in Myotonic Dystrophy 1 are due to PKC-mediated hyper-phosphorylation. Mol Cell. 2007;28(1):68.

46. Jones K, Jin B, Iakova P, Huichalaf C, Sarkar P, Schneider-Gold C, *et al*. RNA Foci, CUGBP1, and ZNF9 Are the Primary Targets of the Mutant CUG and CCUG Repeats Expanded in Myotonic Dystrophies Type 1 and Type 2. Am J Pathol. 2011;179(5):2475.

47. Ho TH, Savkur RS, Poulos MG, Mancini MA, Swanson MS, Cooper TA. Colocalization of muscleblind with RNA foci is separable from mis-regulation of alternative splicing in myotonic dystrophy. J Cell Sci. 2005;118(Pt 13):2923–33.

48. Michalowski S, Miller JW, Urbinati CR, Paliouras M, Swanson MS, Griffith J. Visualization of double-stranded RNAs from the myotonic dystrophy protein kinase gene and interactions with CUG-binding protein. Nucleic Acids Res.1999;27(17):3534–42.

49. Lee JE, Cooper TA. Pathogenic mechanisms of myotonic dystrophy. Biochem Soc Trans. 2009;37(0 6):10.1042/BST0371281.

50. Ozimski LL, Sabater-Arcis M, Bargiela A, Artero R. The hallmarks of myotonic dystrophy type 1 muscle dysfunction. Biol Rev. 2021;96(2):716–30.

51. Charlet-B N, Savkur RS, Singh G, Philips AV, Grice EA, Cooper TA. Loss of the muscle-specific chloride channel in type 1 myotonic dystrophy due to misregulated alternative splicing. Mol Cell. 2002;10(1):45–53.

52. Lueck JD, Mankodi A, Swanson MS, Thornton CA, Dirksen RT. Muscle chloride channel dysfunction in two mouse models of myotonic dystrophy. J Gen Physiol. 2007;129(1):79–94.

53. Nakamori M, Sobczak K, Puwanant A, Welle S, Eichinger K, Pandya S, *et al*. Splicing biomarkers of disease severity in myotonic dystrophy. Ann Neurol. 2013;74(6):862–72.

54. Fugier C, Klein AF, Hammer C, Vassilopoulos S, Ivarsson Y, Toussaint A, *et al*. Misregulated alternative splicing of BIN1 is associated with T tubule alterations and muscle weakness in myotonic dystrophy. Nat Med. 2011;17(6):720–5.

55. Buj-Bello A, Furling D, Tronchère H, Laporte J, Lerouge T, Butler-Browne GS, *et al*. Muscle-specific alternative splicing of myotubularin-related 1 gene is impaired in DM1 muscle cells. Hum Mol Genet. 2002;11(19):2297–307.

56. Bosè F, Renna LV, Fossati B, Arpa G, Labate V, Milani V, *et al*. TNNT2 Missplicing in Skeletal Muscle as a Cardiac Biomarker in Myotonic Dystrophy Type 1 but Not in Myotonic Dystrophy Type 2. Front Neurol. 2019;10:992.

57. Freyermuth F, Rau F, Kokunai Y, Linke T, Sellier C, Nakamori M, *et al*. Splicing misregulation of SCN5A contributes to cardiac-conduction delay and heart arrhythmia in myotonic dystrophy. Nat Commun. 2016;7:11067.

58. Savkur RS, Philips AV, Cooper TA. Aberrant regulation of insulin receptor alternative splicing is associated with insulin resistance in myotonic dystrophy. Nat Genet. 2001;29(1):40–7.

59. Jiang H, Mankodi A, Swanson MS, Moxley RT, Thornton CA. Myotonic dystrophy type 1 is associated with nuclear foci of mutant RNA, sequestration of muscleblind proteins and deregulated alternative splicing in neurons. Hum Mol Genet. 2004;13(24):3079–88.

60. Goodwin M, Mohan A, Batra R, Lee KY, Charizanis K, Gómez FJF, *et al*. MBNL Sequestration by Toxic RNAs and RNA Mis-Processing in the Myotonic Dystrophy Brain. Cell Rep. 2015;12(7):1159–68.

61. Weber YG, Roebling R, Kassubek J, Hoffmann S, Rosenbohm A, Wolf M, *et al*. Comparative analysis of brain structure, metabolism, and cognition in myotonic dystrophy 1 and 2. Neurology. 2010;74(14):1108–17.

62. Sznajder ŁJ, Khan M, Ciesiołka A, Tadross M, Nutter CA, Taylor K, *et al*. Autism-related traits in myotonic dystrophy type 1 model mice are due to MBNL sequestration and RNA mis-splicing of autism-risk genes. Nat Neurosci. 2025;28(6):1199–212.

63. Souidi A, Nakamori M, Zmojdzian M, Jagla T, Renaud Y, Jagla K. Deregulations of miR-1 and its target Multiplexin promote dilated cardiomyopathy associated with myotonic dystrophy type 1. EMBO Rep. 2023;24(4):e56616.

64. Piasecka A, Szcześniak MW, Sekrecki M, Kajdasz A, Sznajder ŁJ, Baud A, *et al*. MBNL splicing factors regulate the microtranscriptome of skeletal muscles. Nucleic Acids Res. 2024;52(19):12055–73.

65. Thomas JD, Sznajder ŁJ, Bardhi O, Aslam FN, Anastasiadis ZP, Scotti MM, *et al*. Disrupted prenatal RNA processing and myogenesis in congenital myotonic dystrophy. Genes Dev 2017;31(11):1122-1133.

66. Fardaei M, Larkin K, Brook JD, Hamshere MG. In vivo co-localisation of MBNL protein with DMPK expanded-repeat transcripts. Nucleic Acids Res. 2001;29(13):2766–71.

67. Ketley A, Chen CZ, Li X, Arya S, Robinson TE, Granados-Riveron J, *et al*. High-content screening identifies small molecules that remove nuclear foci, affect MBNL distribution and CELF1 protein levels via a PKC-independent pathway in myotonic dystrophy cell lines. Hum Mol Genet. 2014;23(6):1551–62.

68. Gu X, Richman J, Langfelder P, Wang N, Zhang S, Bañez-Coronel M, *et al*. Uninterrupted CAG repeat drives striatum-selective transcriptionopathy and nuclear pathogenesis in human Huntingtin BAC mice. Neuron. 2022;110(7):1173-1192.e7.

69. Li LB, Yu Z, Teng X, Bonini NM. RNA toxicity is a component of ataxin-3 degeneration in Drosophila. Nature. 2008;453(7198):1107–11.

70. Casci I, Krishnamurthy K, Kour S, Tripathy V, Ramesh N, Anderson EN, *et al*. Muscleblind acts as a modifier of FUS toxicity by modulating stress granule dynamics and SMN localization. Nat Commun. 2019;10:5583.

71. Izzo M, Battistini J, Provenzano C, Martelli F, Cardinali B, Falcone G. Molecular Therapies for Myotonic Dystrophy Type 1: From Small Drugs to Gene Editing. Int J Mol Sci. 2022;23(9):4622.

72. Pascual-Gilabert M, López-Castel A, Artero R. Myotonic dystrophy type 1 drug development: A pipeline toward the market. Drug Discov Today. 2021;26(7):1765–72.

73. Gomes-Pereira M, Monckton DG. Chemically induced increases and decreases in the rate of expansion of a CAG·CTG triplet repeat. Nucleic Acids Res. 2004;32(9):2865–72.

74. Reddy K, Jenquin JR, McConnell OL, Cleary JD, Richardson JI, Pinto BS, *et al*. A CTG repeat-selective chemical screen identifies microtubule inhibitors as selective modulators of toxic CUG RNA levels. Proc Natl Acad Sci U S A. 2019;116(42):20991–1000.

75. Lee JE, Bennett CF, Cooper TA. RNase H-mediated degradation of toxic RNA in myotonic dystrophy type 1. Proc Natl Acad Sci U S A. 2012;109(11):4221–6.

76. Sobczak K, Wheeler TM, Wang W, Thornton CA. RNA Interference Targeting CUG Repeats in a Mouse Model of Myotonic Dystrophy. Mol Ther. 2013;21(2):380–7.

77. Wheeler TM, Sobczak K, Lueck JD, Osborne RJ, Lin X, Dirksen RT, *et al*. Reversal of RNA-dominance by displacement of protein sequestered on triplet repeat RNA. Science. 2009;325(5938):336–9.

78. Nakamori M, Gourdon G, Thornton CA. Stabilization of Expanded (CTG)•(CAG) Repeats by Antisense Oligonucleotides. Mol Ther. 2011;19(12):2222–7.

79. García-López A, Llamusí B, Orzáez M, Pérez-Payá E, Artero RD. In vivo discovery of a peptide that prevents CUG–RNA hairpin formation and reverses RNA toxicity in myotonic dystrophy models. Proc Natl Acad Sci U S A. 2011;108(29):11866–71.

80. Nakamori M, Taylor K, Mochizuki H, Sobczak K, Takahashi MP. Oral administration of erythromycin decreases RNA toxicity in myotonic dystrophy. Ann Clin Transl Neurol. 2015;3(1):42–54.

81. Chen G, Masuda A, Konishi H, Ohkawara B, Ito M, Kinoshita M, *et al*. Phenylbutazone induces expression of MBNL1 and suppresses formation of MBNL1-CUG RNA foci in a mouse model of myotonic dystrophy. Sci Rep. 2016;6:25317.

82. Bargiela A, Sabater-Arcis M, Espinosa-Espinosa J, Zulaica M, Lopez de Munain A, Artero R. Increased Muscleblind levels by chloroquine treatment improve myotonic dystrophy type 1 phenotypes in in vitro and in vivo models. Proc Natl Acad Sci U S A. 2019;116(50):25203–13.

83. Kanadia RN, Shin J, Yuan Y, Beattie SG, Wheeler TM, Thornton CA, *et al*. Reversal of RNA missplicing and myotonia after muscleblind overexpression in a mouse poly(CUG) model for myotonic dystrophy. Proc Natl Acad Sci U S A. 2006;103(31):11748–53.

84. Cerro-Herreros E, Sabater-Arcis M, Fernandez-Costa JM, Moreno N, Perez-Alonso M, Llamusi B, *et al*. miR-23b and miR-218 silencing increase Muscleblind-like expression and alleviate myotonic dystrophy phenotypes in mammalian models. Nat Commun. 2018;9:2482.

85. Overby SJ, Cerro-Herreros E, Espinosa-Espinosa J, González-Martínez I, Moreno N, Fernández-Costa JM, *et al*. BlockmiR AONs as Site-Specific Therapeutic MBNL Modulation in Myotonic Dystrophy 2D and 3D Muscle Cells and HSALR Mice. Pharmaceutics. 2023;15(4):1118.

86. Wojciechowska M, Taylor K, Sobczak K, Napierala M, Krzyzosiak WJ. Small molecule kinase inhibitors alleviate different molecular features of myotonic dystrophy type 1. RNA Biol. 2014;11(6):742–54.

87. Jones K, Wei C, Iakova P, Bugiardini E, Schneider-Gold C, Meola G, *et al*. GSK3β mediates muscle pathology in myotonic dystrophy. J Clin Invest. 2012;122(12):4461–72.

88. Brockhoff M, Rion N, Chojnowska K, Wiktorowicz T, Eickhorst C, Erne B, *et al*. Targeting deregulated AMPK/mTORC1 pathways improves muscle function in myotonic dystrophy type I. J Clin Invest. 2017;127(2):549–63.

89. Hashem VI, Sinden RR. Chemotherapeutically induced deletion of expanded triplet repeats. Mutat Res Mol Mech Mutagen. 2002;508(1):107–19.

90. Coonrod LA, Nakamori M, Wang W, Carrell S, Hilton CL, Bodner MJ, *et al*. Reducing levels of toxic RNA with small molecules. ACS Chem Biol. 2013;8(11):2528–37.

91. Mittelman D, Moye C, Morton J, Sykoudis K, Lin Y, Carroll D, *et al*. Zinc-finger directed double-strand breaks within CAG repeat tracts promote repeat instability in human cells. Proc Natl Acad Sci U S A. 2009;106(24):9607–12.

92. Xia G, Gao Y, Jin S, Subramony SH, Terada N, Ranum LPW, *et al*. Genome Modification Leads to Phenotype Reversal in Human Myotonic Dystrophy type 1 iPS-cell Derived Neural Stem Cells. Stem Cells Dayt Ohio. 2015;33(6):1829–38.

93. Cinesi C, Aeschbach L, Yang B, Dion V. Contracting CAG/CTG repeats using the CRISPR-Cas9 nickase. Nat Commun. 2016;7:13272.

94. Dastidar S, Ardui S, Singh K, Majumdar D, Nair N, Fu Y, *et al*. Efficient CRISPR/Cas9-mediated editing of trinucleotide repeat expansion in myotonic dystrophy patient-derived iPS and myogenic cells. Nucleic Acids Res. 2018;46(16):8275–98.

95. François V, Klein AF, Beley C, Jollet A, Lemercier C, Garcia L, *et al*. Selective silencing of mutated mRNAs in DM1 by using modified hU7-snRNAs. Nat Struct Mol Biol. 2011;18(1):85–7.

96. Klein AF, Varela MA, Arandel L, Holland A, Naouar N, Arzumanov A, *et al*. Peptide-conjugated oligonucleotides evoke long-lasting myotonic dystrophy correction in patient-derived cells and mice. J Clin Invest. 2019;129(11):4739–44.

97. Wojtkowiak-Szlachcic A, Taylor K, Stepniak-Konieczna E, Sznajder LJ, Mykowska A, Sroka J, *et al*. Short antisense-locked nucleic acids (all-LNAs) correct alternative splicing abnormalities in myotonic dystrophy. Nucleic Acids Res. 2015;43(6):3318–31.

98. Pandey SK, Wheeler TM, Justice SL, Kim A, Younis HS, Gattis D, *et al*. Identification and Characterization of Modified Antisense Oligonucleotides Targeting DMPK in Mice and Nonhuman Primates for the Treatment of Myotonic Dystrophy Type 1. J Pharmacol Exp Ther. 2015;355(2):329–40.

99. Jauvin D, Chrétien J, Pandey SK, Martineau L, Revillod L, Bassez G, *et al*. Targeting DMPK with Antisense Oligonucleotide Improves Muscle Strength in Myotonic Dystrophy Type 1 Mice. Mol Ther Nucleic Acids. 2017;7:465–74.

100. Bisset DR, Stepniak-Konieczna EA, Zavaljevski M, Wei J, Carter GT, Weiss MD, *et al*. Therapeutic impact of systemic AAV-mediated RNA interference in a mouse model of myotonic dystrophy. Hum Mol Genet. 2015;24(17):4971–83.

101. Thornton C, Moxley R, Day J, Ashizawa T, Barohn R, Leung D, *et al*. Study Design of a Phase 1/2a Trial with ISIS-DMPKRx for the Treatment of Myotonic Dystrophy Type 1 (P3.167). Neurology. 2016;86:P3.167.

102. Thornton CA, Moxley RT, Eichinger K, Heatwole C, Mignon L, Arnold WD, *et al*. Antisense oligonucleotide targeting DMPK in patients with myotonic dystrophy type 1: a multicentre, randomised, dose-escalation, placebo-controlled, phase 1/2a trial. Lancet Neurol. 2023;22(3):218–28.

103. Angelbello AJ, González ÀL, Rzuczek SG, Disney MD. Development of Pharmacophore Models for Small Molecules Targeting RNA: Application to the RNA Repeat Expansion in Myotonic Dystrophy Type 1. Bioorg Med Chem Lett. 2016;26(23):5792–6.

104. Childs-Disney JL, Parkesh R, Nakamori M, Thornton CA, Disney MD. Rational Design of Bioactive, Modularly Assembled Aminoglycosides Targeting the RNA that Causes Myotonic Dystrophy Type 1. ACS Chem Biol. 2012;7(12):1984–93.

105. Warf MB, Nakamori M, Matthys CM, Thornton CA, Berglund JA. Pentamidine reverses the splicing defects associated with myotonic dystrophy. Proc Natl Acad Sci U S A. 2009;106(44):18551–6.

106. Chamberlain CM, Ranum LPW. Mouse model of muscleblind-like 1 overexpression: skeletal muscle effects and therapeutic promise. Hum Mol Genet. 2012;21(21):4645–54.

107. Davis J, Salomonis N, Ghearing N, Lin SCJ, Kwong JQ, Mohan A, *et al*. MBNL1-mediated regulation of differentiation RNAs promotes myofibroblast transformation and the fibrotic response. Nat Commun. 2015;6:10084.

108. Cerro-Herreros E, Fernandez-Costa JM, Sabater-Arcis M, Llamusi B, Artero R. Derepressing muscleblind expression by miRNA sponges ameliorates myotonic dystrophy-like phenotypes in Drosophila. Sci Rep. 2012;6(1):36230.

109. Overby SJ, Cerro-Herreros E, González-Martínez I, Varela MA, Seoane-Miraz D, Jad Y, *et al*. Proof of concept of peptide-linked blockmiR-induced MBNL functional rescue in myotonic dystrophy type 1 mouse model. Mol Ther Nucleic Acids. 2022;27:1146–55.

110. Zhang F, Bodycombe NE, Haskell KM, Sun YL, Wang ET, Morris CA, *et al*. A flow cytometry-based screen identifies MBNL1 modulators that rescue splicing defects in myotonic dystrophy type I. Hum Mol Genet. 2017;26(16):3056–68.

111. Pascual-Gilabert M, Artero R, López-Castel A. The myotonic dystrophy type 1 drug development pipeline: 2022 edition. Drug Discov Today. 2023;28(3):103489.

112. Li LC, Okino ST, Zhao H, Pookot D, Place RF, Urakami S, *et al*. Small dsRNAs induce transcriptional activation in human cells. Proc Natl Acad Sci. 2006;103(46):17337–42.

113. Janowski BA, Younger ST, Hardy DB, Ram R, Huffman KE, Corey DR. Activating gene expression in mammalian cells with promoter-targeted duplex RNAs. Nat Chem Biol. 2007;3(3):166–73.

114. Meng X, Jiang Q, Chang N, Wang X, Liu C, Xiong J, *et al*. Small activating RNA binds to the genomic target site in a seed-region-dependent manner. Nucleic Acids Res. 2016;44(5):2274–82.

115. Voutila J, Reebye V, Roberts TC, Protopapa P, Andrikakou P, Blakey DC, *et al*. Development and Mechanism of Small Activating RNA Targeting CEBPA, a Novel Therapeutic in Clinical Trials for Liver Cancer. Mol Ther. 2017;25(12):2705–14.

116. Portnoy V, Lin SHS, Li KH, Burlingame A, Hu ZH, Li H, *et al*. saRNA-guided Ago2 targets the RITA complex to promoters to stimulate transcription. Cell Res. 2016;26(3):320–35.

117. Wang J, Place RF, Portnoy V, Huang V, Kang MR, Kosaka M, *et al*. Inducing gene expression by targeting promoter sequences using small activating RNAs. J Biol Methods. 2015;2(1):e14.

118. Li LC. Small RNA-Guided Transcriptional Gene Activation (RNAa) in Mammalian Cells. Adv Exp Med Biol. 2017;983:1–20.

119. Place RF, Noonan EJ, Földes-Papp Z, Li LC. Defining Features and Exploring Chemical Modifications to Manipulate RNAa Activity. Curr Pharm Biotechnol. 2010;11(5):518–26.

120. Chu Y, Yue X, Younger ST, Janowski BA, Corey DR. Involvement of argonaute proteins in gene silencing and activation by RNAs complementary to a non-coding transcript at the progesterone receptor promoter. Nucleic Acids Res. 2010;38(21):7736–48.

121. Schwartz JC, Younger ST, Nguyen NB, Hardy DB, Monia BP, Corey DR, *et al*. Antisense transcripts are targets for activating small RNAs. Nat Struct Mol Biol. 2008;15(8):842–8.

122. Paugh SW, Coss DR, Bao J, Laudermilk LT, Grace CR, Ferreira AM, *et al*. MicroRNAs Form Triplexes with Double Stranded DNA at Sequence-Specific Binding Sites; a Eukaryotic Mechanism via which microRNAs Could Directly Alter Gene Expression. PLoS Comput Biol. 2016;12(2):e1004744.

123. Kang MR, Yang G, Place RF, Charisse K, Epstein-Barash H, Manoharan M, *et al*. Intravesical delivery of small activating RNA formulated into lipid nanoparticles inhibits orthotopic bladder tumor growth. Cancer Res. 2012;72(19):5069–79.

124. Place RF, Wang J, Noonan EJ, Meyers R, Manoharan M, Charisse K, *et al*. Formulation of Small Activating RNA Into Lipidoid Nanoparticles Inhibits Xenograft Prostate Tumor Growth by Inducing p21 Expression. Mol Ther Nucleic Acids. 2012;1(3):e15.

125. Matsui M, Sakurai F, Elbashir S, Foster D, Manoharan M, Corey DR. Activation of LDL Receptor (LDLR) Expression by Small RNAs Complementary to a Noncoding Transcript that Overlaps the LDLR Promoter. Chem Biol. 2010;17(12):1344–55.

126. Watts JK, Yu D, Charisse K, Montaillier C, Potier P, Manoharan M, *et al*. Effect of chemical modifications on modulation of gene expression by duplex antigene RNAs that are complementary to non-coding transcripts at gene promoters. Nucleic Acids Res. 2010;38(15):5242–59.

127. Yoon S, Huang KW, Reebye V, Mintz P, Tien YW, Lai HS, *et al*. Targeted Delivery of C/EBPα -saRNA by Pancreatic Ductal Adenocarcinoma-specific RNA Aptamers Inhibits Tumor Growth In Vivo. Mol Ther. 2016;24(6):1106–16.

128. Huang V, Qin Y, Wang J, Wang X, Place RF, Lin G, *et al*. RNAa Is Conserved in Mammalian Cells. PLoS ONE. 2010;5(1):e8848.

129. Junxia W, Ping G, Yuan H, Lijun Z, Jihong R, Fang L, *et al*. Double strand RNA-guided endogeneous E-cadherin up-regulation induces the apoptosis and inhibits proliferation of breast carcinoma cells in vitro and in vivo. Cancer Sci. 2010;101(8):1790–6.

130. Yang K, Shen J, Tan FQ, Zheng XY, Xie LP. Antitumor Activity of Small Activating RNAs Induced PAWR Gene Activation in Human Bladder Cancer Cells. Int J Med Sci. 2021;18(13):3039–49.

131. Wang J, Place RF, Huang V, Wang X, Noonan EJ, Magyar CE, *et al*. Prognostic value and function of KLF4 in prostate cancer: RNAa and vector-mediated overexpression identify KLF4 as an inhibitor of tumor cell growth and migration. Cancer Res. 2010;70(24):10182–91.

132. Sarker D, Plummer R, Meyer T, Sodergren MH, Basu B, Chee CE, *et al*. MTL-CEBPA, a Small Activating RNA Therapeutic Upregulating C/EBP-α, in Patients with Advanced Liver Cancer: A First-in-Human, Multicenter, Open-Label, Phase I Trial. Clin Cancer Res Off J Am Assoc Cancer Res. 2020;26(15):3936–46.

133. Qian Y, Liu C, Zeng X, Li LC. RNAa: Mechanisms, therapeutic potential, and clinical progress. Mol Ther Nucleic Acids. 2025;36(2):102494.

134. Ractigen Therapeutic Development of saRNA for Duchenne Muscular Dystrophy by Targeted Activation of Utrophin (Poster) - Ractigen Therapeutics [Internet]. 2024 [cited 26 June 2025].https://www.ractigen.com/therapeutic-development-of-sarna-for-duchenne-muscular-dystrophy-by-targeted-activation-of-utrophin-poster-2/

135. Frohman MA, Dush MK, Martin GR. Rapid production of full-length cDNAs from rare transcripts: amplification using a single gene-specific oligonucleotide primer. Proc Natl Acad Sci U S A. 1988;85(23):8998–9002.

136. Yeku O, Frohman MA. Rapid amplification of cDNA ends (RACE). Methods Mol Biol Clifton NJ. 2011;703:107–22.

137. Musiała-Kierklo N, Plewka P, Jasiok A, Stępniak-Konieczna E. Promoter-targeted small RNA duplexes increase MBNL1 transcription and mitigate myotonic dystrophy-associated spliceopathy. Nucleic Acids Res. 2025;53(15).

138. Dallmeier K, Neyts J. Simple and inexpensive three-step rapid amplification of cDNA 5' ends using 5' phosphorylated primers. Anal Biochem. 2013;434(1):1–3.

139. Wu HL, Li SM, Hu J, Yu X, Xu H, Chen Z, *et al*. Demystifying the mechanistic and functional aspects of p21 gene activation with double-stranded RNAs in human cancer cells. J Exp Clin Cancer Res CR. 2016;35:145.

140. Nakanishi K. Anatomy of four human Argonaute proteins. Nucleic Acids Res. 2022;50(12):6618–38.

141. Portnoy V, Huang V, Place RF, Li LC. Small RNA and transcriptional upregulation. Wiley Interdiscip Rev RNA. 2011;2(5):748–60.

142. Frietze S, O'Geen H, Blahnik KR, Jin VX, Farnham PJ. ZNF274 Recruits the Histone Methyltransferase SETDB1 to the 3' Ends of ZNF Genes. PLoS ONE. 2010;5(12):e15082.

143. Meister G, Landthaler M, Patkaniowska A, Dorsett Y, Teng G, Tuschl T. Human Argonaute2 Mediates RNA Cleavage Targeted by miRNAs and siRNAs. Mol Cell. 2004;15(2):185–97.

144. Childs-Disney JL, Stepniak-Konieczna E, Tran T, Yildirim I, Park H, Chen CZ, *et al*. Induction and reversal of myotonic dystrophy type 1 pre-mRNA splicing defects by small molecules. Nat Commun. 2013;4:2044.

145. Livak KJ, Schmittgen TD. Analysis of relative gene expression data using real-time quantitative PCR and the 2(-Delta Delta C(T)) Method. Methods San Diego Calif. 2001;25(4):402–8.